ESR STUDIES OF RADICAL IONS

A thesis

submitted in partial fulfilment

of the requirements for the Degree

of

Doctor of Philosophy in Chemistry

in the

University of Canterbury

by

C.M. Kirk

University of Canterbury

1975

To

Marg and my Family

ACKNOWLEDGEMENT

I wish to sincerely thank my supervisor, Dr R.F.C. Claridge, for his help, enthusiasm and encouragement during the course of this project.

PUBLICATIONS

The following paper relating to research described in this thesis has been published:

'^{13}C Coupling in the esr spectrum of the pyrene anion in tetrahydrofuran', R.F.C. Claridge, C. M. Kirk and B. M. Peake, Aust. J. Chem., 26, 2055 (1973).

A reprint of this paper is included inside the back cover of this thesis.

CONTENTS

ABSTRACT

The formation and behaviour of ion pairs have been examined by esr spectroscopy for the pyrene, perylene, naphthalene and dimethylnaphthalene systems. The alkali metal hyperfine splittings and the linewidths, in particular, provide much information on the nature and dynamics of these ion pairs. For some systems thermodynamic and kinetic data have been obtained. Various Molecular Orbital calculations were carried out and from these the most likely position of the alkali metal ion in the ion pairs is suggested. The trends in ion pair formation with cation, anion, solvent and temperature are discussed. In the symmetric dimethylnaphthalene series, the effect of the methyl groups on the counter-ion position is considered, with the 1,4- and 2,3- systems being particularly interesting. The hyperfine splittings of the unsymmetric dimethylnaphthalenes allow an additivity model for methyl-group substitution to be completed. Five of the six ^{13}C coupling constants for the pyrene anion were determined.

CHAPTER ONE

INTRODUCTION AND REVIEW

When an alkali metal is reacted with an aromatic hydrocarbon in an ether solvent, different types of product may result. These could be free ions, ion pairs or higher agglomerates and may exist either independently or in equilibria.

Traditional techniques for investigating these systems, such as conductivity measurements, have in recent years been supplemented by a variety of spectroscopic techniques, such as ultraviolet, infra-red and magnetic resonance methods. Of these, electron spin resonance (esr) has probably yielded the most detailed information, particularly on the structure and behaviour of ion pairs in solution.

This thesis continues the application of esr to the study of radical anions and ion pairs in solution. No section is devoted to a description of the esr method or its basic theory. This is readily available in a number of standard texts.[1]

1.1 Earlier studies

The reaction of alkali metals with aromatic hydrocarbons has been known for over a hundred years. In 1867 Bertholt[2] described the formation of a black addition product on fusing metallic potassium with naphthalene in a closed tube. The first comprehensive investigations were carried out by Schlenk and his co-workers[3] in the first quarter of this century; they found that a large number of aromatic hydrocarbons and ketones reacted with alkali metals in ethereal solutions to form coloured free radical

products - the free radical nature was confirmed by magnetic susceptibility measurements.[4] Early formulations[5] of these addition products emphasised this radical nature and considered the alkali metal to be covalently bound to a carbon atom. For example, sodium naphthalene was described by the formula

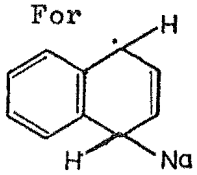

Perhaps the most significant report of these early studies came in 1936 from Scott[6] et al. who investigated the reaction of sodium with naphthalene in a variety of ether solvents. They found that the characteristic green colour of the alkali adduct rapidly appeared when the more polar ethers [such as dimethyl ether (DM), dimethoxyethane (DME) and tetrahydrofuran (THF)] were used, but did not appear at all in other less polar solvents [such as diethyl ether (DEE) or benzene]. Furthermore, the addition of DEE to a pre-formed solution of sodium naphthalene in DM caused it to decompose to the original naphthalene and sodium. Scott also noted that the green solution showed a relatively high electrical conductance, but he failed to follow up the implication of this and of all his observations: that the adduct possessed ionic character.

It was left to Huckel and Bretschneider[7] to raise objections to the earlier formulation of the adducts. They suggested, for the first time, that the hydrocarbon was converted into an anion by the transfer of an electron from the metal.

Proof of this radical anion nature was provided by the pioneering esr studies of Weissman[8] and his associates. They found these solutions showed intense resonance absorptions and this, plus the fact that the overall reaction involved one aromatic molecule per atom of sodium[6,9], conclusively indicated that free radical ions were formed by the transfer of one electron to

the aromatic compound. The observed hyperfine structure also showed that the extra electron was delocalized over the whole molecule, occupying the lowest anti-bonding orbital. Weissman now represented these reactions by the scheme:

$$Na + Ar \rightleftharpoons Na^{+} + [Ar]^{-}$$

and considered the position of equilibrium to depend mainly on the energy of solvation of the metal ion.

With interest revived in the formation and properties of radical anions, many successful investigations using a variety of techniques were initiated. Hoijtink employed polarographic measurements[10] and potentiometric titrations[11] to study quantitatively the ease of reduction of many aromatic hydrocarbons and showed that, besides mononegative ions, dinegative ions can also be formed. He also studied the electronic spectra of the anions[12] while Weissman and others continued esr investigations.[13] Theories accounting for these observations were developed[13-16] and most spectra could be satisfactorily interpreted in terms of Molecular Orbital (MO) theory.

The most significant development in these studies was the detection of hyperfine splitting (hfs) due to the interaction of the unpaired electron of the radical anion with the nucleus of the cation. Weissman and his colleagues first observed this phenomenon with the sodium ketyl of benzophenone[17] and later with sodium naphthalene.[18] This additional hfs was unambiguous proof of the presence of ion pairs. However, the absence of such cation splittings does not necessarily indicate that ion pairs are absent.

Ion pairs represent a strong association between cation and anion and to be detected by the esr technique, each anion must

retain its counter-ion for longer than $\sim 10^{-6}$ sec.* Since 10^{-6} sec. is long in terms of molecular motions, (Brownian motion is of the order of 10^{-10} sec.) these ion pairs may be considered to be thermodynamically stable species, distinct from free ions.

Although esr studies provided the first direct proof of the existence of ion pairs as distinct, stable species, their formation had been postulated more than thirty years earlier by Bjerrum to account for the low conductance of strong electrolytes in non-aqueous solutions.[20] The "sphere-in-continuum" model proposed by Bjerrum[20] and improved by Fuoss[21] described electrolyte solutions by assuming all the ions to be charged spheres and the solvent to be a continuum, characterised electrostatically by its macroscopic dielectric constant and hydrodynamically by its macroscopic viscosity. They derived an expression for the association constant from which the centre-to-centre distance of the oppositely-charged ions could be calculated. The Bjerrum-Fuoss approach was widely used in the next twenty years and despite its oversimplifications it was successful in interpreting the properties of many solutions.[22] However this treatment has certain inherent defects which led Fuoss to propose a modified theory[23] in 1958 based on a new definition of ion pairs.

The first thermodynamic approach to ion pair formation was made by Denison and Ramsey.[24] Using the thermodynamic cycle of Born[25], they studied the dissociation scheme of an ion pair and derived an expression for the free energy of dissociation; this interpreted the increased degree of solvation as the main driving force for ion pair dissociation. A slightly improved expression

---

* Since the mean lifetime, τ , of a species cannot be shorter than the reciprocal of its linewidth, σ, $\tau > \sim 10^{-6}$ sec. for typical esr lines.

noted later by Ramsey[26] was of the same form as that which Fuoss independently derived using statistical methods.[23] As with the preceeding theories, this approach took no account of the interaction of ions with solvent molecules and treats the solvent as simply a dielectric continuum. The first attempt to include ion-solvent interactions in calculations of the association constant was that of Gilkerson[27] who attacked the problem from a microscopic point of view and used partition functions to calculate entropy contributions to the free energy. Although this and other theories have led to some agreement between calculated and observed quantities, ion-solvent interactions are still far from being completely understood.[28]

In their pioneering study, Weissman and Atherton[18] not only detected metal hfs but under some conditions also observed both "split" and "unsplit" spectra simultaneously. They assigned these to ion pair and free ion species respectively and, using the observed spectrum intensities, calculated the thermodynamic parameters for the dissociation of the ion pair. This demonstrated for the first time the vast potential of esr for studying both dynamic and structural aspects of ion pair formation.

In the next few years the esr studies of Weissman, Symons, Reddoch, de Boer, Hirota, Fraenkel, Bolton and many others greatly extended the amount of data on radical ions and ion pairs.[19] Many types of radical anions and cations have now been studied under a large variety of conditions. Alkali metal splittings in particular have provided much insight into the structure of ion pairs. A number of theoretical attempts to calculate these splittings have been made and several different mechanisms proposed.[18,29-31]

Another very useful result to emerge from these studies was that of linewidth alternation, which arises from the out-of-phase modulation of spin densities. This modulation can be caused by a number of processes such as the interconversion of chair and boat forms of a radical or the jumping of a cation between equivalent sites in an anion. This latter process, first observed by de Boer and Mackor in the pyracene anion,[32] often yields valuable information on the relative positions of the cation and anion (i.e. ion pair structure) as well as activation energy and lifetime data. Other types of line broadening have also been analysed to give useful information on ion pair processes.[33,34]

The ability of radical anions to associate with cations in low-polarity solvents also emerged from other types of studies. For instance, Szwarc[35] undertook an elegant series of conductimetric measurements in which he repeated and improved many of Hoijtink's earlier values[11] for the reduction potentials of hydrocarbons. He also determined the dissociation constants of a number of aromatic radical anions by conductance measurements.[36] Perhaps the most extensive studies of the equilibria between alkali metals and aromatic hydrocarbons were carried out during the 1960's by Shatenshtein and his co-workers.[37] These provided much data on the solvating powers of different solvents.

In the ultraviolet and visible spectra of ion pair solutions, the position of absorption maxima was shown to depend on the positive ion and on the solvent.[38] McClelland explained many of these systematic shifts by allowing for the perturbing effects of the cation in Huckel MO calculations.[39] In fact, optical studies were the first to provide physical evidence for the existence of distinct ion pairs in solution. Hogen-Esch and Smid[40] found two absorption peaks in solutions of alkali salts of fluorenyl; their

relative intensities were not affected by dilution but varied significantly with solvent, metal and temperature. This indicated that two ion pair species coexisted in equilibrium (conductance studies verified that the free ion concentration was too low to be important). One absorption peak was assigned to a tight ion pair and the other to a loose ion pair.*

The concept of different types of ion pairs was, in fact, introduced much earlier. In 1954, Winstein[41] and Fuoss and Sadek[42] independently suggested their existence, Winstein to account for the mechanism and stereochemistry of solvolysis reactions and Fuoss and Sadek to explain electrolytic data. They envisaged that an ion surrounded by a tight solvation shell may approach a counter-ion without hindrance until its solvation shell contacts the partner. Then, either the associate maintains its structure as a loose, solvent-separated ion pair, or expels the solvent molecules separating the ions forming a tight ion pair. Grunwald formalised these ideas, which are discussed in the next section.

Hogen-Esch and Smid[40] also found they could interpret much previous data in terms of tight-loose ion pair equilibria. Hirota[44-47] meantime found that two rapidly equilibrating ion pairs could explain much of the extensive esr data he had collected on naphthalene and anthracene radical anions. In particular, he had much success in accounting for the temperature dependence of many alkali metal splittings. The most convincing evidence for this equilibrium process was that the dependence of the linewidth on the alkali magnetic quantum number which this "dynamic" model predicts, has been observed on a number of

---

* Tight, contact or intimate ion pairs consist of a pair of ions with no interposed solvent molecules.

Loose, solvent-separated or external ion pairs consist of a pair of ions with solvent molecules between them.

occasions.[19] Such broadening has usually been assigned to equilibria between tight and loose ion pair structures but Hirota has also interpreted some broadenings as arising from equilibria between different types of tight ion pairs.[46] Although some aspects of Hirota's analysis have been questioned,[48] it has been applied with considerable success to interpreting esr data and represents a significant contribution to the understanding of ion pair processes.

More subtle variations, such as the effect of ion pairing on the proton splitting[49] and g-values[49,50] of the radical anion, have been studied and also discussed in terms of such models. Another approach involving esr is that used in electron exchange studies. The pioneering work of Weissman and his colleagues[34] showed that the rate of electron exchange between radical anions and their parent molecules depends on the state of association of the anions and is generally slower for ion pairs than for free ions. Rate constants for the exchange process may be calculated from the shapes of the esr lines. There have been many subsequent studies, using both the slow and fast exchange limits, and considerable insight into ion pair equilibria has resulted.

Many other important contributions to the applications of esr to the study of radical ions and ion pairs have been made over the last 15 years. Recently the application of alkali nuclear magnetic resonance (nmr) to the study of ion pairs has attracted much interest.[19] A special advantage of the nmr method is that the sign as well as the magnitude of the hfs of a given nucleus can be determined directly, while only the latter is given by esr. However, the high radical concentration necessary (~0.1 - 1 M) is often a complication and limits the usefulness of the method.

As mentioned at the beginning of this chapter, a variety of

techniques are available to study ions and ion pairs. Although the most detailed information has probably been obtained from esr studies, the importance of other approaches should be emphasised. For instance, while optical methods are not usually the most detailed, they are not limited to paramagnetic molecules (as is esr) or to high concentrations (as is nmr). And while ion pair types are often distinguished by typical esr studies, loose ion pairs and free ions usually are not, a fact which has caused considerable misinterpretation in the past; electron exchange or conductance studies, on the other hand, will usually distinguish the free ion from ion pairs.

In summary, the presence of a cation can considerably modify the esr spectrum of a radical anion. The main source of structural information are the metal hyperfine coupling constants, particularly their temperature dependence. Linewidth variations and the observation of more than one species (simultaneously) can lead to a great deal of thermodynamic and kinetic data on the processes of ion pairs.

1.2 The concept of structurally different ion pairs and its limitations.

A brief description of the concept of different ion pairs will now be given to clarify the nature of loose and tight ion pairs and when they may and may not be regarded as distinct entities. This concept and its limitations has been lucidly dealt with by Szwarc.[19,36]

Grunwald[43] described the interactions leading to the separation of ions by a solvent molecule(s) in terms of the potential energy of the two ions as they are pulled away from their contact

FIGURE 1.1

POTENTIAL ENERGY WELLS FOR ION PAIRS

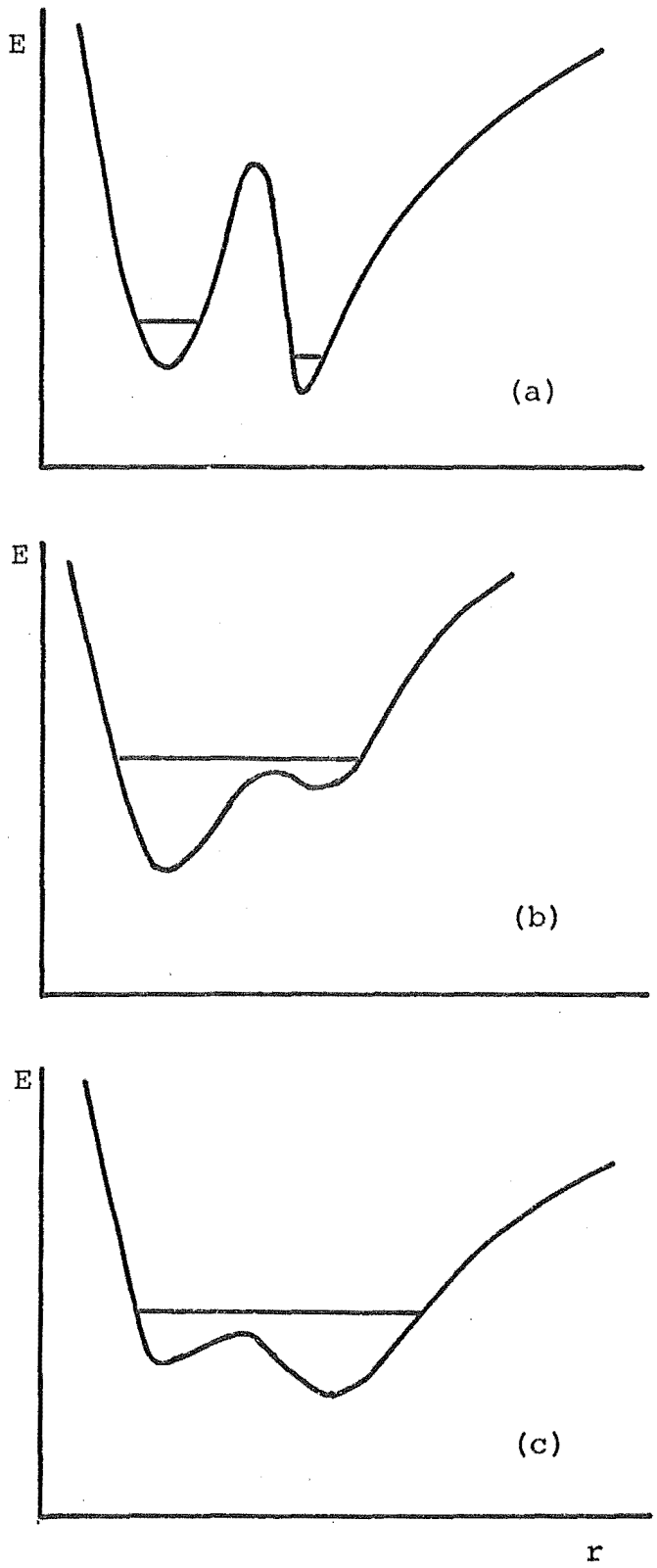

position. Initially, the solvent shells of the two ions are very incomplete and powerful electrostatic forces are important in stabilising the ion pair.

Because the medium is not a continuum but is composed by discrete molecules of definite size, separation of the ions requires energy. In ascending to the top of this energy barrier, more energy is required to oppose the attractive forces than is compensated for by increased solvation. However, beyond a certain separation, which allows a solvent molecule(s) to enter between the ions, increased solvation more than compensates for the energy input required for further separation of the ions, and a second minima occurs. Since the inner shell of solvation molecules determines most of the energy of solvation, still further separation again increases the potential energy which eventually reaches its plateau value at infinite separation [Fig. 1.1a]. The two minima correspond to two distinct species, a contact ion pair and a solvent-separated ion pair coexisting in equilibrium.

In this oversimplified description, Grunwald assumed the potential energy of an ion pair to be uniquely determined by the interionic distance, r. Although this is the usual case for gaseous ions, the situation for ions in solution is more complex. As Szwarc has pointed out[37], the ion pair is embedded in a fluctuating environment of solvent molecules, whose properties change with temperature. This means the average configuration of solvent molecules varies with temperature and the shape of the potential energy curve may be temperature dependent. Therefore the deep minima depicted in Grunwald's model may appear at one temperature, but not at another. It should also be noted that whenever the solvating power of a medium changes, the average interionic distance, r, in both solvent-separated and contact ion

pairs may also change.

In considering whether the concept of two types of ion pairs is valid for all systems containing associated ions, two extreme situations can be imagined. For narrow, deep wells (Fig 1.1a) the concept of two thermodynamically distinct ion pair species is justified over a wide temperature range. The whole system may be regarded as an equilibrium mixture of the two ion pair types and is described as the dynamic model. The observed properties of the system depend on temperature as well as on the lifetime of each species. The esr spectrum should show two sets of lines for slow rates of interconversion, sharp, averaged lines for fast equilibration, and broadening in the intermediate region.

On the other hand, for broad potential energy wells, [Fig. 1.1 b,c] the distinction between ion pair types may not be valid. Since potential energy curves are temperature dependent, these shapes may change considerably; for instance, a well may be like Fig.1.1b at high temperatures, but like Fig.1.1c at low temperatures. This represents a gradual transformation from a contact to a solvent-separated ion pair as the temperature decreases. Thus, in this static model, one structure describes the ion pair at each temperature but this structure may be gradually modified over a temperature range. At some temperatures, the two ions may vibrate between the two minima and the concept of two thermodynamically distinct species becomes meaningless. For this type of system the esr parameters should show a steady shift with temperature.

Distinction between the static and dynamic models is not easy when only one metal hfs is observed. This is always anticipated by the static model but is also predicted by the dynamic model when the rate of interconversion between the various ion

FIGURE 1.2

STRUCTURAL FORMULAE FOR MOLECULES STUDIED IN THIS PROJECT

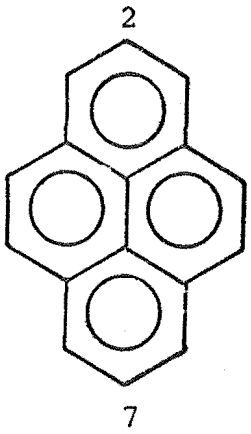

PYRENE

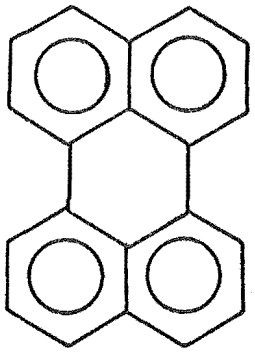

PERYLENE

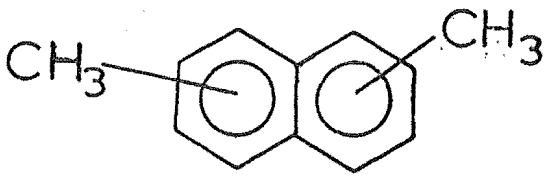

NAPHTHALENE AND DIMETHYL DERIVATIVES

pair types is sufficiently fast. In some systems only one type of ion pair may exist. For instance, when ions do not coordinate with the solvent molecules, their association gives contact ion pairs only. Alternatively, for very strong coordination with the solvent, contact ion pairs may not exist. Thus the concentration of one form may become vanishingly small under some conditions.

1.3 Introduction to Present Study

In this project the radical anions of pyrene (PY), perylene (PYL) and of naphthalene (N) and its dimethyl derivatives (DMN) were studied by esr spectroscopy. [Fig 1.2].

A brief survey of previous esr studies using these compounds and the reasons for this investigation will now be given.

Pyrene

When de Boer and Weissman[13] first studied this anion, they assigned one proton splitting (by isotopic substitution) but found a serious discrepancy between the observed spectrum and that calculated on the basis of spin densities using Huckel Molecular Orbital (HMO) theory, which predicts a nodal plane and thus no spin density at the 2,7 positions. This led to the first postulate of negative π spin density for radical anions. In 1960, McLachlan[51] showed how this might arise at the 2,7 carbon positions of the pyrene anion. Soon afterwards improved resolution allowed Hoijtink[51] to observe and assign all three coupling constants. Nishiguchi et al.[52] have reported Rb and Cs metal splittings using tetrahydropyran as the solvent and Hirota[53] has recently published sodium splittings, as measured by nmr, for the DME and MTHF systems. Mobius[54] reported the proton hfs for an electrolytically prepared sample. Reddoch[55] has noted the

variation with temperature of the proton hfs for the Na/THF system and concluded the free ion to be present throughout the temperature range. Segal[56] investigated the Na salt in DME at low temperature and Hirota[57] concluded from electron transfer studies that this system contained either the free ion or a loose ion pair. Recently, a slightly slower rate was measured for the Na/THF system[58] indicating a greater degree of ion pairing in this solvent than in DME. The g-values have been reported by Blois,[59] Mobius,[54] Segal[60] and Fraenkel.[50]

Perhaps the most interesting report discussed the PY/K/THF system. Lyons, Moore and Morris[61] interpreted small peaks astride the main proton line as due to a potassium splitting (0.14 G) from a K^+ PY^- ion pair, and concluded a free ion-ion pair equilibrium was present. As well, some of these small lines appeared to broaden as the temperature was decreased. They concluded this was due to linewidth alternation caused by migration of the K^+ ion between the equivalent sites 2 and 7. The first part of this project was devised around this paper.

As outlined above (Chap 1.1), linewidth alternation, equilibria between distinct species, and alkali metal coupling constants are among the most useful esr observations for probing ion pair formation. Of these, Lyons' work indicated the first two should be evident in a number of solvent/metal systems and the third had been only lightly studied. Thus, it was thought that a systematic study of this anion might result in considerable data on ion pairing processes and ion pair structure.

Perylene

In contrast to the pyrene case, de Boer and Weissman's[13] initial esr work with the perylene anion showed an excellent fit between the calculated and observed spectra. Shortly afterwards,

Carrington et al.[62] measured the proton hfs for K reduction in THF. Bolton reported new values in 1963[63] and slightly modified ones a little later.[64] As with pyrene, Mobius[54] published coupling constants for an electrolytically prepared sample and Reddoch[55] studied their temperature dependence in the Na/THF system. Hnoosh and Zingero[65] unexpectedly observed the perylene anion spectrum when studying the reaction between tris-(1-naphthalene) phosphine and lithium (accidentally lithium had initially reacted with the glass vessel). de Boer[66] obtained the esr spectrum of the PYL/Na/DME system from +20°C to -95°C but was interested in linewidth measurements and reported no coupling constants or ion pairing. The g-values for the negative ion have been published a number of times[54,59,60,62] and the perylene cation is a well-studied cation species.[67]

From this brief survey, it is evident that esr data on ion pairing effects with perylene as the anion is negligible. Certainly most evidence predicts that large, diffuse ions like perylene form mainly solvent-separated ion pairs or free ions, neither of which is likely to yield a great deal of information via the esr technique. However, no attempt at a systematic study appeared to have been made. It was with the aim of extending esr investigations of ion pairs to larger anions that the perylene anion was studied.

Naphthalene (N) and the dimethylnaphthalenes (DMN).

An enormous amount of work has been carried out with the naphthalene anion and it was not intended in this project to reinvestigate this radical. Naphthalene samples were observed only for those systems used with the DMNs, so that a comparison with the unsubstituted molecule under the same preparative and operating conditions could be made. Such systems also serve as

a check for the methods used in this project. Thus no survey of the data available on naphthalene will be made except to note that Hirota,[45,46] in particular, has reported a large number of metal splittings and linewidth effects, and Reddoch[49] has studied the proton splittings most accurately.

The initial work on DMN anions was that of de Waard and Henning[68] who used a K/dioxane system at room temperature to reduce the six symmetrically substituted compounds. Gerson[69] investigated these anions in Na/DME at -70°C and correlated the methyl proton splittings with the Huckel spin densities allowing for the inductive effect of the methyl groups. About the same time, the spectrum of the 2,3DMN anion in liquid NH_3 was reported by Maximadsky,[70] but apparently no analysis was made. Moss et al.[71] produced a sizeable report in 1969 in which they extended the number of systems investigated and found that changes in the proton coupling constants on methyl-substitution obeyed an additivity relationship. They also discussed the various models for the effects of methyl group substitution and performed a large number of correlations between calculated and observed quantities. In these studies no metal splittings or ion pairing effects were noted.

Rieke[72] observed the 2,3DMN/K/DME system in the course of his studies on ring strain effects and noted a large change in splitting constants as the temperature was decreased. He attributed this to an unsymmetrical ion pair which reverts to the free ion at low temperatures, although again no metal splitting was detected. Very recently he reported[73] that the above system in a DME-HMPA mixture produced the free ion and temperature-independent proton coupling constants.

The first metal splitting for DMN anions was reported by

Goldberg and Bolton[31] for the 1,5DMN/Na/MTHF system. The Na hfs ranged from 0.5 (-120°C) to 0.9 G (+30°C). More recently Peake[74] observed Cs splittings for 1,8- and 2,6-DMN in both DME and THF, and Na hfs for these anions in THF. He also observed the spectra of three of the four unsymmetrical DMN anions, but because of insufficient resolution was unable to analyse them. There appears to be no other reports for the unsymmetrical anions.

Although some comprehensive investigations of DMN anions had already taken place, they were mainly concerned with the effects of methyl-substitution on the spin density distribution. Few had investigated ion pair formation, in obvious contrast to the unsubstituted compound where ion pairing studies brought many interesting results. In this section of the project, it was hoped to obtain some esr data on ion pairing effects in these compounds. Besides its own intrinsic interest, such data could be used to test ideas such as that of Goldberg and Bolton.[31] On the basis of their calculations for the naphthalene system, they suggested that differences in alkali metal splittings shown by the DMNs on the one hand, and N on the other, could be explained by steric arguments.

Although this project was not principally a theoretical investigation, a few simple calculations were planned for comparison with the experimental data.

CHAPTER TWO

EXPERIMENTAL

2.1 Radical Anion Preparations

All the radical anions used in this project were prepared by the reduction of the parent hydrocarbons with alkali metals. The standard vacuum techniques employed in these preparations are well documented.[9,74,75] About 1 mg. of hydrocarbon was used. Cesium was formed by gently heating a mixture of calcium turnings and cesium chloride[76] while sodium and potassium were simply freshly cut metal pieces.[75] Purified sodium, potassium and cesium mirrors were formed by distilling the metal three times. The procedure suggested by Fraenkel[50] was followed for lithium reductions. The solvents were purified and dried by the usual methods[75] and stored in vacuo over potassium anthracenide.

2.2 Chemicals

Solvents:

1,2-Dimethoxyethane (DME): BDH

Tetrahydrofuran (THF): Fluka Purum

2-Methyltetrahydrofuran (MTHF): Eastman Organic Chemicals White Label

Diethylether (DEE): Riedel-de Haen

Ethanol (96%): Fluka Co., for UV spectroscopy

Hydrocarbons:

Pyrene (PY): Aldrick Chemical Co., Inc.

Perylene (PYL): Koch Light Laboratories Ltd.

Naphthalene (N): BDH

1,6-; 2,3-; 2,6-Dimethylnaphthalene (DMN): L. Light and Co. Ltd.

1,4-; 1,3-; 1,5-DMN: Fluka Co.

2,7-; 1,2-DMN: K and K Laboratories

1,7-DMN: prepared by R.F.C. Claridge and D.A.R. Happer from a succinic acid condensation and subsequent methylation.[77]

1,8DMN: prepared by S. Blackstock from the reduction of naphthalic anhydride.[78]

Metals:

Potassium: BDH

Lithium: Riedel-de Haen

Sodium: BDH

Cesium chloride: Riedel-de Haen

The purity of the aromatic hydrocarbons was checked by nmr spectroscopy. Pyrene and naphthalene were used without further purification. Perylene was recrystallised from acetic acid and some of the DMNs were purified by recrystallisation (from ethanol) or column chromatography.

2.3 Esr spectra

The esr spectra were recorded on a Varian E12 spectrometer equipped with a Varian V4557 temperature controller. The sample temperature was monitored with a copper-constantan thermocouple connected to a calibrated digital voltmeter and was steady to within 1.0°C over the time required to obtain a spectrum. The microwave frequency was measured using a Systron Donner Frequency Counter, Model 6016.

The scan range was calibrated from the smaller coupling constant of a N/K/DME* sample at room temperature. The absolute magnitude of this splitting was taken to be 1.835 Gauss[49] [1 Gauss (G) = 0.1 millitesla (mT)]. In the early part of this project the linearity of the recorder was found to be unacceptable. This fault was eventually corrected by replacing the X-Y scan potentiometer. Such nonlinearity can introduce serious errors into the measured coupling constant values if it is not recognised. This problem was overcome by confining all measurements and computer simulations to lines which occured in a small, accurately calibrated portion of the scan.**

Early experiments showed that if 100 KHz modulation frequency was used the effect of sidebands became evident when the lines were narrow (30 mG); in fact, this artifact resulted in a spectrum for the PY/K/MTHF system where each proton signal was split into a five-lined multiplet. This could very easily be misinterpreted as a K hfs plus a free-ion line. To eliminate this effect, all spectra were obtained using 10KHz modulation. No sidebands were observed under these conditions. In almost all cases the lowest modulation amplitude was also used, to prevent any lineshape distortion.

To avoid saturation effects the power levels were always low (0.05 - 0.2 mW). This was most important for perylene samples,

---

* The symbolism R/M/S refers to a system in which R is the parent hydrocarbon, M is the metal, and S is the solvent.

** For example, for pyrene, simulated lines were all within 3.5 G of the central line, on the low field side. Using the principal line (M_β=0, M_α=-1, M_γ=0), a_α may be determined; there are then a number of lines whose position in the above portion of the scan is determined by either a_β or a_γ. Hence all three coupling constants can be measured within the calibrated region.

which were usually recorded at a power level of 0.05 mW. Most pyrene, naphthalene and DMN spectra were run at 0.1 mW.

The most critical parameter in obtaining well-resolved spectra was the concentration of the radical anion. As the concentration was lowered, the linewidth approached a minimum value, and any further dilution merely reduced the amplitude of the signal. The optimum concentration was always sought by trial and error, and was of the order of 10^{-4} - 10^{-5} M. Spectra were usually recorded with a scan range of 10 G/40 cm, a time constant of 0.3 sec, and a scan time of 16 min.

g-values

On two occasions where both free ion and ion pair were observed simultaneously, the g-value of the ion pair was calculated. The free ion g-value was assumed to be that of the pyrene anion in the K/DME system which has been very accurately determined by Fraenkel.[50] The ion pair g-value can then be found from the measured microwave frequency and the field difference between the centres of the two spectra.

Concentration measurements

For systems which involve a free ion-ion pair equilibrium, the total concentration of radical anion is required to calculate the equilibrium constant. Immediately after the esr spectra had been recorded, the height of the solution in the calibrated esr tube was noted, the tube carefully opened and the solvent evaporated off. The hydrocarbon was taken up in a known volume of 96% ethanol and the concentration obtained using UV-visible absorption. The required molar extinction coefficient of pyrene in 96% ethanol was determined from six experiments to be:

ε_λ at 319nm = 2.92×10^4; ε_λ at 334nm = 4.82×10^4

and was accurate to within 10%.

The extinction coefficient of perylene in 96% ethanol was taken to be:[79]

ε_λ at 434nm = 3.39×10^4; ε_λ at 405nm = 2.75×10^4

The UV-visible spectra were obtained on a Varian Techtron Spectrometer, Model 635, with a digital readout.

Calculations

All the experimental coupling constants were determined by visually comparing computer simulated spectra with the observed spectra until the best agreement was achieved. The computer program used, SIMESR,[74] assumed each hyperfine line of a spectrum was of equal width but had provision for more than one spectrum to be superimposed. Spectra showing hyperfine lines of different widths could be simulated by decomposing the spectra into a number of pseudo-spectra with equal linewidth, but differing from each other. All hyperfine lines were taken to be 100% Lorenztian in shape. The minimum plotting interval was 1/100".

Theoretical coupling constants were determined using a modified HMO method (program MOCALC)[74] and an INDO calculation (program CNINDO, QCPE 141).[80]

All calculations were performed on an IBM 360/44 or a Burroughs 6718 computer at the University of Canterbury. All plotting was done on a Calcomp X-Y plotter controlled by a PDP11/20.

FIGURE 3.1

STRUCTURAL FORMULA AND NUMBERING SYSTEM

FOR PYRENE

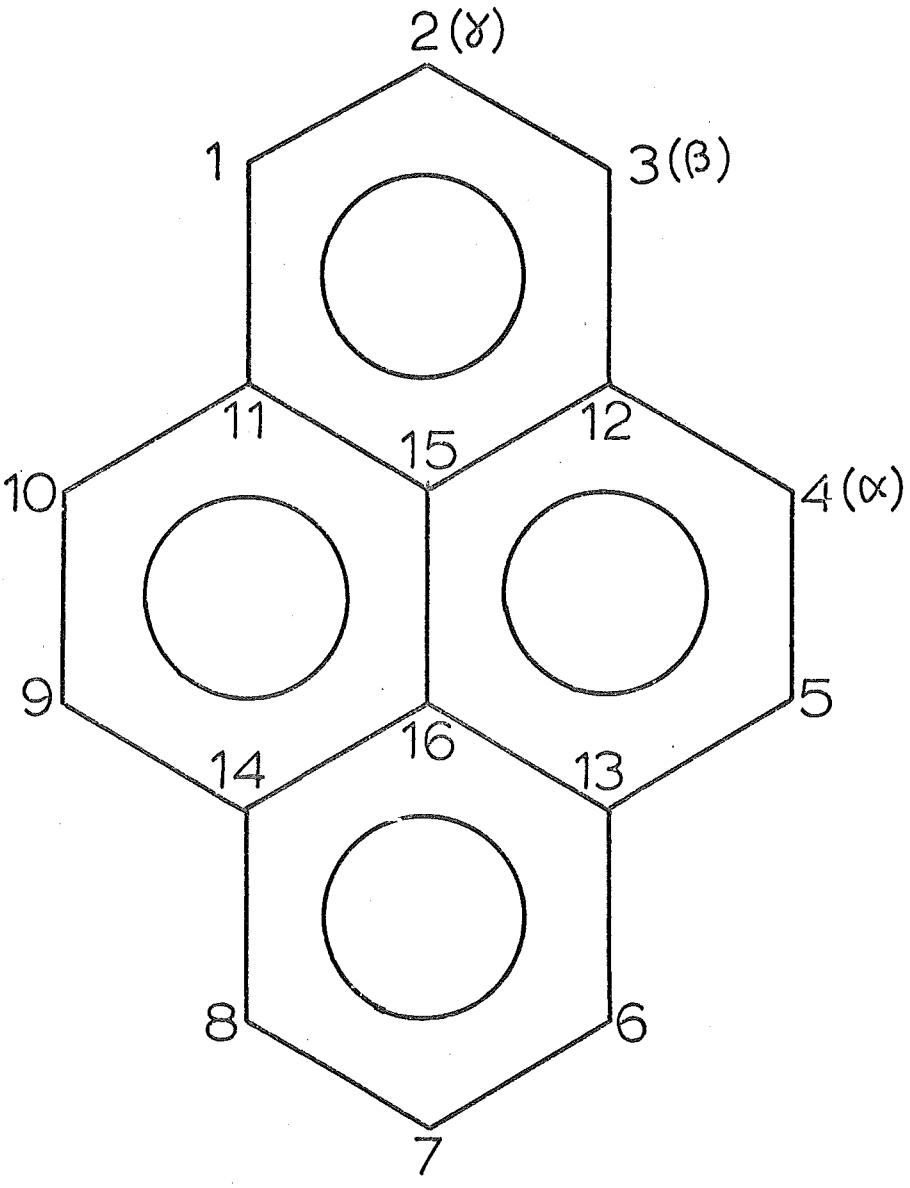

CHAPTER THREE

PYRENE

Pyrene was rapidly reduced, using the procedures of Chapter Two, to a stable, reddish-brown solution, characteristic of the pyrene anion.[61] Four alkali metals (Li, Na, K, Cs) and four ether solvents (DME, THF, MTHF, DEE) were used in all combinations. Only Cs/DEE gave no detectable changes.

Pyrene has 3 sets of magnetically inequivalent protons, denoted α, β, γ [fig. 3.1] by esr spectroscopists; these sets contain four, four, and two protons respectively and give rise to seventy-five lines in the absence of metal splitting. The coupling constants have been assigned to positions in the molecule.[51]

3A. Esr spectra: observations

The coupling constants which best simulated the experimental spectra are listed for each system in Table A.1., Appendix A

K/DME, Li/DME, Na/DME, K/THF, Li/THF

These systems produced esr spectra with very narrow (25 - 30 mG linewidth) lines arising from the proton splittings. In some, broadening occurred at higher temperatures probably due to an unresolved metal splitting. For such cases, an estimate of this "implied" coupling constant is given in parentheses in Table A.1. For K/DME some broadening also occurred at lower temperatures; this may again be due to a small metal coupling constant or perhaps to the increased viscosity of the solvent.

An interesting feature, first noted for the K/DME system but

subsequently for many others, was that the first derivative lines were slightly asymmetric. The lines, recorded in the - + phase ( ), had a greater height from the crossover point to the top of the signal than to the bottom of the signal. Attempts to remove this distortion by adjusting the experimental variables were unsuccessful and it was concluded to be a real effect arising from second order shifts, as discussed in part B. Computer simulations incorporating this effect for the larger proton coupling constant showed considerably better agreement with the observed lineshape than those without it. On this basis, subsequent pyrene simulations always included this second order calculation.

Na/THF Extremely narrow lines (23 mG) were found for this system from -80°C to 0°C with broadening gradually increasing at higher temperatures (40 mG at +25°C). The asymmetry due to second order effects was probably best illustrated in these low temperature spectra. Reddoch's values[55] are in close agreement at +25°C and the temperature dependence of a_α and a_γ are almost identical. However, he reports that a_β is also temperature dependent, although the shifts are very small (~0.4%). Reddoch makes no mention of the increasing linewidth above 0°C but he probably worked with higher minimum linewidths than were achieved in this work.

Cs/DME Well-resolved spectra were found for this system at temperatures below -30°C. The linewidths were broader than those in the above systems (~40 mG), probably due to a small cesium splitting. Above -30°C an additional species was indicated by

FIGURE 3.2

ESR SPECTRA[a] OF THE PY/Cs/THF SYSTEM

Main free ion lines marked *

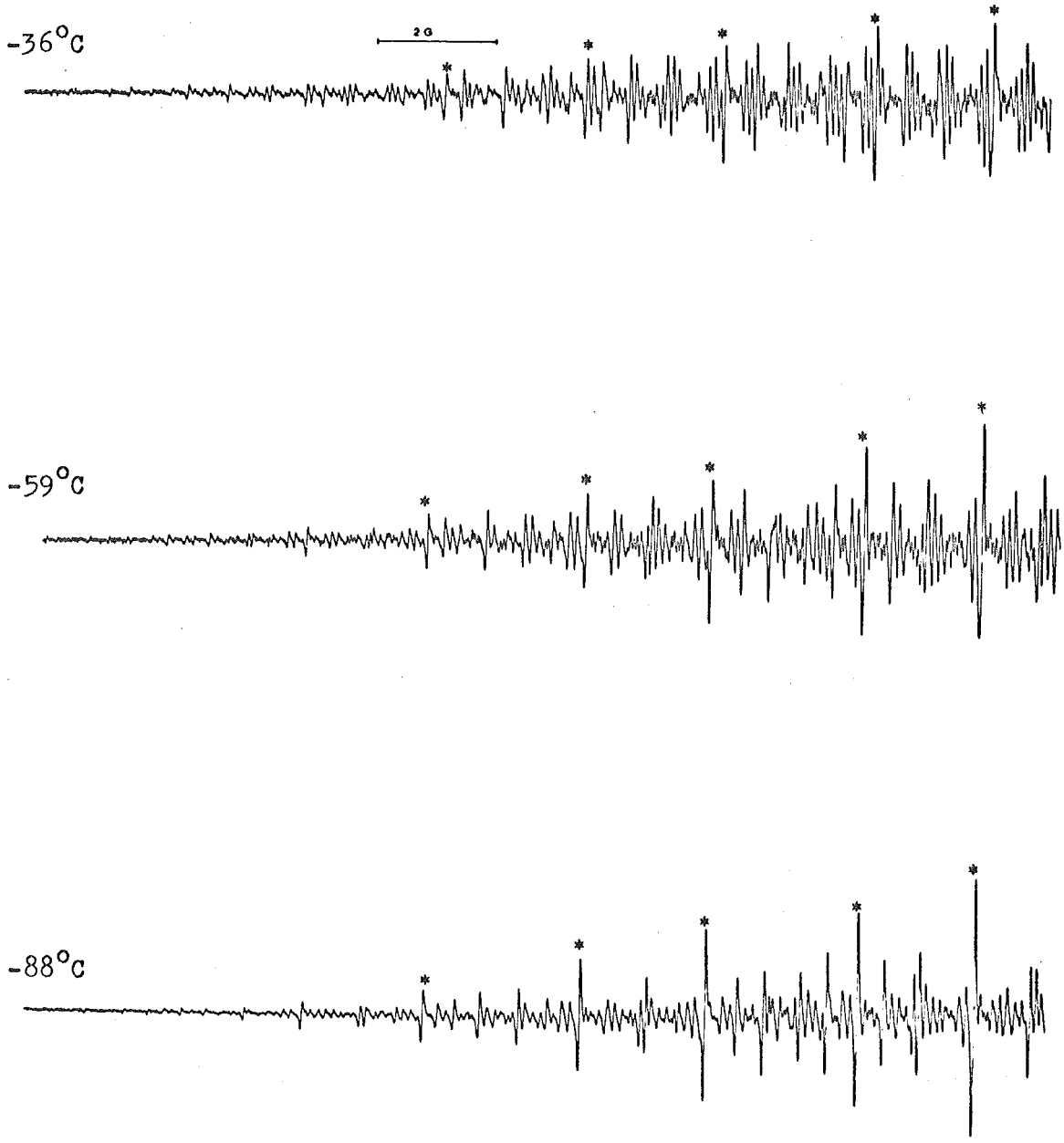

a) Only the downfield half of the first derivative esr spectrum is shown. Magnetic field always increases to the right.

the appearance of extra lines. These lines changed considerably over the temperature range where they were observed and were clearly due to an ion pair with a rapidly increasing Cs hfs. Despite a number of attempts to simulate these extra lines, little success was achieved, mainly because of the large number of lines, the lack of resolution and the low intensity of this species. A Cs hfs of the order of 0.3 G at +17°C gave some reasonable simulation.

Cs/THF The spectra from this system displayed a large number of lines at all temperatures studied [Fig 3.2]. These were analysed as a superposition of two simpler spectra; one with each of the usual lines further "split" into eight components. Such a splitting can only arise from a hyperfine interaction of the unpaired electron and the Cs nucleus (I_{Cs} = 7/2). Since both sets of lines are narrow, each species has a lifetime of at least 10^{-6} sec. Both "normal" and "split" spectra are present throughout the temperature range observed and their ratio changes with temperature. The former predominates at low temperatures, the latter at higher temperatures. If the sample is diluted at constant temperature, the relative intensity of the unsplit component increases. All phenomena are reversible. The g-values of the two species are different and the difference is temperature dependent [Table 3.1]. For reasons detailed in the discussion, the "normal" spectrum was assigned to the free ion species, and the system taken to represent a free ion-ion pair equilibrium.

Table 3.1: g-factor differences and alkali metal hyperfine splittings

System	Temperature (°C)	$\Delta g^{a)} \times 10^{+6}$	$\lvert a_M \rvert$ (G)
Cs/THF	-88	123	0.761
	-65	126	0.753
	-59	129	0.747
	-45	132	0.741
	-36	136	0.741
	-23	139	0.734
	-8	142	0.728
	+3	145	0.721
	+17	148	0.714
K/MTHF[b)]	-88	14	0.048
	-81	14	0.050
	-71	12	0.053
	-60	11	0.055
	-55	9	0.057
	-43	9	0.057
	-35	9	0.057
	-24	9	0.057

a) $\Delta g = g_{\text{free ion}} - g_{\text{ion pair}}$ where $g_{\text{free ion}}$ is taken to be the g-value found for the K/DME system;[50] both $g_{\text{free ion}}$ and $g_{\text{ion pair}}$ are corrected for second order effects; estimated error in Δg is $\pm 3 \times 10^{-6}$.

b) from 1 G/40 cm spectra.

Li/MTHF At lower temperatures this system displayed typically narrow single lines, which broaden only slightly above +10°C, again possibly due to unresolved cation splitting. Above -10°C additional small lines appeared on either side of the main ones and increased in relative intensity and separation as the temperature was raised. These lines (also 30 mG linewidth) are presumably the outer lines of an IP species. This species has a slightly lower g value ($\Delta g \simeq 6 \times 10^{-6}$) but no frequency measurements were made.

Cs/MTHF This system exhibited esr spectra with a large number of narrow lines (30 mG). Spectral simulation showed that one ion pair species accounted for these throughout the temperature range.

Na/MTHF The esr spectra of this system displayed narrow (26 mG) lines from -80°C to -45°C. At -29°C the lines were definitely broadened and by -20°C sodium hfs was resolved which increased as the temperature was raised. Some small asymmetry of the resolved sodium hyperfine pattern was noted in the -20°C to +20°C region which could arise from a small amount of another species, or, as discussed below, could be due to second order effects.

K/MTHF As for the Cs/THF case, this system was analysed in terms of an ion pair and a free ion species [Fig. 3.3]. Above 0°C the free ion concentration became negligible in the samples studied. All lines were narrow (27 mG) so again both species exist for at least 10^{-6} sec. The ion pair and free ion have slightly different g values (Table 3.1). For the centre line

FIGURE 3.3

ESR SPECTRA OF THE PY/K/MTHF SYSTEM

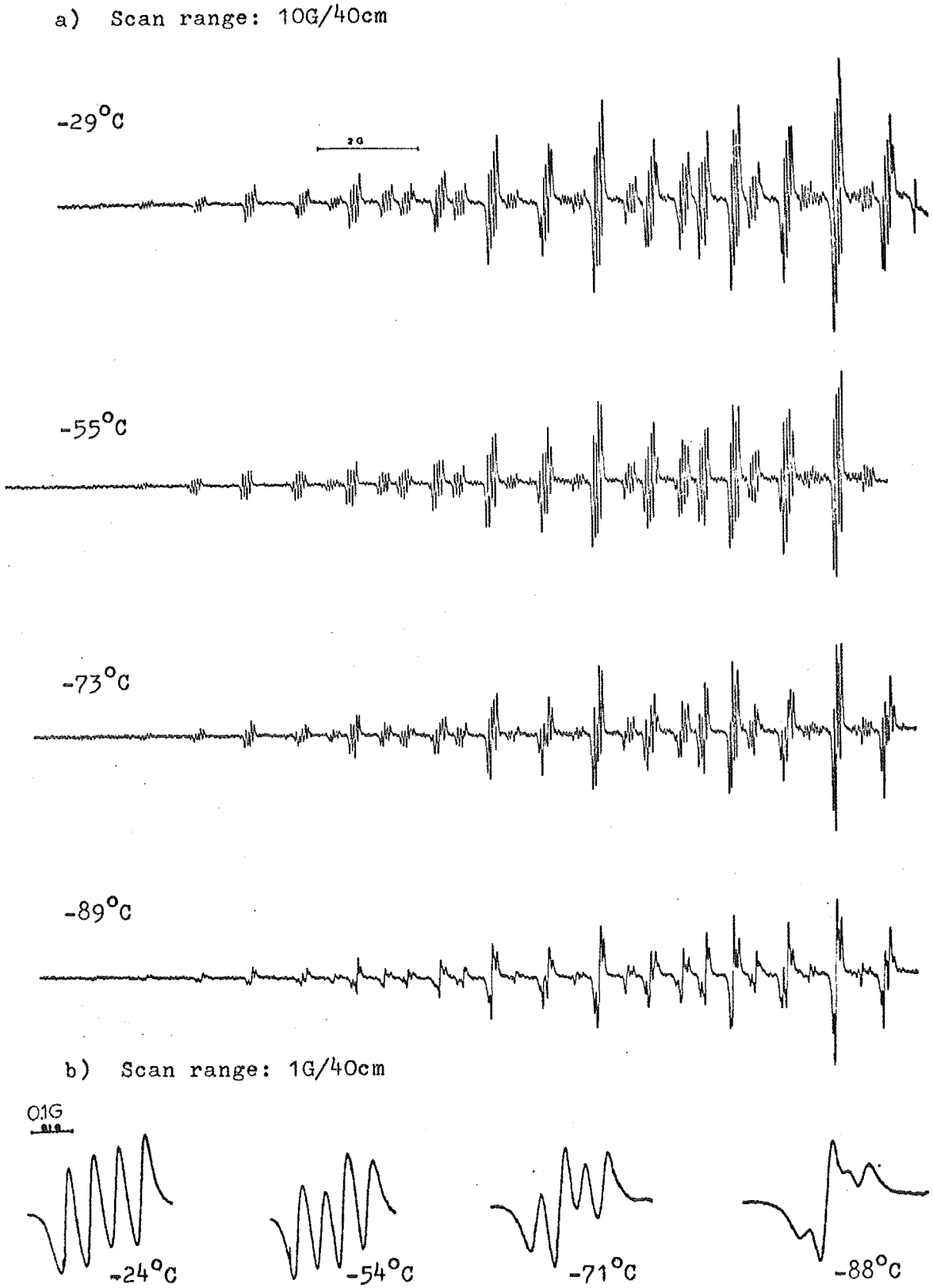

this causes the free ion signal to be superimposed on the second component of the K^+ splitting. Because of this complexity, it was exceedingly difficult to determine which parameters to vary to obtain the best spectral simulations. For instance, small variations in the ion pair : free ion ratio (Γ), Δg, a_K or the linewidths all affect the overall shape of the central quartet considerably. Since the thermodynamic parameters for this equilibrium depend directly on Γ, the central lines were reinvestigated on an expanded scale (1G/40cm). These spectra indicated the relative g-values and variations in the K hfs much more accurately so that the original spectra could be confidently simulated by adjusting the ratio of the two species.

K/DEE These spectra showed a K hfs which varied only slightly in the temperature range studied. The linewidths were again very small (27 mG), with a slight increase above $0^\circ C$ (40 mG at $+22^\circ C$).

Na/DEE Esr spectra for this system exhibited an interesting effect: as the temperature was decreased the Na hfs decreased to zero ($\sim -55^\circ C$) and then reappeared again. The lines were again narrow (28 mG), with some increase at very low temperatures and near room temperature. Below $-60^\circ C$, a second species was apparently present as additional small signals appeared on either side of the main lines, and grew in intensity and separation as the temperature was lowered. However, samples prepared later to check reproducibility showed no second species. This strongly suggests the original extra lines were the result of impurities. Tuttle[81] has pointed out that impurities, especially from potassium ions in sodium preparations, can readily contaminate

FIGURE 3.4

ESR SPECTRA OF THE PY/Li/DEE SYSTEM

Main free ion lines marked *

a) Scan range: 10G/40cm

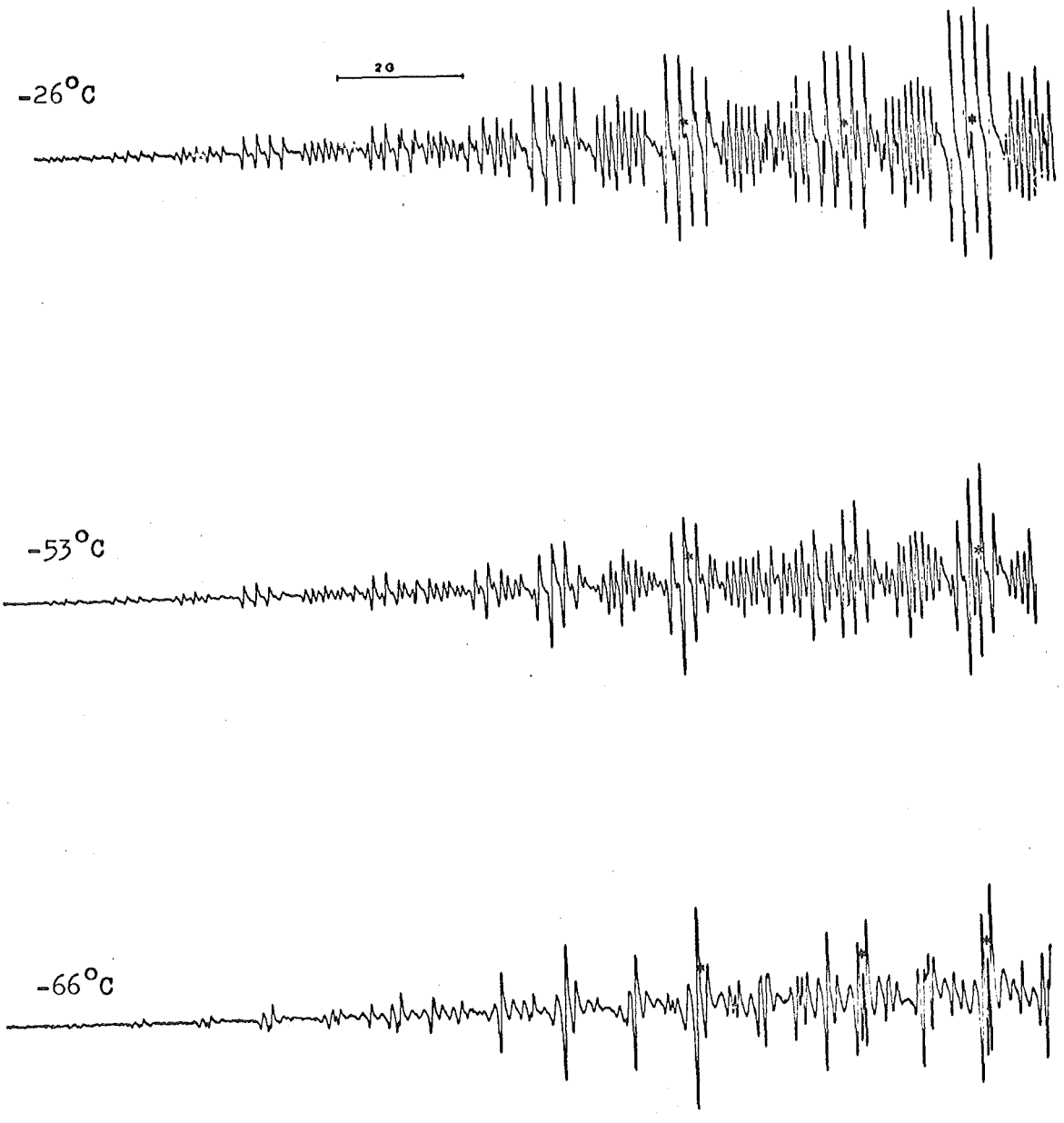

...ctd

radical anion preparations, and lead to the incorrect analysis of spectra. For instance, Hirota[45] initially interpreted extra metal splittings he observed in a N/Na/DEE sample as providing direct esr evidence for the simultaneous existance of two types of ion pairs, but he later[46] found that the concentration of the second species strongly depended on the preparation. It seems that potassium salts present as impurities in commercial metallic sodium or on glass surfaces may exchange with ion pairs containing sodium to give an appreciable concentration of ion pairs containing potassium. It is interesting to note that the metal splitting of this "impurity" (assuming it to be an ion pair species) is definitely larger than that found for a_K in the K/DEE system. [$|a_M|$ = 0.146 G at 112°C; 0.133 G at -86°C; 0.127 G at -68°C]

Li/DEE From room temperature to about -35°C, spectra for this system displayed narrow lines (26 mG) with a large, increasing Li hfs. Then, as the temperature was lowered further, two interesting effects were observed: the Li hfs decreased quite rapidly and the outer components ($m_I = \pm 3/2$) of this splitting broadened relative to the inner components ($m_I = \pm 1/2$). By about -80°C the $\pm$ 3/2 components were broadened beyond detection, and by -100°C only narrow (28 mG) "normal" lines for proton splittings were observed [Fig. 3.4]. An additional single line spectrum was superimposed on the ion pair spectra. This was due to the free ion (see discussion) and grew in intensity relative to the ion pair spectrum as the temperature was decreased or the sample diluted at constant temperature. The free ion spectrum had a slightly higher g value ($\Delta g \simeq 6\text{-}9 \times 10^{-6}$), at lower temperatures at least. All effects are reversible and reproducible. This

FIGURE 3.4 (ctd)

b) Scan range 1G/40cm. Centre lines only.

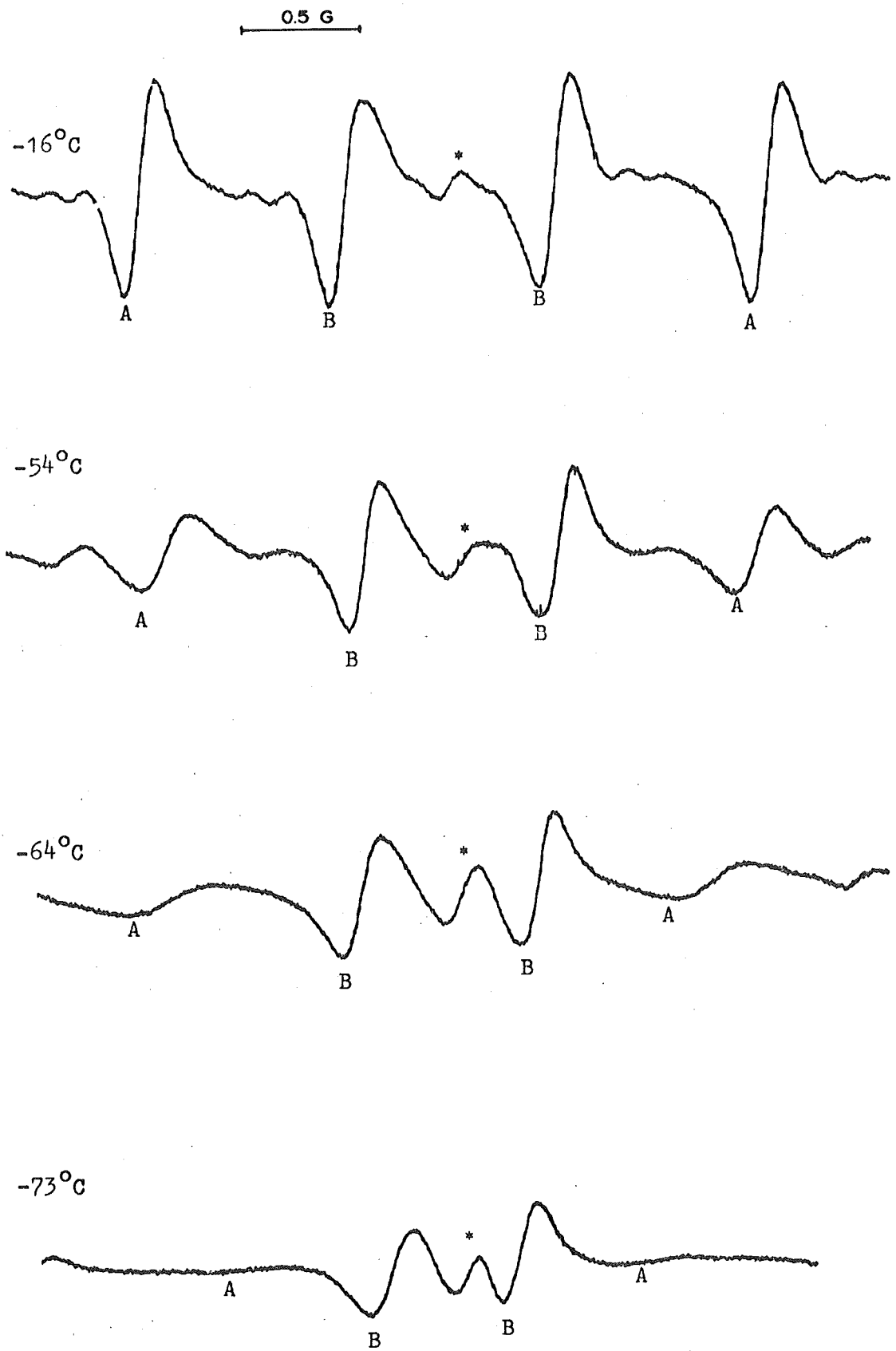

A: ± 3/2 components of lithium hyperfine splitting

B: ± 1/2 components of lithium hyperfine splitting

system was analysed in terms of two rapidly interconverting ion pairs (below -30°C) and a free ion. The computer simulations were necessarily performed using one set of coupling constants for the total ion pair spectrum and another set for the free ion.

Cs/DEE Six attempts were made to reduce pyrene in this system, but no reaction was observed. Hirota[46] has noted that anthracene does not react with cesium in this solvent.

3B. Discussion

3B.1: Second order shifts

Second order corrections always result in a downfield shift,[82] given by:

$$\Delta B = -(a^2/2B_o)[I(I+1) - m^2] \qquad (3.1)$$

where B_o is the external magnetic field,

a is the hyperfine splitting,

I is the nuclear spin (for n equivalent nuclei of spin I, $J = \sum_n I_n$ replaces I in Eqn. 3.1)

and m is the z component of I. Since most aromatic hydrocarbons have coupling constants which are less than 5G, the resultant second order shifts (only a few milligauss) are usually masked by the linewidths and therefore disregarded. In molecules with larger splittings these shifts can provide useful structural information - for example, Gooijer and Maclean[83] recently deduced the structure of the potassium pyrazine ion pair from asymmetries in the potassium hyperfine splitting induced by second order shifts (here a_N = 7.15 G and maximum shift was 48 mG.)

For pyrene, the downfield second order shifts for the components of the centre line (M_J = 0), using B_o = 3250 G and the

largest coupling constant a_β = 4.85 G, are: 0.0213 G, (J=2, M_J=0), 0.0072G (J=1, M_J=0) and 0.0 G (J=0, M_J=0). These components are of relative intensity 1:3:2 respectively.[82] When shifts are not resolved, an averaging procedure is often used to calculate the total shift for the degenerate lines.[60] With the three sets of ccupling constants, this gives shifts for the centre line of 7.2 mG (β), 1.4 mG (α) and 0.15 mG (γ). The total second order shift is then 8.6 mG. Since the observed linewidths were only $\sim$25 - 30 mG, the observed asymmetry can clearly arise from second order effects. These calculations also show that most of the shift arises from the β coupling constant, and justifies neglecting the contributions from the α and γ coupling constants in the computer simulated spectra.

Second order shifts probably explain the observed asymmetry of the sodium splitting pattern in the Na/MTHF system, for small values of a_{Na}. According to Gooijer and Maclean,[83] asymmetry may be expected when the cation hfs is less than twice the maximum second order shift, as observed here.

3B.2: Line broadening

There is no evidence to indicate any linewidth alternation in these systems although it was the likely prospect of observing this effect[61] that originally prompted this study (Chapter 1.) When line broadening did occur (apart from the Li/DEE case), it was the same for all lines. The increased linewidth noted occasionally at low temperature was probably due to the increased viscosity of the solvent, rather than any changes in actual ion pair structure. This causes the correlation time of species in solution to increase and anisotropic interactions, which are usually averaged to zero by rapid rotation, may contribute to

the linewidth.* However, the increased linewidth often noted at higher temperatures may well reflect a change in structure. Aten et al.[84] concluded from electron transfer studies, that ion pair formation is favoured by increasing temperature and increasing cation radius, and this trend has been reported in many studies.[19] The observed line broadening may be due to unresolved metal splittings resulting from ion pair formation. Jones[85] has studied the shape of such lines in much detail and found them to be broader in the wings than a single pure Lorenztian line. No attempt to perform such an analysis was attempted in this work and therefore ion pair formation as the source of the broadening is only speculative.

Where two species are observed simultaneously, the linewidth sets lower limits[1] on the lifetime, τ, of each entity: for widths of 25 - 30 mG, $\tau > \sim 2 \times 10^{-6}$ sec. A given species with sharp lines may itself be experiencing very rapid processes, such as the vibration of a cation.

3B.3: Free ion - ion pair equilibria.

For the K/MTHF, Cs/THF and Li/DEE systems, two species were observed simultaneously. Whenever this happens it is important

---

* According to Ayscough,[1] an estimate of correlation time can be found from

$$\tau_c = \frac{4\pi\eta a^3}{3kT}$$

where η is the viscosity, a is the radius of a tumbling sphere and k is Boltzmann's constant. Then, if $\delta\omega$ is the contribution from anisotropic hyperfine interactions, the linewidth from this source is

$$\frac{1}{T_2} = \tau_c . \delta\omega^2$$

Hence increased viscosity will increase the linewidth.

to establish the identity of the species involved. The usual problem is to distinguish between loose ion pairs and free ions. The presence of metal splitting in one spectrum indicates that an ion pair is certainly one of the species. However, the absence of metal coupling in the other spectrum does not prove it arises from the free ions; for example, the metal coupling may be too weak to resolve or it could be averaged to zero by rapid cation exchange processes. One potential way of solving this difficulty is to apply the law of mass action. For a free ion (FI) - ion pair (IP) equilibrium

$$IP \rightleftharpoons FI^- + M^+ \qquad (3.2)$$

the dissociation constant is given by

$$K_d = \frac{[FI^-]\,[M^+]}{[IP]} = \frac{\alpha^2 c}{1-\alpha} \qquad (3.3)$$

where α is the degree of dissociation, c is the total concentration and activity coefficients are assumed to be unity. Hence the free ion is favoured by dilution. On the other hand, an ion pair-ion pair equilibrium

$$IP_1 \rightleftharpoons IP_2 \qquad (3.4)$$

leads to an equilibrium constant given by

$$K = \frac{[IP_2]}{[IP_1]} \qquad (3.5)$$

which is independent of concentration.* The dilution experiments [Part A] prove that a dissociation - association process is taking place [eqn 3.3]. Since one of the species is an ion pair, the other must be the free ion.

The thermodynamic quantities characterising this dissociation process were found by calculating the equilibrium constant at a number of temperatures. Using Atherton and Weissman's notation,[18] a particularly useful form for the equilibrium constant is, from

---

* In the limit of infinite dilution.

Table 3.2: Experimental Dissociation Constants.

PY/K/MTHF	Temperature (K)	K_D (mol l^{-1})	Sample [a]
	260	1.91×10^{-8}	1
	251	5.18×10^{-8}	1
	249	3.97×10^{-8}	2
	238	7.83×10^{-8}	2
	232	2.06×10^{-7}	2
	230	2.21×10^{-7}	2
	218	3.40×10^{-7}	2
	215	4.18×10^{-7}	1
	213	5.07×10^{-7}	2
	206	7.18×10^{-7}	1
	202	7.40×10^{-7}	2
	192	1.52×10^{-6}	2
	185	2.18×10^{-6}	2

PY/Cs/THF	Temperature (K)	K_D mol l^{-1}
	290	1.8×10^{-6}
	265	2.0×10^{-6}
	250	2.28×10^{-6}
	237	3.91×10^{-6}
	228	6.37×10^{-6}
	214	8.41×10^{-6}
	208	1.27×10^{-5}
	185	2.44×10^{-5}

PY/Li/DEE	Temperature (K)	K_D (TIP) mol l^{-1}	K_D (LIP) mol l^{-1}
	291	1.67×10^{-7}	
	283	1.44×10^{-7}	
	268	2.07×10^{-7}	
	255	2.44×10^{-7}	
	247	3.26×10^{-7}	
	236	9.09×10^{-7}	
	232	1.77×10^{-6}	2.56×10^{-5}
	220	2.54×10^{-6}	1.34×10^{-5}
	207	8.95×10^{-6}	1.42×10^{-5}
	196	2.06×10^{-5}	1.05×10^{-5}

3.2 and 3.3:

$$K_D = \frac{C}{\Gamma^2 + \Gamma} \qquad (3.6)$$

where C is the total anion concentration (i.e. [IP] + [FI]) and Γ is the ratio of the concentrations of the two species ($\frac{[IP]}{[FI]}$). Γ was obtained directly from the computed spectra* and C was measured by absorption spectroscopy [Chapter 2].

This method of determining the concentration assumes:

1) that all the radical anions present in the esr sample tube reverted to pyrene once the tube was opened; this is reasonable since the characteristic colour of the anions disappeared immediately and, after removal of the solvent, a yellow-white solid (colour of pyrene) remained.

2) that no neutral or dianion pyrene was present during the esr experiment. The narrow linewidths preclude the presence of unreacted pyrene. Dianion formation can be neglected since the pyrene anion has a very low electron affinity[11,35] and shows little tendency to disproportionate.[11,35]

3) that the concentration remained constant throughout the esr experiment. When temperatures already recorded were rechecked, this was found to be true.

The values of K found by this analysis are presented in Table 3.2. From the relationships

$$\Delta G = \Delta H - T\Delta S = - RT \ln K \qquad (3.7)$$

a plot of log K vs 1/T [Fig 3.5] yields the enthalpy and entropy

---

* For the Li/DEE system, Γ = [all ion pairs]/[FI] was obtained from spectral simulations. This relates to the apparent equilibrium:

$$\text{all ion pairs} \rightleftharpoons[K_{app}] \text{free ions.}$$

K_{app} is required to calculate the dissociation constants of the individual ion pairs. (Eqn 3.15, page 37).

FIGURE 3.5

PLOTS OF LOGK vs $\frac{1}{T}$ FOR THE DISSOCIATION OF PYRENE ION PAIRS

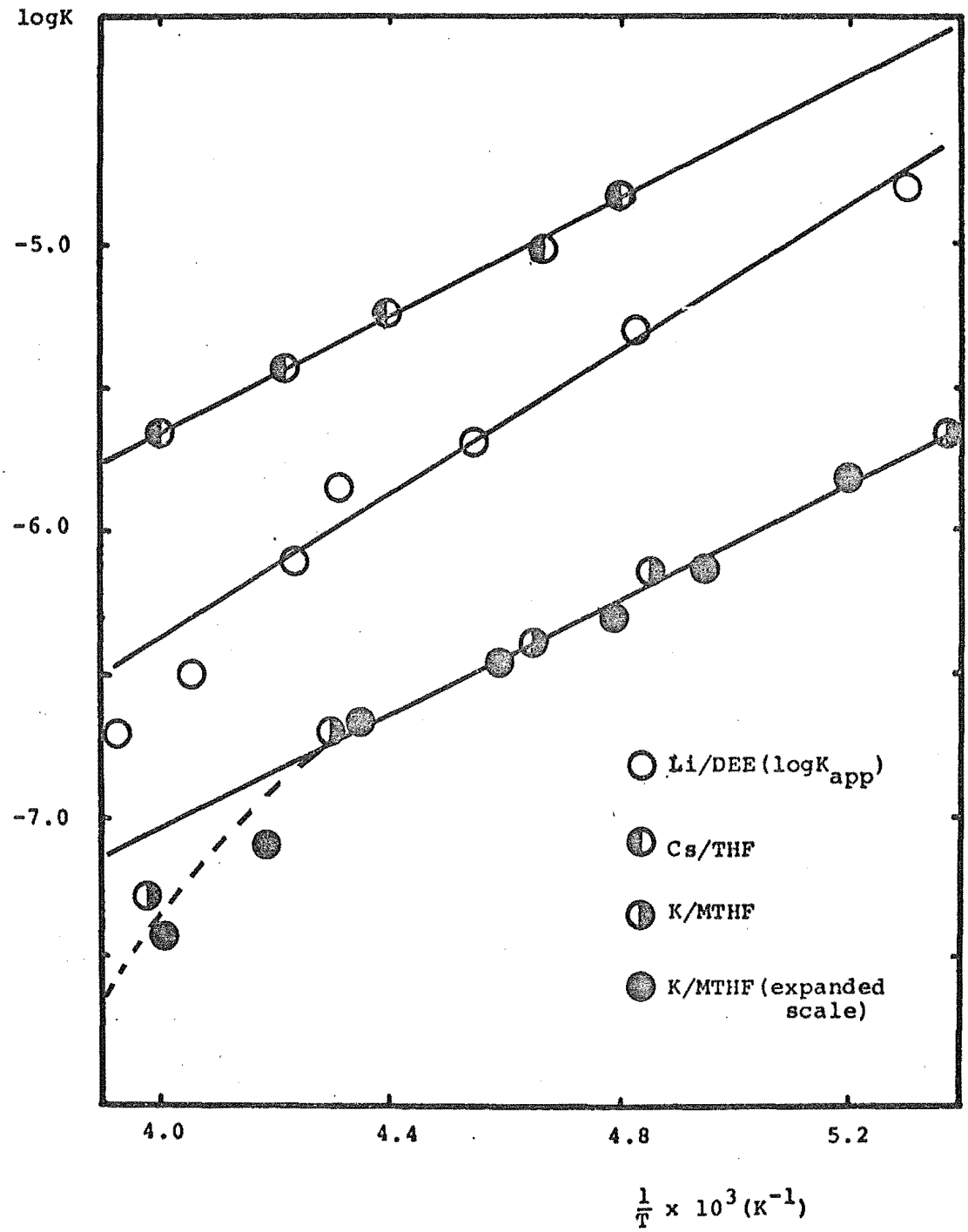

of dissociation, as listed in Table 3.3.

Table 3.3 Thermodynamic data for dissociation of ion pairs to free ions.

System		ΔH_D^o / kJ mol^{-1}	ΔS_D^o / J K^{-1} mol^{-1}
K/MTHF		-19.3	-210
Cs/THF		-16.7	-176
Li/DEE	(app)	-29.7	-243
	(TIP)	-28.0	-230
	(LIP)	+5.0	-67

ΔH_D^o $\pm$ 2.0 kJ mol^{-1}; ΔS_D^o $\pm$ 10 J K^{-1} mol^{-1}

3B.4: The Li/DEE system

The variations in linewidth observed for the Li/DEE system (Fig 3.4) were analysed in terms of an equilibrium between two distinct ion pairs:

$$IP_{tight} \underset{k_{-1}}{\overset{K}{\rightleftharpoons}} IP_{loose} \qquad (3.8)$$

The interconversion rate has to be rapid enough to average the cation hfs but not fast enough to produce exchange-narrowed lines. This region is often called the "limit of rapid exchange."[45]

Hirota has discussed such a model in detail[45] and shown that the equilibrium constant is given by

$$K = \frac{a_{TIP} - a_{obs}}{a_{obs} - a_{LIP}} \qquad (3.9)$$

FIGURE 3.6

TEMPERATURE DEPENDENCE OF LITHIUM HYPERFINE SPLITTING

SYSTEM : PY/Li/DEE

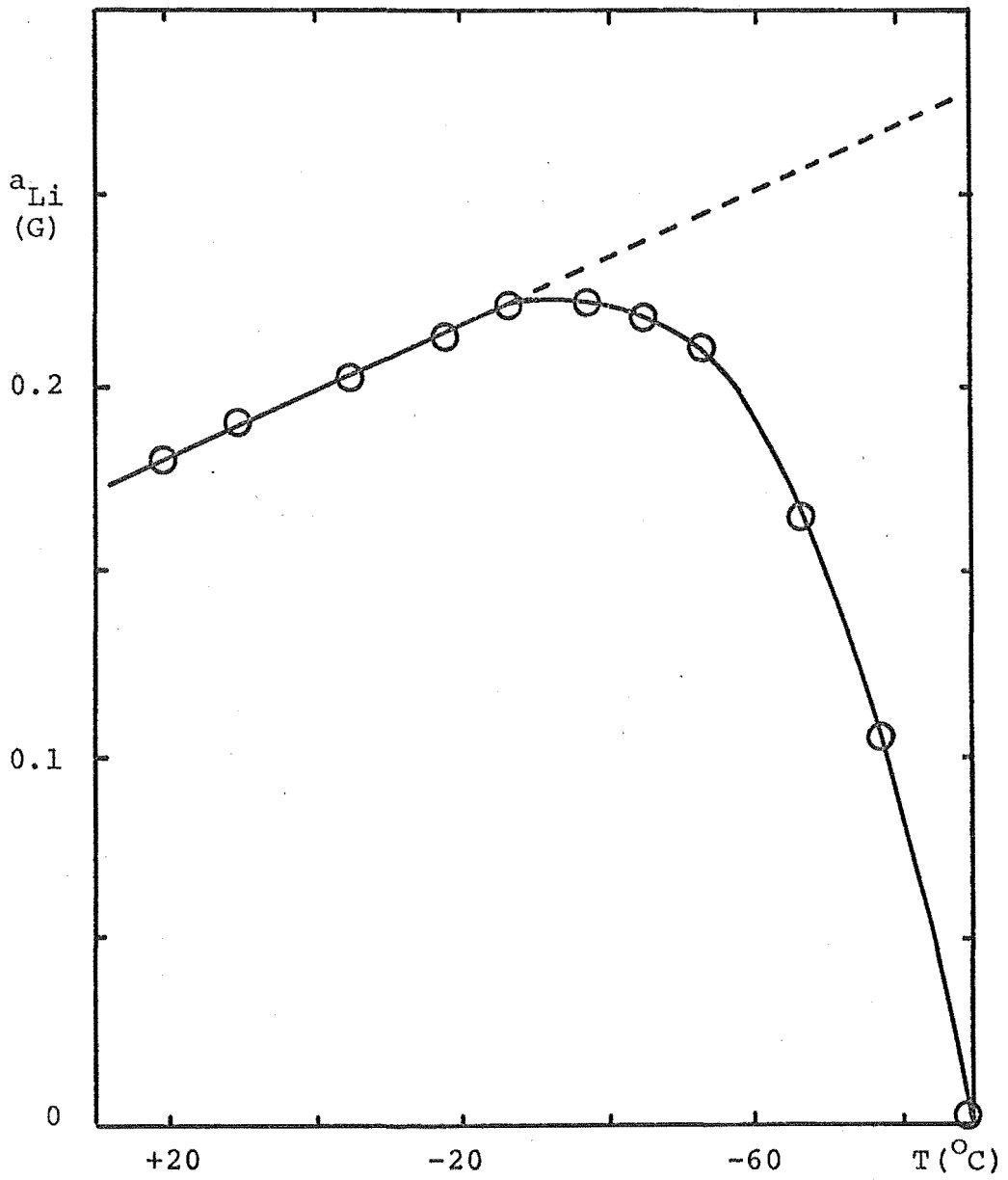

where a_{TIP} and a_{LIP} are the cation hfs for the tight and loose ion pairs respectively; a_{obs} is the observed cation coupling constant. In a number of systems, Hirota found that an "s-shaped" curve resulted from plotting a_M vs T. He usually assumed a_{TIP} to be the plateau value of a_M on such a graph and a_{LIP} to be zero. The validity of these assumptions is important for they are the basis of his thermodynamic calculations. Szwarc has criticised this approach,[48] pointing out that the assumption of temperature independent a_{TIP} and a_{LIP} values is at best doubtful since it implies that the ion pairs have the same structure throughout a whole temperature range. If either or both of these splittings are temperature dependent, then the magnitude of the calculated equilibrium constants would be modified which strongly influences the derived ΔH and ΔS values. Hirota's method, however, often gives good straight lines for log K vs 1/T plots and he has claimed his ΔH and ΔS values are within 15% for sodium naphthalide salts.[47]

The $|a_{Li}|$ v. T graph for the Li/DEE system is shown in Fig. 3.6. For the calculation of the equilibrium constant, values of a_{TIP} and a_{LIP} at each temperature were estimated on the following basis:

1) For the initial portion of the graph (T = 30°C to ~-30°C) $a_{TIP} = a_{obs}$ - i.e. the solution is regarded as being 100% tight ion pairs at these temperatures;

2) The rest of the graph results from the rapid interconversion of the two ion pairs (eqn 3.8); this equilibrium is changing so that the relative concentration of loose ion pairs increases as the temperature is lowered. The line broadening was first observed at ~-30°C;

Table 3.4: Thermodynamic and kinetic data for the interconversion of tight and loose ion pairs in the PY/Li/DEE system.

Temperature (°C)	K [a]	p_{TIP}	k_1 [b] / s^{-1} x 10^{-6}	k_{-1} [b] / s^{-1} x 10^{-6}
-34	0.044	0.97		
-40	0.060	0.94		
-45	0.098	0.91	3.02	30.9
-50	0.14	0.88	2.76 [c]	19.5 [c]
-54	0.20	0.83	2.81	14.0
-60	0.37	0.73	2.80 [c]	7.58 [c]
-64	0.51	0.65	2.71	5.33
-70	0.87	0.54		
-73	1.1	0.48	2.67	2.91
-80	2.2	0.31		

ΔH^o / kJ mol^{-1}	ΔS^o / J K^{-1} mol^{-1}	$\Delta H_1^{\ddagger}$ / kJ mol^{-1}	$\Delta S_1^{\ddagger}$ / J K^{-1} mol^{-1}	$\Delta H_{-1}^{\ddagger}$ / kJ mol^{-1}	$\Delta S_{-1}^{\ddagger}$ / J K^{-1} mol^{-1}
-34.3 ± 1.0	-172 ± 5	-1.5 ± 2.0	-113 ± 10	+36.4 ± 2.0	+ 60 ± 10

a) ± 5% b) ± 20% c) values found from interpolation of linewidth data.

3) $a_{LIP} = 0$ at all temperatures. Any deviation from zero is probably very small since no Li hfs was observed in any other solvent where loose ion pairs might be expected (the only exception is a very minor component in MTHF) and the plot approaches zero very quickly.

4) Below $\sim -30^{\circ}C$, the value of a_{TIP} can be found by extrapolation, assuming a_{TIP} continues to vary linearly with temperature (see graph). Linear temperature dependence is displayed by nearly all the cation splittings in the pyrene systems studied here and has been found in many other systems.[19] A similar type of extrapolation was applied by de Boer to the metal splitting in an nmr study of the cesium biphenyl ion pair in diglyme.[86]

From this model, K was calculated using eqn 3.9 and ΔH° and ΔS° found by plotting log K vs 1/T [Table 3.4 and Fig 3.7].

Selective broadening of the type observed here results from an in-phase modulation of the metal splitting.[44,87,88] When this modulation is due to an equilibrium between structurally different ion pairs, then the rate of this interconversion, in the limit of rapid exchange, is given by[47]

$$k_1 = 2.03 \times 10^7 \cdot p_{LIP}^2 \cdot p_{TIP}^2 \cdot (1+K) \frac{\Delta B^2_{\pm 3/2} - \Delta B^2_{\pm 1/2}}{\delta_{\pm 3/2} - \delta_{\pm 1/2}} \quad s^{-1} \qquad (3.10)$$

where: p_{LIP} is the fraction of loose ion pairs; p_{TIP} the fraction of tight ion pairs:

$\Delta B_{\pm 3/2(\pm 1/2)}$ is the field difference in the $\pm 3/2(\pm 1/2)$ components of the two ion pairs; and

$\delta_{\pm 3/2(\pm 1/2)}$ is the contribution to the width of the $\pm 3/2(\pm 1/2)$ hyperfine lines that is due to the interconversion process.

FIGURE 3.7

PLOTS OF LOGK AND LOGk vs $\frac{1}{T}$ FOR THE INTERCONVERSION OF TIGHT AND LOOSE ION PAIRS

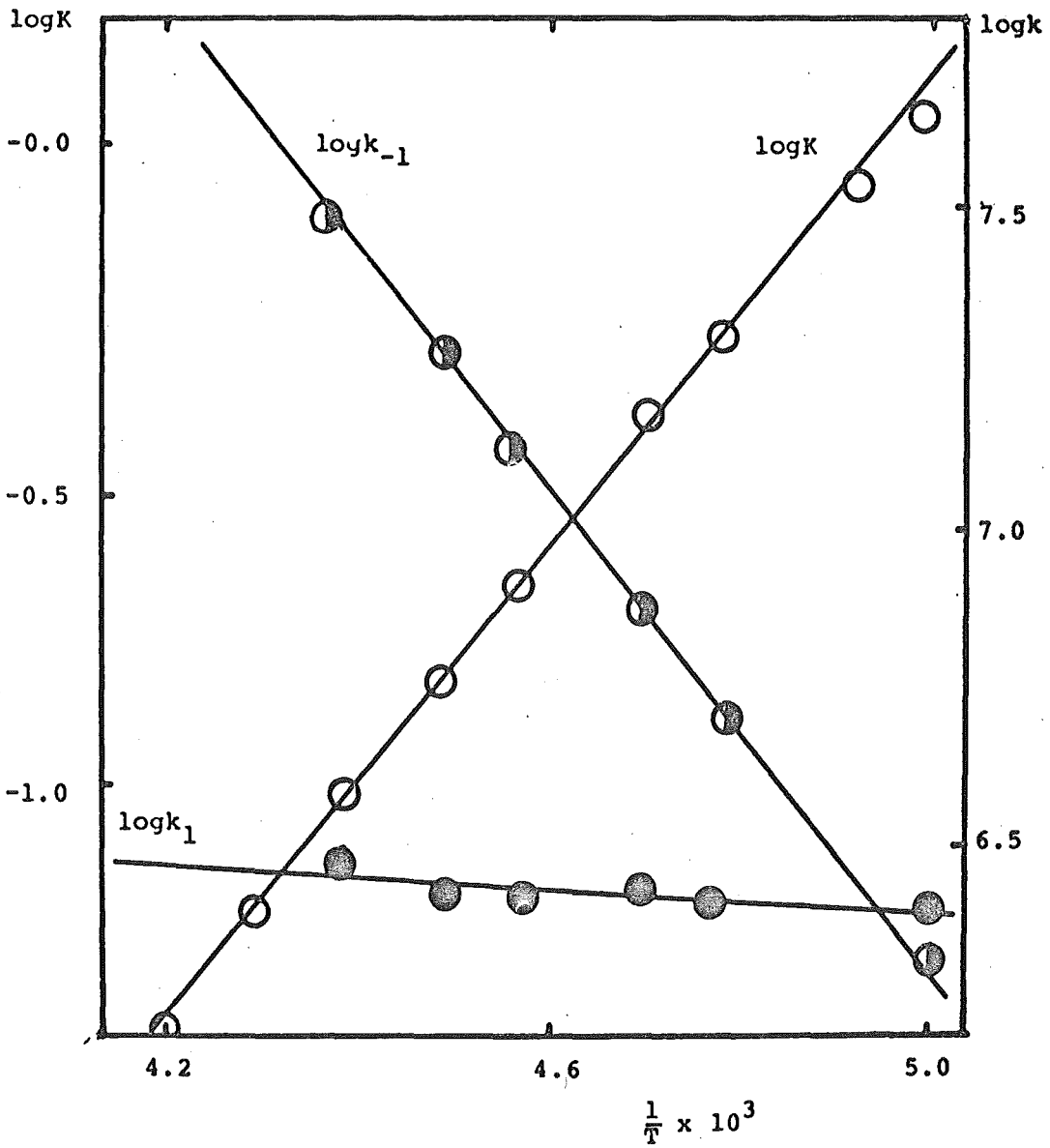

Since

$$K = \frac{p_{LIP}}{p_{TIP}} = \frac{k_1}{k_{-1}} = \frac{a_{TIP} - a_{obs}}{a_{obs} \quad a_{LIP}} \qquad (3.11)$$

and

$$p_{TIP} = \frac{a_{obs}}{a_{TIP}} = 1 - p_{LIP} \qquad (3.12)$$

all the variables in eqn 3.10 may be calculated or directly measured and k_1 can be determined for each temperature. From eqn 3.11, k_{-1} may also be found [Table 3.4]. From the theory of absolute reaction rates, the rate constant is given by:

$$k = \frac{kT}{h} \quad \exp \quad (-\Delta G^{\ddagger}/RT) \qquad (3.13)$$

where k is the Boltzmann constant, h is Planck's constant, R is the gas constant and $\Delta G^{\ddagger}$ is the free energy of activation. Using eqns 3.13 and 3.7, plots of log k_1 and log k_{-1} vs 1/T provide the enthalpy ($\Delta H^{\ddagger}$) and entropy ($\Delta S^{\ddagger}$) of activation for the forward and reverse reactions. These are included in Figure 3.7 and Table 3.4. Since the free ion is also observed, the total system may be represented as:

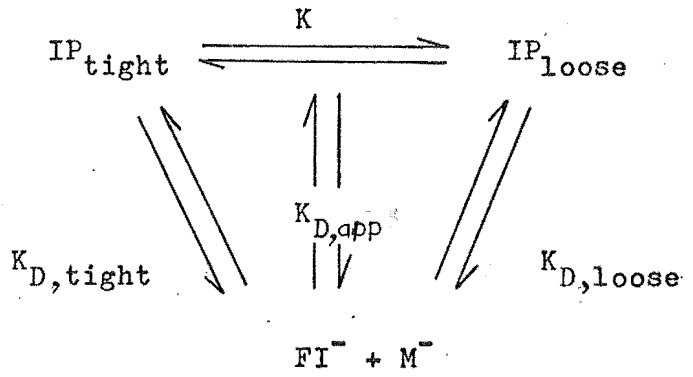

(3.14)

The dissociation constant for the tight and loose ion pairs can now be determined at each temperature, using:*

$$K_{D,app} = \frac{K_{D,TIP}}{1 + K} = \frac{K_{D,LIP}}{1 + K} \cdot K \qquad (3.15)$$

Log K vs 1/T plots allow the appropriate enthalpy and energy terms to be calculated [Table 3.3]. Thus, the thermodynamic parameters for all the processes in 3.14 have been determined from the esr spectra alone.

3B.5: Interpretation of Thermodynamic Quantities

a) Ion-pair - free ion equilibria

Negative ΔH^{o} and large negative ΔS^{o} values are characteristic of these equilibria** The entropy term arises from two main effects:

1) loss of freedom in the solvent: a partial ordering of solvent molecules results from the increased solvation of the cation in the dissociated state;

2) loss of vibrational entropy of the ion pair: since the cation of an ion pair is in a potential energy well (Chapter 1.2), it has a large number of close-lying vibrational states available to it which are lost on dissociation.

---

* By definition, $K_{D,tight} = \frac{[FI^-][M^+]}{[IP_{tight}]}$ and

$K_{D,loose} = \frac{[FI^-][M^+]}{[IP_{loose}]}$

From $K_{D,app} = \frac{[FI^-][M^+]}{[IP_{tight}]+[IP_{loose}]} = \frac{[FI^-][M^+]}{[IP_{tight}](1+K)}$

$$= \frac{[FI^-][M^+]}{[IP_{loose}](1+\frac{1}{K})}$$

** Aromatic radical anions are considered to be only very weakly solvated in these solvents.[36]

Both effects cause a negative entropy contribution and combine to give the unusually high negative ΔS° values for the dissociation of an ion pair. There is a positive entropy term which arises because a single entity (the ion pair) dissociates to form two species (the free ions) but its contribution is small.

The enthalpy change can be divided into two important terms:

$$\Delta H^{\circ} = \Delta H^{\circ}_{\text{ion-ion}} + \Delta H^{\circ}_{\text{ion-solvent}}$$

($\Delta H^{\circ}_{\text{solvent-solvent}}$ is considered to be much less important and is neglected). For a dissociation process, $\Delta H^{\circ}_{\text{ion-ion}}$ represents the enthalpy associated with breaking the ionic bond of the ion pair, and is positive; $\Delta H^{\circ}_{\text{ion-solvent}}$ represents the heat of solvation of the created ions, and is negative.* Usually $|\Delta H^{\circ}_{\text{ion-solvent}}| > |\Delta H^{\circ}_{\text{ion-ion}}|$ so that ΔH° is negative, in accord with most observations. If $|\Delta H^{\circ}_{\text{ion-solvent}}|$ is small, $|\Delta H^{\circ}_{\text{ion-ion}}|$ may become the larger term, resulting in a positive ΔH°. This is most likely in solvents of poor solvating power or when the change in structure on dissociation is small. Both situations apply for the dissociation of the loose ion pair of lithium in DEE: this ion pair is already significantly solvated (TIP $\rightleftharpoons$ LIP, $\Delta S^{\circ} = -172$ J K^{-1} mol^{-1}) leading to a low entropy of dissociation (-67 J K^{-1} mol^{-1}) and DEE is a relatively weak solvation agent for cations. This probably accounts for the slightly positive ΔH found for this system.

Large magnitudes of ΔH° and ΔS° imply large changes in the solvation sphere. In a number of aromatic systems, Szwarc[90,36] found $-\Delta H^{\circ} \simeq 25 - 38$ kJ mol^{-1}, $-\Delta S^{\circ} \simeq 200 - 250$ J K^{-1} mol^{-1} for

---

* Allendoerfer and Papez[89] have pointed out that since the heat of solvation is expected to be temperature dependent (D changes with temperature), a plot of log K vs 1/T should not be linear unless this effect on ΔH is itself linear with temperature or is negligible.

the dissociation of contact ion pairs, and $-\Delta H^{o} \simeq 0 - 9$ kJ mol^{-1}, $-\Delta S^{o} \simeq 80 - 125$ J K^{-1} mol^{-1} for solvent-separated ion pairs.

The data for the Li/DEE system [Table 3.3] is consistent with this classification of tight and loose ion pairs. On the basis of their ΔH^{o} and ΔS^{o} values the ion pairs of Cs/THF and K/MTHF systems are classified as tight ion pairs.

It is not easy to compare the magnitudes of the ΔH and ΔS terms because both cation and solvent are varying. Some insight into the state of solvation in the ion pair may be gained by considering the simple "sphere-in-continuum" model for describing ion pair dissociation. Using this model, Fuoss[23] calculated that the dissociation constant is given by

$$K_d = (3000/4\pi a^3 N)\exp(-e^2/aDkT) \qquad (3.16)$$

where D is the macroscopic dielectric constant, N is Avogadro's constant, e is the charge on each of the ions, T the temperature and a is the centre-to-centre distance between the two ions. From the standard thermodynamic relation

$$\Delta H_d^{o} = -R\, d(\ln K_d)/d(1/T) \qquad (3.17)$$

the enthalpy of dissociation is given by

$$\Delta H_d^{o} = (Ne^2/aD)[1 + \partial(\ln D)/\partial(\ln T)] \qquad (3.18)$$

which is the same expression Denison and Ramsey[24] arrived at from their Born cycle approach.

This model gives reasonable results when specific solvent-cation interactions are absent in both free ions and ion pairs. Smid[40] found close agreement between calculated and experimental K_d values for the fluorenyl/Cs/THF system using an interionic distance of 3.76 Å at all temperatures. On substituting this distance into eqn 3.18, he found excellent agreement between calculated and observed ΔH values. He considered that any specific solvation between the Cs^{+} ion and the THF molecules must be

Table 3.5: Calculated values using sphere-in-continuum model.

	Best-fit values				
	Temperature (K)	$a^{a)}(K_d)$ (Å)	$a^{b)}(\Delta H^o)$ (Å)	$\Delta H^{o\,c)}$ using a = 5.0Å kJ mol^{-1}	
PY/Cs/THF	185	6.5	1.03	-3.5	
	208	6.0	1.18	-3.9	
	214	6.0-5.5	1.21	-4.0	
	228	5.5	1.30	-4.4	
	237	5.5	1.37	-4.6	
	250	5.0	1.45	-4.9	
	265	5.0	1.55	-5.2	
				-16.7	ΔH^o_{obs}
PY/K/MTHF	206	5.5	0.95	-3.6	
	215	5.5	1.01	-3.8	
	232	5.0	1.09	-4.2	
	251	4.5	1.19	-4.6	
	260	4.5	1.24	-4.7	
				-19.3	ΔH^o_{obs}

a) interionic distance which gives best agreement between calculated and experimental K_d values: a varied by 0.5Å

b) interionic distance found by using experimental ΔH^o value.

c) calculated ΔH^o values using interionic distances which give best K_d.

small, a conclusion arrived at independently by Szwarc[91] who found the Stokes radius of Cs^+ in THF ($\sim$2.4Å) to be only slightly larger than the radius of the "bare" Cs^+ ion ($\sim$1.9Å).

Applying this model to the PY/Cs/THF system, the interionic distances which give the best agreement between calculated and observed K_d values are shown in Table 3.5, and are of a reasonable order of magnitude. Since the "height" of aromatic molecules like pyrene is 2.0 - 2.5 Å,[31,36] these distances (5.5 - 6.5Å) indicate the Cs^+ ion in the pair is considerably solvated, contrary to both the conclusion reached earlier that the ion pairs are tight and to the work of Smid[40] and Szwarc.[91] Substituting these values into eqn 3.18 yields ΔH values which are very different from that observed, showing that the model is inadequate for the PY/Cs/THF system.

The sphere-in-continuum treatment, in neglecting specific solvent-cation interactions, considers the solvation enthalpy to arise only from the difference in electrostatic potential energy of an ion pair as compared to that of the free ion in a continuum of dielectric constant D. The increased exothermicity observed is due to the increased extent of cation solvation ($\Delta H^o_{ion\text{-}solvent}$) in the dissociated state. This increased solvation has an opposite effect on the two energy terms, ΔH and $-T\Delta S$: ΔH becomes more negative and $-T\Delta S$ more positive. Because of this strong compensation effect, and the relation $-RT \ln K = \Delta H - T\Delta S$, the sphere-in-continuum model can appear to calculate reasonable dissociation constants when it is, in fact, an inadequate description of a given system.

Similar considerations apply to the PY/K/MTHF system [Table 3.5]: the calculated enthalpy of dissociation is again in poor agreement with that observed (again the K_d values are

reasonable), indicating significant changes in the extent of solvation on dissociation of this ion pair also.

The best description of these systems still requires the formation of tight ion pairs so that the extent of cation solvation can increase significantly on dissociation and account for the observed enthalpy and entropy changes. The fluorenyl/Cs/THF system also required tight ion pairs ($a = 3.76\text{Å}$); the difference between the fluorenyl and pyrene systems is in the degree of solvation of the Cs^+ ion in the ion pair, the former being more like the free ion and hence probably further from the anion. This may indicate an interionic distance of ~ 3.6 Å for the Cs^+PY^- ion pair.

b) Tight ion pair - loose ion pair equilibrium:

The Li/DEE system

For the same reasons that apply to the dissociation of ion pairs, the conversion of a tight to a loose ion pair is an exothermic process. Since it also involves freezing solvent molecules around the cation, it has a negative entropy change. The large magnitude of both terms clearly indicates that the loose ion pair is a much more solvated species than the tight ion pair.

The separation of kinetic data into enthalpy and entropy of activation terms usually provides some insight into the rate process being considered. Thus from the $\Delta S_1^{\neq}$ values it appears that a significant amount of solvation takes place in going from the tight ion pair to the activated complex. The slightly positive $\Delta H_1^{\neq}$ indicates that the rate of the forward reaction is almost temperature independent while $\Delta H_{-1}^{\neq}$ shows that the reverse reaction is considerably slower at lower temperatures. Put another way, the lifetime of the tight ion pair (τ_{TIP}) is

approximately independent of temperature while τ_{LIP} is very sensitive to temperature. The activation energy for the conversion of tight to loose ion pairs is disturbingly low. Sometimes enthalpy and entropy diagrams are drawn to describe the interconversion process,[45,91] but this approach can be misleading.

Considerable care is needed in considering these $\Delta H^{\ddagger}$ and $\Delta S^{\ddagger}$ terms, because they are obtained over a range of temperatures. The true enthalpy and entropy of activation, as found from the theory of absolute reaction rates using equation 3.13, describe the rate characteristics of a particular process, A⇌B, where A and B are well defined, unchanging systems and the reaction proceeds via a transition state or activated complex. The real situation in liquids is often more complicated since a change in temperature often influences more than just the rate process itself. For instance, in this Li/DEE system, the structure of tight ion pair is changing with temperature, as indicated by the temperature dependence of its lithium coupling constant. If this change (or any other temperature-dependent change) is in any way connected to the rate of the interconversion process, then $\Delta H^{\ddagger}$ and $\Delta S^{\ddagger}$ include these contributions and no longer characterize just the rate process itself. Furthermore, any changes which accelerate the rate at lower temperatures can readily explain an apparently very small (or negative) activation energy such as that observed here ($\Delta H_1^{\ddagger} \simeq -1.5$ kJ mol^{-1}).

For these reasons, it seems preferable to consider the rate constants at particular temperatures. This is conveniently done by considering $\Delta G^{\ddagger}$, the free energy of activation at temperature T, which is related to the rate constant by eqn 3.13. Using the parameters in Table 3.4, ΔG° and $\Delta G^{\ddagger}$ terms for the interconversion process have been calculated at a number of temperatures and are

FIGURE 3.8

FREE ENERGY DIAGRAMS FOR THE INTERCONVERSION OF TIGHT AND LOOSE ION PAIRS AND THE DISSOCIATION OF THE ION PAIRS

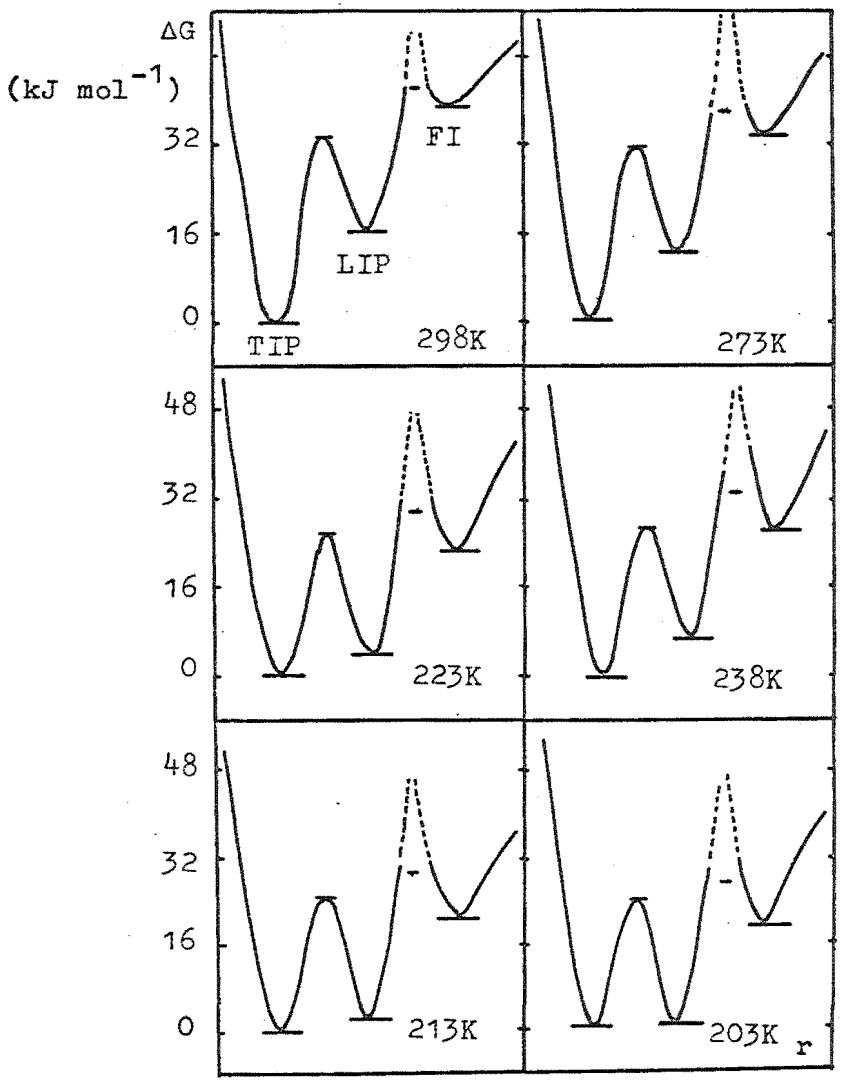

Table 3.6: Exchange regions for the PY/Li/DEE system

Temperature °C	$\tau \times 10^{+7}$ [a] s	$[\lvert\gamma\rvert\lvert\Delta a\rvert]^{-1}$ [b] s	p_{TIP}	Exchange region [c]
-34	0.097	2.5×10^{-7}	0.97	fast
-54	0.60	2.4×10^{-7}	0.83	fast
-73	1.8	2.2×10^{-7}	0.48	fast-intermediate
-87 [d]	3.8	2.1×10^{-7}	0.07	intermediate-slow

a) $\tau = \dfrac{\tau_{TIP}\ \tau_{LIP}}{\tau_{TIP} + \tau_{LIP}}$; b) $\Delta a = a_{TIP} - a_{LIP}$;

c) Conditions for exchange: $\tau^2 < [\gamma_e^2 < (\Delta a)^2 >]^{-1}$ and $\tau > [\lvert\gamma_e\rvert\lvert\Delta a\rvert]^{-1}$ for fast and slow motion respectively.[93]

represented in Fig 3.8. Also included is an estimate of the minimum free energy of activation for the association of the free ions into an ion pair. This energy barrier corresponds to the reverse process in the equilibrium

$$\text{all ion pairs} \underset{k'_{-1}}{\overset{k'_1}{\rightleftharpoons}} \text{free ions} \qquad (3.19)$$

where $K_{D,app} = k'_1/k'_{-1}$ is already known. In the absence of interconversion, the "ion pair" of the above equilibrium shows narrow lines ($\sim$30 mG); this places a lower limit on the lifetime of the "ion pair" and hence an upper limit on k'_1 (assuming the rate of dissociation is first order). An upper limit to the reverse process can then be found and from Eqn 3.13 a minimum free energy of association.

The Li/DEE system may now be examined more quantitatively. The free energy diagrams indicate that at higher temperatures the free energy barrier for the conversion of loose to tight ion pairs becomes sufficiently low for the loose ion pairs to collapse immediately, and no longer "exist" (at -34°C, p_{TIP} = 97%). This explains why only tight ion pairs and free ions are present at these temperatures. On cooling, τ_{LIP} increases and the rate enters the fast exchange limit, [Table 3.6]. As can be seen from the expression for k_1 [Eqn 3.10], the linewidth in this region is governed by a number of changing factors and not just the rate of the interconversion process. The fast exchange region exists from $\sim$-30°C to $\sim$-80°C. Below these temperatures, p_{TIP} decreases rapidly and the spectrum becomes that of the loose ion pair and the free ion [at -83°C, p_{TIP} = 22%; at -87°, p_{TIP} = 7%].

FIGURE 3.9

EXPERIMENTAL AND SIMULATED ESR SPECTRA FOR THE PY/Li/DEE SYSTEM

Simulated spectra include effects of exchange on the linewidths but not the lines due to the free ion species.

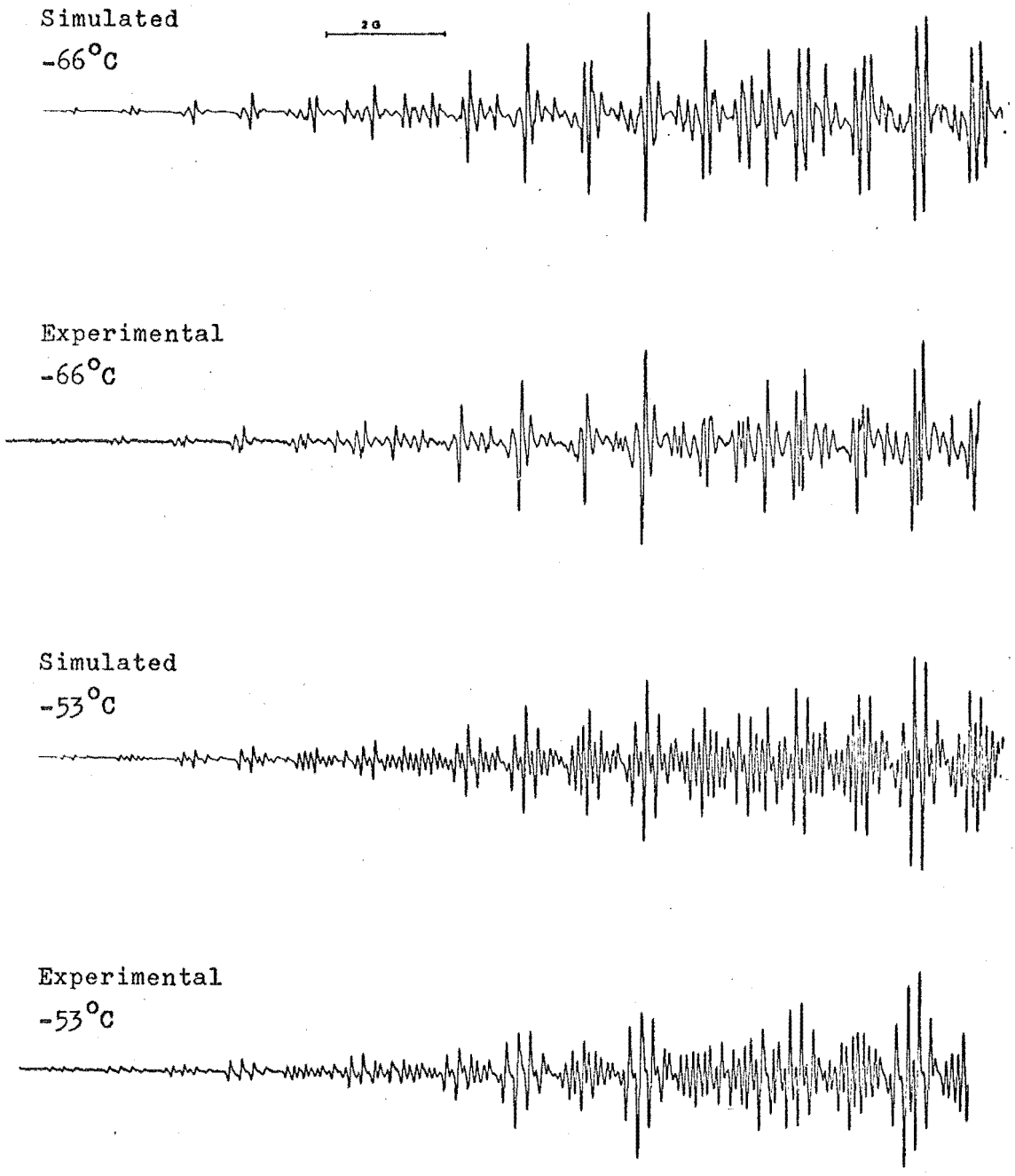

In summary, all spectra can be explained by assuming that a rapid equilibrium between tight and loose ion pairs operates between -30°C and -90°C. Beyond these temperatures the concept of equilibrium becomes meaningless because one of the species can no longer be considered to be a thermodynamic entity. At high temperatures the tight ion pair is in equilibrium with the free ion only, but probably passes through the now unstable loose ion pair configuration during the process.

Strong evidence supporting this model was obtained from spectral simulations using a program[94] which calculated the effects of exchange on the lineshapes.[95] Using the parameters k_1, k_{-1}, p_{TIP}, p_{LIP}, a_{TIP} and a_{LIP} [Tables A.1, 3.4] from the above analysis and without any alteration, excellent agreement was found between computed and experimental spectra [Fig 3.9].

3B.6: Alkali metal coupling constants and ion pair structure

The isotropic hyperfine coupling of the cation in the ion pair depends on both the spin density at the metal nucleus and the nuclear magnetic moment of that nucleus. By taking the spin density on the cation as the ratio of the observed coupling constant to that of the free atom, i.e.:

$$\rho = \frac{a_{obs}}{a_{atom}} \qquad (3.20)$$

the effect of different nuclear magnetic moments is eliminated. Fig 3.10 represents the temperature dependence of ρ in those systems where cation splittings were observed.

The magnitude, sign and temperature dependence of ρ reflect the structure of ion pairs in a sensitive way. However, the mechanisms accounting for the spin density of the cation are quite complex. Recent Configuration Interaction (CI) calcula-

FIGURE 3.10

TEMPERATURE DEPENDENCE OF CATION SPIN DENSITY
IN PYRENE ION PAIRS

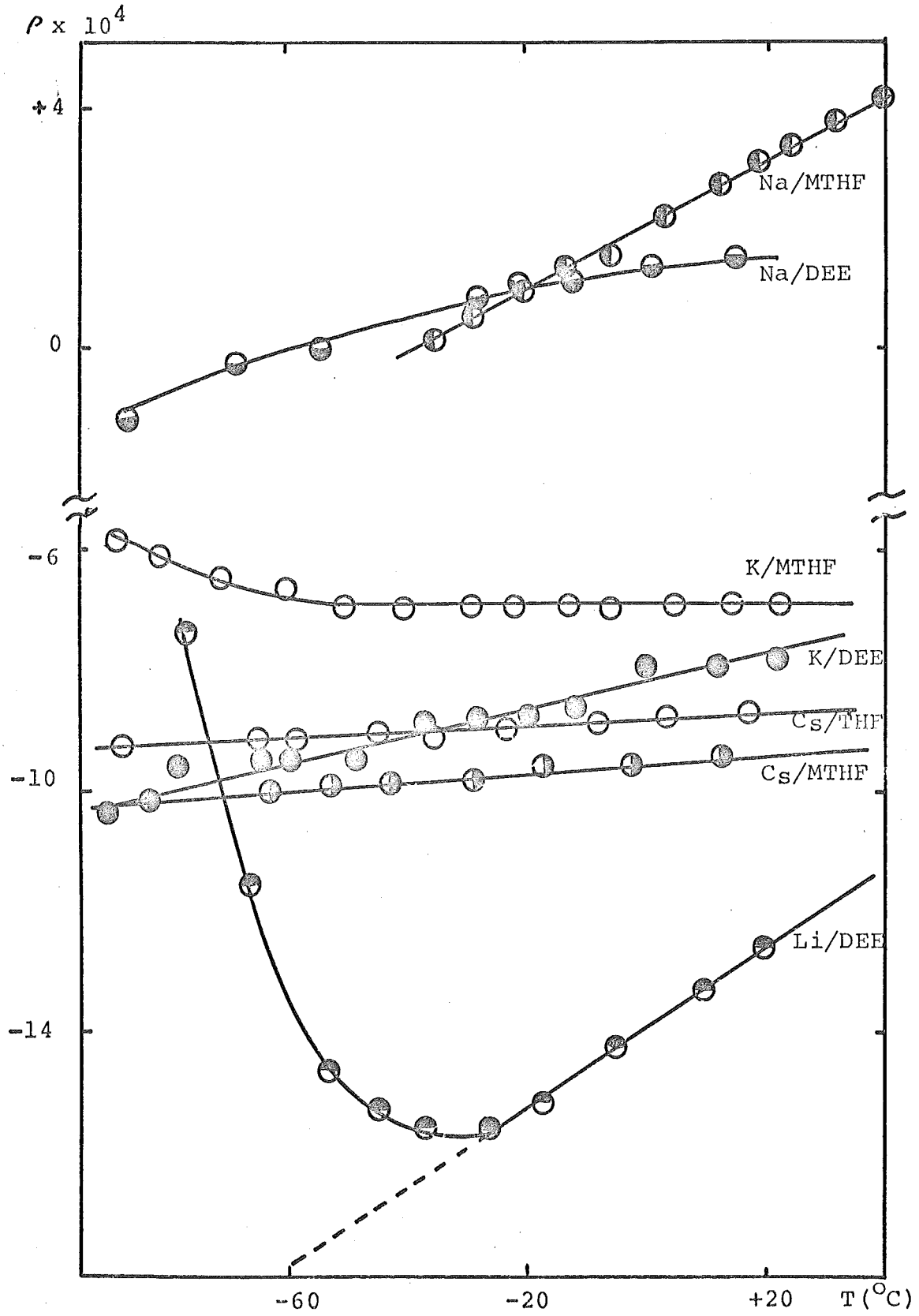

tions which incorporate electron exchange effects account satisfactorily for the occurrence of both positive and negative spin density.[30] There appear to be two main contributions to the cation spin density:

1) a zero-order, positive one (ρ_o) from the direct mixing of the valence shell metal s orbital in the unpaired electron molecular orbital (MO) [the overlap mechanism];

2) a first order negative contribution (ρ_1) arising from electron excitation from the aromatic system into the empty metal s orbital [exchange mechanism].

A third contribution, also first order, arises from excitation inside the aromatic system and can have either sign; it is usually considered to be negligible. Although both ρ_o and ρ_1 decrease with increasing interionic distance, ρ_1 becomes relatively more important at larger distances.

Since the spin density at the alkali metal nucleus is the sum of positive and negative contributions, both dependent on temperature and cation-anion position, knowing the sign of the coupling constant can be of much assistance in determining ion pair structure. Negative coupling constants are observed if ρ_o is small, as when the cation resides in a nodal plane of the aromatic anion or when the interionic distance is large. Although direct determination of the sign at present requires nmr measurements, it is often strongly indicated by the temperature dependence of the cation hfs in esr spectra. From the known experimental data, it appears that the temperature coefficient of metal hyperfine coupling constants (da_M/dt) is, in most cases, positive* so that if the magnitude of a splitting increases on

---

* Some authors[96] feel it is safe to conclude that da_M/dt is always positive.

cooling, the splitting is negative. In systems where nmr measurements have been made, this relationship has been found to be valid.[53,97,98]

On this basis, negative metal coupling constants were assigned to the systems: K/DEE, Cs/THF, Cs/MTHF, Li/DEE and Na/DEE (low temperature only). The K/MTHF system is uncertain using this critereon since a_K is 0.057 G almost throughout the temperature range. However, a further relationship often observed for esr spectra indicates this splitting is probably negative also: ρ often changes regularly with increasing size of the alkali ion.[19,49] For the MTHF systems this follows only if potassium has a negative spin density. The remaining coupling constants are taken to be positive, which is definitely so for the Na/MTHF system, where nmr measurements have been made.[53]

As well as the sign, the variation of the metal hfs with temperature often points to ion pair structure. Three models have been proposed to account for the temperature dependence:

1) Hirota's model of a dynamic equilibrium between different ion pair types[44-46] (discussed in section 3B.4)

2) Szwarc's static model which relates the metal coupling constant variation to changes in solvation and ion pair structure with temperature.[36]

3) Atherton and Weissman's vibrational model where variations are caused by thermal changes in the populations of the vibrational energy levels of the ion pair.[18]

In those pyrene systems where negative coupling constants were observed, the cation must be located near a nodal plane ($\rho_o \simeq 0$). For the highest unpaired MO of pyrene both the xy and yz plane (Fig. 3.11) are nodal.*

---

* The molecular plane (xy) is also nodal, but the cation is considered to be always above or below this plane.

FIGURE 3.11

INTERACTION ENERGY CALCULATIONS FOR PYRENE ION PAIRS

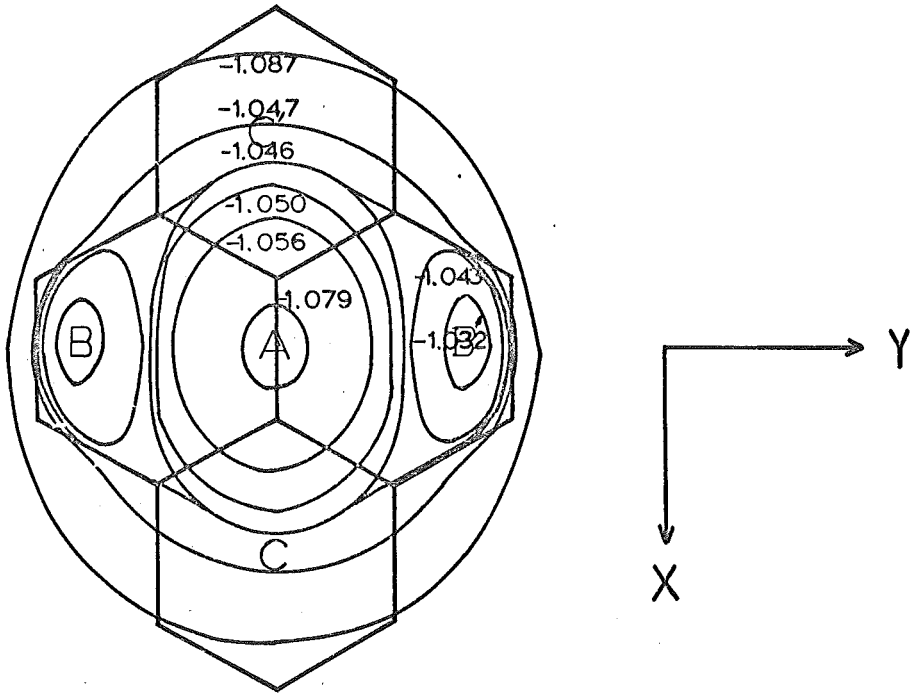

z = 0.3 nm

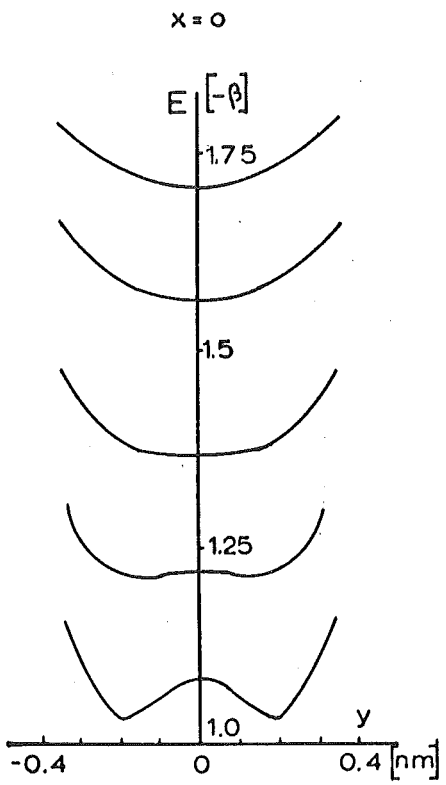

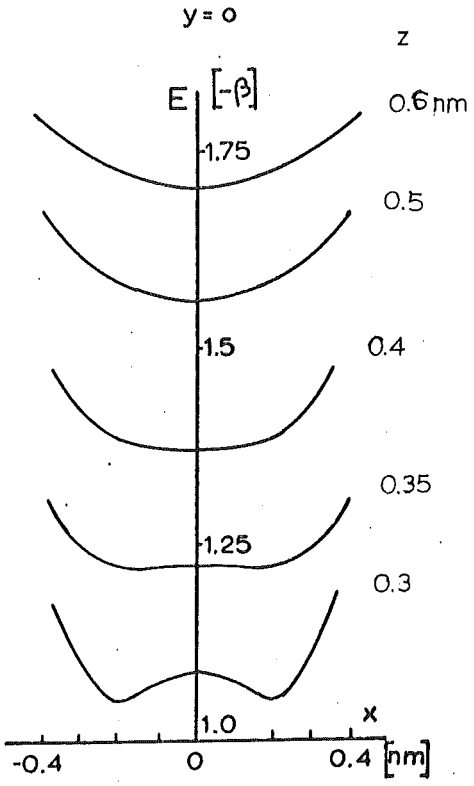

The observed temperature dependence can then be explained by combining the static and vibrational models. At low temperatures the cation is located somewhere in a nodal plane and, as the temperature is raised, it vibrates through this plane with increasing amplitude. This increases the positive contribution to the spin density (ρ_o) thus decreasing the total splitting. According to the static model, as the solvation changes, the position of the cation above the plane of the anion as well as the distance between the ions may vary. Both ρ_1 and ρ_o depend differently on these two factors. Thus increasing the cation-anion distance by increasing the degree of solvation (lowering the temperature) decreases both ρ_o and ρ_1, but alters their relative importance because ρ_1 decreases more slowly. At sufficiently large interionic distances no metal hyperfine coupling is expected.

Because of the presence of two nodal planes, the cation can be located in a number of positions and still lead to negative spin densities. There are three likely sites for the cation: A, B and C of figure 3.11. Clearly, if the cation is at B or C it must spend an equal time at B' and C' since the spin distribution as found by esr conformed to the symmetry of the molecule at all times. Interaction energy calculations (details in 3B.10) were performed to find the most favourable position energetically. At short interionic distances (3Å), these showed there are double energy minima along both the x and y axes, with B the most favourable position [Fig. 3.11]. Electron repulsion effects, which must be considered at small interionic distances, also favour positions B and C rather than A. As the cation is placed at greater distances above the aromatic plane, the potential wells become shallower and the double minima tend to disappear.

FIGURE 3.12

CALCULATED SPIN DENSITY AT A SODIUM NUCLEUS

0.3nm FROM THE PYRENE ANION.

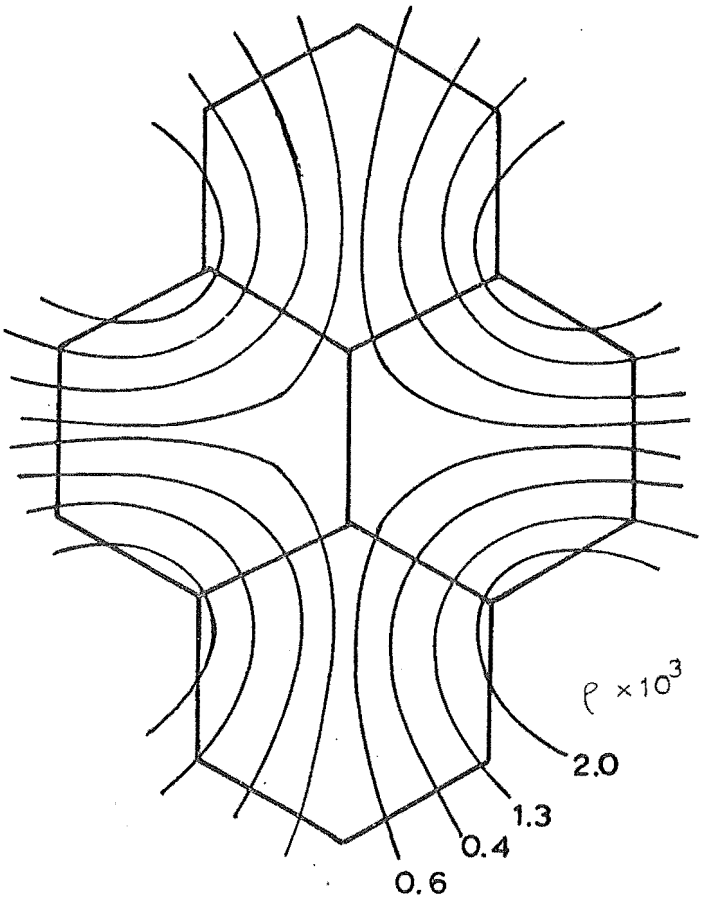

with the most favourable energy position shifting to over the centre of the molecule. A similar shift in minimum energy position was found for naphthalene calculations.[31]

To try and locate the position of the cation more precisely, the positive spin density contribution (ρ_o) was calculated using the method of Goldberg and Bolton.[31] These calculations were performed for sodium and lithium ion pairs only and are summarised in figure 3.12 for the former (z = 0.3nm = 3Å).

For the Na/MTHF system the observed sodium spin density decreases steadily from 0.44×10^{-3} at +50°C to zero (-40°C). No negative splitting was observed at lower temperatures. The calculations show that if the cation is 4Å above the pyrene plane a spin density of 0.4×10^{-3} is possible only if the cation moves a large distance from its energetically most favourable position above the centre of the anion. Placed 3.0Å above the anion plane, the sodium cation can readily acquire a positive of 0.4×10^{-3} by vibrating short distances about positions B or C. Interaction energy calculations and electron repulsion considerations indicate an energy minimum at both B and C, with B the most favoured position. However, if the cation remains at this short distance above the plane as the temperature decreases, a negative spin would be expected below -40°C [Fig. 3.10]. The lack of negative splitting is accounted for if, as the temperature decreases, the cation is slowly pulled away from the anion by the increasing solvating power of the solvent. By -40°C the cation may be sufficiently far from the anion for both ρ_o and ρ_1 to be vanishingly small. Inserting a solvent molecule(s) between the sodium and pyrene ions is expected to increase the distance between them considerably.

Thus a combination of the vibrational and static model can

explain the observed spin density changes for the Na/MTHF system. At low temperatures, the ion pairs can be regarded as solvent-separated with the cation probably located above the centre of the anion and greater than 4.0Å from it. As the solvating power of the solvent decreases with increasing temperature, the interionic distance decreases, the average position of the cation shifts (probably to position B) and the amplitude of vibration increases. At higher temperatures, the system consists of tight ion pairs, with the cation perhaps 3.0 - 3.5Å above the anion, according to the spin density calculations. Such an interionic distance is reasonable when van der Waal's and ionic radii are considered, if solvent molecules surround the ion pair but do not separate the ions. The same interpretation of ion pairs in Na/MTHF was proposed for the tetraphenyl boride anion: the contact ion pairs formed at higher temperatures become gradually more solvated as the temperature decreased.[90]

For the Na/DEE system, a spin density of 0.16×10^{-3} was found at +16°C and -0.22×10^{-3} at -112°C. If the cation is placed 3.0 - 3.5 Å above the nodal plane, then, at higher temperatures, vibration about positions B or C gives the correct order of magnitude to the positive spin density [Fig. 3.12]. DEE is a weaker solvent than MTHF [see 3B.7] and it does not gain sufficient solvating power to "pull off" the sodium cation as the temperature is lowered. Hence the cation remains in the potential energy well, probably at position B, with about the same interionic distance at lower temperatures. Since the amplitude of vibration also decreases, the sodium ion spends more time in the nodal plane, leading to a negative spin density below -60°C. These ion pairs are regarded as tight ion pairs at all temperatures. Above -40°C the sodium cation in DEE has a lower positive spin density

than in MTHF [Fig. 3.10]. This probably arises because the cation is slightly closer to the anion in DEE, which will have less peripheral solvation of a tight ion pair than MTHF; this allows the cation to spend more time in the position of minimum energy about the nodal plane where ρ_o is small.

In the Li/DEE system, the positive contribution to the spin density of the tight ion pair is low at all temperatures [Fig. 3.10]. With the cation 3.0Å above the molecular plane, vibration about position B leads to very small ρ_o values, according to the calculations. On the other hand, the same degree of vibration about C leads to a significantly larger positive spin density. This again suggests position B is the more likely site for the cation at short interionic distances. For a tightly-bound lithium ion pair, 3.0Å is about the expected distance.

The remaining systems where alkali metal splittings were observed contain the larger K^+ and Cs^+ ions. At the larger interionic distances expected for their tight ion pairs, 3.5 - 4.0 Å, the most likely location of the cation is above the centre of the anion at position A. From the calculations for the lithium and sodium ion pairs it is evident that the amount of positive spin density acquired by vibration about position A is always small in all directions. The negative splittings observed are therefore expected for these cations. The small changes in these spin densities with temperature indicate little change in the interionic distance and therefore little change in the solvation state of these tight ion pairs.

3B.7 Solvent properties and ion pair structure

Since the solvent competes with the anion for coordination to cation sites, variation in solvent properties can lead to extensive changes in ion pair structure. Differences in solvating power cannot be explained merely in terms of dielectric constant - i.e. electrostatic considerations. An important role is played by donor-acceptor interactions (basicity) and by steric factors.[37,99] Although the basicity of MTHF is higher than that of THF,[37] MTHF is a poorer solvent because the bulky methyl group increases the average distance between the ion and the solvent's coordination site. DME is a more powerful solvating agent than THF, despite its slightly lower dielectric constant at +25°C (7.20 and 7.39 respectively).[91] DME possesses two oxygen atoms in a favoured steric arrangement to coordinate simultaneously with the cation, whereas THF can form only a single donor-acceptor bond. This means the number of solvent molecules in the solvation shell is reduced in DME (probably two in DME compared to four in THF) and the entropy of solvation is favoured.

Shatenshtein[37] has shown that the nature of the metal is also important and that solvation interactions are determined by the specific features of both metal and solvent. Usually smaller cations have a stronger interaction with the solvent molecules because of their more intense electric fields.

The generally accepted order of decreasing solvating power is DME > THF > MTHF > DEE. Hence solvent-separated ion pairs are expected in DME and tight ion pairs in DEE, while the larger cations should form tight ion pairs in THF and MTHF, in agreement with earlier conclusions on ion pair structure. The lack of reduction in the Cs/DEE system indicates that even in very tight

ion pairs, some degree of solvation is necessary to stabilise the structure.

3B.8 Proton coupling constants and ion pairing effects.

The effects of ion pair formation on the proton coupling constants of radical anions potentially contain much information on ion pair structure since they reflect the electronic distribution within a molecule. However, these effects are usually small and are much more difficult to monitor accurately than changes in metal splittings. Hirota,[46] Iwaizumi,[100] and Reddoch[101] have been able to correlate changes in proton coupling constants with changes in ion pair structure for acenaphthylene, azulene and other anions where they found variation in splittings of up to 10%. However Reddoch[49] could find no correlation between the coupling constants of naphthalene and the effects of ion pair formation. Similarly, there seems to be no single trend for the proton coupling constants of pyrene [Table A.1]. This is hardly surprising, since the solvent-cation interactions depend on the detailed nature of both species and vary with temperature. As the average interionic distance varies so does the perturbation of the proton spin densities caused by the metal ions.

In all the systems observed in this work, the γ coupling constant decreases as the temperature is lowered, in agreement with Reddoch's findings.[55] This seems to be an intrinsic property of the pyrene anion and is probably due to out-of-plane vibrations.[55]

There are some noteworthy features of the observed α and β coupling constants. Firstly, in both the K/MTHF and Cs/THF systems, α_β(IP) is greater than α_β(FI) and a_α(IP) is less than

a_α(FI). Theoretical calculations [3B.10] predict this trend when the cation is situated above the centre of the anion but not if it is oscillating in the x and y directions [Fig. 3.11].

Secondly, the free ion values in MTHF and THF are similar to each other and to those found in Li/THF and K/DME (Reddoch has noted that free ion splittings can be solvent dependent[49]). This may indicate that "free" ions are present in the latter two systems rather than loose ion pairs. All four systems have temperature independent α and β coupling constants.

A third feature is that in nearly all cases where the coupling constants are temperature dependent, both $|a_\beta|$ and $|a_\alpha|$ increase on cooling, as observed by Reddoch.[55] He considered this was probably a property of the free ion due to proton vibration out of the molecular plane. In this work, some coupling constants shift towards the area of the "free ion" values while others move further away, which may arise from the existence of opposing effects. Usually lowering the temperature increases the proportion of loose ion pairs,[36,40,45] but if the ion pair is solvent-separated initially, lowering the temperature may cause the solvent sheath to become tighter so that the ionic distance decreases and cation perturbation increases. On the other hand, the improved solvating power on decreasing the temperature may gradually pull the cation further away from the anion and decrease its perturbing influence on the proton spin densities. This further underlines the complications in trying to predict ion pair effects as solvent, cation and temperature are altered.

FIGURE 3.13

PLOT OF g-SHIFT vs CESIUM HYPERFINE SPLITTING

SYSTEM : PY/Cs/THF

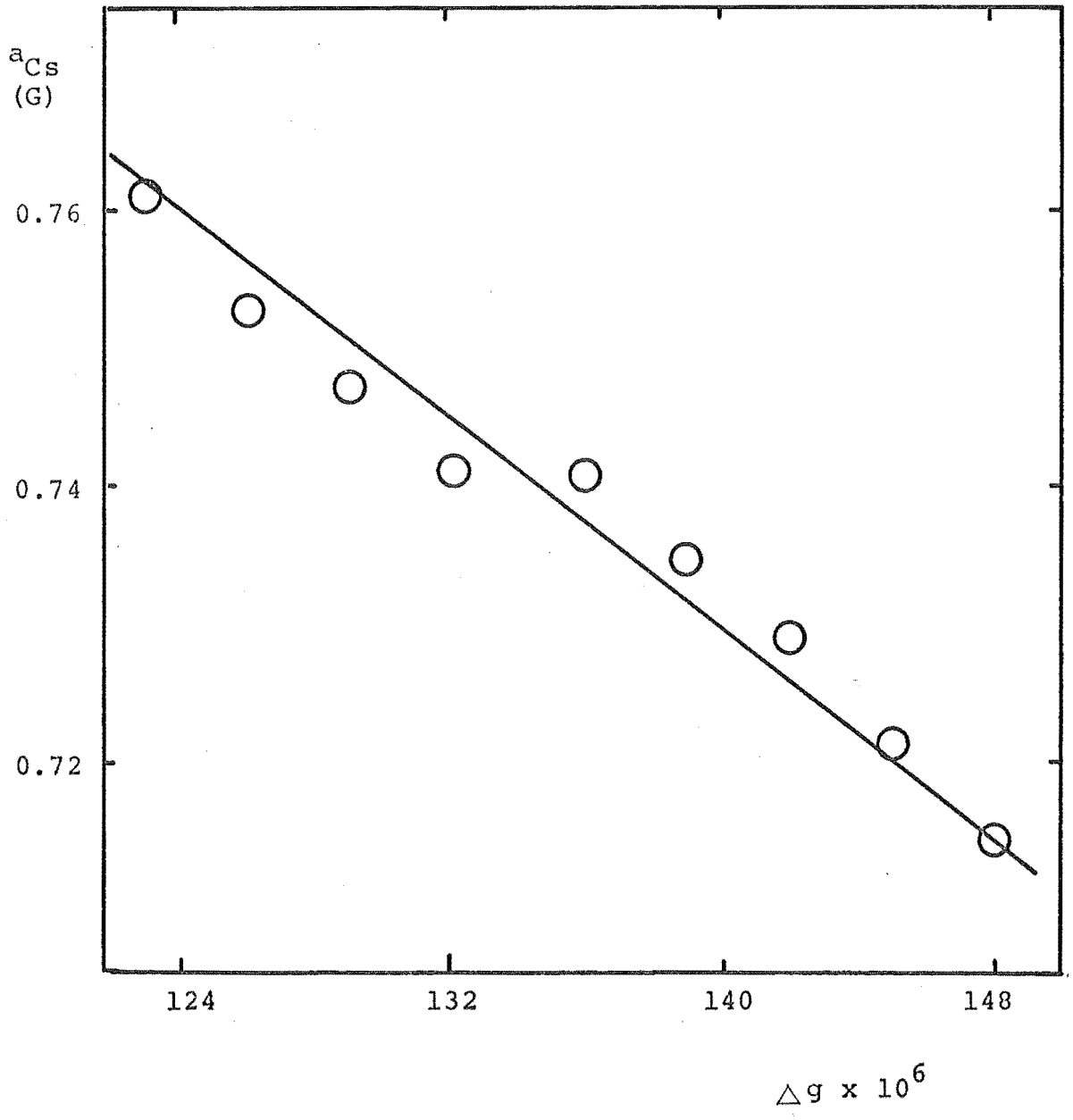

3B.9 The g-values and ion pairing effects.

Reddoch[49] and Fraenkel[50] have recently shown that the g-value of a radical anion may change upon ion pair formation. Their results suggest a strong correlation between the g-factor and the appropriate metal spin orbit coupling (soc) parameter (ζ). For the Cs/THF and K/MTHF pyrene systems, both ion pairs and free ions were present simultaneously and $\Delta g = g_{FI} - g_{IP}$ could be found [Table 3.1]. In both cases Δg increased as $|a_M|$ decreased and, as expected,[49,50] g_{IP} was less than g_{FI}. Fraenkel[49] investigated the temperature variation of the g-factor in the same terms that are used for metal hfs changes: 1) thermal changes in the population of the vibrational energy levels causing gradual changes with temperature (static model), and 2) a rapid equilibrium between two distinct ion pairs (dynamic model). He showed that a linear relationship between Δg and a_M should result if the dynamic model applied, and found this held for the naphthalene (N)/Na/THF system but not for N/Cs/DME.

The linear relationship found between Δg and $|a_{Cs}|$ for the PY/Cs/THF system [Fig. 3.13] is surprising since, from the linewidths and the temperature dependence of a_{Cs}, there is no reason to suspect the involvement of a rapid equilibrium. As noted by Fraenkel,[49] this linearity does not prove that two ion pair species are present but means this could be the case. A static model is still favoured to describe this PY/Cs/THF system where the temperature dependence of Δg and a_{Cs} is due to variations in the relative populations of the vibrational levels of a single ion pair species. Fraenkel's g-value analysis,[50] de Boer's detailed nmr measurements of linewidths,[86] and Reddoch's esr studies[49] indicate that the static model usually

suffices to describe cesium ion pairs.

The data for PY/K/MTHF is limited. Both Δg and a_K are constant above $\sim -50^{\circ}C$, and linearly related below this. The low temperature deviation in the ρ v T graph [Fig. 3.10] and the linear dependence of Δg and a_K both indicate two ion pairs could be present below $\sim -60^{\circ}C$.*

3B.10 Calculations

An attempt was made to calculate the effects of a counter-ion on the proton hfs, based on the modified Huckel approach of McClelland.[39] He suggested that the electrostatic interaction of the cation and anion could be approximated by adding a term $-e^2/r$ (r is the distance between the ions) to the unmodified Huckel Hamiltonian; the eigenvalues and eigenfunctions are then calculated in the usual way and the spin densities found from the relation $\rho_i = C'^2_{oi}$, where C'_{oi} is the coefficient of the MO containing the unpaired electron, Ψ_o', at atom i. Usually McConnell's[15] relation

$$a_i = Q\rho_i \qquad (3.21)$$

is then used to estimate the coupling constant, a_i, of proton H_i bonded to carbon C_i.

Since a simple MO treatment cannot explain the occurrence of negative proton spin density, McLachlan's[16] method was used to calculate corrected spin densities for the anion system, the McClelland-type calculation then performed, and McLachlan's method used again. McLachlan's calculation is a semi-empirical

---

* If this is the case, then the rate of interconversion is very fast since no linewidth effects are noted. Such an equilibrium would have a negligible effect on the thermodynamic parameters derived for the IP⇌FI process since, in the region used for this analysis, $p_{LIP} \simeq 0$.

FIGURE 3.14

CALCULATED PROTON HYPERFINE SPLITTINGS IN PYRENE ION PAIRS FOR VARIOUS CATION POSITIONS AND HEIGHTS ABOVE THE ANION PLANE

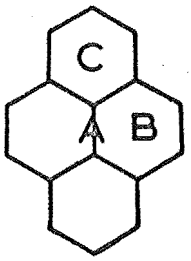

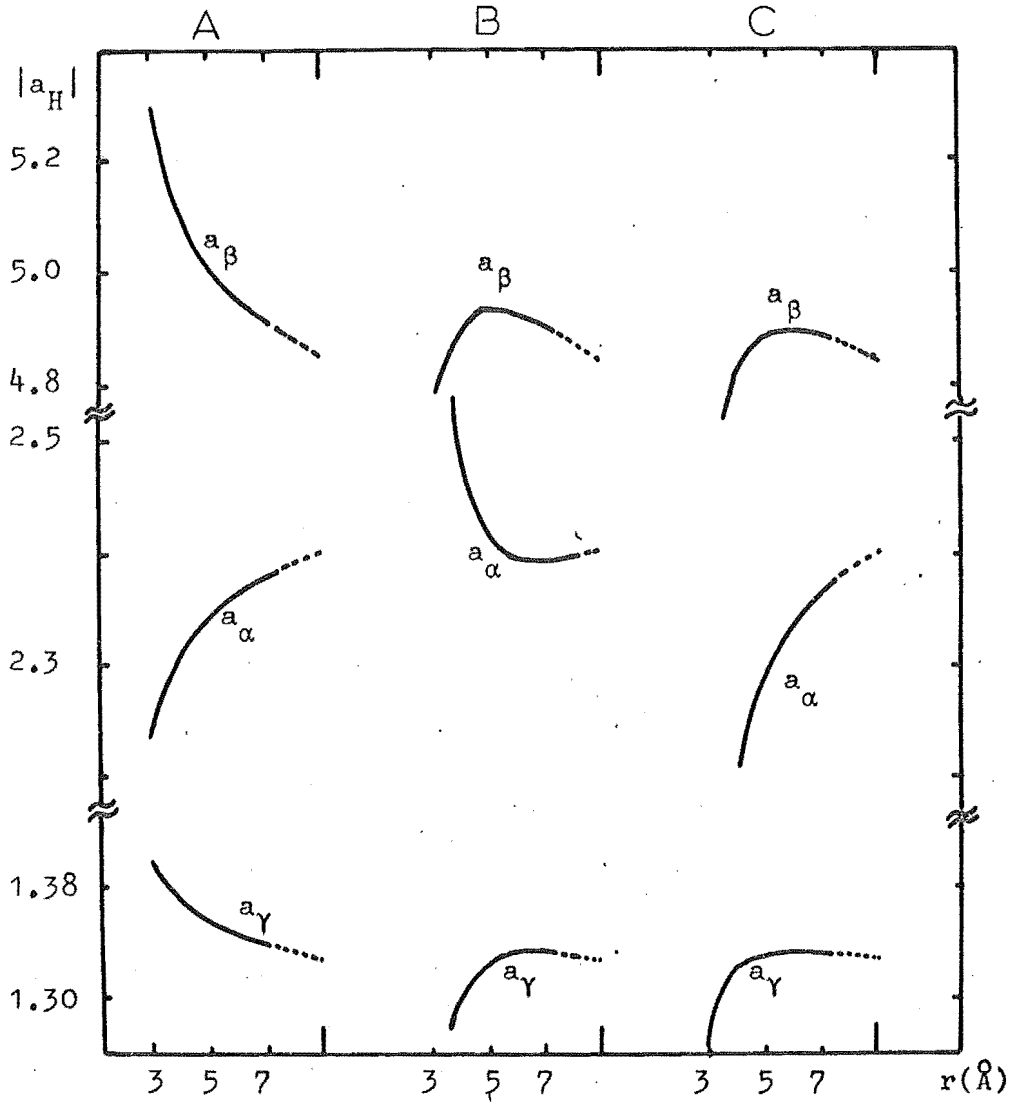

way of accounting for π-π spin interactions and is usually preferable to a simple HMO calculation, especially where there are nodes in the unpaired electron's MO. Electrostatic interaction energy calculations were carried out at the same time to locate the cation-anion positions that are energetically favoured. These calculations measure the energy difference between a perturbed (ion pair) and an unperturbed (free ion) system, allowing for the repulsion between the effective positive carbon cores and the positive charge of the cation, at a given position.

The three locations of the counter-ion discussed earlier: A, B and C, were considered from 2 - 7 Å above the molecular plane. McConnell's relation[15] was used with a value for Q of 26.0 G. The calculated proton coupling constants are expressed graphically in Fig. 3.14 and the calculated interaction energy maps shown in Fig. 3.11. It is the trends in calculated values, rather than their magnitude, which are usually considered most useful.

As noted earlier, in two cases where ion pairs and free ion were simultaneously observed, $|a_\beta(IP)| > |a_\beta(FI)|$ and $|a_\alpha(IP)| < |a_\beta(FI)|$, as predicted by position A only. However, for Li/DEE in the region where loose and tight ion pairs were rapidly interconverting, the resulting lineshapes indicated that $|a_\beta(LIP)| > |a_\beta(TIP)|$, as predicted by positions B and C. Exactly the same conclusions were reached from considerations of the spin density (3B.6): i.e. in tight ion pairs the Li^+ ion resides over ring positions (probably position B) while the K^+ and Cs^+ ions are located above the centre of the anion.

In these calculations, trends are a function of interionic distance. Any changes due to some mechanism other than the perturbing effect of the cation are ignored.

Table 3.7 Experimental hyperfine coupling constants for PY/K/THF at -30°C.

Position	coupling constant[a] (G)	linewidth[b] (G)	%
a_1^H	(-)4.813	0.03	
a_2^H	(+)1.029	0.03	
a_4^H	(-)2.121	0.03	
a_1^C	+ 7.10	0.06	2.2
a_2^C	- 6.00	0.04	1.1
a_4^C	(+)1.84	0.04	2.2
a_{11}^C	(-)2.58	0.03	2.2
a_{15}^C	0.20	-	1.1

a) ± 0.02 G; signs in brackets are predicted by theory, the others determined from experiment.

b) linewidth of low field component.

3C: ^{13}C coupling constants

From the original K/THF spectra it was clear that the extra lines Lyons had earlier observed for this system[61] were not due to a potassium ion pair. Lyons had considered the lines were too intense to be due to the natural abundance of ^{13}C nuclei present. However additional minor peaks were present in all the spectra discussed above which did suggest hyperfine coupling to ^{13}C nuclei as their source. To try and resolve this question, an attempt was made to determine the ^{13}C hfs of the pyrene anion.

The ^{13}C nucleus has a natural abundance of 1.1% and a spin quantum number of $I = \frac{1}{2}$. Thus the intensity of each ^{13}C satellite relative to the parent proton line is given by $(n/2) \times 0.011$ where n is the number of equivalent positions that can accommodate a ^{13}C nucleus. This "intensity criterion" is often useful in assigning ^{13}C splittings but must be used with due caution in view of the linewidth effects discussed below. To detect all the hyperfine components arising from ^{13}C nuclei present in natural abundance in complex molecules like pyrene, spectra of very high resolution and an extremely good signal-to-noise ratio are vital. Since dilute solutions and low microwave power are still required (to avoid masking the ^{13}C components with broad proton lines), stringent requirements are placed on spectrometer performance. To achieve adequate sensitivity, the system (K/THF at $-30^{\circ}C$) was investigated under high-gain slow-scan conditions.* The coupling constants listed in Table 3.7

---

* Conditions used: Receiver Gain: 8.0×10^3; Power 0.1 mW; Time Constant: 3.0 sec; Scan time: 2 hr.; Modulation Frequency: 10 KHz; Modulation Amplitude: 1.25×10^{-2}.

FIGURE 3.15

LOW-FIELD REGION OF THE ESR SPECTRUM OF THE PY/K/THF SYSTEM

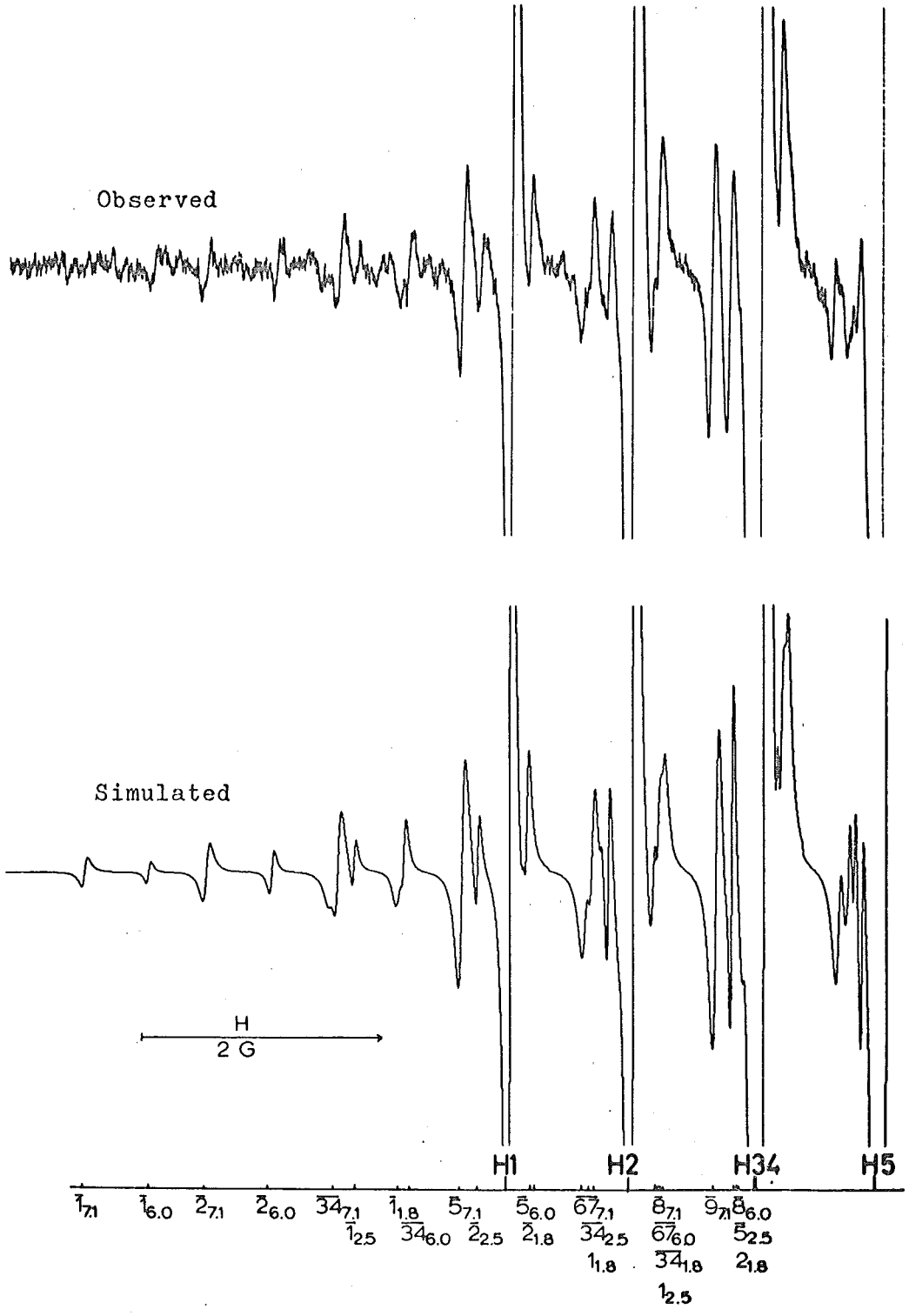

The large lines labelled H1, H2 etc, are the outermost lines due to the protons. The remaining lines are due to ^{13}C and are labelled as low-field, $\bar{1}$, or high-field, 1, satellites of the proton lines. The subscripts are the respective coupling constants.

gave excellent simulation of the wings of these high gain spectra. With these values, no lines were observed in any part of the spectrum which could not be reasonably accounted for [Fig. 3.15]. The coupling constants were assigned to the five distinct C positions on the basis of theoretical splittings, intensity ratios and linewidth effects.

Table 3.8 lists the π spin densities of the carbon positions, $\rho^{\pi}(C_i)$, calculated by a variety of methods. The expressions of Karplus and Fraenkel [105]

$$a_C = 35.6\rho^{\pi}(C) - 13.9\Sigma_i\rho^{\pi}(C_i) \text{ for } C\text{-}C_2H \text{ fragments} \qquad (3.22)$$

and

$$a_C = 30.5\rho^{\pi}(C) - 13.9\Sigma_i\rho^{\pi}(C_i) \text{ for } C\text{-}C_3 \text{ fragments} \qquad (3.23)$$

were used to calculate the corresponding coupling constants.

Linewidths provide information on the sign of coupling constants because of their linear dependence on nuclear magnetic quantum numbers (M). In dilute solutions, two of the most important effects in causing linewidth variations among different hyperfine lines are the anisotropic dipolar electron-nuclear interaction and the g-tensor anisotropy. According to the theory of lineshapes developed by Freed and Fraenkel, [106] the width of the principal* hf lines arising from an equivalent set of nuclei and characterised by M (say) are given by

$$T_2^{-1} = A + BM + CM^2 \qquad (3.24)$$

where A, B and C are parameters related to the anisotropic contributions.

B involves a cross term between the anisotropic dipolar and and g-tensor interactions which de Boer and Mackor [107] have shown

---

* Principal hf lines are lines characterised by only one quantum number unequal to zero.

Table 3.8: Calculated ^{13}C hyperfine coupling constants and spin densities.

Position	Spin densities			Coupling constants (G)				
	HMO[a]	McL[b]	UHF[c]	HMO	McL	UHF	INDO[d]	Expl
1	0.136	0.187	0.174	+4.467	+7.352	+6.625	+9.9	+ 7.10
2	0	-0.052	-0.042	-3.781	-7.050	-6.332	-7.1	- 6.00
4	0.087	0.092	0.085	+1.512	+1.968	+1.692	-2.9	(+)1.84
11	0.027	0.002	0.011	-2.276	-3.650	+3.278	-	(-)2.58
15	0	-0.012	-0.001	-0.751	-0.255	-0.389	-	0.20

a) Simple Huckel method[102]

b) McLachlan method[16]

c) Unrestricted Hartree-Fock method[103]

d) INDO method[104]

is always negative for ^{13}C nuclei. Since A and C are positive, a positive (negative) coupling constant will have broader lines at high (low) field. Hence measurement of the appropriate linewidths can determine the sign of coupling constants.*

The C parameter is a function of the anisotropic intramolecular dipolar interaction and although it is of no value in determining the sign of hfs, Bolton and Fraenkel[108] have shown it can be of assistance in assigning ^{13}C splittings. They found that for any skeletal carbon, the largest part of this dipolar line broadening arises from the spin density on the atom containing the nucleus (the local spin density). Further, the linewidth contribution is approximately proportional to the square of this local spin density. This is most accurate when the local spin density is large, but is still a reasonable guide for low values.[108] Hence, whenever the dipolar interactions are large enough to cause a measurable effect on the widths, the lines from nuclei with a large local spin density will be broader than those from nuclei with a small spin density.

Analysis of the linewidths of the observed spectra led to these conclusions: the sign of the 7.10 G splitting was positive; the sign of the 6.0 G splitting was probably negative (lines not as clearly resolved); the linewidth of the 2.58 G coupling constant was narrower than that of the 1.84 G splitting. There was some evidence that the 1.84 G splitting was positive but this was not conclusive.

---

* Although this procedure is general, it is much more useful for ^{13}C than for proton sign determinations; this is because the anisotropic hf interaction varies as r^{-3}, where r is the distance between the unpaired electron and the magnetic nuclei in question. When C atoms are part of the π-electron system, the hf anisotropic effects are much larger at their nuclei than at the neighbouring proton nuclei; hence the linewidth variations are greater.

All the coupling constants calculated by the Karplus-Fraenkel method[105] predict positive values for positions 1 and 4, and negative values for positions 2,11 and 15 [Table 3.8] The two largest splitting constants could be assigned to positions 1 and 2 respectively on the basis of their magnitudes, relative intensities and signs. The two remaining constants observed were present in equal ratios (2.2%), were of similar magnitude and clearly belong to positions 4 and 11, since for position 15 a 1.1% intensity ratio and a much smaller coupling constant are predicted. From Bolton and Fraenkel,[108] the dipolar anisotropic contribution to the linewidth should be significantly greater for the 4 position; hence the 1.84 G splitting can be assigned to position 4 and the 2.58 G constant to position 11. As no other ^{13}C hfs could be found, the coupling constant for position 15 must be less than 0.20 G and hidden by the massive proton lines.

Spectra taken at +17°C and -78°C showed some slight variations in the ^{13}C hfs, but no thorough analysis was carried out.

Since analysis of the proton spectra for the PY/K/THF system indicated that a_γ was temperature dependent (while a_α and a_β were not), it seemed likely that the apparent broadening that Lyons[61] observed was due to this temperature variation. To check this, several simulations were made of the ordinary proton spectra including the appropriate of ^{13}C splittings. Although these simulations are limited in that both high and low peaks have to be assigned the same linewidths, they did indicate that the variation in a_γ with temperature causes linewidth variations in some regions of the spectra. Furthermore, with linewidths

attained in this study, a potassium hfs of 0.14 G would have been clearly evident. The coupling constants listed in Table 3.7 explain the total observed spectrum satisfactorily.

3D. Conclusions

Based on the data and evidence of this chapter, the following ion pair classifications are suggested; the Li/DME, THF, MTHF; Na/DME, THF; K/DME, THF and Cs/DME systems consist of well-solvated loose ion pairs. The Li/THF and K/DME systems may even contain the "free" pyrene anion. Na/MTHF and Li/DEE also contain loose ion pairs at low temperature while the remaining systems consist of tight ion pairs only. In loose ion pairs the cation is localised above the centre of the anion and greater than 4.5Å from it. The tight ion pairs of cesium and potassium are of similar structure but with a shorter inter-ionic distance (3.5 - ~4.0Å). Lithium and sodium tight ion pairs involve a shorter distance between the ions (~3.0 - 3.5Å) with the cation located above ring positions.

FIGURE 4.1

STRUCTURAL FORMULA AND NUMBERING SYSTEM

FOR PERYLENE

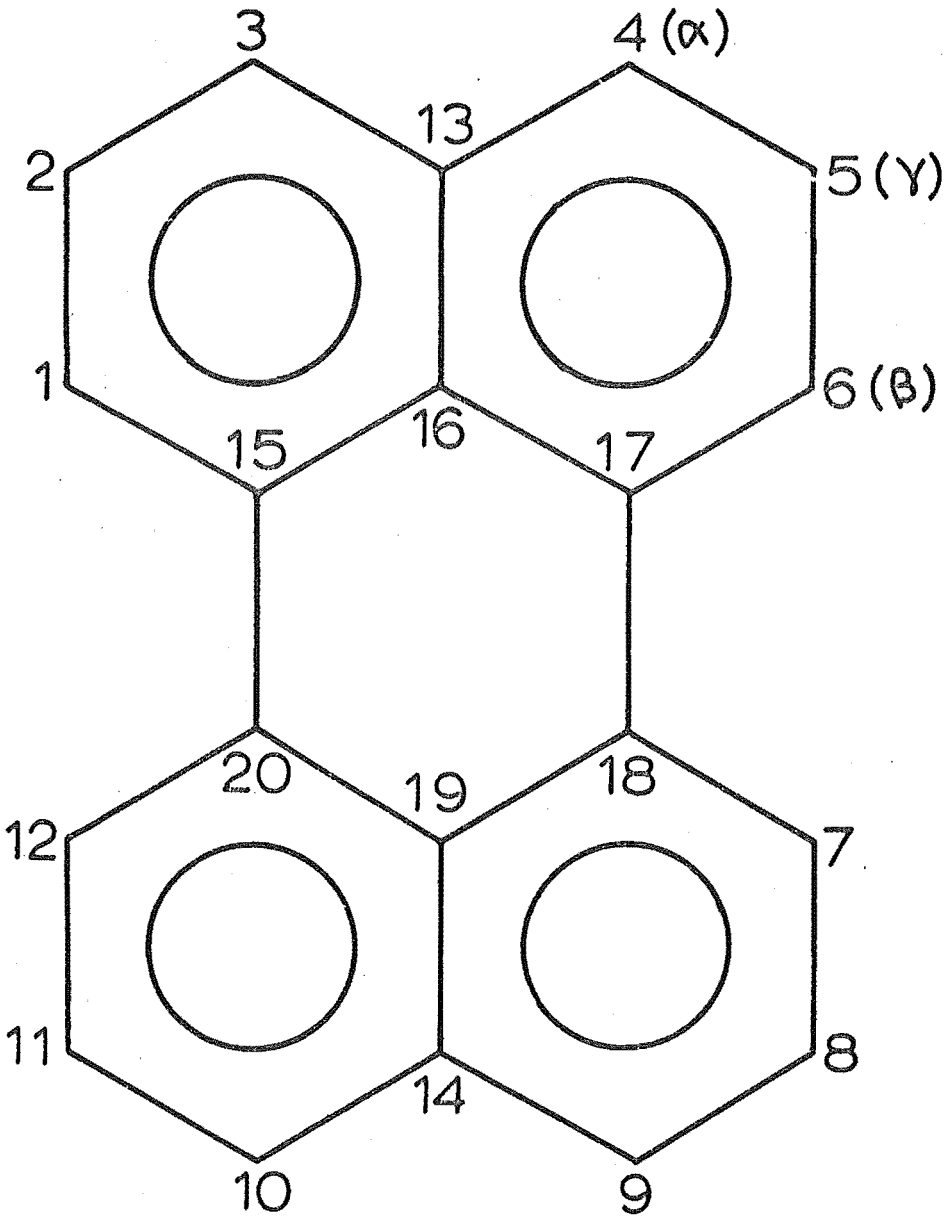

CHAPTER FOUR

PERYLENE

The perylene anion was readily formed using the methods of Chapter Two. The four alkali metals Li, Na, K, Cs and the four ether solvents DME, THF, MTHF, DEE were used in all combinations. As with pyrene, the Cs/DEE system would not reduce the hydrocarbon.

Perylene has three magnetically distinct sets of protons, usually labelled α, β, γ [Fig. 4.1]. Each set contains four protons giving rise to 125 lines but, as most previous investigators[62-67] have noted, these are not all resolved because of accidental overlap arising from the magnitude of the small coupling constant being about equal to the difference between the two larger ones.

4A: Esr spectra observations

The coupling constants listed in Table A.2, [Appendix A, page 124] were found by spectral simulation. As noted in Chapter Two, the use of lower power levels often narrowed the lines for perylene systems considerably.

Li/THF, K/THF, Na/THF

The spectra from these systems exhibited extremely narrow linewidths (20 mG) and at low temperature the γ proton coupling constants were resolved [Fig. 4.2]. As for many of the pyrene systems, asymmetry due to second order effects was observed.*

---

* The average downfield second-order shift, as calculated by eqn. 3.2, is $\sim$6.7 mG for the perylene anion.

FIGURE 4.2

ESR SPECTRA OF THE PYL/K/THF AND PYL/K/DME SYSTEMS

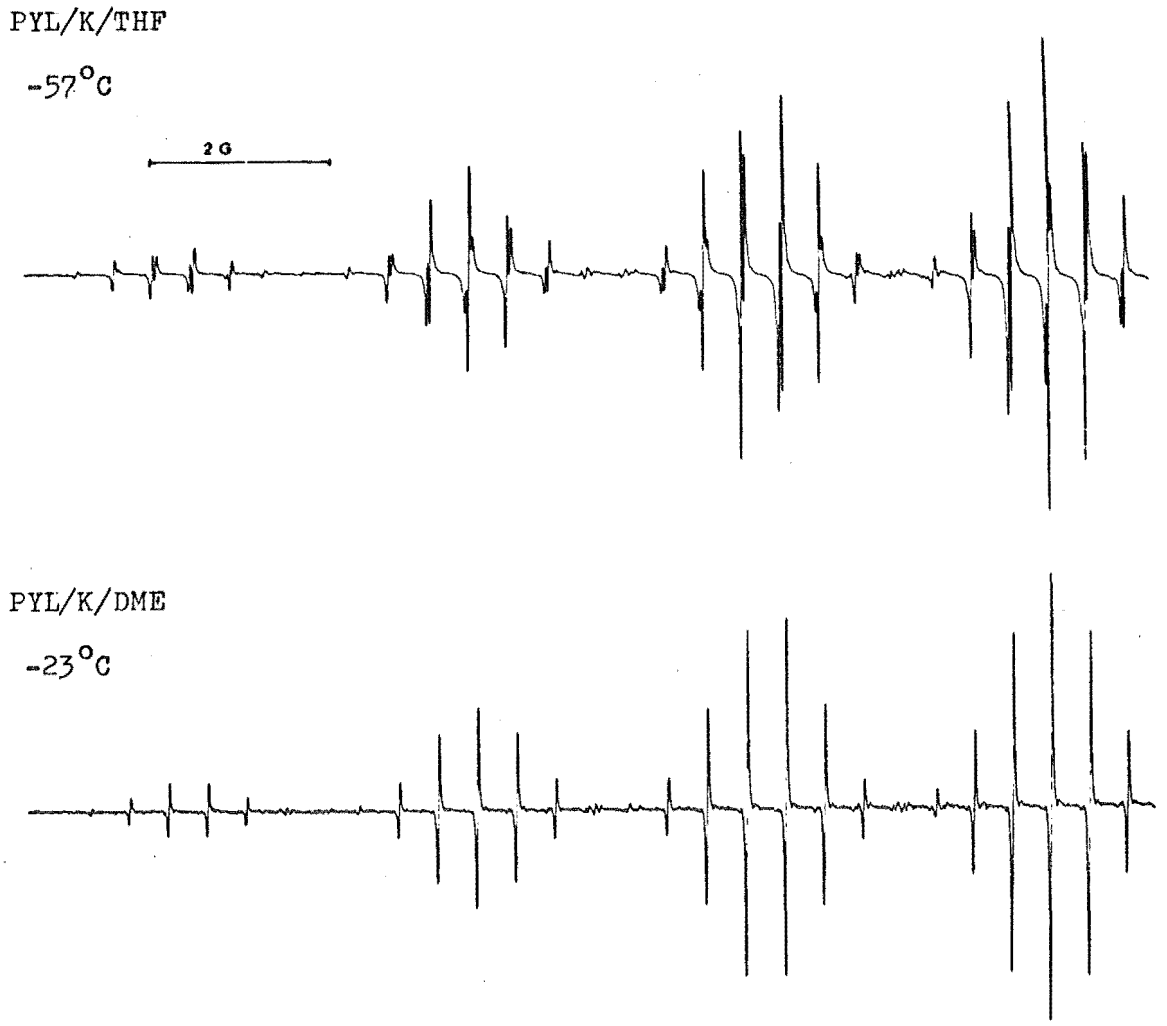

FIGURE 4.3

ESR SPECTRUM OF THE PYL/K/MTHF SYSTEM

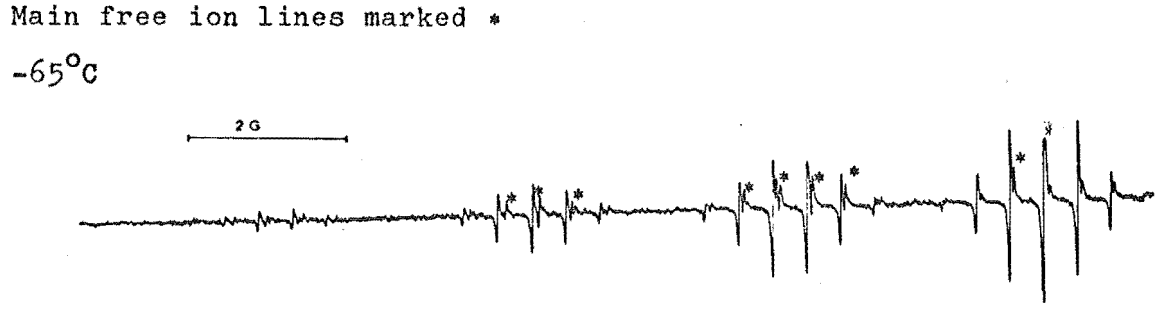

Li/DME, K/DME, Na/DME These spectra were again extremely narrow (20 mG) but unlike the THF systems, the Y coupling constant was never resolved [Fig. 4.2]. Very small additional lines astride the main proton lines were observed in all three systems, as was asymmetry of the signals due to second order shifts.

Cs/DME This system produced lines which broadened considerably on increasing the temperature, although no cesium splitting was resolved.

Cs/THF Dilution experiments showed both ion pair and free ion were present for this system at low temperatures (linewidth 30 mG). The ion pair had a slightly higher g-value than the free ion* ($g_{IP} - g_{FI} \simeq 6 \times 10^{-6}$) and the outer components of the Cs hfs were broadened relative to the inner ones. Above $-40^{\circ}C$, the lines broadened and overlapped so much that spectral simulation in terms of two species was no longer possible.

K/MTHF With very dilute solutions both ion pair and free ion lines were distinguished [Fig. 4.3]. No metal hfs was detected at any temperature (linewidth 23 mG) but some broadening was noted at higher temperatures. Again, the ion pair had a higher g-value than the free ion ($g_{IP} - g_{FI} \simeq 15 \times 10^{-6}$).

Li/MTHF At high dilution and low temperatures, ion pair and free ion lines could be partially resolved ($g_{IP} - g_{FI} \simeq 3 \times 10^{-6}$) but on increasing the temperature the lines merged and the species could not be distinguished. No lithium hfs was observed at any temperature.

---

* The g-value of the free ion was taken as that determined for the Na/DME system,[60] allowing for Allendoerfer's correction[109] and second order effects.

FIGURE 4.4

ESR SPECTRUM FOR THE PYL/Cs/MTHF SYSTEM

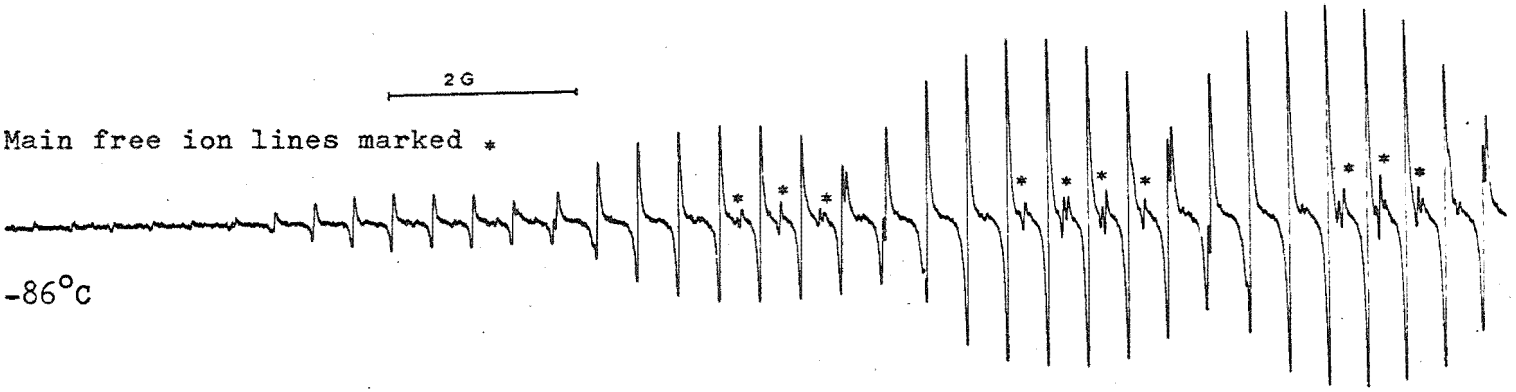

FIGURE 4.5

ESR SPECTRUM FOR THE PYL/K/DEE SYSTEM

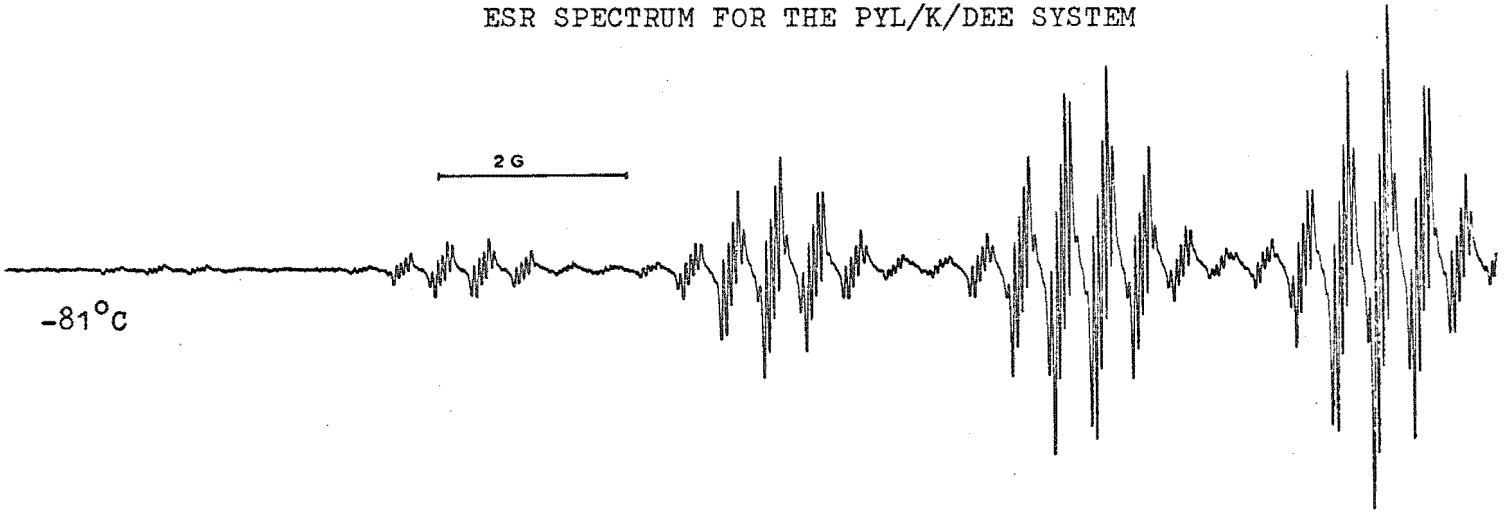

Na/MTHF The extremely narrow (20 mG) single lines found at low temperature for this system were split by hyperfine coupling to the sodium cation at higher temperatures. The free ion was indicated in these spectra, but its relative concentration and coupling constants were difficult to simulate because of overlap complications, especially that caused by the relation: $|a_\gamma| \simeq |a_\alpha| - |a_\beta|$.

Cs/MTHF This system also produced spectra of both free ion and ion pair simultaneously. At low temperatures (-80°C) all lines were sharp (20 mG) with the ion pair present in greater concentration than the free ion. Above -50°C the free ion intensity was too low to be detected. Frequency measurements showed the g_{IP} was 222 x 10^{-6} greater than g_{FI}, from -100°C to -60°C [Fig. 4.4].

Li/DEE These spectra displayed narrow, single lines (linewidth 20 mG) at low temperature which were broadened at -43°C and resolved into four components at -23°C. The Li hfs increased to 0.051 G at -3°C and remained constant as the temperature was increased.

K/DEE For this system, a potassium splitting was observed throughout the temperature range, decreasing very slightly as the temperature was raised [Fig. 4.5]. All systems showed narrow linewidths (25 mG).

Na/DEE The extremely narrow lines for this system at low temperature (20 mG) allowed resolution of the Y coupling constant. A sodium hfs was resolved at -89°C which increased steadily with temperature. At higher temperatures the linewidth was slightly increased (28 mG).

Table 4.1 Experimental Dissociation Constants.

	Temperature (K)	K_D (mol l^{-1})
Cs/THF	175	2.96×10^{-5}
	192	9.15×10^{-6}
	211	4.42×10^{-6}
	231	2.93×10^{-6}
K/MTHF	168	8.15×10^{-6}
	188	4.45×10^{-6}
	208	1.67×10^{-6}
	228	1.25×10^{-6}
	248	8.9×10^{-7}
Na/MTHF	245	2.61×10^{-6}
	261	2.01×10^{-6}
	277	1.23×10^{-6}
Cs/MTHF	170	1.77×10^{-6}
	187	9.89×10^{-7}
	189	8.33×10^{-7}
	208	5.45×10^{-7}

K_D: $\pm$ 20%

Table 4.2 Thermodynamic data for the dissociation of ion pairs to free ions.

System	ΔH_D^o / kJ mol^{-1}	ΔS_D^o / J K^{-1} mol^{-1}
K/MTHF[a)]	-9.6	-155
Cs/THF[a)]	-12.9	-162
Na/MTHF[b)]	-14.9	-167
Cs/MTHF[a)]	-5.7	-146

a) $\Delta H_D^o = \pm 2$ kJ mol^{-1}, $\Delta S_D^o = \pm 10$ J K^{-1} mol^{-1}.

b) $\Delta H_D^o = \pm 4$ kJ mol^{-1}, $\Delta S_D^o = \pm 20$ J K^{-1} mol^{-1}.

Values found within temperature range ~170 - 240 K except Na/MTHF: 245 - 280 K.

4B. Discussion

4B.1 Free ion - ion pair equilibria

Thermodynamic data [K_{diss}, ΔH, ΔS - Tables 4.1, 4.2, Fig 4.6] were obtained for the dissociation of perylene ion pairs to free ions:

$$PYL^- M^+ \rightleftharpoons PYL^- + M^+ \qquad (4.1)$$

in the Cs/THF, Na/MTHF, K/MTHF and Cs/MTHF systems. The presence of free ions was established by dilution at constant temperature, and the thermodynamic analysis carried out as detailed in section 3B.3. The determination of the total concentration required in the expression for the equilibrium constant [Eqn. 3.6] is more complicated for perylene than for pyrene systems for two reasons: the formation of the dinegative ion and the disproportionation of the anion occur more readily for perylene[35,110] (cf. assumption 2, page 32). Considerable care was taken to allow the metal and perylene to remain in contact for only a short time to minimize any direct reduction to the dianion. Szwarc[110] has recently shown that the equilibrium constant for disproportionation reactions

$$2\ PYL^- M^+ \rightleftharpoons PYL^{2-}, 2M^+ + PYL \qquad (4.2)$$

is very small when the cation is poorly solvated in both the anion and dianion. Since weak cation solvation is expected in all the systems studied and since the narrow lines indicate that no significant amount of perylene hydrocarbon is present (as required by eqn 4.2), the effect of disproportionation was considered negligible.

Small ΔH^o and ΔS^o terms were found for the dissociation of perylene ion pairs in the Na/DME, Na/THF and Li/THF systems by Szwarc and his co-workers.[36,90] They concluded these systems

FIGURE 4.6

PLOTS OF LOG K vs $\frac{1}{T}$ FOR THE DISSOCIATION OF

PERYLENE ION PAIRS

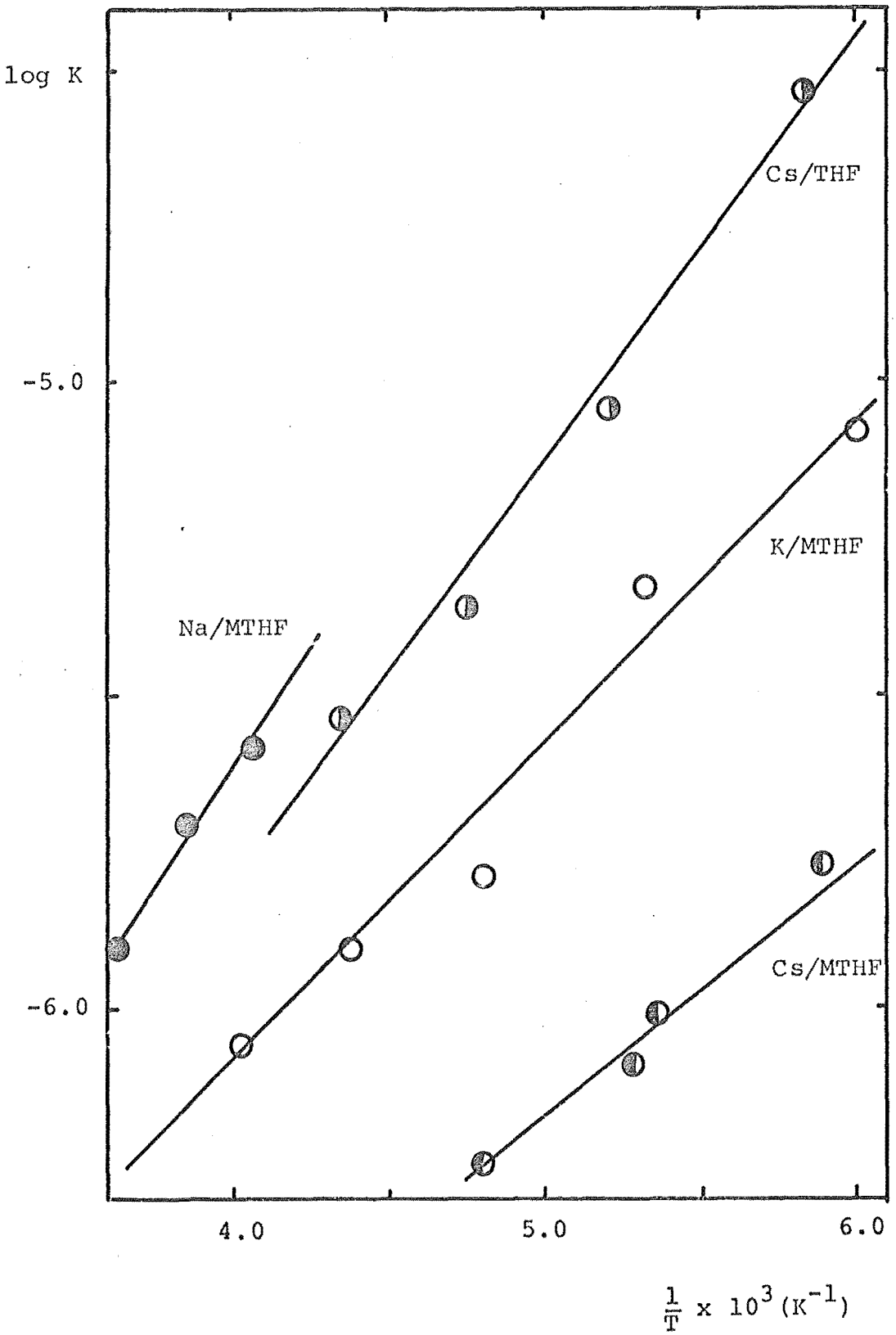

contained solvent-separated ion pairs only. The dissociation enthalpy for the Cs/MTHF system is of the same small order of magnitude but in this case does not arise from the presence of loose ion pairs. As discussed in section 3B.5, small ΔH^{o} terms are expected when $|\Delta H^{o}_{\text{ion-solvent}}|$ is small. This can occur:
1) when well-solvated ion pairs dissociate to fully-solvated free ions (e.g. loose ion pair in PY/Li/DEE system); or
2) when tight ion pairs with little specific solvation dissociate to free ions which also have weak coordination with the solvent.
Since the Cs^{+} ion has only a small specific interaction with THF[40,91] molecules and MTHF is an even weaker solvating agent,[40,90] the second situation applies and the dissociation of tight $Cs^{+}PYL^{-}$ ion pairs gives rise to only a small negative ΔH^{o} term.

The larger ΔH^{o} terms for the sodium and potassium ion pairs in MTHF indicate a greater change in the solvation sphere on dissociation. Assuming these ion pairs are still tight ion pairs,* this change arises mainly from an increased degree of solvent coordination with the free cation. Since a smaller "bare" ion generates a greater polarising field in its vicinity, the expected order of these cation-solvent interactions is $Na^{+} > K^{+} > Cs^{+}$, in agreement with the trend in the observed enthalpy changes. Similarly the order of the negative entropy changes is $Na^{+} > K^{+} > Cs^{+}$, consistent with the stronger cation-solvent interactions inducing more order in the solvent.

Tight cesium ion pairs are proposed for the THF and MTHF systems, so that the larger negative ΔH^{o} and ΔS^{o} values in THF

---

* The classification of tight ion pairs for the Na/MTHF system applies only to the higher temperature region ($> \sim -25^{o}C$) where thermodynamic data was obtained.

Table 4.3: Calculated K_{diss} and ΔH° values using the "sphere-in-continuum" model

Solvent: MTHF

Temperature K	Interionic distance 4.0 Å		5.0 Å		6.0 Å	
	$\frac{K_{diss}}{mol\ l^{-1}} \times 10^{+9}$	$\frac{\Delta H}{kJ\ mol^{-1}}$	$\frac{K_{diss}}{mol\ l^{-1}} \times 10^{+7}$	$\frac{\Delta H}{kJ\ mol^{-1}}$	$\frac{K_{diss}}{mol\ l^{-1}} \times 10^{+6}$	$\frac{\Delta H}{kJ\ mol^{-1}}$
168	5.83	-3.6	1.91	-2.9	1.76	-2.4
188	4.53	-4.1	1.56	-3.3	1.49	-2.7
208	3.59	-4.6	1.29	-3.7	1.28	-3.1
228	2.78	-5.1	1.06	-4.1	1.08	-3.4
248	2.14	-5.6	0.86	-4.5	4.54	-3.7

again reflect this solvent's greater solvation of the free Cs^+ ion. Both these solvents must contribute some solvation stability to cesium ion pairs which the weaker DEE is apparently unable to provide.

The dissociation of perylene ion pairs may be compared with that of pyrene ion pairs in the K/MTHF and Cs/THF systems [3B.3]. The less negative ΔH^o and ΔS^o terms observed for perylene ion pairs arise because of the greater delocalisation of negative charge in the perylene anion. This lowers the Coulombic attraction between anion and cation and, since the degree of cation solvation depends on the competitive interactions of anion and solvent for the cation binding sites, leads to more extensive solvation in perylene ion pairs. Thus dissociation to the free ion state requires less change in the solvation sphere of the cation, resulting in smaller negative values for ΔH^o and ΔS^o.

Calculations based on the simple "sphere-in-continuum" model [section 3B.5] have often been in good agreement with observed dissociation parameters when bulky ions are present or when specific ion-solvent interactions are absent. On both counts, reasonable agreement might be expected for a number of these systems, especially Cs/MTHF. Using eqns 3.16 and 3.18 , values for K_{diss} and ΔH^o were calculated at a number of temperatures for MTHF solutions [Table 4.3]. Although none of the observed and calculated values correspond closely, the best agreement is found for the Cs/MTHF system. As with pyrene ion pairs, it appears that the sphere-in-continuum treatment is too simple to describe adequately the dissociation of the ion pairs of perylene studied in this project. Szwarc[36] found this model gave reasonable results for solvent-separated ion pairs in THF solution.

FIGURE 4.7

PLOT OF LOG K vs $\frac{1}{T}$ FOR THE INTERCONVERSION OF TIGHT AND LOOSE ION PAIRS

SYSTEM: PYL/Li/DEE

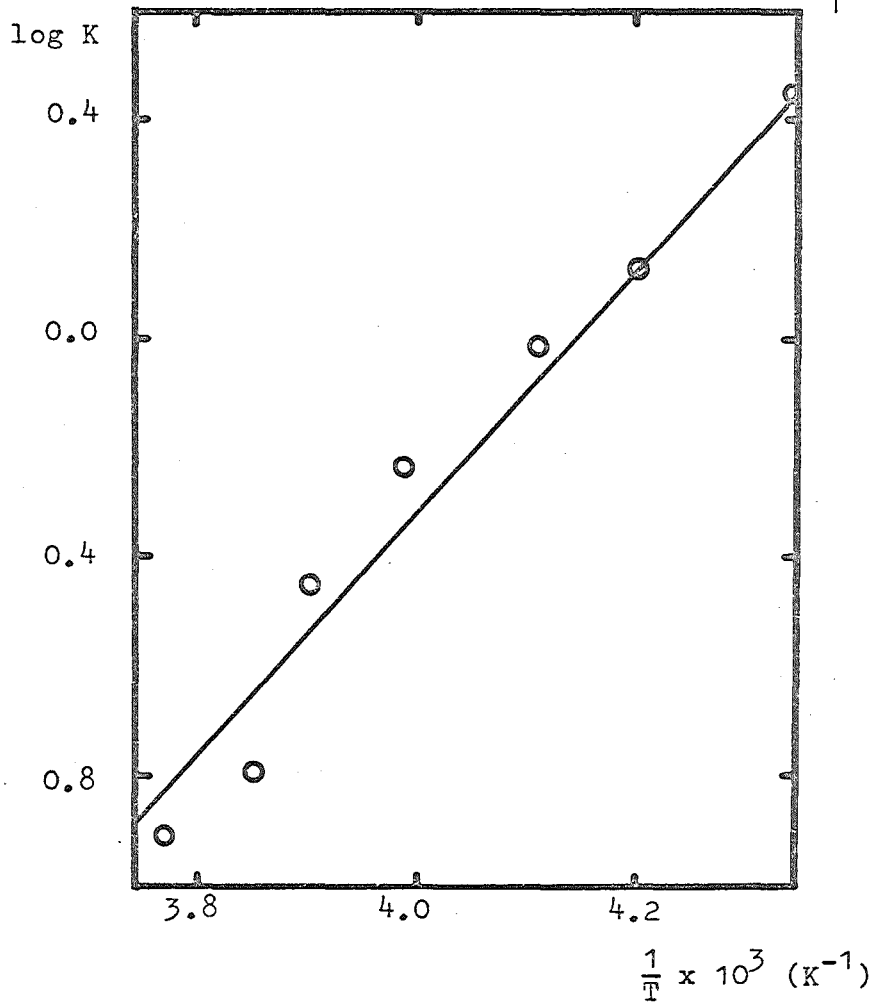

Table 4.4: Thermodynamic data for the interconversion of tight and loose ion pairs

System: PYL/Li/DEE

Temperature °C	K
-43	2.92
-35	1.37
-30	0.98
-22.5	0.59
-17	0.36
-13.5	0.16
-8	0.12
-3	0.0

$\Delta H^\circ = -39.0 \pm 1.5$ kJ mol^{-1}

$\Delta S^\circ = -165 \pm 8$ J k^{-1} mol^{-1}

K: $\pm$ 2%

4B.2 The Li/DEE system

The type of temperature dependence shown by the lithium hfs in DEE [Table A.1, Fig. 4.8] is often interpreted in terms of a dynamic equilibrium between different ion pair types.[44-46] In many such cases additional evidence is provided by linewidth effects, as found for the PY/Li/DEE system [section 3B.4]. However if the rate of interconversion of the ion pairs is very fast the lines become exchange-narrowed, so the absence of linewidth effects for the PYL/Li/DEE system does not preclude such an equilibrium.

If the equilibrium exists, the equilibrium constant may be determined from eqn 3.9:

$$K = \frac{a_{TIP} - a_{obs}}{a_{obs} - a_{LIP}}$$

From Figure 4.8, likely values for a_{TIP} and a_{LIP} are 0.051 G and 0.0 G respectively. Since the observed value of 0.051 G is constant over a temperature range, it seems reasonable, in this case, to assume this value of a_{TIP} is temperature independent. K may then be calculated and, from its temperature dependence, ΔH^{o} and ΔS^{o} may be found [Table 4.4]. A reasonably linear plot results from log K vs 1/T [Fig. 4.7], but this does not prove the process exists. The derived ΔH^{o} and ΔS^{o} values are almost identical to those for the same process in the pyrene system: ΔH^{o} = -34.3 kJ mol^{-1} and ΔS^{o} =-171 J K^{-1} mol^{-1}. The slightly higher enthalpy change for the perylene anion may reflect the fact that solvent-separated perylene ion pairs will be more solvated because of the more extensive delocalization in the larger molecule.

The existence of this equilibrium between tight and loose perylene ion pairs is only speculative. If it does exist, this analysis shows the derived thermodynamic parameters that describe

FIGURE 4.8

TEMPERATURE DEPENDENCE OF CATION SPIN DENSITIES IN PERYLENE ION PAIRS

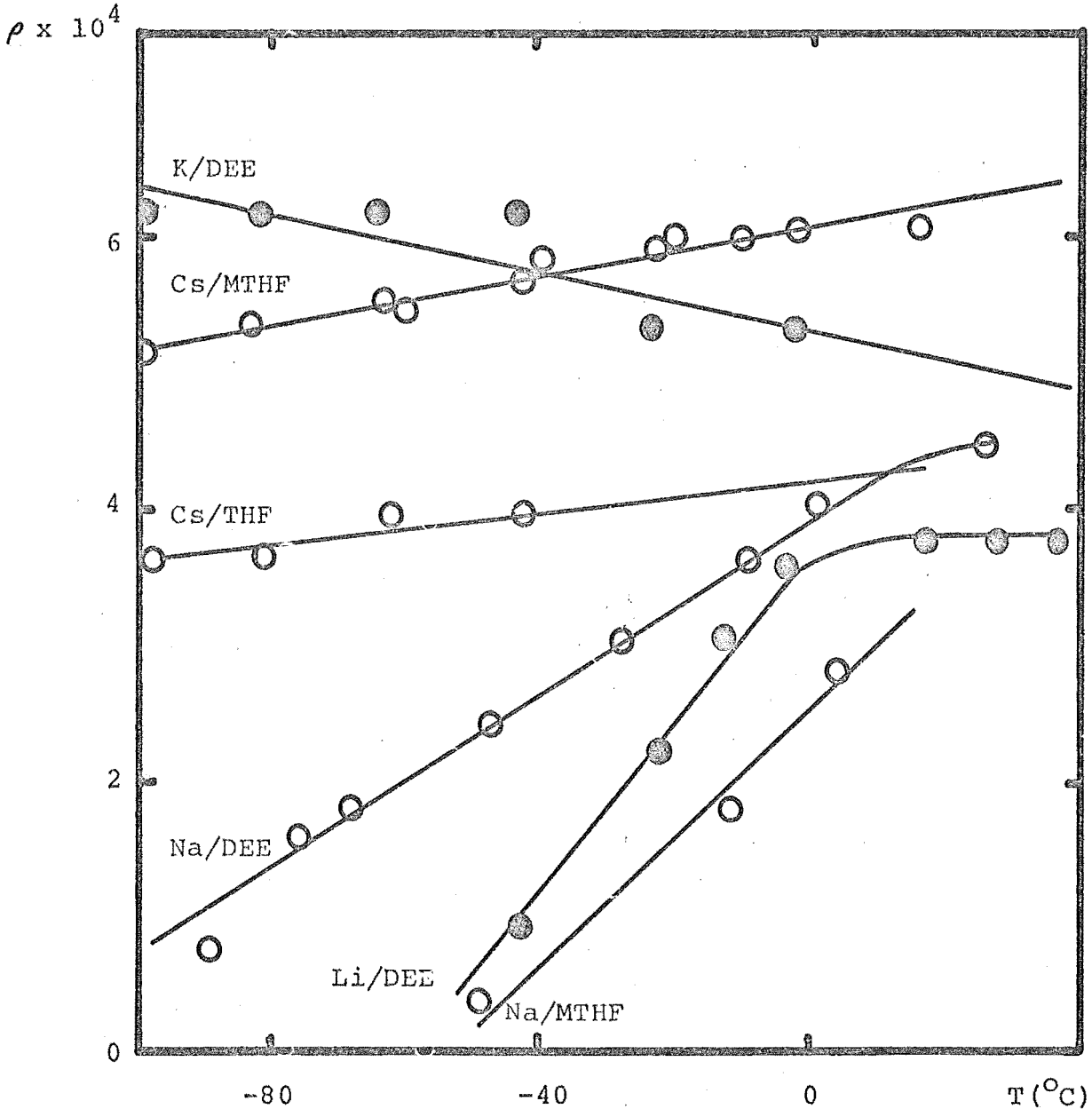

it are of the expected order of magnitude.

4B.3 Alkali metal coupling constants and ion pair structure

As detailed in section 3B.6, the sign, magnitude, and temperature dependence of the cation spin density often provide insight into the structure of ion pairs. A graph of $|\rho_m|$ vs T is shown in Figure 4.8 for perylene ion pairs. From the fact that da_M/dt is usually positive, the alkali metal hyperfine coupling constants in the Na/DEE, Na/MTHF and Cs/MTHF systems can be confidently assigned to be positive. For the Cs/THF system the data are limited but the coupling constant appears to be positive. In K/DEE, the coupling constant magnitude changes from 0.044 G to 0.051 G (experimental plotting limits:0.006 G) over a 100°C range. On the basis of a smooth change of ρ with increasing atomic number this coupling constant should be positive also. If the Li/DEE system can be represented by one species only (static model) then the lithium coupling constant is positive from its temperature dependence, but if the dynamic model applies [4B.2], it could equally well be negative.

To locate which positions correspond to minimum potential energy, interaction energy calculations [section 3B.10] were carried out*. The results, summarised in Figure 4.9, show energy minima above the "peri"-bonds, [position C of Fig. 4.9], and above the naphthalenic rings [position E], at short interionic distances. These minima disappear at greater ionic separations, being replaced by a shallow well above the centre of the molecule. However this calculation does not consider repulsion

---

* The "peri"-bonds that join carbon 15 (17) to carbon 20 (18) were taken to be 1.50 Å[111]; all other C-C distances were assumed to be 1.39 Å, and all bond angles 120°.

FIGURE 4.9

INTERACTION ENERGY CALCULATIONS FOR PERYLENE ION PAIRS

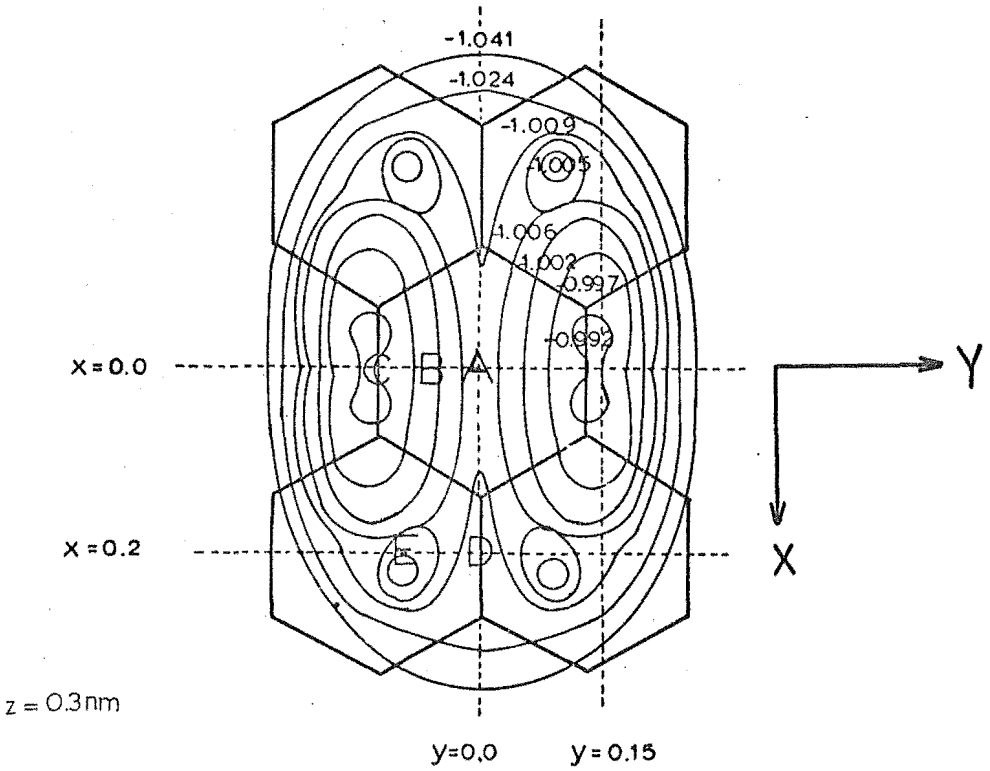

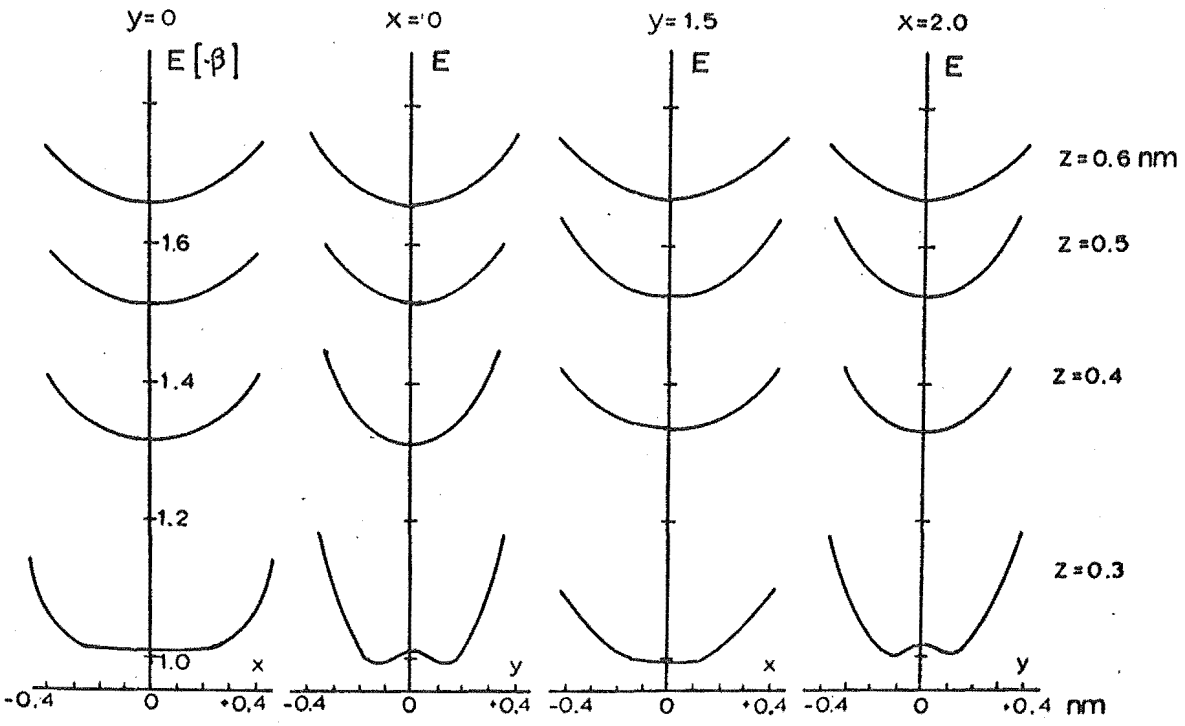

between the electrons in the π-system and those of the cation. At close interionic distances, the repulsion becomes important. At 3.0 Å, the most favoured position (from interaction energy calculations) is also a region where significant electron repulsion is expected. While it is difficult to estimate the precise effect of these opposing interactions, they probably shift the position of true minimum energy to somewhere between positions A and C, near position B. The energy minima over the naphthalenic rings are not shifted by these considerations.

To help locate the most likely position of the counter-ion, the unpaired electron density on sodium and lithium ions in ion pairs with the perylene anion were determined. When the centre of a sodium ion is 3.0Å above the nuclear plane of the anion, the spin density map shown in Figure 4.10 was calculated.

For the Na/MTHF system, the observed spin densities [Fig. 4.8] are readily obtained if the cation is situated near the centre of the molecule, even up to 4.0 Å from the molecular plane. The lack of negative hyperfine splitting at lower temperatures implies that the spin density decreases because of increased solvation. Insertion of a solvent molecule(s) between the ions greatly increases the interionic distance, so both ρ_o and ρ_1 are vanishingly small. The spin density calculations suggest this system contains tight ion pairs at higher temperatures, with the cation at position B or perhaps E, and loose ion pairs at lower temperatures, with the cation well away from the anion and probably above the centre. A similar description fits the Na/DEE system, where, because of the weaker solvating power of DEE, a lower temperature is required to produce the solvent-separated

FIGURE 4.10

CALCULATED SPIN DENSITY AT A SODIUM NUCLEUS

0.3nm FROM THE PERYLENE ANION

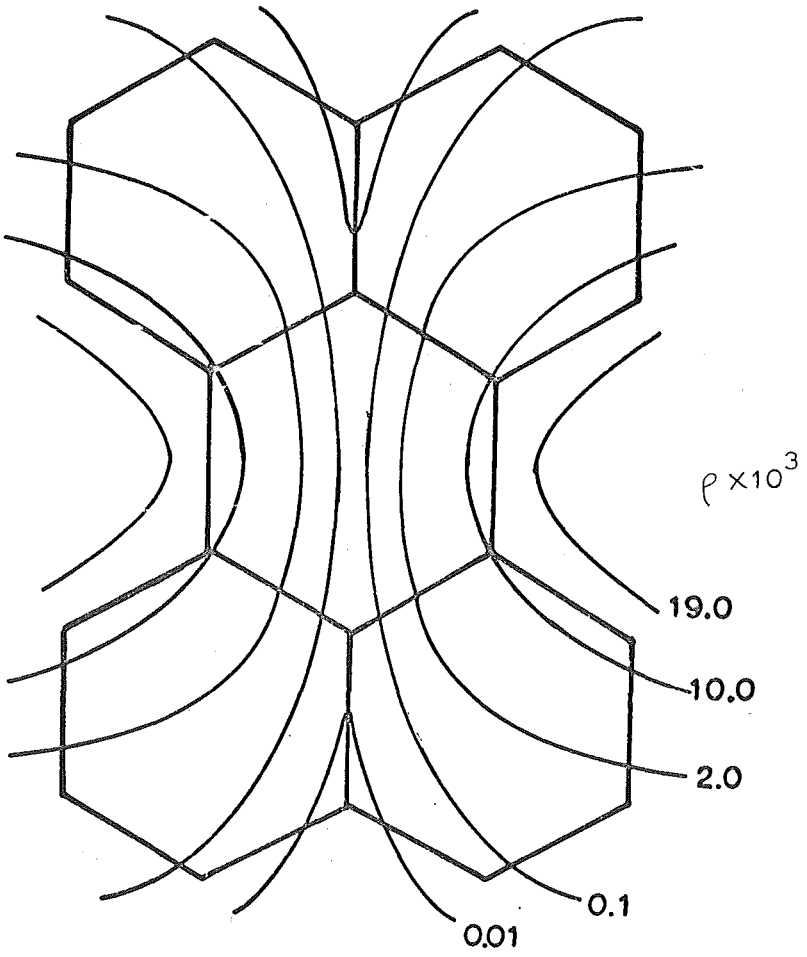

ion pairs [Fig 4.8].* Alternatively, this system could contain tight ion pairs at all temperatures, as it does with the pyrene anion.

Since the Li^+ ion is smaller and has a considerably greater polarizing field than the Na^+ ion, DEE solvates the lithium cation more easily. Thus, solvent-separated ion pairs are formed at considerably higher temperatures in Li/DEE than in Na/DEE [Fig. 4.8]. The variation in cation spin density between -60°C and 0°C may be explained in two ways: an equilibrium between tight and loose ion pairs as discussed in part 4B.2, or by the gradual formation of tight ion pairs from loose pairs as the solvating power of the solvent decreases with increasing temperatures and the cation moves closer to the anion. In this case the constant ρ may indicate a distance of minimum approach has been reached at $\sim$ 0°C. Such a minimum distance was envisaged by Goldberg and Bolton[31] when electron repulsion and interaction energy interactions oppose each other. For an ionic separation of 3.0 Å, the spin density calculations predict a value of 0.4×10^{-3} at about the positions expected for minimum energy: positions B or E. Since the dynamic model with very fast interconversion between the different ion pairs and the static model predict similar observations, they cannot be distinguished for this system.

The weaker solvation characteristic of larger cations allows the ion pairs in the Cs/THF, Cs/MTHF and K/DEE systems to remain tight throughout the temperature range. The average position of

---

* The weaker solvating power of DEE also allows the Na^+ ion to approach the anion more closely, or at least spend more time at the position of minimum energy. Since the most favoured position (B or E) is not a nodal plane, a higher positive spin density results. This is in contrast to the pyrene case, where the minimum energy position was over a nodal plane and the sodium spin density was greater in MTHF than in DEE (pp. 49-50).

FIGURE 4.11

CALCULATED PROTON HYPERFINE SPLITTINGS IN PERYLENE ION PAIRS FOR VARIOUS CATION POSITIONS AND HEIGHTS ABOVE THE ANION PLANE

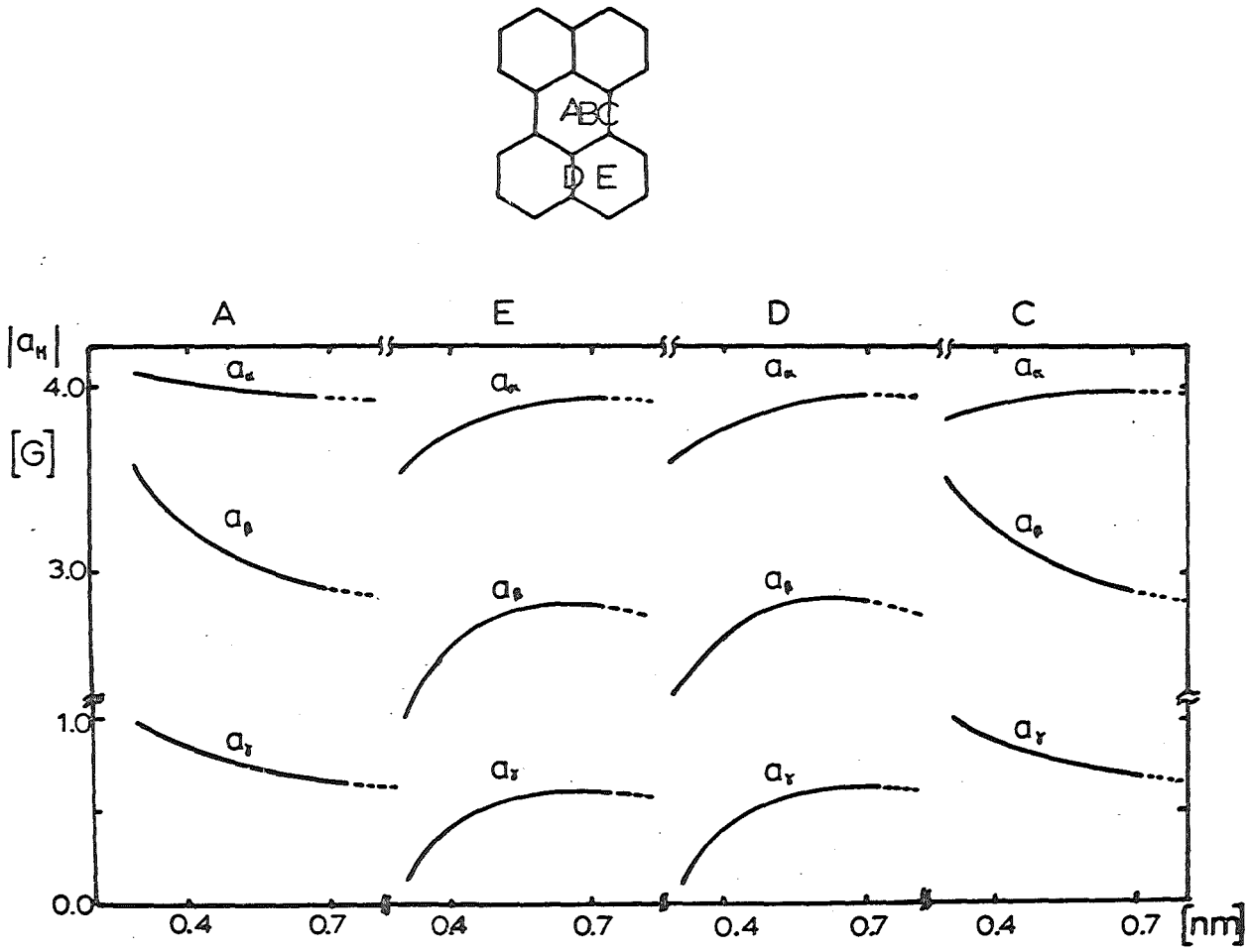

these cations may be slightly out of the nodal plane, between A and B. This is consistent with the movement toward the centre of the molecule of the minimum energy position as the interionic distance increases and with the (assumed) positive sign of the coupling constant.

In the K/MTHF system, no metal hfs was resolved although broadening was noted at higher temperatures. Because the magnetic moment of potassium is small, a coupling constant of only 0.025 G (would lead to the observed broadening) gives rise to a spin density of $\sim 3 \times 10^{-3}$. This is of the same order as the spin density in the tight ion pairs of Na/MTHF and Na/DEE. Hence the lack of a resolved potassium splitting does not rule out the formation of tight ion pairs that was indicated by the thermodynamic data [4B.1].

4B.4 Proton coupling constants: observations and calculations

McClelland-type calculations [section 3B.10] were performed with the cation placed in a number of likely sites: A, C, D, E. The calculated coupling constants are shown in Figure 4.11.

As with pyrene systems, there appears to be no single trend correlating all the observed coupling constants in perylene ion pairs. For those systems where both ion pairs and free ions were present simultaneously, the magnitudes of the coupling constants of the free ion were smaller than those of the ion pair. This behaviour is predicted by placing the cation at A or perhaps C, but not at D and E. The γ coupling constant in particular, seems to be a sensitive indicator of the amount of cation perturbation. In systems where tight ion pairs are formed, $|a_\gamma|$ is always larger than in systems where loose ion pairs or free ions

are present. Only sites A or C predict this observation.

From considering the interaction energy and cation spin density calculations [4B.3] it was concluded that the most likely cation position in tight ion pairs was either between A and C or near E. The calculations of this section strongly favour the former site. Although only limited weight should be given to calculations of this type, because of the small nature of the observed changes and the various approximations in the treatment, a cation position near position B in tight ion pairs and A in loose ion pairs does provide agreement between the calculated and observed quantities.

4B.5 The g-values and ion pair structure

The positive g-shift on ion pair formation observed in these perylene systems is unusual. Frequency measurements were made only for the large g-shift in the Cs/MTHF system but small positive shifts were noted for three other systems where ion pair and free ion spectra were simultaneously observed. The magnitude and direction of g-shifts has been used by Brustolon et al.[112] to assign likely structures to ion pairs of the naphthalene (negative shift) and biphenylene (positive shift) systems.

From Stone's theory of g-values,[113] changes due to ion pairing require a small contribution from a metal p orbital to the ground state wave function of the ion pair. Only the p_z orbital has an appreciable overlap with the single electron's MO if the cation is located over the radical plane. Spin orbit interaction can then couple this ground state with configurationally excited states involving p metal orbitals, resulting in a g-value shift; this shift is proportional to ζ and inversely

proportional to the energy difference between the ground and excited states.[113] On both counts, greater g-value shifts are expected for the larger alkali atoms. According to Brustolon,[112] a negative g-value shift arises from excited states which mix metal p orbitals with the singly occupied π MO (Ψ^{π}_{m+1}), while a smaller positive shift may arise from excited states which mix the p orbitals with the highest doubly occupied π MO (Ψ^{π}_{m}). Brustolon reasoned that since these contributions to the g-factor depend on the location of the cation relative to the anion, the magnitude and sign of the shifts may provide some insight into the geometry of the ion pair.

For naphthalene, Brustolon[112] considered that placing the cation in a position where Ψ^{π}_{m} has a nodal plane but Ψ^{π}_{m+1} does not, resulted in a negative shift. For biphenylene, a position where Ψ^{π}_{m} is not nodal but Ψ^{π}_{m+1} is, was predicted to give a positive shift in agreement with experiment. However, consideration of the likely cation sites [A,C,D and E of Fig. 4.9] and the nodal properties* of Ψ_{10} and Ψ_{11} of the perylene anion, predicts negative and not positive shifts. With this approach it is also difficult to predict the negative shifts observed in the pyrene systems [section 3B.9]. Fraenkel[50] has noted that the direction of the g-factor change on ion pair formation may not be as significant as the usual trends might suggest.

4C. Conclusion

Loose ion pairs are formed throughout the temperature range studied in all the DME and THF systems, except Cs/THF. This and the K/DEE, K/MTHF, and Cs/MTHF systems form tight ion pairs at all temperatures. In the Li/DEE and Na/MTHF systems, the tight pairs which are present at higher temperatures are converted to

---

* For Ψ_{10}, xz and yz are nodal planes; for Ψ_{11}, xz is nodal

loose ion pairs on cooling. The same may apply to the Na/DEE and K/MTHF systems or they may remain as tight ion pairs at lower temperatures.

In the solvent-separated ion pairs the cation is probably centred over the anion and 5.0Å or more from it. The cation appears to reside somewhere between the central position and the "peri"-bonds in the tight ion pairs, at ionic separations varying from 3 - 4Å.

FIGURE 5.1

STRUCTURAL FORMULAE FOR NAPHTHALENE AND THE DIMETHYL NAPHTHALENES

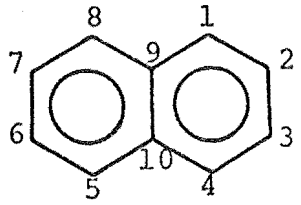

NAPHTHALENE

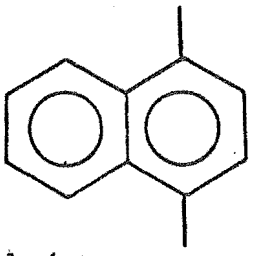

1,4DMN

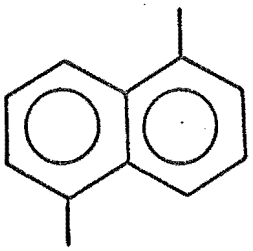

1,5DMN

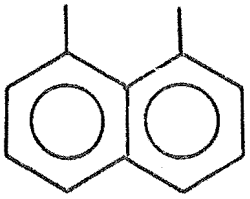

1,8DMN

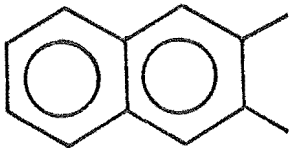

2,3DMN

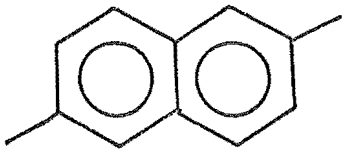

2,6DMN

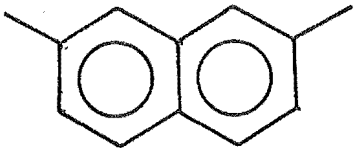

2,7DMN

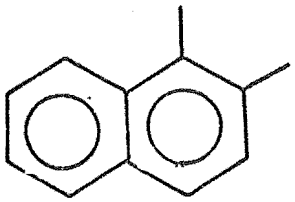

1,2DMN

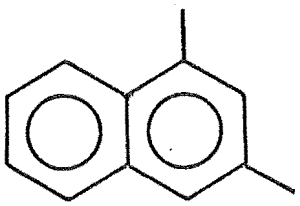

1,3DMN

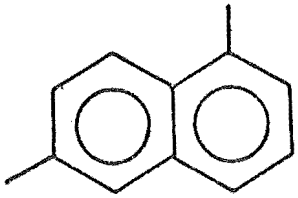

1,6DMN

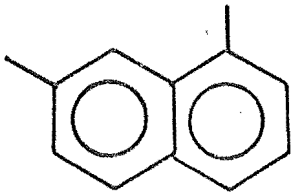

1,7DMN

CHAPTER FIVE

NAPHTHALENE AND THE DIMETHYLNAPHTHALENES

This chapter is subdivided. The Introduction (section 5.1) contains details of the preparations, spectral simulation, and types of calculations performed. The spectra of naphthalene and the symmetric dimethylnaphthalenes are discussed for individual metal/solvent systems in sections 5.2 - 5.9. The trends for this series of compounds are then discussed and compared in section 5.10 and the unsymmetric dimethylnaphthalenes are considered in section 5.11.

5.1 Introduction

Naphthalene (N) and the six symmetrical dimethylnaphthalenes (DMN) [Fig. 5.1] were reduced by sodium and potassium metals in DME, THF, MTHF and DEE. The Na/DEE combination produced no significant reduction of the DMNs over a period of two weeks, despite several attempts for each compound and storing at various temperatures. The four unsymmetric dimethylnaphthalenes [Fig. 5.1] were prepared in the K/DME system only.

Spectra were usually obtained at $\sim 20^{\circ}C$ intervals from about $-100^{\circ}C$ to room temperature, with the central lines recorded more frequently when metal hyperfine coupling was present. All spectra were measured manually, and spectral simulation then carried out of representative spectra of a given system. All metal hfs were determined by computer simulation. The coupling constants used in the simulated spectra are listed in Tables A.3 A.4 and A.5 [Appendix A]. Spectra at intervening temperatures fit

observed trends. Where a metal splitting was assumed because of line broadening but was not resolved, it is in brackets.

The methyl- and ring- proton splittings were assigned to molecular positions on the basis of calculated values and previous assignments.[69,71] The aromatic proton coupling constants are undoubtedly negative and those of the methyl-protons positive.[71] The temperature dependence of the metal hfs indicated positive coupling constants in all cases.

Interaction energy and coupling constant calculations using the McClelland treatment[39] [section 3B.10] were again performed to assess the electrostatic perturbing effect of the cation and its most favoured position relative to the anion. Various models have been proposed to account for the effects produced by substituting a methyl group for a hydrogen in an aromatic system and discussed many times.[71,114,115] It appears that the hyperconjugation model plus a small inductive effect gives the most satisfactory results.[71,114,115] In this model, the methyl group is treated as a modified vinyl group, $C\text{-}C'\text{-}H_3$, where C is the substituted carbon atom of the original π system, C' represents the carbon of the methyl group, and H_3 is the pseudo-atom corresponding to a group of three hydrogens. The Coulomb- and resonance- integral parameters are then defined by the expressions:

$$\begin{aligned} \alpha_C &= \alpha + \delta_C\beta, & \beta_{CC'} &= k_{CC'}\beta \\ \alpha_{C'} &= \alpha + \delta_{C'}\beta, & \beta_{C'H_3} &= k_{C'H_3}\beta \\ \alpha_{H_3} &= \alpha + \delta_{H_3}\beta, & & \end{aligned} \qquad (5.1)$$

The parameters determined by Lazdins and Karplus[115] for the toluene anion:

$$\delta_{C'} = -0.05, \quad \delta_{H_3} = -0.5, \quad k_{CC'} = 0.86, \quad k_{C'H_3} = 2.50 \qquad (5.2)$$

were used, with the small inductive effect included as $\delta_C = 0.15$.

FIGURE 5.2

INTERACTION ENERGY CALCULATIONS FOR NAPHTHALENE AND DIMETHYLNAPHTHALENE ION PAIRS

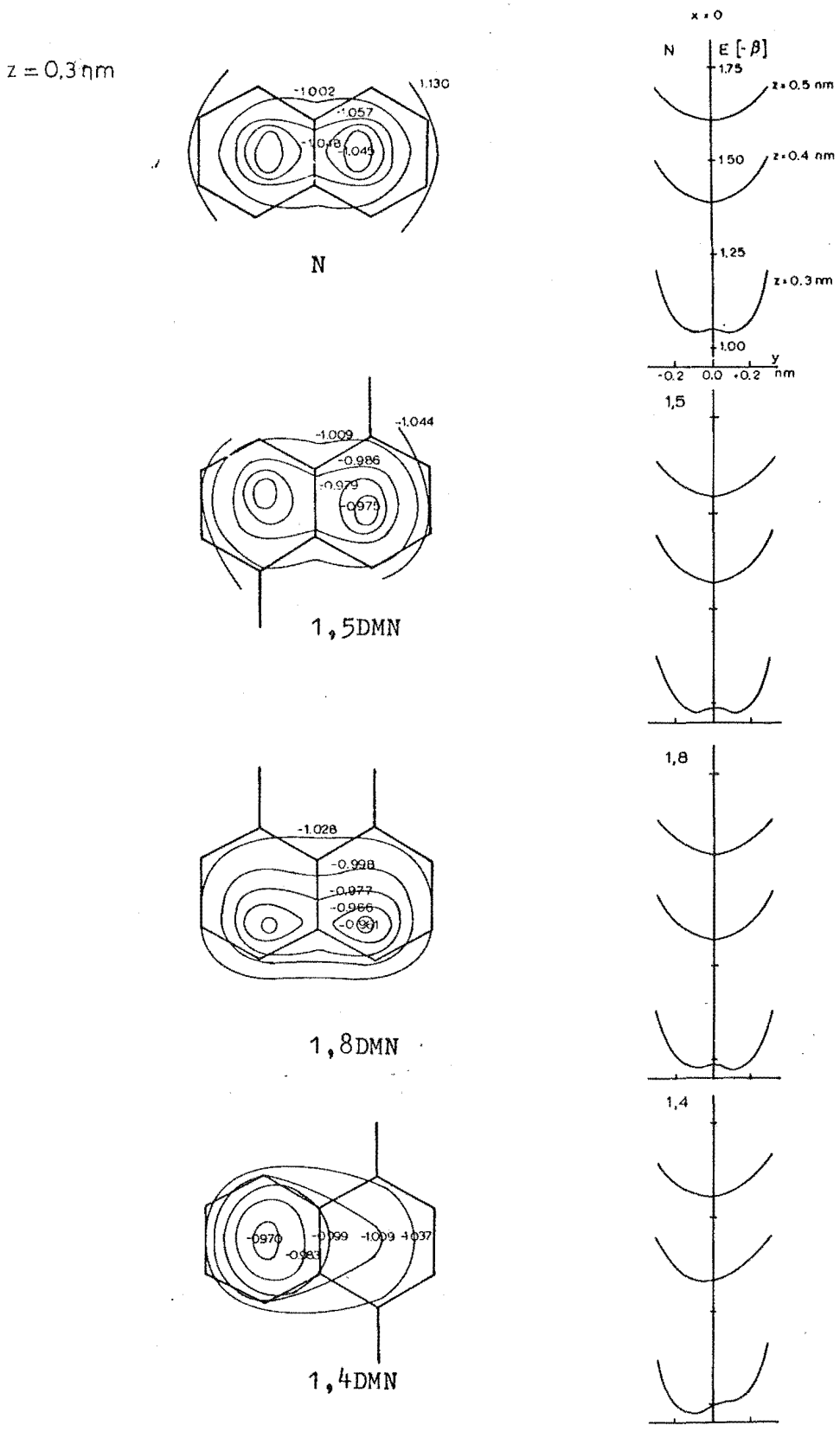

...ctd

The spin densities calculated by this model were compared to the observed ring proton coupling constants (a_{H_i}) by using McConnell's relation [15]

$$a_{H_i} = Q\rho_{C_i} \qquad (5.3)$$

where proton H_i is attached to carbon C_i. Q was taken to be -26.0G. For calculating the methyl-proton splittings from spin densities, an expression analogous to McConnell's can be used [117]

$$a_{CH_3{}_i} = Q'\rho_{C_i} \qquad (5.4)$$

where the i^{th} methyl group is bonded to the i^{th} aromatic carbon*. Values of Q' vary from ~20 - 35 G; Q' = 26.0 G was chosen unless otherwise stated. Correlations of theoretical spin densities with experimental coupling constants have been performed a number of times to test other expressions relating the two,[71,74,115] but since the purpose of this project was to investigate ion pairing effects, only the simple expressions [Eqns. 5.3 and 5.4] were used.

The interaction energy maps calculated by this model [Fig. 5.2] determine the most favourable cation positions allowing for only the electrostatic effects of the methyl groups. There is an additional steric interaction arising from the bulk of the methyl group and the finite size of the cation, which favours cation positions away from the site of methyl substitution. This tends to reinforce the electrostatic effect, producing an extra "hardening" of the walls of the potential energy well near the methyl groups. Both effects mean that the 2,3- and 1,4- DMNs, with both methyl groups in the same ring, are different from the other compounds in the series. They have energetically favoured

---

* In this project, $a_{CH_3} \equiv a_{Me}$ always relates to the proton constant of the methyl group.

FIGURE 5.2 (ctd).

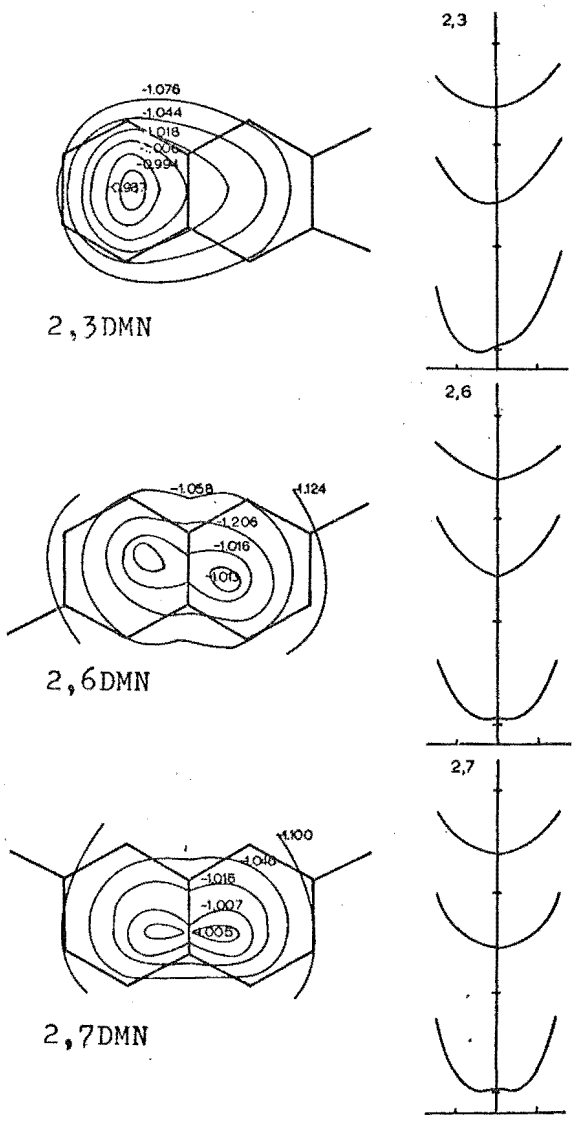

sites which are no longer symmetrically placed about the centre of the naphthalene skeleton and these sites are of unequal energy. Thus any motion of the cation between the two most favoured positions is between inequivalent sites for the 2,3- and 1,4- compounds, but between equivalent sites in the remaining compounds. This has important consequences in determining ion pair structure and cation motion.

Two pertinent observations can be made from Table A.3 regarding the proton hfs in the DMN anions. Firstly, the values of a_5 and a_{Me} in 1,4DMN and of a_5 and a_1 in 2,3DMN change considerably ($\sim$ 0.5 G) as the solvent/metal combination is altered, with the more strongly solvating systems (e.g. Na/DME) having smaller a_5 and larger a_{Me} (a_1) coupling constants than the weaker solvating systems (such as Na/MTHF). In all other DMN systems, the changes in coupling constants with changes in metal and solvent are much smaller ($\sim$ 0.1 G). This strongly suggests that the geometries of tight and loose ion pairs in 2,3- and 1,4- DMN are significantly different, apart from the usual increase in ionic separation. The McClelland-type perturbation calculations show that when the cation is placed over a ring position, the coupling constants in that ring increase considerably while those in the other ring decrease. Thus the observed changes in the proton hfs indicate that the mean position of the cation in the tight ion pairs of 1,4- and 2,3- DMN is nearer the unsubstituted ring than it is in loose ion pairs. Further, the lack of coupling constant change in the other DMNs indicates that the mean position of the cation in their tight and loose ion pairs is the same. These conclusions also follow from the interaction energy maps discussed earlier [Fig 5.2] which predict the mean position of the cation to be over the centre of the

Table 5.1: Calculated Coupling Constants[a] for naphthalene and the symmetric dimethylnaphthalenes.

Compound	Position	HMO	McL	INDO	Exptal[b]
N	2	1.8	1.1	0.9	1.8
	1	4.7	5.9	5.3	4.9
1,5DMN	2	1.5	0.9	1.1	1.1
	3	1.8	1.2	0.8	2.4
	4	4.5	5.7	5.0	4.5
	CH_3	4.6	5.8	6.5	4.4
1,8DMN	2	1.3	0.6	1.3	1.7
	3	2.0	1.5	0.5	1.8
	4	4.4	5.4	5.1	4.5
	CH_3	4.7	6.0	7.5	4.6
1,4DMN	2	1.5	0.9	1.0	1.7
	6	1.8	1.2	0.8	1.8
	5	5.1	6.4	4.6	5.6
	CH_3	4.1	5.1	7.3	3.0
2,3DMN	CH_3	1.9	1.4	1.4	1.7
	6	1.8	1.1	0.9	1.8
	1	4.3	5.5	5.7	4.3
	5	4.7	6.0	4.9	5.2
2,6DMN	CH_3	1.4	0.7	1.8	1.2
	3	2.3	1.9	0.7	2.8
	1	4.4	5.7	5.3	4.6
	4	4.7	5.8	5.2	4.8
2,7DMN	CH_3	1.7	1.2	1.8	2.1
	3	2.0	1.4	0.8	1.8
	1	4.2	5.3	5.3	4.4
	4	4.9	6.2	5.1	5.2

a) Details of calculations in text; the aromatic proton coupling constants are negative, the methyl proton coupling constants are positive; methods abbreviated as in Table 3.8.

b) Since the experimental coupling constants depend on metal, solvent, and temperature, only an approximate value can be listed here. Accurate values for each system are in Table A.3.

anions for all interionic distances, except for the 2,3 and 1,4 compounds.

It follows that for 2,3- and 1,4- DMNs the values of a_5 and a_1 and of a_5 and a_{Me} respectively provide an indication of the state of solvation in a given system. Larger a_5 and smaller a_1 (a_{Me}) values indicate tighter ion pairs. The precise value of the coupling constants in the tight and loose ion pairs will depend on metal, solvent, and temperature.

The second observation from Table A.3 is that in most systems, the values of the large coupling constant decrease slightly as the temperature rises. This implies that, for a given type of ion pair structure, the effect of weaker solvent interaction (equated with increasing temperature) decreases the large splittings slightly, as the McClelland calculations[39] generally predict for structures where the cation is placed above the centre of the molecule or is oscillating between positions above the two rings.

Combining these two observations, the conversion of a loose to a tight ion pair in the 2,3- and 1,4- DMNs should be accompanied by a large decrease in a_1 (a_{Me}) and a smaller increase in a_5. For the other anions no significant changes are expected.

INDO calculations[80] were also carried out to assess the accuracy of this approximate self-consistent field method in predicting the observed coupling constants through a series of methyl-substituted compounds. For naphthalene, the calculated values tend to be too high for the β and too low for the α positions. Deviations from the experimental values is even greater with the dimethylnaphthalenes [Table 5.1]. The much more empirical Huckel method predicts the trends and

FIGURE 5.3

TEMPERATURE DEPENDENCE OF SODIUM HYPERFINE SPLITTINGS

SYSTEM : Na/DME

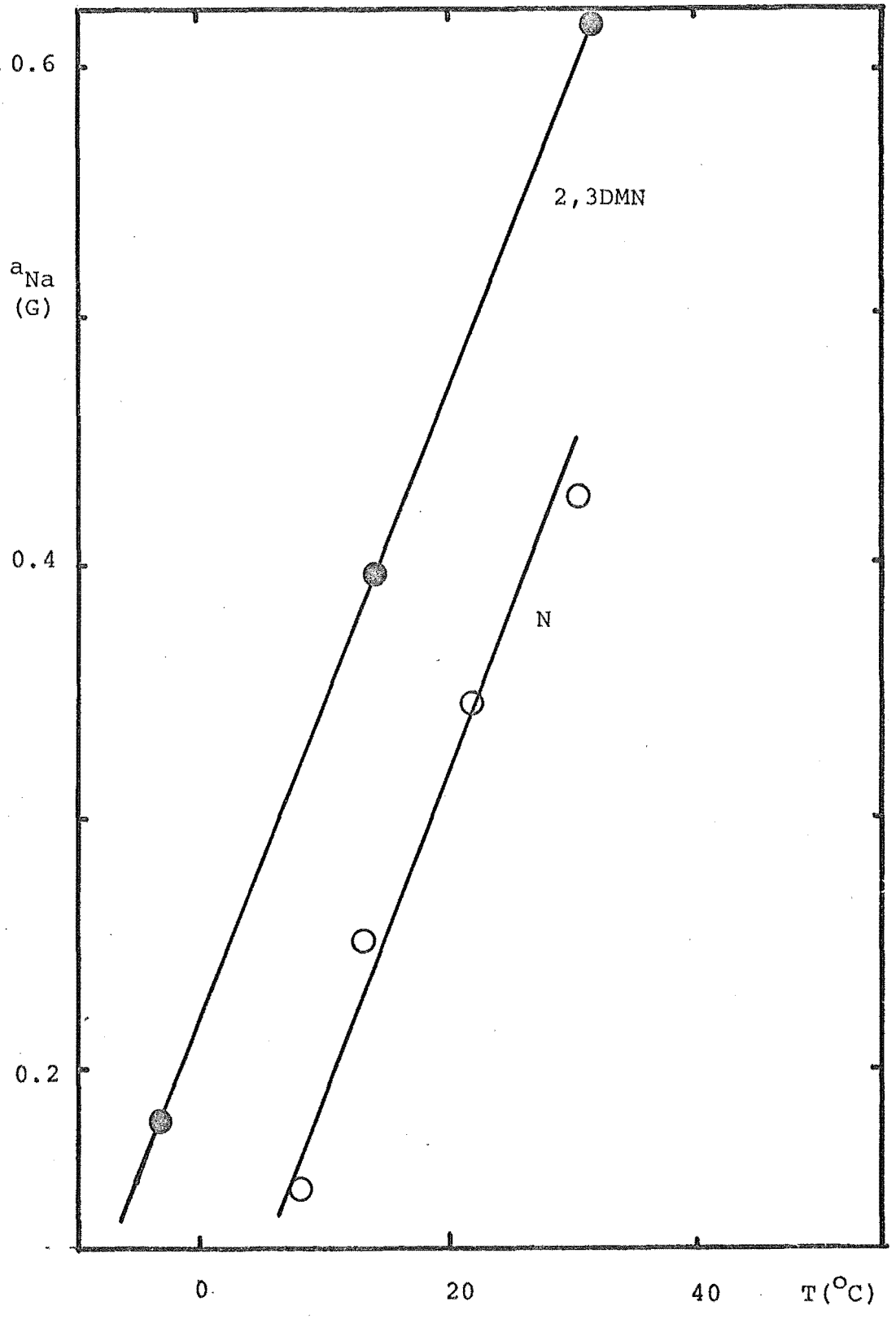

observed values far more accurately. The lack of success with the INDO treatment may be partly due to the choice of bond lengths and angles. For all calculations, the aromatic bond lengths were taken to be 1.39Å, the C-H bond lengths 1.084Å, and the aromatic carbon-methyl carbon distance 1.52Å. The aromatic bond angles were all assumed to be 120° and HCH angles of the methyl group 109.47°.* The orbital energy convergence factor was decreased by an order of magnitude to 10^{-5}, and the calculations performed in single precision.

5.2: Na/DME systems

A Observations

For all six DMNs and N, this combination of metal and solvent resulted in narrow lines and well-resolved spectra at low temperatures. From above $\sim -60° - -50°C$ the lines broadened and led to spectra of low intensity at higher temperatures. This observation was quite general and reversible and was not a concentration effect. With the 2,3-, 2,6- and 2,7- DMNs and N, a sodium splitting was resolved above $\sim 0°C$ [Fig. 5.3], while all lines of the 1,5-, 1,4- and 1,8- DMNs continued to broaden. For N and 2,3DMN, the $\pm$ 3/2 components of the resolved sodium hfs were clearly broader than the $\pm$ 1/2 components, as shown for the

---

* There is a good deal of evidence to show that in some DMNs there is a significant amount of steric interaction. In particular, peri-interactions between the methyls in 1,8DMN causes molecular distortions, as determined by its crystal structure[118] and by ^{13}C[119] and ^{1}H[120] nmr spectroscopy. There is also steric interaction between the peri-H (on C8) and a methyl group on Cl.[119,121] and between the methyls in 1,2- and 2,3- DMN.[119]. None of these distortions were allowed for in the molecular geometries assumed for the calculations.

naphthalene centre lines:

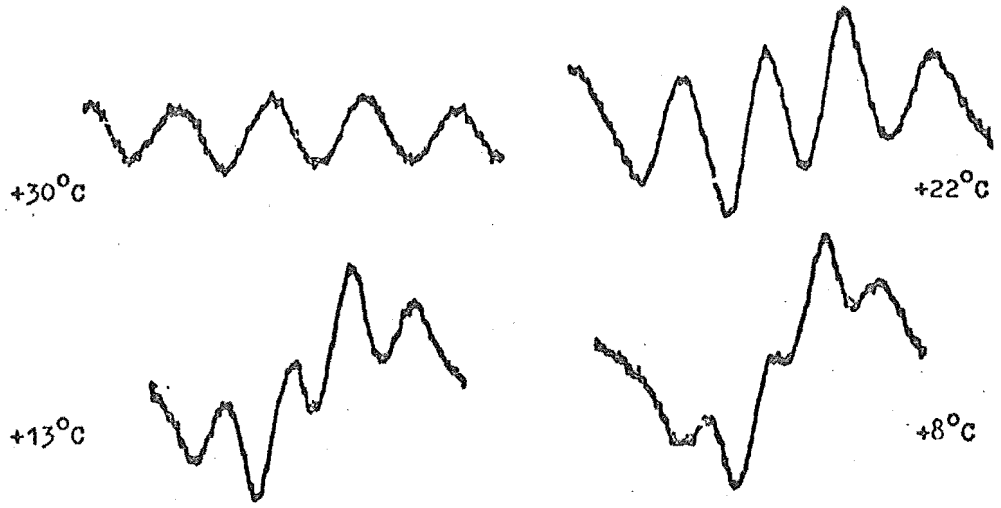

The remaining spectra had such low intensity and broad features at higher temperatures that this effect could not be conclusively determined, but was probably present. Previously reported "free ion" signals[49] were not observed in this system and were probably due to potassium impurities in those samples.[81]

A Discussion

No previous studies of this system reported any metal hfs for the DMNs.[69,71,74] However, sodium splitting in the naphthalene system has been noted by Hirota[53], Reddoch,[49] Fraenkel,[50] and Tuttle[123], although only Hirota has reported the linewidth effect. These sodium hfs compare well with those observed in this project, as does the temperature dependence reported by Hirota and Tuttle [Fig. 5.3]. The nmr experiments of Hendricks[98] and Hirota[53] have shown this splitting is positive at all temperatures. Reddoch's[49] proton splittings are also in close agreement to those found in this work.

Proton coupling constants have been reported for all six DMNs in this system by Gerson[69] (at -70°C) and by Peake[74] (at -85°C), who found temperature independent values and considered this system to contain free ions, with the exception

of 2,3DMN (and possibly 1,8DMN) at higher temperatures. Although there are a few differences [Table A.3], the agreement is satisfactory. The only other DMN coupling constants reported for this system are those of Campion[71] for the 1,4 compound at -70°C [Table A.3], and these values are identical to those found here.

Since metal coupling constants were resolved in some systems at high temperatures, the broadening observed in all others was considered to be due to unresolved metal splittings. To account for the observed M_I(Na)- dependent linewidth broadening, it is tempting to postulate an equilibrium between tight and loose ion pairs [section 3B.4]. This situation usually gives rise to a characteristically curved temperature dependence for a_M. Although followed over a limited temperature range only, the resolved sodium hfs increases smoothly as the temperature is raised in these systems* [Fig. 5.3], so that, as has been pointed out for the N/Li/MTHF system,[87] there is no justification for assuming the existence of only two types of ion pair. Hirota's more extensive data[53] suggests that, at higher temperatures, the temperature dependence of a_{Na} for the N/Na/DME system becomes nonlinear.

Assuming an equilibrium between tight and loose ion pairs does exist, the thermodynamic parameters cannot be confidently derived for it, since a realistic value of a_{TIP} is needed at each temperature to estimate K [eqn. 3.9], and K is required to calculate the rate data [eqn. 3.10]. The existence of this equilibrium would suggest that only solvent-separated ion pairs are present below ~-50°C, as concluded by Szwarc from spectro-

---

* The static model, depicting a gradual change from a loose to tight ion pairs, predicts this type of temperature dependence, but not the linewidth effect.

FIGURE 5.4

CENTRE LINES OF THE ESR SPECTRA FOR THE N/Na/THF SYSTEM

Scan range: 4G/40cm

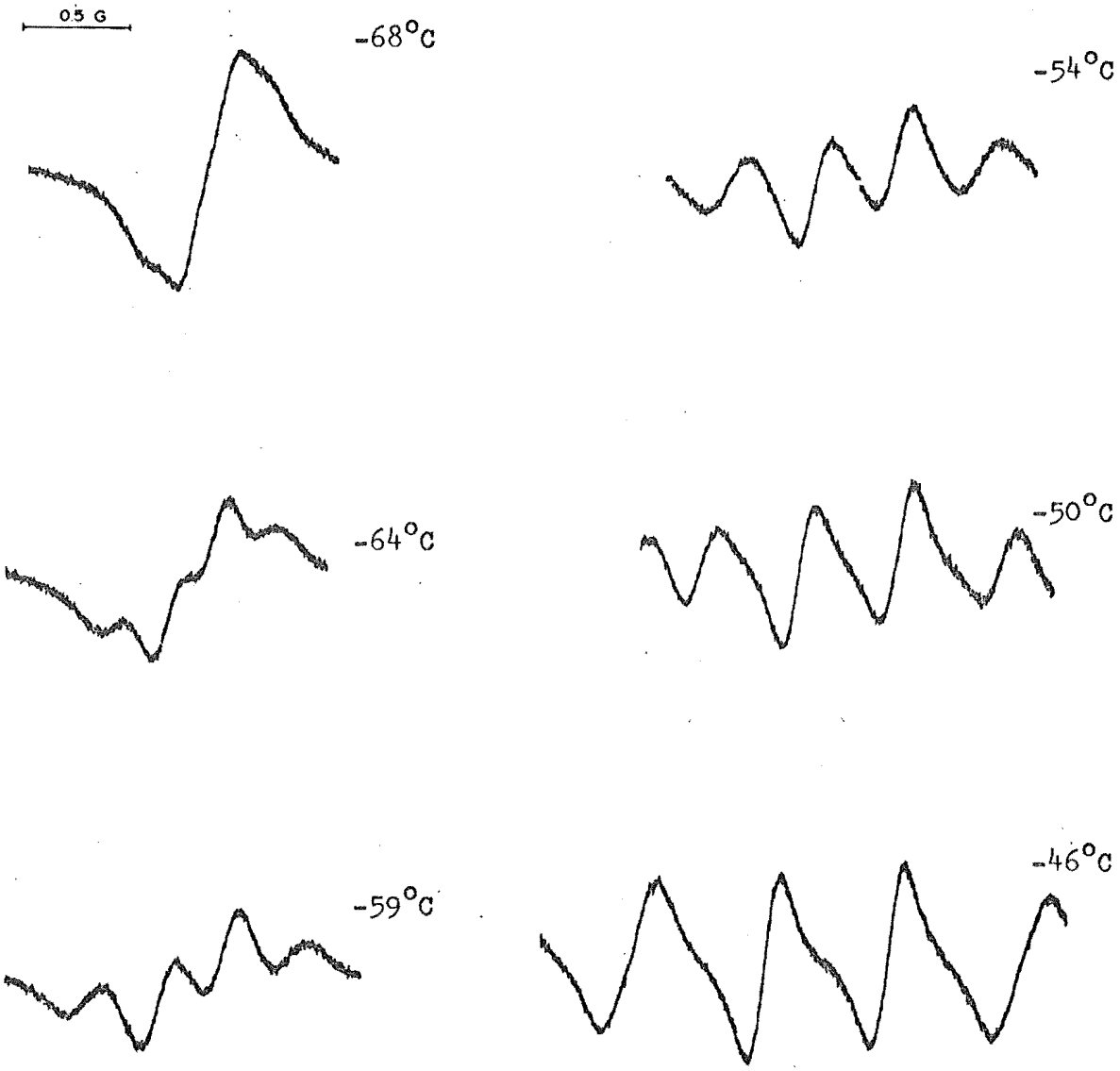

photometric methods.[122] Above this temperature, the free energy gain due to cation solvation is no longer enough to prevent some loose ion pairs from collapsing to tight ion pairs, which increase in relative concentration as the temperature is further increased. The equilibrium would need to operate over a large temperature range, as the spin density expected for a sodium cation in a tight ion pair with naphthalenic systems is not realised until at least 100°C, according to Hirota's graph.[53] The decrease in the proton hfs as the temperature is raised [Table A.3] presumably reflects the formation of tight ion pairs.

In summary, the limited data available indicates ion pairs are formed in this system but does not allow analysis of the ion pair equilibria involved. A rapid tight to loose ion pair equilibrium appears to be operating over a large temperature range, above $\sim$-50°C.

5.3: Na/THF systems

A Observations

All spectra exhibited the same kind of changes with temperature. At low temperature ($<\sim$-100°C) single, narrow lines were obtained. As the temperature was increased, these lines broadened and by -70°C the amplitude of all signals was very low. Between $\sim$ -70 to -45°C, a sodium hyperfine splitting emerged with the outer components ($M_I = \pm 3/2$) broader than the inner lines ($M_I = \pm 1/2$) [Fig. 5.4]. Increasing the temperature sharpened all the lines and increased the sodium splitting. Because of the similarity of the behaviour of these compounds in this metal/solvent system, only one system, N/Na/THF, was more thoroughly analysed for linewidth broadening by recording spectra

FIGURE 5.5

TEMPERATURE DEPENDENCE OF SODIUM HYPERFINE SPLITTINGS

SYSTEM : Na/THF

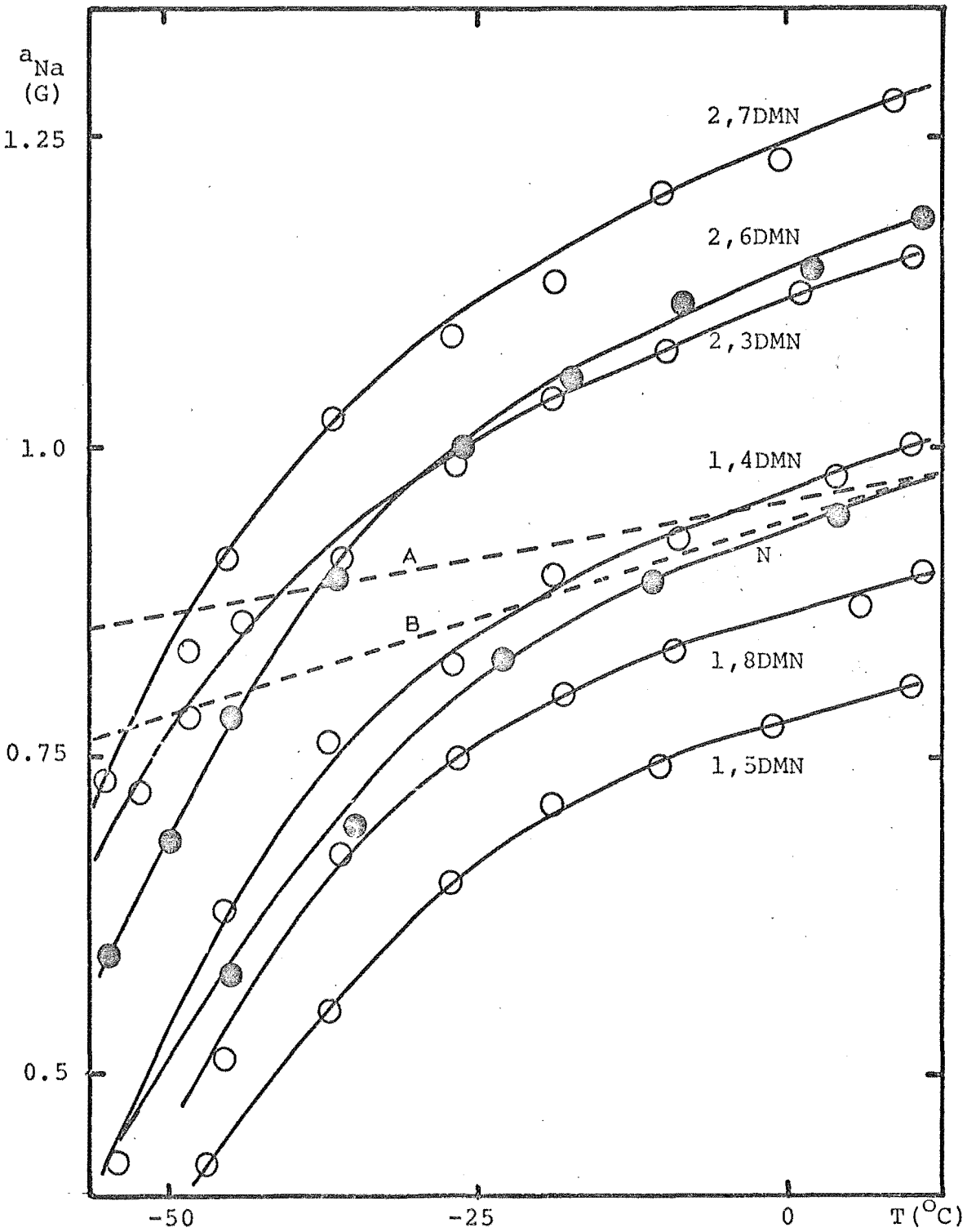

on an expanded scale (4G/40 cm). The temperature dependence of the metal coupling constants is shown in Figure 5.5.

B Discussion

The N/Na/THF system has been the subject of numerous studies. Atherton and Weissman,[18] Reddoch,[49] Hirota,[45] and Fraenkel[49] have all reported sodium hyperfine constants in good agreement with those observed here, as are Reddoch's[49] proton splittings. Nmr studies[53,98] have shown that the sodium coupling constant is positive. A number of these studies also report the superposition of free ion and ion pair spectra, but peaks due to the free ion were not detected under the conditions used in this study. Conductance studies[36] have proved that the concentration of free ions was too low to account for the reported intensities of "free ion" peaks in early esr studies.[18] Similarly, electron transfer rate studies [34,47,124] indicated these signals (or at least part of them) were not due to the free ion. Recently Tuttle[125] provided some explanation for the discrepency between the esr and other results in terms of potassium impurities [section 3A, PY/Na/DEE system]. From Szwarc's[36] ion pair dissociation constants, some free ion lines would have been expected under the conditions used here, and the failure to observe them is surprising. Tuttle[123] found a similar absence of free ion signal in the biphenylene/Na/THF system where calculations showed an equal amount of ion pair and free ion should have been present. An additional set of spectral lines of low intensity was observed in the 2,6DMN system and were simulated at -45°C with a_{Me} = 1.222 G, a_3 = 2.629 G, a_1 = 4.656 G, a_4 = 4.797 G, a_{Na} = 0.0G. An additional set of lines of even lower intensity was observed for 2,3DMN in this system. These species may be the free ion.

FIGURE 5.6

PLOTS OF LOGK vs $\frac{1}{T}$ FOR THE INTERCONVERSION OF TIGHT AND LOOSE ION PAIRS

SYSTEM : N/Na/THF

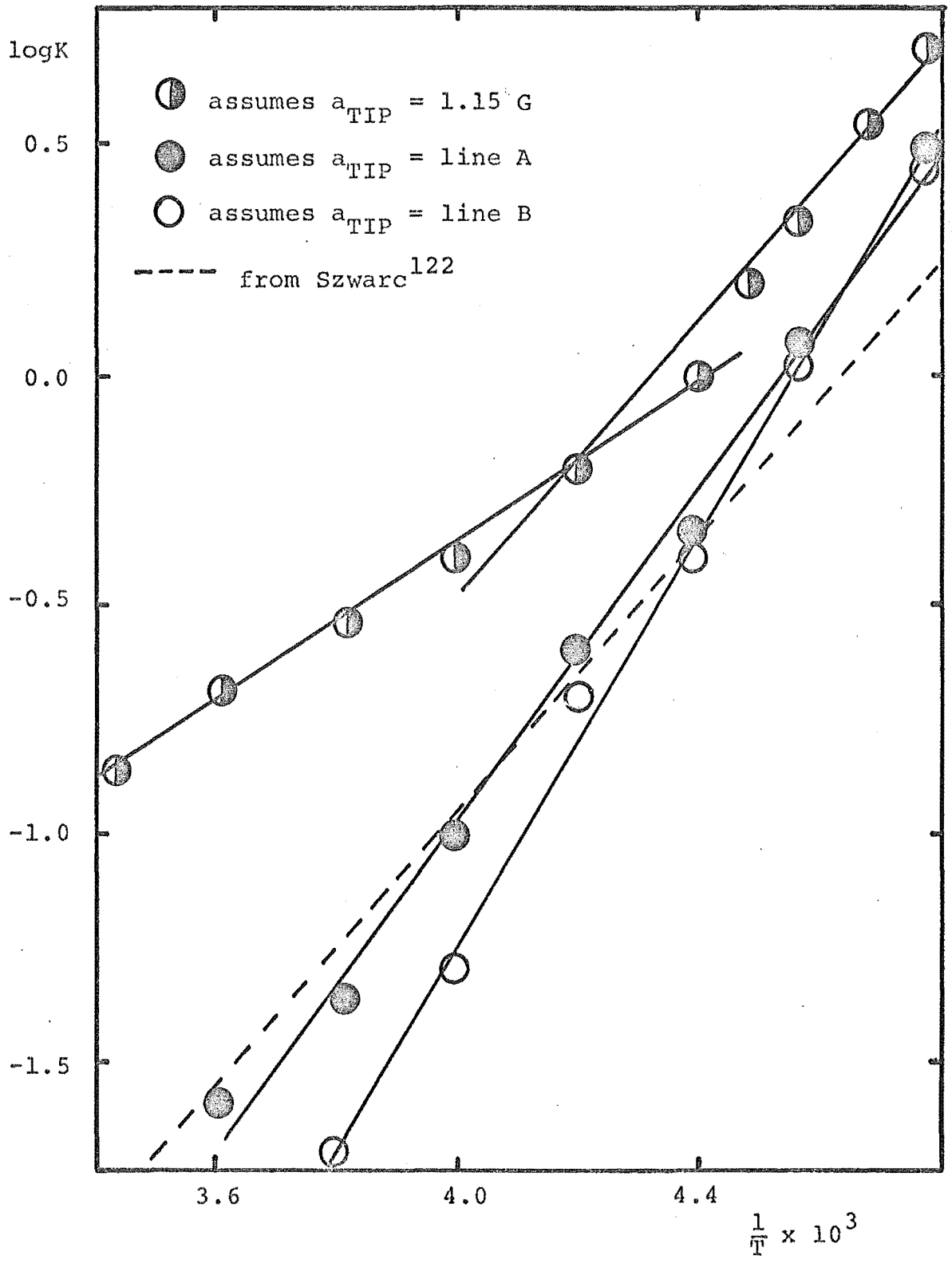

The temperature dependence of the sodium hfs has been attributed to a reduced amplitude of vibration of the cation about the centre of the anion[18] or to a shifting equilibrium between tight and loose ion pairs.[45] Using the latter model, Hirota obtained thermodynamic parameters for the interconversion. Although he also noted the selective broadening of the outer sodium hfs components and has published full kinetic data for the mixed solvent THF-DEE systems,[49] Hirota does not appear to have fully analysed the THF system. Only $\tau_{TIP} \simeq 5 \times 10^{-9}$ s and $\Delta H_1^{\ddagger} \simeq 20.9$ kJ mol^{-1} have been reported as far as is known.

There seems little doubt that solvent-separated and tight ion pairs are prcsent in the N/Na/THF system; besides Hirota's evidence,[45] Smid[40] has observed both species by optical methods and Fraenkel[49] has found the shift in g-value with temperature is linearly dependent on $|a_{Na}|$, a result expected if the ion pair equilibrium model applies. Szwarc's[36] studies of ion pair dissociation yield values characteristic of contact ion pairs at high temperatures and loose ion pairs at low temperatures. Further evidence is supplied by the proton coupling constants of the 1,4- and 2,3- DMN anions: as outlined at the beginning of this chapter, a large decrease in a_{Me} (a_1) and an increase in a_5 are characteristic of a change from a loose to a tight ion pair structure with these anions. The substantial changes observed in this Na/THF system as the temperature is altered clearly indicate loose ion pairs at low and tight ion pairs at high temperatures.

On the basis of these observations and the similarity of all spectra, a tight-loose ion pair equilibrium was assumed for all seven systems studied here.

Hirota's method of analysis has been described in section 3B.4 along with the equations and definitions involved. The

Table 5.2: Calculated equilibrium constants and tight ion pair fractions, for the interconversion of tight and loose ion pairs.

System: N/Na/THF

Temperature (°C)	Method (see text) a_{TIP} = 1.15 G		a_{TIP} - line A		a_{TIP} - line B	
	$Kx10^{-1}$	p_{TIP}	$Kx10^{-1}$	p_{TIP}	$Kx10^{-1}$	p_{TIP}
-64	55.34	0.15	35.14	0.22	32.4	0.24
-54	21.25	0.32	12.33	0.45	11.2	0.47
-45	9.86	0.50	4.56	0.69	3.91	0.72
-35	6.64	0.60	2.58	0.80	2.10	0.83
-23	3.82	0.72	0.82	0.92	0.48	0.95
-11	2.91	0.78	0.44	0.96	0.20	0.98

K: ± 5% p_{TIP}: ± 2%

Table 5.3: Thermodynamic data for the interconversion of tight and loose ion pairs

System N/Na/THF

Method (see text)	ΔH^o kJ mol^{-1}	ΔS^o J K^{-1} mol^{-1}	References
a_{TIP} = 1.15	-16.3 -28.6	-72 -122	This work
a_{TIP} - line A	-34.4	-156	"
a_{TIP} - line B	-42.9	-195	"
a_{TIP} = 1.15	-23.4 -20.1	-100 -84	Hirota[45,46]
non-esr	-28.9	-134	Szwarc[122]

ΔH^o: ± 1.5 kJ mol^{-1}; ΔS: ± 8 J K^{-1} mol^{-1}

equilibrium constant for the process:

$$TIP \underset{k_{-1}}{\overset{k_1}{\rightleftharpoons}} LIP \qquad (3.8)$$

is given by:

$$K = \frac{a_{TIP} - a_{obs}}{a_{obs} - a_{LIP}} \qquad (3.9)$$

Szwarc[48] has questioned this method of analysis because it is generally assumed that a_{TIP} and a_{LIP} are temperature independent. If this is not the case, the derived thermodynamic parameters can be in considerable error. To assess the effect of these assumptions for the N/Na/THF, the data obtained in this project were treated in two ways:

1) a_{TIP} and a_{LIP} were taken to be temperature independent and equal to 1.15 G and 0.0 G respectively, the values assumed by Hirota.[45]

2) a_{TIP} was assumed to vary linearly with temperature, similar to the approach used for the PY/Li/DEE system. The lines labelled A and B in Figure 5.5 were considered reasonable choices for estimating a_{TIP} at different temperatures. The most reasonable value for a_{LIP} seems to be zero, throughout the temperature range.

From the experimental coupling constants and using Eqns 3.9 and 3.11, K and p_{TIP} were found at a number of temperatures for each approach [Table 5.2]. From plots of log K vs 1/T [Fig. 5.6], the enthalpy and entropy changes can be found [Table 5.3]. The points resulting from approach 1, with a_{TIP} = 1.15 G at all temperatures, appear to lie along two linear portions (in contrast to that found by Hirota[45]) and the results for both portions are given. While approach 2, with temperature dependent a_{TIP} values, yields a more linear dependence of log K, none of the lines

Table 5.4: Thermodynamic and kinetic data[a] for the interconversion of tight and loose ion pairs.

System: N/Na/THF

Temperature	Method		
	a_{TIP} = 1.15 G	a_{TIP} - line A	
°C	$\frac{k_1}{s^{-1}} \times 10^{-7}$	$\frac{k_1}{s^{-1}} \times 10^{-7}$	
-23	29.7	1.75	b
-23	32.1	2.62	c
-34	15.5	2.44	c
-35	17.1	3.38	b
-45	11.1	3.24	b
-45.5	10.9	3.37	c
-50	11.2	4.69	c
-54	9.93	4.69	b
-54	9.85	4.85	c

$\Delta H_1^{\ddagger}$ = +12.3 kJ mol^{-1} $\quad$ $\Delta H_1^{\ddagger}$ = -11.2 kJ mol^{-1}

$\Delta S_1^{\ddagger}$ = -33 J K^{-1} mol^{-1} $\quad$ $\Delta S_1^{\ddagger}$ = -147 J K^{-1} mol^{-1}

$\Delta H_{-1}^{\ddagger}$ = +43.1 kJ mol^{-1} $\quad$ $\Delta S_{-1}^{\ddagger}$ = +27.3 kJ mol^{-1}

$\Delta S_{-1}^{\ddagger}$ = +100 J K^{-1} mol^{-1} $\quad$ $\Delta S_{-1}^{\ddagger}$ = +27 J K^{-1} mol^{-1}

a) k = ± 20%; $\Delta H^{\ddagger}$: ± 3.5 kJ mol^{-1}; $\Delta S^{\ddagger}$: ± 15 J K^{-1} mol^{-1}

b) uses a_{obs} from 10 G/40 cm spectra

c) uses a_{obs} from 4 G/40 cm spectra

correspond to that found independently by Szwarc [122] from studies of electron transfer reactions.

The validity of Szwarc's earlier criticism[48] of Hirota's approach is clearly evident from Tables 5.2 and 5.3 and from Figure 5.6. If Szwarc's thermodynamic parameters are correct, it appears that the temperature dependence of the tight (and perhaps loose) ion pair sodium splitting must vary in a non-linear way in order to fit the observed esr data. There is no a priori reason for a_{TIP} to vary linearly with temperature, but in the absence of other indications it seems a reasonable assumption.

Since approach 1 (with the "best" slope) and approach 2 using line A gave reasonable agreement with Szwarc's ΔH^{o} and ΔS^{o} values respectively, they were both employed for the kinetic analysis of the linewidth broadening. Rate constants for the interconversion process can be found from Eqn. 3.10 [Table 5.4].* The calculated values are again very dependent on the approach used, especially at higher temperatures. The large variation in these values, when the only difference in the calculations is the value assigned to a_{TIP} at a given temperature, is quite remarkable. Plots of log k_1 vs 1/T and log k_{-1} vs 1/T are shown in Figure 5.7 and the derived activation parameters, $\Delta H^{\ddagger}$ and $\Delta S^{\ddagger}$ are listed in Table 5.4. As pointed out previously [3B.4], the breakdown of kinetic data into thermodynamic terms may not be valid for these systems, so the $\Delta H^{\ddagger}$ and $\Delta S^{\ddagger}$ values may not be meaningful. It is preferable to consider the rate data at different temperatures, by using free energy diagrams [Fig. 5.8].

---

* Rate constants were calculated using the linewidth data from the 4G/40 cm spectra; the fact that the metal coupling constants used were those observed in both 4G- and 10G-/40 cm spectra and were not "smoothed" out by graphical procedures, accounts for small variations only.

FIGURE 5.7

PLOTS OF LOGk vs $\frac{1}{T}$ WITH DIFFERENT VALUES OF a_{TIP} ASSUMED

SYSTEM : N/Na/THF

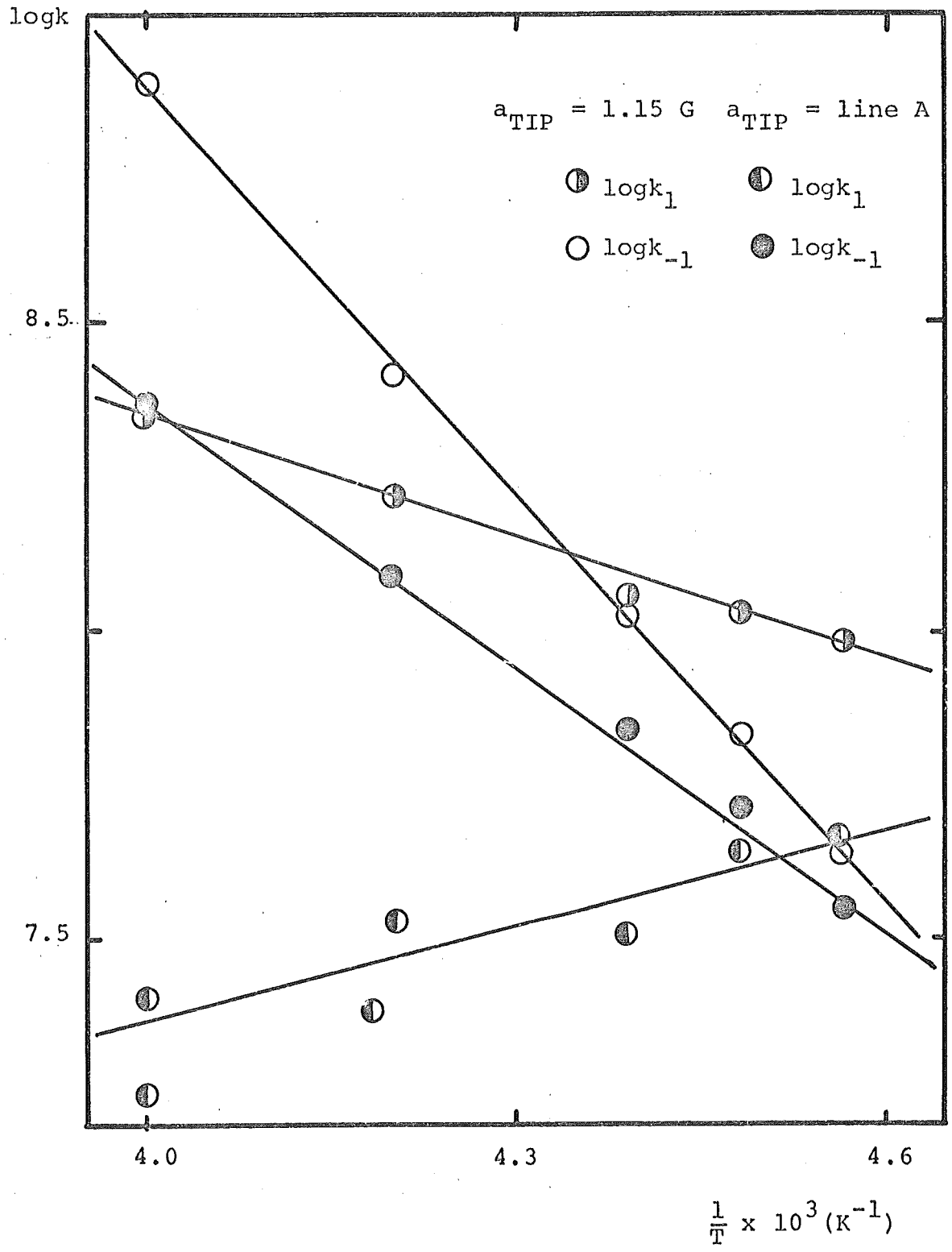

FIGURE 5.8

FREE ENERGY DIAGRAMS FOR THE INTERCONVERSION OF TIGHT AND LOOSE ION PAIRS

SYSTEM : N/Na/THF

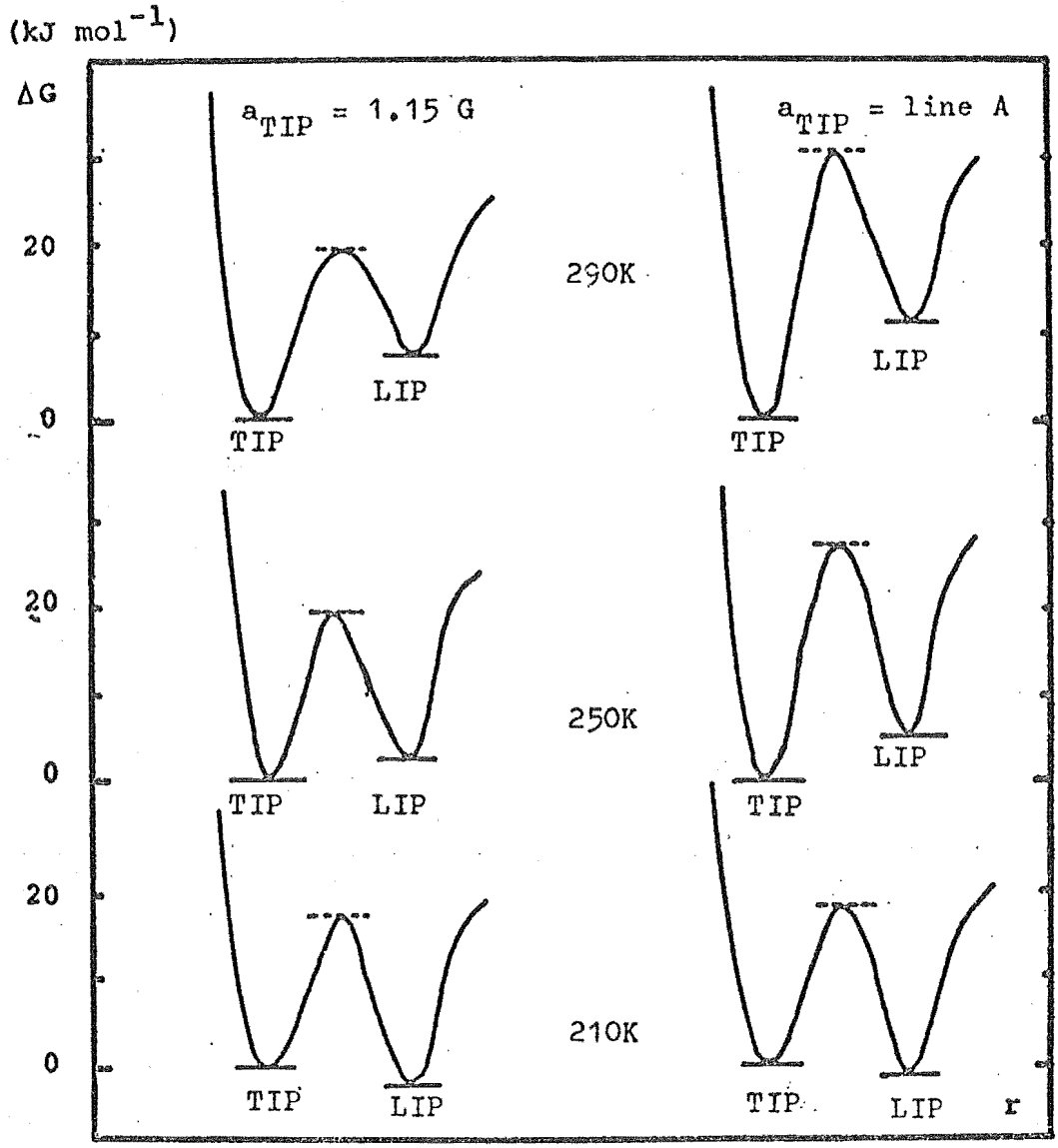

These show that the same trends are predicted by both approaches as the temperature varies, but that the free energy differences involved are very dependent on the assumptions involved. Clearly the thermodynamic parameters obtained using Hirota's traditional treatment[45,46] must be viewed with much caution unless the accuracy of the initial assumptions can be verified.

FIGURE 5.9

TEMPERATURE DEPENDENCE OF SODIUM HYPERFINE SPLITTINGS

SYSTEM : Na/MTHF

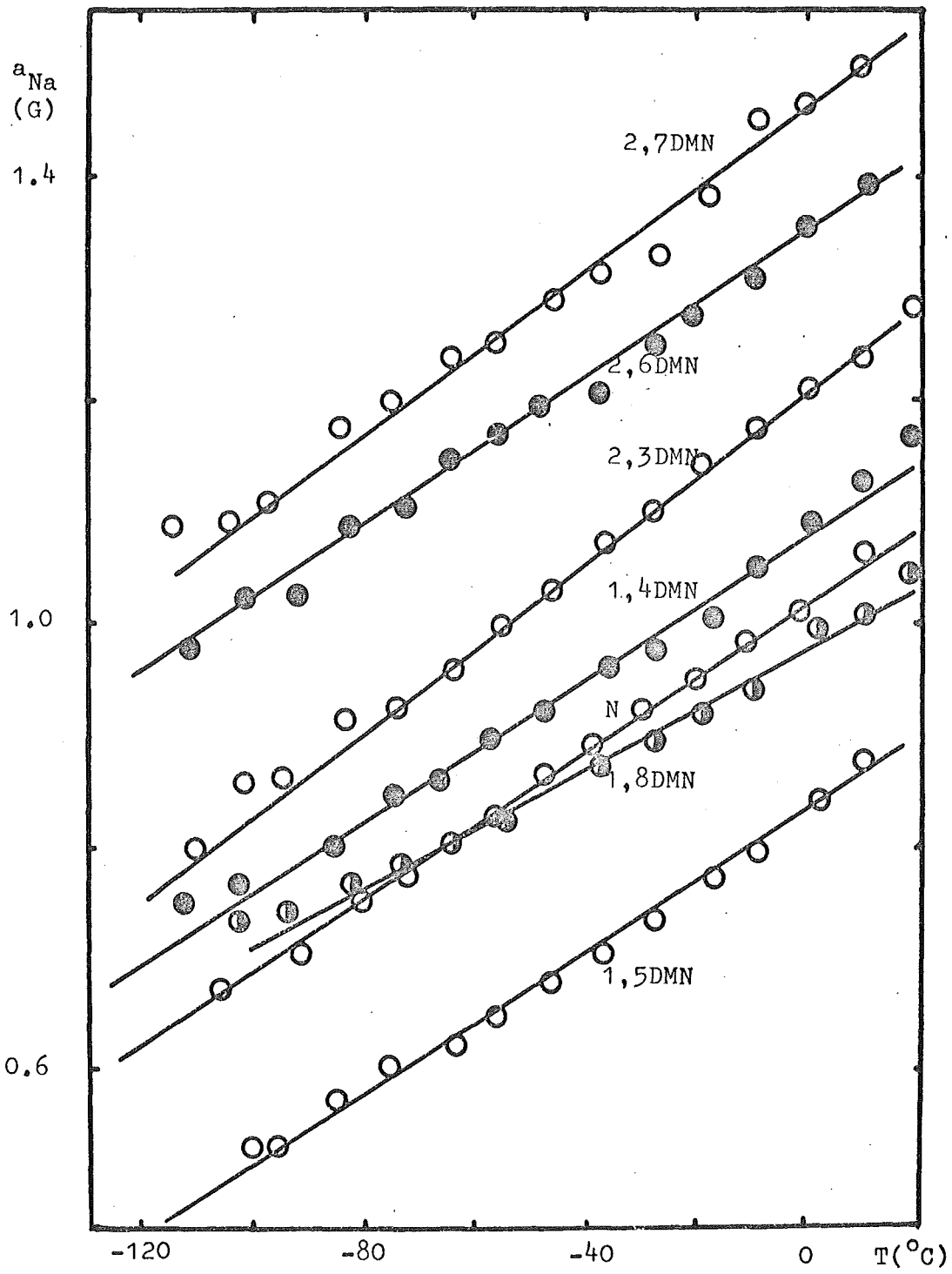

Analysis of the temperature dependence of the sodium splitting for the DMN anions leads to ΔH^{o} and ΔS^{o} values similar to those of the naphthalene analysis. The effect of methyl-groups substitution causes the absolute value of the sodium splitting to increase in the order (20°C): 1,5< 1,8 < N <1,4 <2,3 <2,6 <2,7. The implications of this will be discussed in part 5.10.

5.4: Na/MTHF Systems

A Observations

At all temperatures, these spectra exhibited sodium splittings [Fig. 5.9]. At most temperatures the lines were narrow [Fig. 5.10] but some broadening occurred at very low temperatures where a second species, without sodium coupling and in low concentration, was sometimes observed (< -100°C). This could have been the free anion or a solvent-separated ion pair but no measurements or dilution studies were carried out. In spectra of the N/Na/MTHF system, the outer components of the sodium splitting appeared to be slightly broader than the inner components at very low temperatures (below ~ -90°C). This was probably true of the DMN spectra but the greater number of overlapping lines makes this uncertain. The differences were too small and the uncertainties too large to make any analysis worthwhile.

B Discussion

The sodium coupling constants obtained in this system are very similar to those found by Atherton and Weissman,[18] Hirota[46] and Goldberg and Bolton[31] for naphthalene and by the latter workers for 1,5DMN.

The large magnitude and the linear temperature dependence of

FIGURE 5.10

ESR SPECTRA FOR DMN/Na/MTHF SYSTEMS

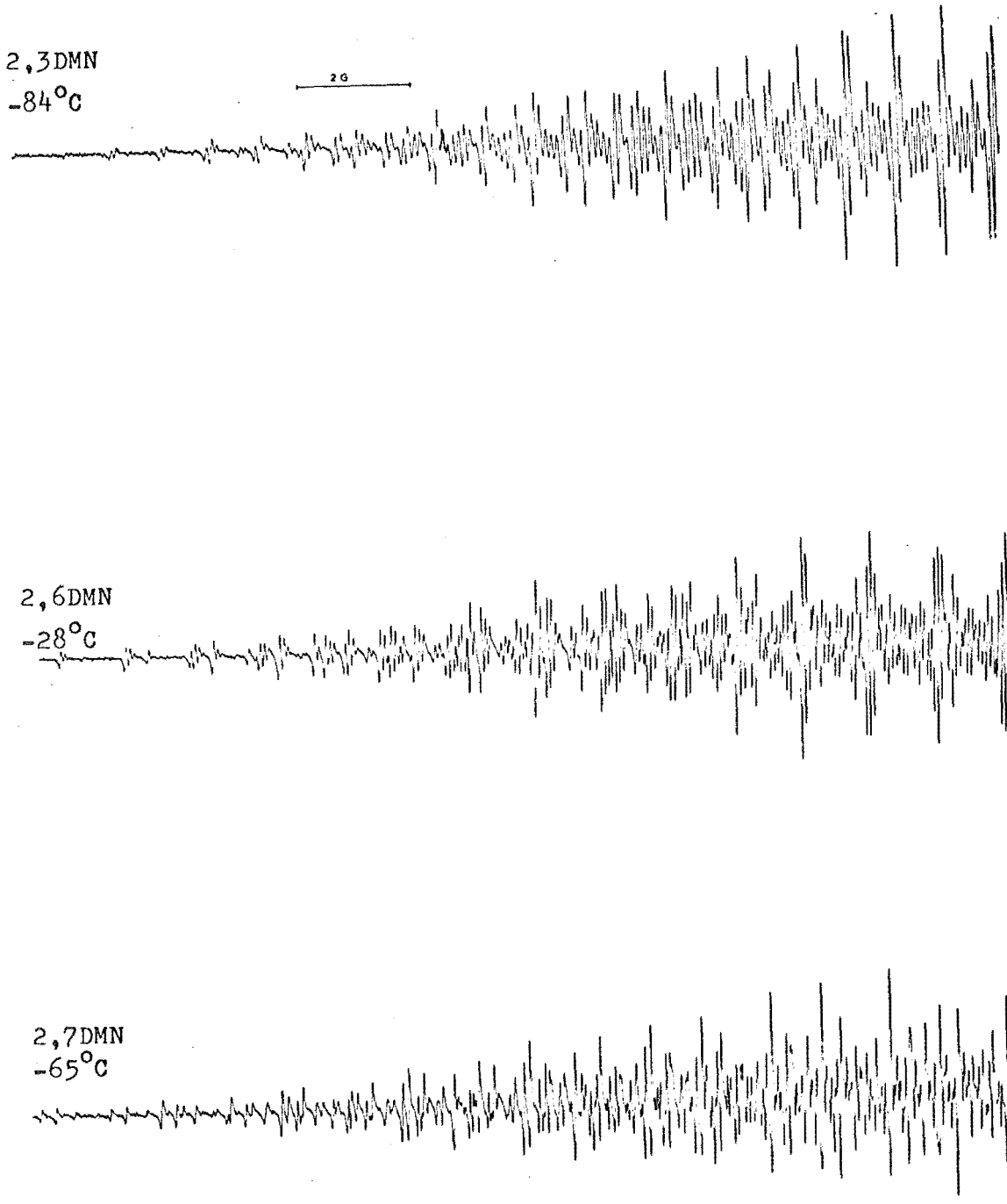

the sodium hfs indicates that only tight ion pairs are present throughout the temperature range studied.* This is in contrast to the situation in THF where loose ion pairs are also present and a rapid equilibrium between the two forms exists, but is in keeping with the greater solvating power of THF. It may also be contrasted with the anthracene/Na/MTHF system where Hirota[45] has shown a tight-loose ion pair equilibrium also exists. Since anthracene has a more diffuse negative charge distribution, its ability to compete with the solvent for interaction with the positive ion is less than that of naphthalene. This difference apparently allows the MTHF molecules enough relative coordinating ability to form loose pairs in the anthracene system, whereas they have insufficient power to form them in the naphthalene system, except perhaps at very low temperatures where this power is greatest.

The magnitude and behaviour of the structure-sensitive proton splittings of 1,4- and 2,3- DMN [a_5 and a_{Me} (a_1)] indicate tight ion pair formation only. The a_5 coupling constant increases considerably on cooling, which may result from some slight changes in geometry within the tight ion pair caused by the large solvent molecules as the external solvation of the pair increases.

At +20°C, the order of increasing sodium splittings among the series of compounds is the same as for Na/THF:

1,5 < 1,8 < N < 1,4 < 2,3 < 2,6 < 2,7.

---

* The apparent M_z-linewidth dependence observed at very low temperatures may indicate a rapid equilibrium between tight and loose ion pairs; thus loose ion pairs may also be formed below ~ -90°C.

FIGURE 5.11

CENTRE LINES OF THE ESR SPECTRA OF THE N/Na/DEE SYSTEM

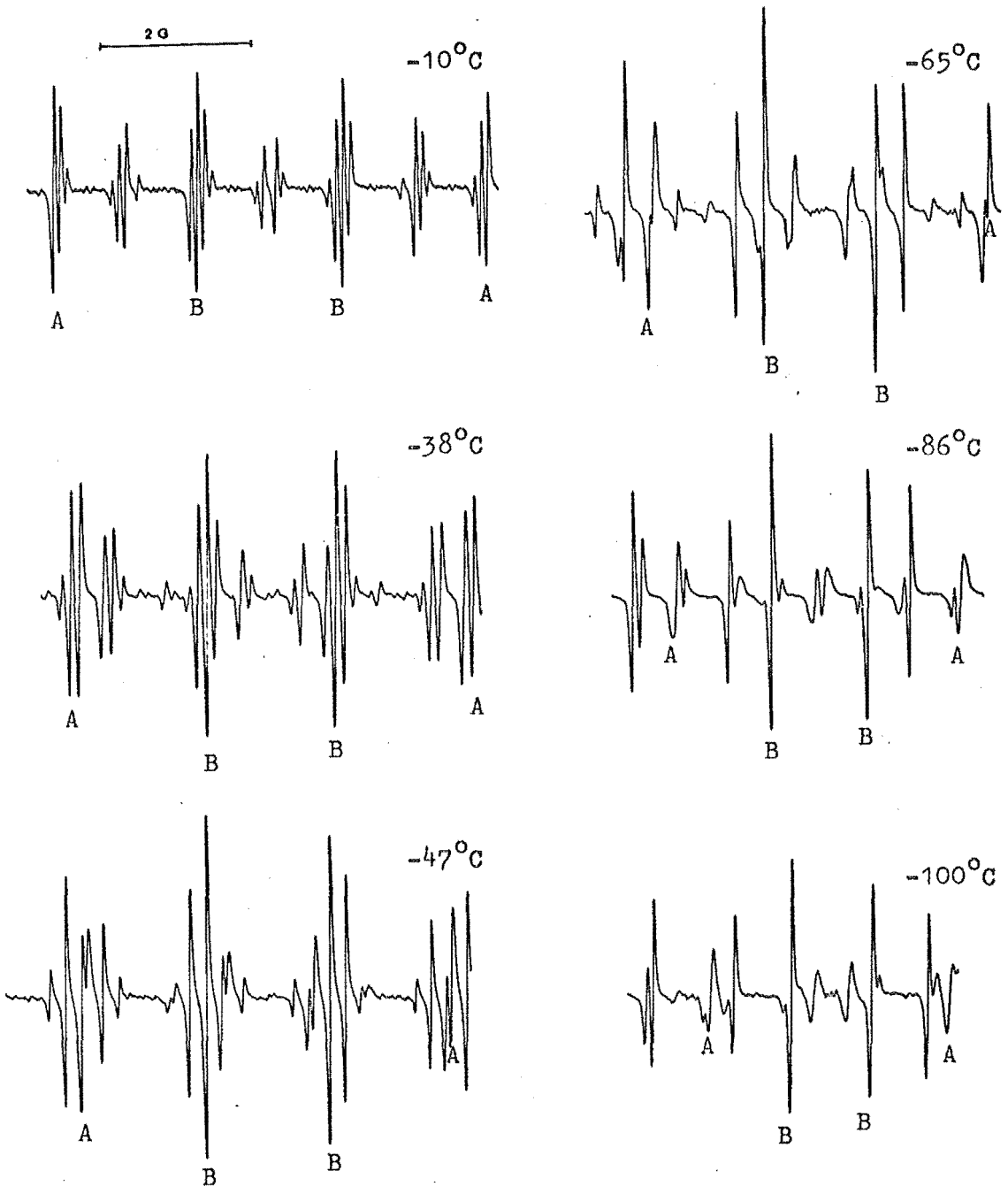

A: ± 3/2 components of sodium hyperfine splitting

B: ± 1/2 components of sodium hyperfine splitting

5.5: Na/DEE systems

A Observations

Of all the compounds, only naphthalene could be reduced to any significant extent in this system, and this reduction occurred more readily at lower temperatures. The spectra of this system showed a large temperature-dependent sodium splitting and, below -30°C, selective broadening of the $M_I = \pm 3/2$ components of this splitting [Fig. 5.11].

B Discussion

Szwarc[127] has reported difficulties in reducing naphthalene in this system and found the process was enhanced by low temperatures. Despite attempts under various experimental conditions, the DMNs could not be reduced sufficiently to produce any esr signals. Since some degree of solvation seems to be necessary to stabilise all ion pairs, the lack of reduction of the DMNs may reflect a steric effect of the methyl groups. Their size may prevent solvent molecules from approaching closely enough to solvate the periphery of the tight ion pairs to a sufficient extent for them to be stable.

In naphthalene spectra, no additional lines due to a second ion pair species, as noted by Hirota[45,46] and Fraenkel,[50] were observed at any temperatures. As Tuttle[81] and Szwarc[122] have pointed out, these extra peaks were almost certainly due to traces of potassium in these samples.

The observed sodium coupling constants seem to be marginally greater than those found by Fraenkel,[50] Szwarc[127] and Hirota[46], but the differences are small and the temperature dependence similar [Fig. 5.12]. At higher temperatures, the a_{Na} vs T plot begins to flatten out, as Hirota observed.[46] Both Szwarc and

FIGURE 5.12

TEMPERATURE DEPENDENCE OF SODIUM HYPERFINE SPLITTING

SYSTEM : N/Na/DEE

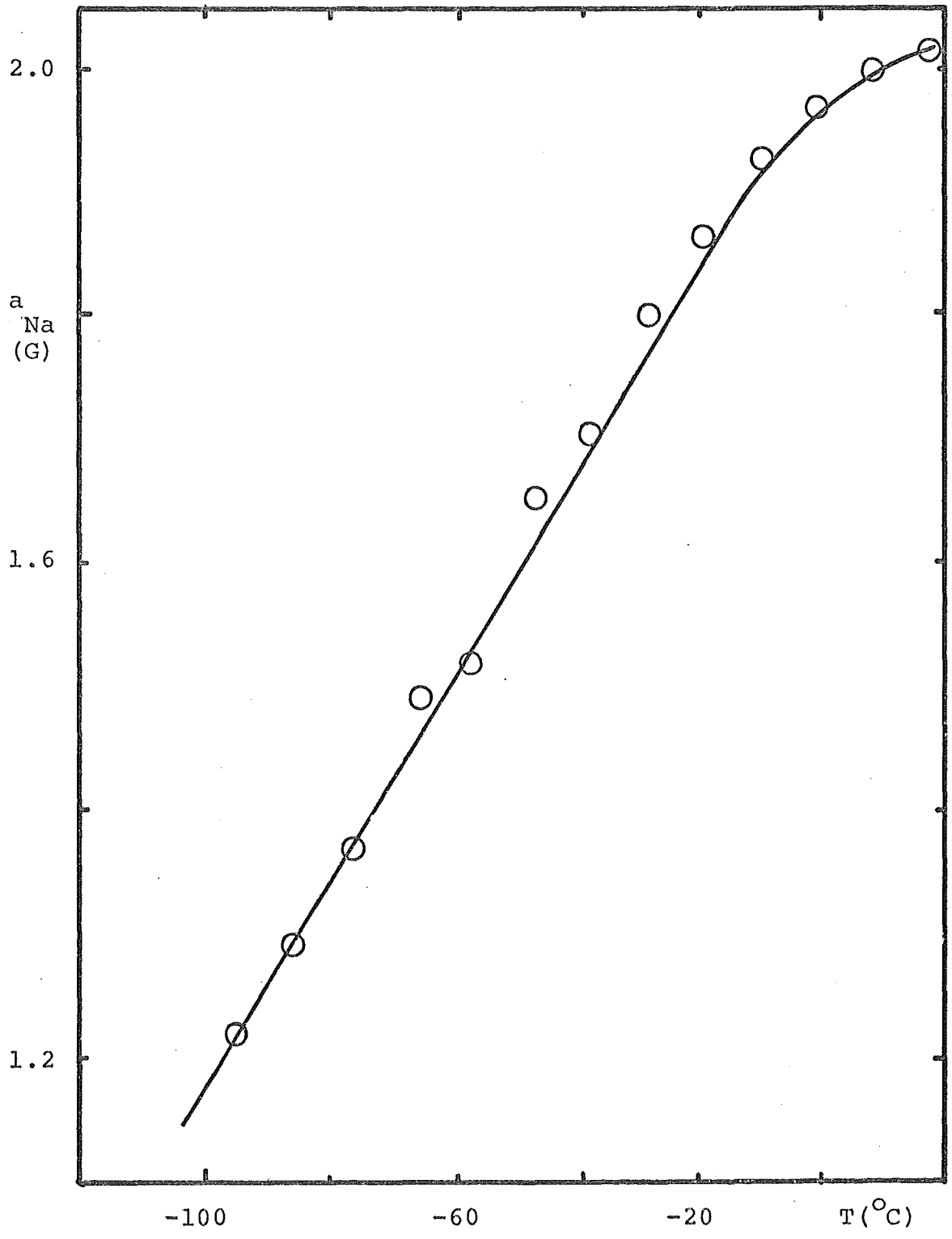

Hirota observed the dependence of the linewidth on the alkali metal magnetic quantum number, although Szwarc noted this only below $\sim -90^{\circ}C$.

The large sodium splitting and the weak solvating power of DEE make it very unlikely that any species other than tight ion pairs exist in this system. Hirota[46] has suggested the broadening in this system is due to a rapid equilibrium between two distinct tight ion pairs. $TIP(1) \underset{k_{-1}}{\overset{k_1}{\rightleftharpoons}} TIP(2)$, in contrast to the PY/Li/DEE and N/Na/THF systems previously considered, where one species was a loose ion pair. Since the observed coupling constants give no indication of reasonable a_{TIP} and a_{LIP} values, which are required for analysis of this equilibrium [Eqns 3.9, 3.10, 3.11], Hirota's values of 2.45 G and 0.75 G respectively were assumed. Analysis of the observed data in the usual way [sections 3B.4 and 5.3] yields the results in Table 5.5 and Figure 5.13. A comparison of the thermodynamic parameters found here and those determined by Hirota shows good agreement. Since the separation of rate data into $\Delta H^{\ddagger}$ and $\Delta S^{\ddagger}$ terms for processes of this type must be treated with caution [section 3B.5], the interconversion between the two species is best represented by free energy diagrams at a number of temperatures [Fig. 5.14].

Unlike the N/Na/THF system, there are no other obvious values to take for a_{TIP} and a_{LIP} so as to compare the results of an analysis with alternative assumptions. As would be expected, the ΔH° and ΔS° terms show the conversion of a tight ion pair into another tight ion pair requires much less change in the solvation sphere (and therefore smaller ΔH° and ΔS° values) than does the change from a tight to a loose ion pair. The rate of this process is also significantly faster. However, in view of the doubt that must be associated with the estimating of the

FIGURE 5.13

PLOTS OF LOG K AND LOG k vs $\frac{1}{T}$ FOR THE INTERCONVERSION OF TWO TIGHT ION PAIRS

SYSTEM : N/Na/DEE

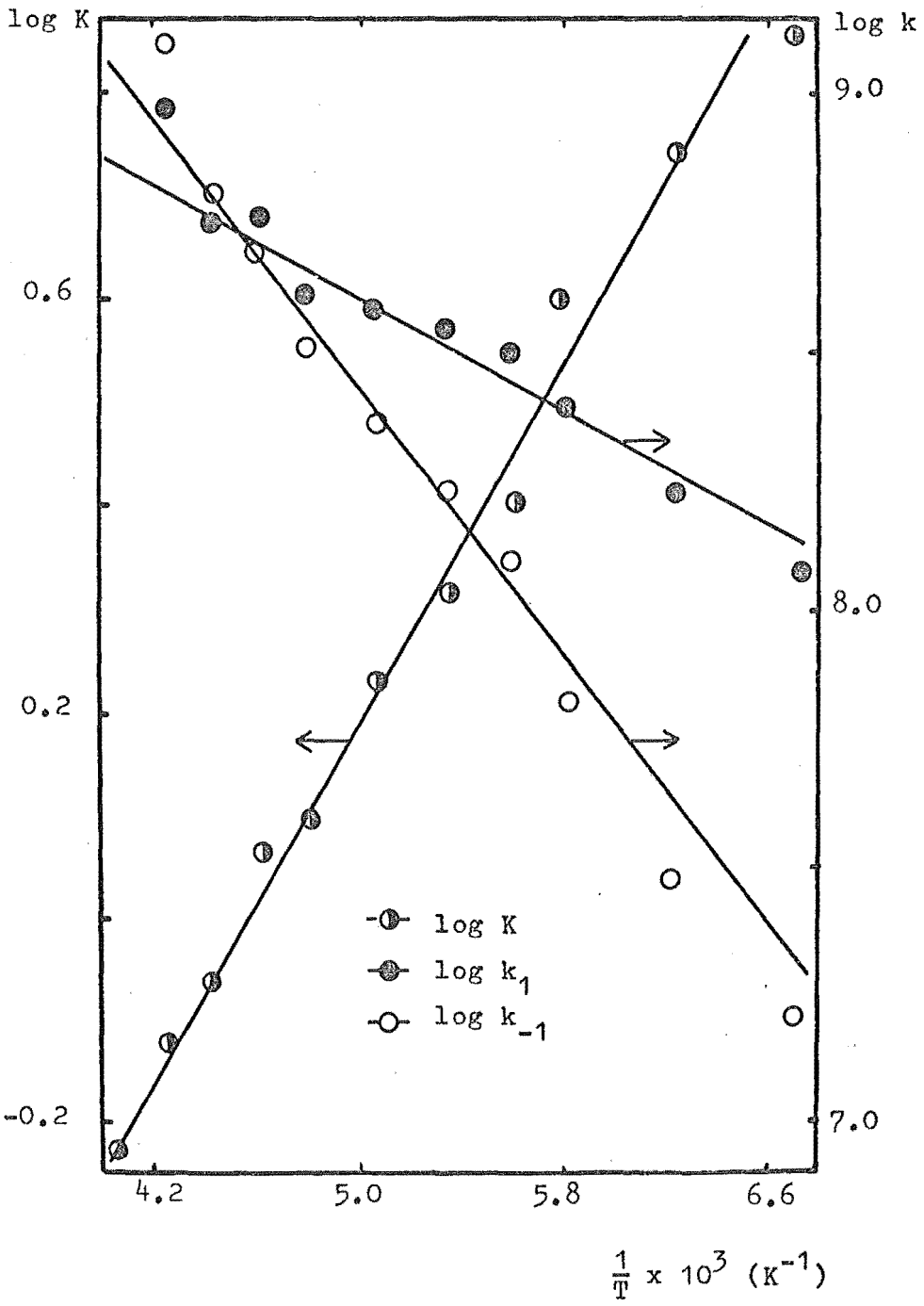

Table 5.5: Thermodynamic and kinetic data for the interconversion of tight ion pairs.

System: N/Na/DEE

	ΔH / kJ mol^{-1}			ΔS / J K^{-1} mol^{-1}	
	This work	Hirota[46]		This work	Hirota[46]
ΔH^{o}	-8.4	-10.0	ΔS^{o}	-38	-46
$\Delta H^{\ddagger}_{1}$	+5.0	+3.8	$\Delta S^{\ddagger}_{1}$	-52	-50
$\Delta H^{\ddagger}_{-1}$	+12.1	+13.0	$\Delta S^{\ddagger}_{-1}$	-20	-10

Temperature / °C	K	k_1 / s^{-1} x 10^{-8}
+9	0.35	
-1	0.37	
-10	0.42	
-19	0.51	
-27	0.59	
-38	0.75	9.50
-47	0.86	5.64
-57	1.16	5.81
-65	1.25	4.02
-76	1.70	3.83
-86	2.07	3.48
-95	2.53	3.22
-100	4.00	2.51
-113	5.54	1.61
-124	7.21	1.10

$\Delta H^{o} \pm 1.0$, $\Delta H^{\ddagger} \pm 2.0$ kJ mol^{-1} $\Delta S^{o} \pm 5$, $\Delta S^{\ddagger} \pm 10$ J K^{-} mol^{-1}

K: $\pm$ 5% k_1: $\pm$ 20%

FIGURE 5.14

FREE ENERGY DIAGRAMS FOR THE INTERCONVERSION OF TWO TIGHT ION PAIRS

SYSTEM: N/Na/DEE

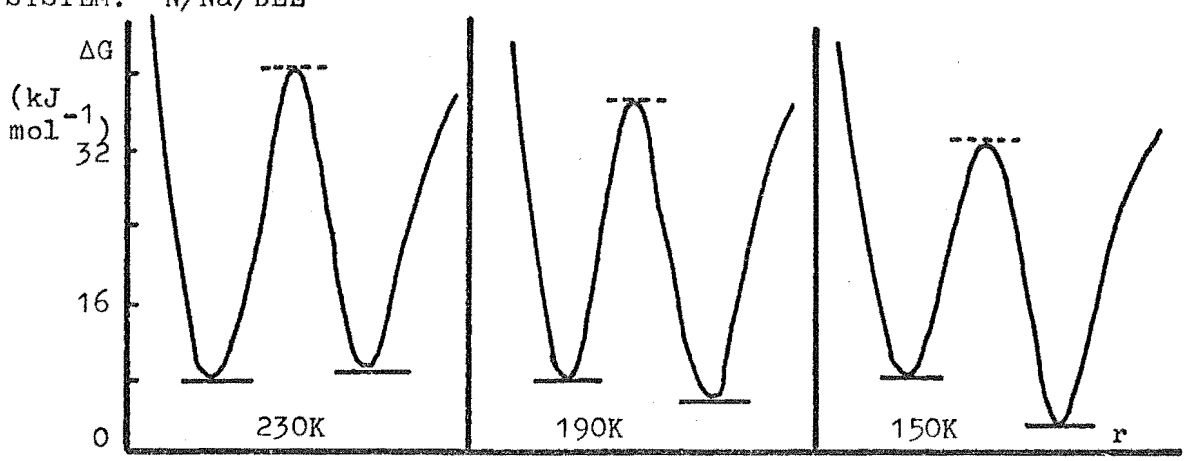

FIGURE 5.15

ESR SPECTRA FOR THE 1,4DMN/K/DME SYSTEM

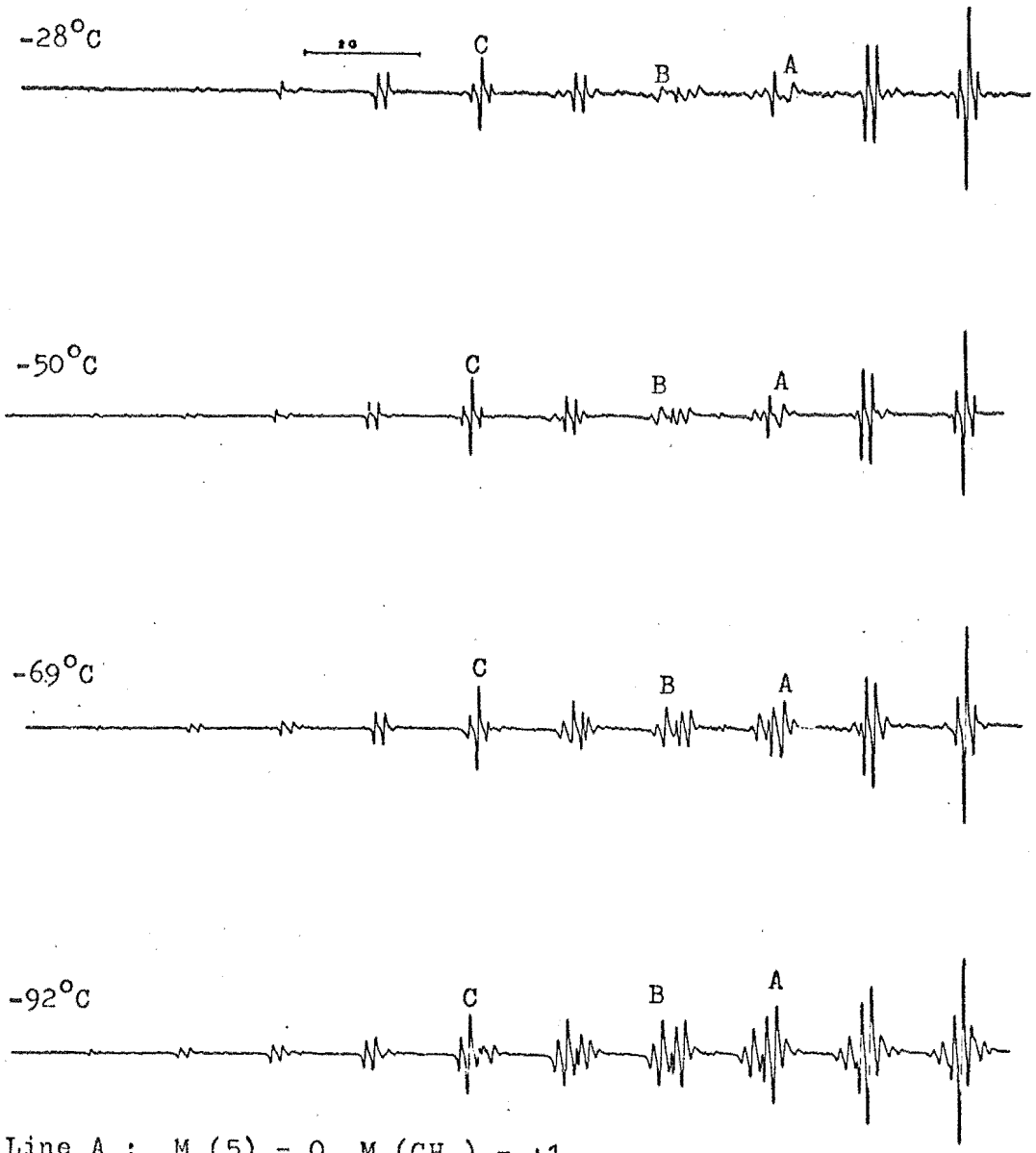

Line A : $M_I(5) = 0$, $M_I(CH_3) = +1$

Line B : $M_I(5) = -1$, $M_I(CH_3) = 0$

Line C : $M_I(5) = -1$, $M_I(CH_3) = +1$

a_{TIP} and a_{LIP} values, it may be unwise to place too much weight on the absolute values of the derived data.

5.6: K/DME systems

A Observations

All systems displayed narrow lines at low temperatures. For N, 1,5- and 1,8- DMN, the linewidths increased only slightly at high temperatures, but for 2,3-, 2,7-, 2,6-, and 1,4- DMN, line-broadening began about -40° to -30°C and was partially or fully resolved into a potassium hfs at higher temperatures [Table A.4].

The 1,4- and 2,3- DMNs also exhibited another linewidth effect. Using the usual notation for describing spectral lines*, only the $M_I(CH_3) = -M_I(5) = 0, \pm 1$ lines remain sharp in 1,4DMN as the temperature is varied [Fig. 5.15]. At -90°C, all lines are reasonably narrow but the height of the lines with $M_I(CH_3) \neq -M_I(5)$ is less than that expected. As the temperature is increased these lines broaden until ~-25°C, above which they increase in height again. Similar behaviour is observed for 2,3DMN in this system, where only lines with $M_I(1) = + M_I(5)$

---

* Each line is described by one of the z components (M_I) of the total spin (I) of each of the sets of nuclei in the molecules. For 1,4DMN, the four sets of proton nuclei have coupling constants denoted a_2, a_6, a_5 and a_{CH_3} a_{Me}, and M_I values denoted by $M_I(2)$, $M_I(6)$, $M_I(5)$ and $M_I(CH_3)$. The lines arising from proton splittings in 2,3DMN are similarly described by $M_I(CH_3)$, $M_I(6)$, $M_I(1)$ and $M_I(5)$. For negative (positive) coupling constants, the downfield lines are described by negative (positive) M_I values. All the ring-proton splittings are considered negative and all methyl-proton splittings positive.[71]

FIGURE 5.16

ESR SPECTRA FOR THE 2,3DMN/K/DME SYSTEM

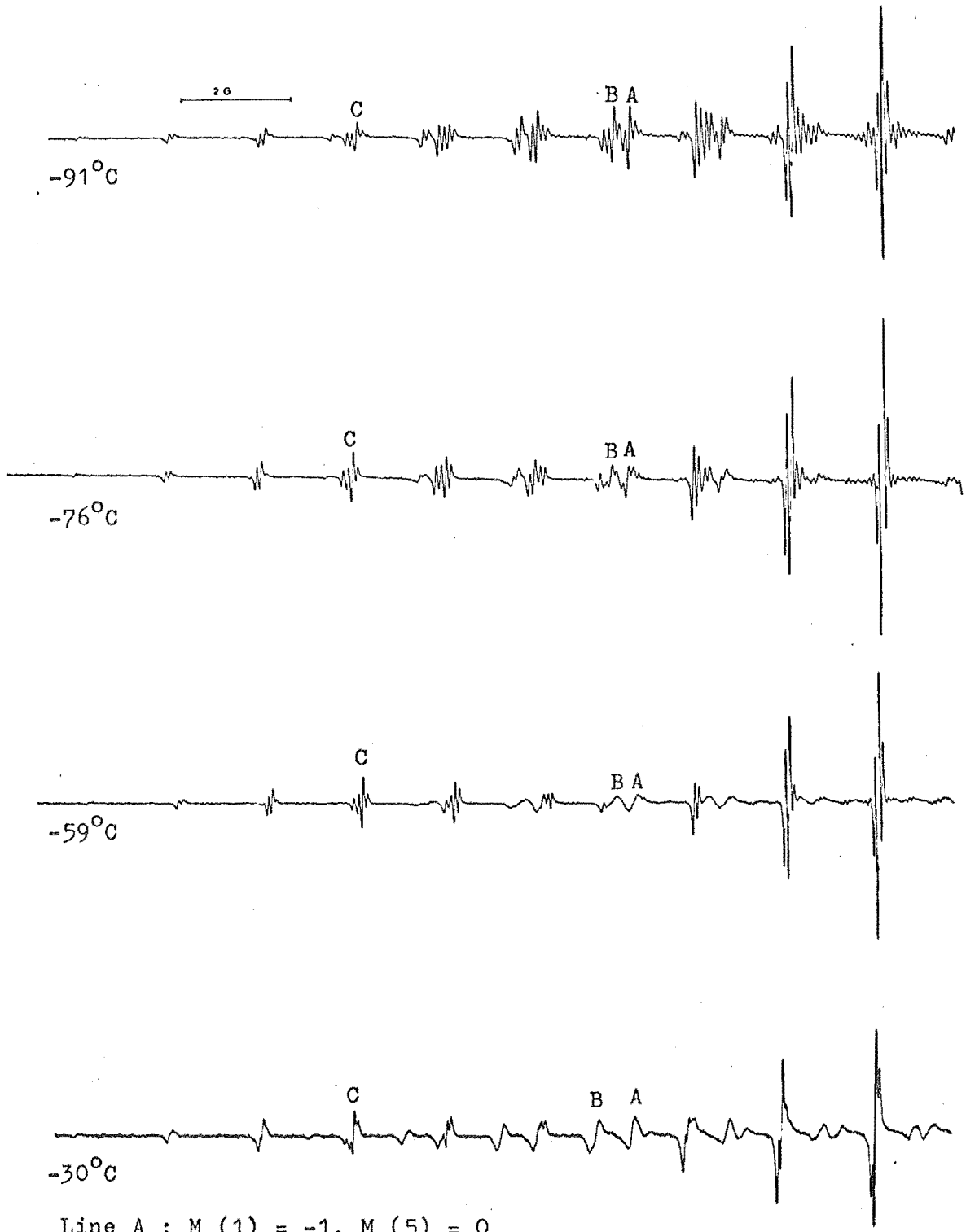

Line A : $M_I(1) = -1$, $M_I(5) = 0$

Line B : $M_I(1) = 0$, $M_I(5) = -1$

Line C : $M_I(1) = -1$, $M_I(5) = -1$

remain narrow as the temperature is varied [Fig. 5.16]. In this case, maximum broadening occurs over a slightly lower temperature range ($\sim$ -50 to -30°C) than in 1,4DMN ($\sim$ -60 to -40°C).

B Discussion

No potassium hfs has been detected by esr measurements for any of the DMNs or N reduced in K/DME. For naphthalene, Hendricks[98] did find a small splitting (positive at high and negative at low temperatures) by the nmr technique and to explain the change of sign, he concluded that contact ion pairs were present over the entire temperature range. Reddoch[49] considered this system contained ion pairs at higher temperature and the free ion at lower temperatures, on the basis of the temperature dependence of the proton coupling constants. His values and those reported here are in excellent agreement [Table A.3]. Of the DMNs, Campion[71] reported the 1,8 compound in K/DME at -70° and Peake[74] found all six compounds gave identical results in K/DME to those in Na/DME, but with less resolution. Rieke[72] observed the 2,3DMN/K/DME system and found similar coupling constants and shifts with temperature to those found in this project [Table A.3]. He considered the low temperature species to be the free ion and the high temperature species an unsymmetrical ion pair, with the large shift on cooling resulting from the dissociation of the ion pair. No mention was made of the broadening of certain lines as observed here, although the spectrum published in Rieke's paper[72] appears to show lines of smaller height than expected.

The most interesting aspects of this K/DME system are the selective broadening of lines and unusual shifts in the proton coupling constants, especially a_1 (a_{Me}), observed for both the 2,3- and 1,4- DMNs.

Changes in the coupling constants of 1,4- and 2,3- DMN were discussed above (p. 80) where it was concluded that a large decrease in a_{Me} (a_1) and a smaller increase in a_5 were expected for these compounds if loose ion pairs were converted into tight ion pairs. Such shifts are observed as the temperature increases within the K/DME system of both 1,4- and 2,3- DMN [Table A.3]. On this basis, change from tight to loose ion pairs on cooling is postulated for these systems. The change may be dynamic (rapid equilibrium between the two ion pairs) or static (gradual transformation) in nature.

Although this process accounts for the observed changes in the proton coupling constants, it does not necessarily cause the broadening of certain lines that was observed for the 1,4- and 2,3- DMN anions in K/DME. The line-broadening results from a modulation of the spin densities on the 1,4,5 and 8 positions. The modulation causes a time-dependent variation in the hyperfine splitting which, from the Uncertainty Principle, leads to broadening when the lifetime of a spin state approaches the inverse of the normal linewidth. In the dilute solutions used, this modulation must be caused by an intramolecular rate process involving the cation. If the cation movement is between two positions in the anion, A and B say, the process may be represented by

$$A \rightleftharpoons B \qquad (5.4)$$

Positions A and B may change with temperature. To preserve the symmetry of the molecule this movement must be in the x, y or z directions. In discussing these motions, the 2,3DMN anion will be used but all considerations apply equally well to the 1,4DMN system.

Cation movement in the x direction can be immediately

discounted because it leads to an out-of-phase* modulation of a_5 and a_1, which causes only alternate lines to broaden.[32] In this case the $M_I(5) = \pm 1$ and the $M_I(8) = \pm 1$ lines would remain sharp and the centre line would broaden, contrary to the observed effects.

Cation movement in the y and z direction produces in-phase modulation* of the anion spin densities. Although the spin density at protons 1 and 4 is changing with time, the two protons are equivalent at any instant. This means the spectral lines can still be described by the total nuclear spin quantum number $M_I = m_I(1) + m_I(4)$ and can be treated as if they result from one interacting nucleus with a total spin density of $I = I(1) + I(4) = 1$. Similarly for the protons at the 5 and 8 positions.

For very fast rates of in-phase modulation, an averaged narrow set of lines appears. For very slow rates, the individual spectra of A and B are superimposed with all lines again sharp. In the limit of "slow" exchange, the lines whose position is altered by the exchange process are broadened by an amount proportional to the exchange rate but almost independent of the induced changes in their position, $(\Delta\omega)$**. For form A, this gives a broadened signal centred at ω_A with the broadening due to the exchange given by [126]

$$T_2^{-1}(ex) = \tau_A^{-1} \qquad (5.5)$$

In the limit of "fast" exchange,** the exchanging lines appear at

---

* For out-of-phase modulation, when a_5 increases, a_8 decreases by the same amount; a_5 and a_8 have the same time-average hyperfine splitting and the proton nuclei are said to be equivalent. Similarly for a_1 and a_4. For in-phase modulation, the nuclei always have the same instantaneous hyperfine splitting and are said to be completely equivalent.[93]

** For "slow" exchange the lifetimes τ_A and τ_B must be sufficiently large compared to the inverse of the frequency separation, $(\omega_A - \omega_B)^{-1} = (\Delta\omega)^{-1}$. The conditions for different exchange regions are more exactly defined in Table 3.6.

an averaged frequency and are broadened by an amount proportional to both the rate and $\Delta\omega^2$.[126]

$$T_2^{-1}(ex) = p_A^2\, p_B^2\, (\omega_A - \omega_B)^2\, (\tau_A + \tau_B) \qquad (5.6)$$

where p_A and p_B are the probabilities of finding forms A and B. At intermediate rates of exchange a more exact equation such as that of Gutowsky and Holm[95] is required to analyse the broadening. Equation 5.6 can be rewritten in terms of the coupling constants of forms A and B, as

$$T_2^{-1}(ex) = \gamma_e^2\, p_A\, p_B\, \tau\, (a_A - a_B)^2\, M^2 \qquad (5.7)$$

where $\tau = \dfrac{\tau_A\ \tau_B}{\tau_A + \tau_B}$ and γ_e is the magnetogyric ratio of a free electron. Hence, in the general case where all the coupling constants in A and B differ, all lines but the central line (M=0) broaden and many different linewidths result. Clearly if the coupling constants for some nuclei are identical in forms A and B, these lines remain sharp ($\Delta a=0$). Since the lines associated with the hyperfine splittings of the nuclei at position 2 and 3 and at 6 and 7 do not broaden, these splittings must be changed little by the motion of the cation (i.e. $\Delta a \simeq 0$).

There are two additional lines which remain sharp: those with $M_I(1) = M_I(5) = \pm 1$ in 2,3DMN and those with $M_I(5) = -M_I(CH_3) = \pm 1$ in 1,4DMN. To account for this a special numerical relationship between the changes in the coupling constants resulting from the exchange process must be satisfied: the magnitude of the change induced in a_1 must be the same as that induced in a_5,

i.e. $|\Delta a_1| = |\Delta a_5|$ for 2,3DMN

and (5.8)

$|\Delta a_{Me}| = |\Delta a_5|$ for 1,4DMN

This means that the lines at distances from the centre given by

$\pm [|a_1| + |a_5|]$ for 2,3DMN, and $\pm [|a_{Me}| + |a_5|]$ for 1,4DMN, will be the same in forms A and B and thus remain sharp.

Of the two directions for cation motion, movement in the z direction represents the interconversion of tight and loose ion pairs by a rapid equilibrium. This process is already postulated to account for the observed proton hfs changes with temperature, but not necessarily as a dynamic equilibrium. There are two observations which show this motion is not responsible for the observed linebroadening:

1) At all temperatures, the $M_I(1) = M_I(5) = \pm 1$ lines broaden to about the same extent [Figs. 5.15 and 5.16]. In the limit of rapid exchange and at constant temperature, Eqn 5.7 gives the ratio of the linewidths of these lines as:

$$\frac{T_2^{-1}\ (M_I(1) = -1)}{T_2^{-1}\ (M_I(5) = -1)} = \frac{\Delta a_1^{\,2}}{\Delta a_5^{\,2}} \qquad (5.9)$$

This indicates that the $M_I(1) = -1$ line should be about 16 times broader than the $M_I(5) = -1$ line, contrary to observation $[|\Delta a_1| \simeq 0.4G,\ |\Delta a_5| \simeq 0.1G]$.

2) From the magnitude of the changes in the coupling constants between the tight and loose ion pairs, the special numerical relationships required [eqn 5.8] clearly do not hold for this type of exchange.

Cation movement in the y direction, between the two rings, has been postulated[31] for the sodium ion pairs of naphthalene. Calculations showed this structure leads to spin densities of the correct order of magnitude for many systems.[30,31] Goldberg and Bolton assumed this type of motion also occurs in the DMNs but that the sites occupied above each ring are altered by the presence of the bulky methyl groups.[31] In N and the 2,6-, 2,7-, 1,5- and 1,8- DMNs, these sites are equivalent and the cation

Table 5.6: Calculated coupling constant[a] differences induced by cation motion between two sites, A and B.

System:

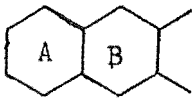

Interionic Distance(Å)	a_1 A	a_1 B	$\lvert\Delta a_1\rvert$ (G)	a_5 A	a_5 B	$\lvert\Delta a_5\rvert$
2.0	2.365	9.250	8.885	9.997	1.020	8.977
3.0	2.295	7.803	5.508	8.524	3.025	5.499
4.0	3.625	6.772	3.147	7.448	4.325	3.125
5.0	4.357	6.224	1.867	6.850	5.002	1.848
6.0	4.757	5.933	1.176	6.525	5.363	1.162

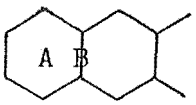

	a_1 A	a_1 B	$\lvert\Delta a_1\rvert$	a_5 A	a_5 B	$\lvert\Delta a_5\rvert$
2.0	0.365	4.138	3.773	9.997	5.743	4.254
3.0	2.295	4.832	2.537	8.524	5.816	2.708
4.0	3.625	5.120	1.495	7.448	5.885	1.563
5.0	4.357	5.257	0.900	6.850	5.922	0.928
6.0	4.757	5.329	0.572	6.525	5.941	0.584

ctd.

must spend an equal time above each ring to preserve the molecule's symmetrical spin distribution. Therefore $p_A = p_B$ and $\tau_A = \tau_B$. The exchange causes out-of-phase modulation of the proton spin densities, but is usually considered to be very fast. With the 2,3 and 1,4 compounds the sites are inequivalent, from both steric and electrostatic considerations [p. 78], and thus the populations of the two sites will be different, so that $p_A \neq p_B$ and $\tau_A \neq \tau_B$. The exchange process produces in-phase modulation of both proton and cation spin densities.

To adequately account for the observations, this cation movement across the molecule must satisfy the relationships of Eqn 5.8 which allow the two additional sharp lines to appear in each spectrum and cause the broadening rates of the exchanging lines to be about the same. As well, the spin densities of the substituents at positions 2 and 3 and 6 and 7 must change only a small amount with cation movement.

Evidence that these conditions are satisfied is provided by the spin density calculations. Table 5.6 lists the results, for various heights above the aromatic plane, of McClelland calculations[39] incorporating McLachlan's approximate treatment of configuration interaction,[16] for rapid cation motion in two cases: (1) between sites above the centres of each ring, and (2) between a site above the centre of the unsubstituted ring to one over the centre of the anion. Although the precise sites for the cation in forms A and B is not known, and are probably not those in the calculations, the calculations serve to show that, wherever these sites are, the changes induced in a_1 and a_5 (2,3DMN) and in a_{Me} and a_5 (1,4DMN) are about the same. Table 5.6 also shows that the induced changes in these coupling constants are large [T_2^{-1} (ex) α Δa^2 - Eqn 5.7], particularly for

Table 5.6 continued

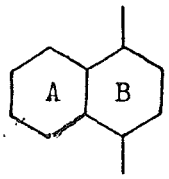

	a_{Me} A	a_{Me} B	$\lvert\Delta a_{Me}\rvert$	a_5 A	a_5 B	$\lvert\Delta a_5\rvert$
2.0	0.725	9.117	8.452 (9.102)[b]	10.134	1.391	8.743
3.0	2.328	7.453	5.125 (5.519)	8.898	3.547	5.351
4.0	3.470	6.367	2.897 (3.120)	7.900	4.846	3.054
5.0	4.114	5.824	1.710 (1.842)	7.311	5.496	1.815
6.0	4.470	5.544	1.074 (1.156)	6.979	5.835	1.144

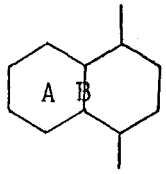

	a_{Me} A	a_{Me} B	$\lvert\Delta a_{Me}\rvert$	a_5 A	a_5 B	$\lvert\Delta a_5\rvert$
2.0	0.725	3.997	2.727 (2.937)[b]	10.134	6.485	3.649
3.0	2.328	4.576	2.248 (2.421)	8.898	6.436	2.462
4.0	3.470	4.818	1.348 (1.452)	7.900	6.425	1.475
5.0	4.114	4.932	0.818 (0.881)	7.311	6.417	0.894
6.0	4.470	4.991	0.521 (0.561)	6.979	6.411	0.568

a) All coupling constants in gauss; $Q = -Q' = -26.0$ G [Eqns 5.3 and 5.4]

b) $\lvert\Delta a_{Me}\rvert$ if $Q' = 28.0$ G.

the short distances characteristic of tight ion pairs. Similar calculations also show that differences in $|a_{Me}|$ and $|a_6|$ of 2,3DMN and in $|a_2|$ and $|a_6|$ of 1,4DMN are small ($\sim$0.2 G). Even allowing for the approximations made in these calculations, they provide valuable evidence that the conditions required for the observed broadening to occur are fulfilled.

At high temperatures, the 2,3- and 1,4 DMN/K/DME systems are assumed to consist of tight ion pairs in which the unsolvated potassium ion oscillates very rapidly in the y direction between two inequivalent sites, A and B. The tight ion pairs of all the other metal/solvent/anion combinations are assumed to be of similar structure - i.e. the cation migrates rapidly across the molecule between sites determined by the exact nature of the metal, solvent and anion and by the temperature. To account for the fact that broadening is observed only for the K/DME systems of the 1,4- and 2,3- DMN anion, the movement of the cation must be slower in these particular systems. Since the electrostatically favoured sites will be the same for all the 1,4- and 2,3- DMN systems, steric interactions appear to play a decisive role in determining the extent of allowed cation movement.

As the temperature is decreased, the K^+ ion of the tight ion pair becomes more tightly coordinated with DME molecules; the cation is probably still relatively close to the anion, but is now significantly bulkier. Since K^+ is a larger cation than Na^+, and DME is the strongest solvating agent, the partially solvated K^+ ion in the ion pair may reach a critical size while still close to the anion, where the additional steric interactions repel the cation from the less favoured site, (say B), thus raising the energy barrier for motion from A to B and slowing down the exchange rate. As the temperature continues to decrease

the group becomes bulkier and the broadening more extensive. At the same time, the cation is also being pulled away from the anion by the increased solvating power of the solvent. At larger interionic distances the sites tend to coalesce into a broad minimum [Fig. 5.2] characteristic of a loose ion pair, and the steric repulsions decrease. The rate process, becoming more like that of vibration about a shallow potential energy well, will be less restricted by steric interaction at these larger ionic distances, so the lines begin to sharpen again at lower temperatures. At sufficiently low temperatures, the lines should be restored to their expected amplitude. Thus the movement of the cation is very fast at high and low temperatures but considerably slower in between.

This model envisages a critical temperature range where the state of cation solvation (i.e. size of solvation cage) is large enough to cause substantial steric interactions with the methyl groups but where the cation is still reasonably close to the anion. In the Na/DME and Na/THF systems with the 1,4- and 2,3- DMN anions, proton lines are not broadened but the outer lines of cation hfs are. This indicates a rapid tight ion pair - loose ion pair equilibrium, in contrast to the gradual interconversion proposed in this model for the K/DME system. The sodium systems therefore have either a tightly bound unsolvated cation oscillating very rapidly between favoured sites, or a well-solvated cation far from the anion where very rapid cation vibration is again expected. The lack of intermediate configurations may account for the absence of broadening in these systems.

Although this interpretation of the linebroadening is speculative, it does seem to be consistent with the observations.

It would also predict that the additional steric effects present in K/DME systems should begin at a higher temperature in 1,4DMN than in 2,3DMN, because less solvation should be required to produce the same amount of interaction with the closer methyl groups.

A more quantitative analysis of the broadening is hampered by a lack of facts. In the usual cases where cation movement in ion pair systems produces an in-phase modulation of spin densities, it is the lines arising from the cation splitting which are broadened. Then an estimate of a_A, a_B, p_A and p_B may be made from the temperature dependence of the metal coupling constant [sections 3B.4, 5.3, 5.5]. A parallel procedure for the situation observed when proton lines are broadened requires an estimate of the proton coupling constants in forms A and B.* If the motion was slow enough to produce two sets of spectral lines at some temperature then a_A and a_B could be found. Since only one set of lines is observed at all temperatures, then either (a) the rate process is always in the fast exchange region and therefore a set of lines with time-averaged coupling constants is always found, or (b) when the rate is in the slow exchange limit, the percentage of the less favoured form, p_B, is very short. The proposed model favours case (a).

In summary, the K/DME system contains loose ion pairs at low temperatures and tight ion pairs at high temperatures. A gradual interconversion, rather than a rapid equilibrium, is postulated because this allows an explanation of the observed linewidth effects for the 1,4- and 2,3- DMNs in terms of cation

---

* It was considered that the calculated values [Table 5.6] were too approximate to use since the precise cation positions in forms A and B are unknown and the calculated values are very dependent on these as well as on interionic distance.

FIGURE 5.17

TEMPERATURE DEPENDENCE OF POTASSIUM HYPERFINE SPLITTINGS

SYSTEM : K/THF

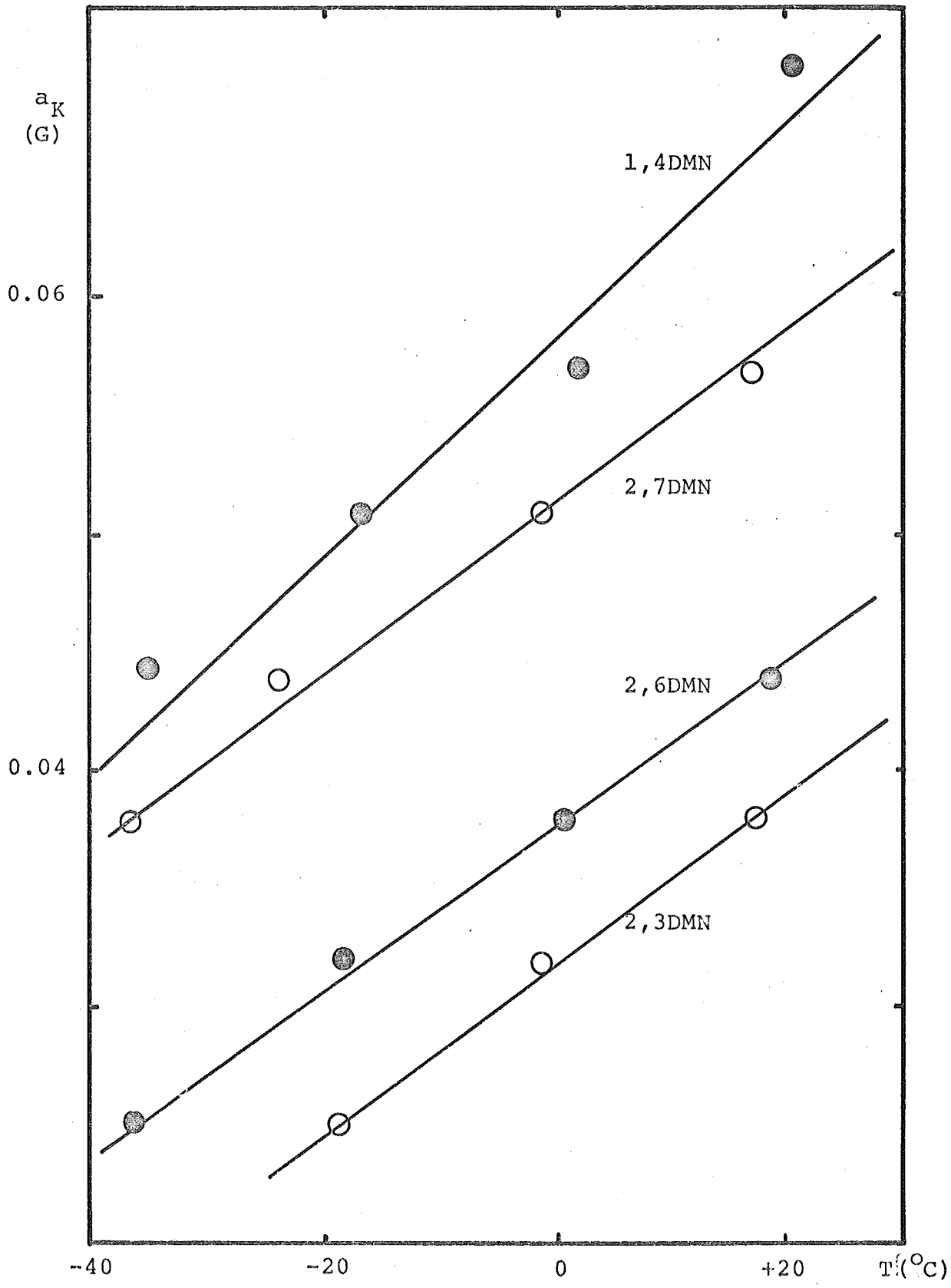

motion along the y axis of the anions. The same processes are assumed to occur in tight ion pairs of the other DMNs (and N), but the steric and electrostatic effects of methyl substitution are less drastic, and the rate remains very fast at all temperatures. In the N/K/DME system, this proposed model is in agreement with Reddoch's[49] conclusion based on the temperature dependence of the proton splittings. The change of sign of a_K observed by Hendricks[98] at lower temperatures is then due to increasing interionic distance, which, as noted in section 3B.6 and confirmed by calculation,[30] can lead to negative cation spin densities whenever the positive spin density is small.

5.7 K/THF systems

A Observations

As the temperature was raised in this system, potassium splittings were resolved for the 1,4-, 2,7-, 2,6-, and 2,3- DMNs, but not for N, 1,5- and 1,8- DMN. This latter group of compounds showed broadened lines at high and low temperatures; 2,3DMN spectra also broadened at low temperatures. Otherwise, narrow lines were detected in all systems. The temperature dependence of the resolved cation couplings is shown in Figure 5.17.

B Discussion

Potassium splittings have not been reported previously for any DMNs in K/THF, although de Waard[71] and Peake[74] have reported proton coupling constants for some compounds. Fraenkel[58] and Reddoch[49] did not detect any metal coupling in the N/K/THF system. Reddoch's[49] proton coupling constants at +26°C are identical to those observed in this study.

Since loose ion pairs involving potassium ions are expected

to have very small potassium splittings, those systems where a resolved splitting is observed will contain tight ion pairs. Two of these, the 2,3- and 1,4- DMNs, provide strong evidence that only tight ion pairs exist at all the studied temperatures. The magnitude of their a_5 and a_1 (a_{Me}) coupling constants, which are sensitive indicators of ion pair structure have values in the region expected for a tight ion pair structure in THF - i.e. between the values in strongly solvating systems like K/DME at low temperature and those found in weakly solvating systems like K/DEE. The lack of any large changes in the coupling constants with temperature is consistent with one type of ion pair structure throughout the temperature range. If solvent-separated ion pairs were formed on cooling, much smaller a_5 and larger a_1 (a_{Me}) values would be expected (p. 80), as are found in some other systems. On this evidence, tight ion pairs are proposed for all the anions in K/THF.

No K hfs was observed for some anions, but this is not uncommon even in tight ion pairs involving potassium because of the small magnetic moment of the K nucleus. If the observed broadening at both high and low temperatures is assumed to be due to unresolved metal splitting, positive and negative respectively, then the change in sign can be rationalised easily in terms of a reduced amplitude of vibration of the cation within the tight ion pairs on cooling.[18]

Although the tight ion pair classification is proposed for all compounds, the detailed ion pair structure depends on the nature of the anion as well as the metal and solvent. Clearly, the precise structure of the tight ion pairs is different for each system and the degree of "tightness" varies with temperature as the solvating properties of the solvent change. The small

FIGURE 5.18

TEMPERATURE DEPENDENCE OF POTASSIUM HYPERFINE SPLITTINGS

SYSTEM : K/MTHF

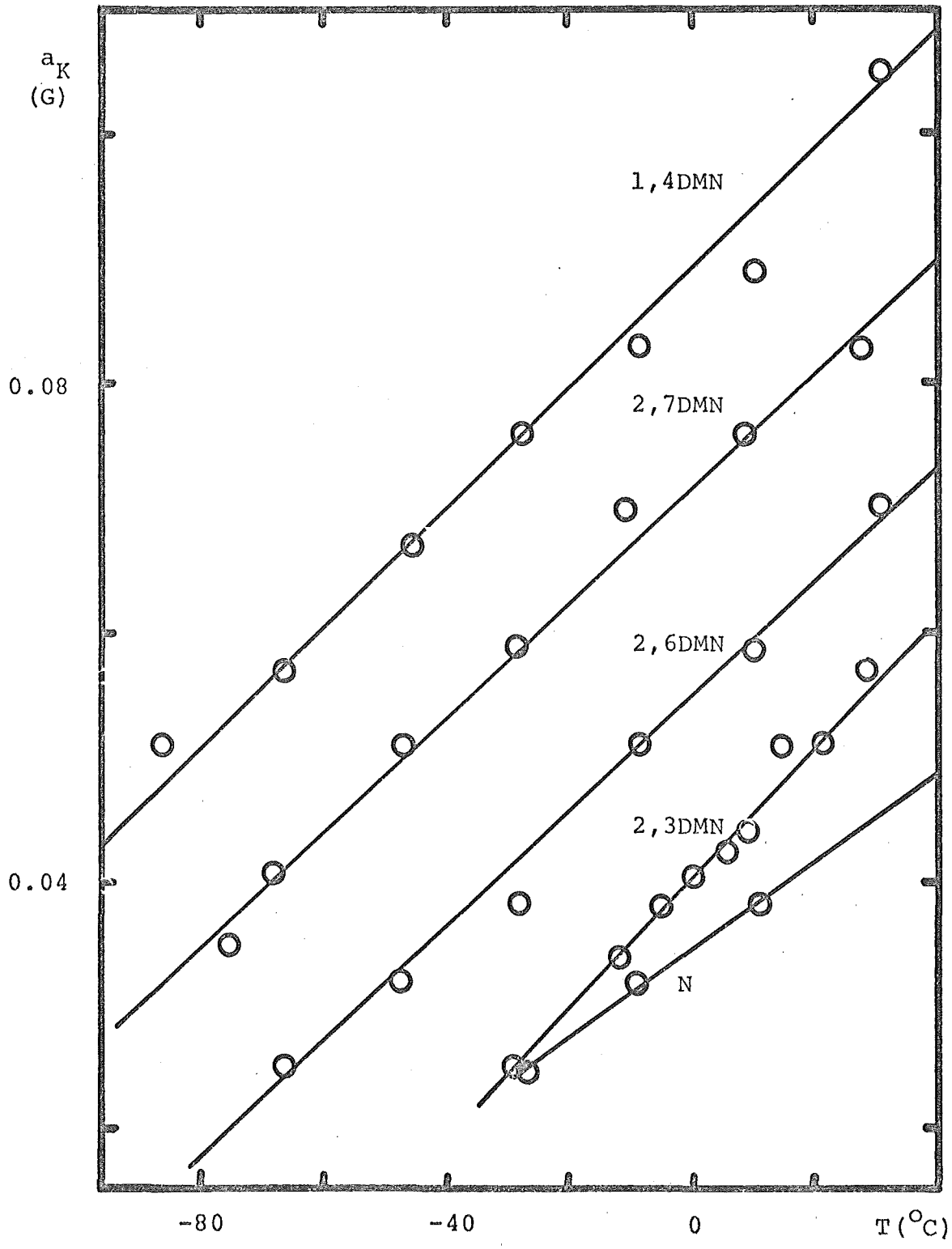

changes in the proton coupling constants and the temperature dependence of the K hfs reflect this latter point. The effect of the methyl substituents on the potassium splitting, which increases in the order 2,3 < 2,6 < 2,7 < 1,4, is interesting because the value in the 1,4 compound is unexpectedly high compared to the results for Na/THF system.

It seems that THF, in the K/THF system with the 1,4- and 2,3- DMN anions, is not able to coordinate with K^+ in the tight ion pairs to the same extent as DME does, since broadening is not observed in this system. This could reflect the fact that only one molecule of DME is required to coordinate with two cation sites, whereas two THF molecules are required [section 3B.7]. The methyl groups may hinder the approach of a second THF molecule sufficiently to prevent significant solvation of the K^+ ion at the temperatures studied.

5.8 K/MTHF systems

A Observations

Potassium couplings were resolved for N, 2,3-, 2,6-, 2,7- and 1,4- DMN, which increased with increasing temperature [Fig. 5.18]. Spectra for the 1,5- and 1,8- DMNs showed some broadening at high and low temperatures, as did those of 2,3DMN and N at very low temperatures (< -100°C). Narrow lines were found for all other conditions.

B Discussion

Potassium hfs have not been reported for any of these compounds in K/MTHF, and the only proton coupling constants available seem to be those of Peake[74] for the 1,8 compound, which are in fair agreement to those found here [Table A.3].

Like the K/THF system and for the same general reasons, this system is considered to contain tight ion pairs at all temperatures. Since ion pairs in MTHF would be expected to have less external solvation, they should form a tighter structure than those in THF. This is reflected in the potassium splittings where the trends are the same, but the magnitudes are greater in MTHF. It is also reflected in the a_5 and $a_1(a_{Me})$ coupling constants of 2,3- and 1,4- DMN in the two solvents where the magnitude of the coupling constants in MTHF is more like those predicted for poorly solvated systems - i.e. larger a_5 and smaller a_1 (a_{Me}) values.

The magnitude of a_5 increases considerably ($\sim$0.2 G) on cooling in both 1,4- and 2,3- DMN. Since this is in the opposite direction to that expected for the formation of loose ion pairs (p. 80) at low temperatures, it does not affect the postulate of tight ion pairs at all temperatures. If the shift is significant, the reason for it is not readily apparent but, since it is not observed when THF is the solvent, it may be related to small changes in structure caused by the extra bulk of the MTHF molecules as the degree of external solvation increases at low temperature. A similar effect was noted for the Na/MTHF system.

5.9 K/DEE systems

A Observations

Spectra for all compounds except 1,5- and 1,8- DMN displayed resolved potassium splittings and narrow lines throughout the temperature range [Fig. 5.19]. 1,5DMN showed a resolved coupling constant above $-70^{\circ}C$, but for the 1,8 compound only increased linebroadening was observed as the temperature was

FIGURE 5.19

TEMPERATURE DEPENDENCE OF POTASSIUM HYPERFINE SPLITTINGS

SYSTEM : K/DEE

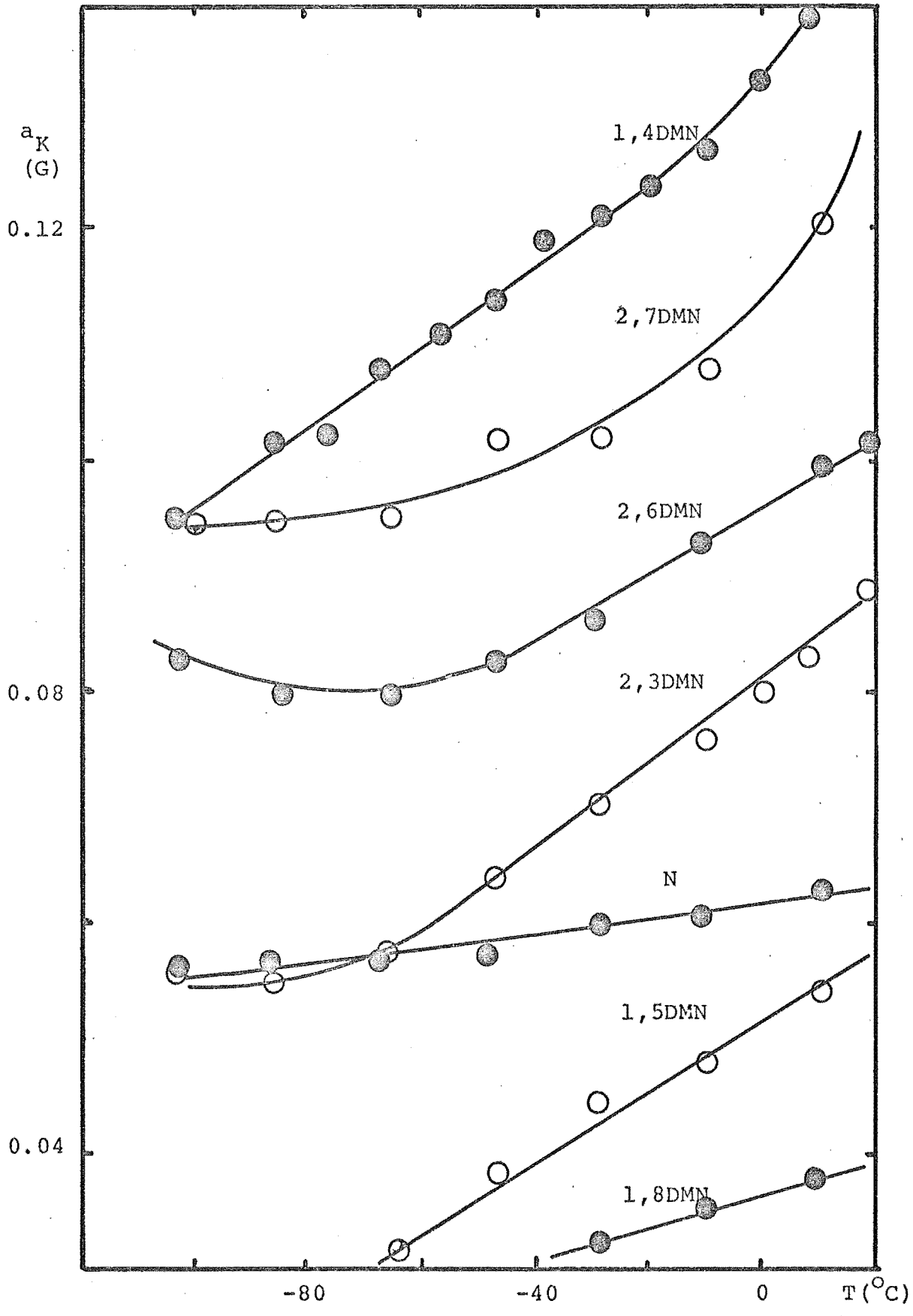

raised.

B Discussion

Hirota[45] and Fraenkel[50] have previously reported K hfs for the N/K/DEE system. Hirota's values are approximately temperature independent but Fraenkel's increase slightly more with temperature than those observed here, although the differences are small. There are no reports of the DMNs in K/DEE.

In this poorly solvating system, tight ion pairs are expected at all temperatures. Since DEE is a weaker solvating agent than MTHF, the extent of external ion pair solvation should be decreased, and the "degree of tightness" of the pair increased in this system. Accordingly, the potassium hfs are larger* and the magnitudes of the a_5 and a_1 (a_{Me}) coupling constants of the 2,3- and 1,4- DMNs are increased and decreased respectively (especially for 1,4DMN), relative to the K/MTHF system. The order of increasing cation splitting is typical of that found with potassium ion pairs, but is more complete than in the other solvents. At +20°C the order is 1,8 < 1,5 < N < 2,3 < 2,6 < 2,7 < 1,4. For the α-substituted compounds, the order is quite different from that found in sodium ion pairs and is discussed in section 5.10.

---

* The "degree of tightness" does not necessarily imply only a decrease in the interionic distance - it may mean that the cation spends more time in the minimum energy positions, as envisaged by Goldberg and Bolton.[51] If this is true, then these minimum energy sites must also correspond to positions of greater unpaired electron density on the cation, or a smaller time-average coupling constant might be expected.

5.10 Trends in the naphthalene and the symmetric dimethylnaphthalene systems.

With both sodium and potassium systems, the expected trends in ion pair type as the solvent is varied [section 3B.7] are found. Thus for sodium systems, loose ion pairs are found throughout the temperature range in DME, with tight pairs being formed only at higher temperatures and having a low relative concentration even at room temperature. In THF, tight ion pairs predominate at higher temperatures and loose ion pairs at low temperatures, the species being in rapid equilibrium in the intermediate range. Tight ion pairs exist throughout most of the temperature range studied in MTHF with loose ion pairs possibly formed at very low temperatures ($<\sim -100^{\circ}C$). Only tight pairs are found in DEE. For potassium systems, loose and tight ion pairs exist in DME only, the conversion taking place gradually as the temperature is varied. In the other solvents only tight pairs are formed, the "degree of tightness" increasing through THF, MTHF, DEE.

In comparing the sodium and potassium systems with each other, it is clear that loose ion pair formation is more favoured, in a given solvent, for sodium pairs. This is an expected trend, since Na^+ is a smaller cation than K^+ and therefore generates a stronger polarising field to interact with the solvent molecules.

In all tight ion pairs, the cation is assumed to be rapidly hopping between favoured sites. For all but the 1,4- and 2,3-DMNs, this process is between equivalent sites above each ring and is very fast under all conditions. For the inequivalent sites of the 1,4- and 2,3- compounds it is usually a very rapid process

FIGURE 5.20

STRUCTURAL FORMULAE FOR SOME ALKYL-SUBSTITUTED AROMATIC HYDROCARBONS

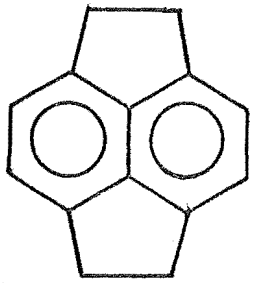

PYRACENE

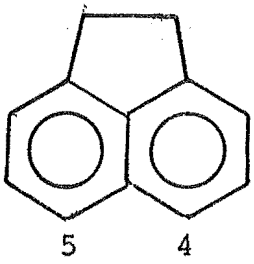

ACENAPHTHENE

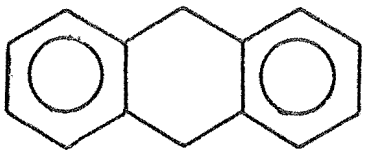

9,10-DIHYDROANTHRACENE

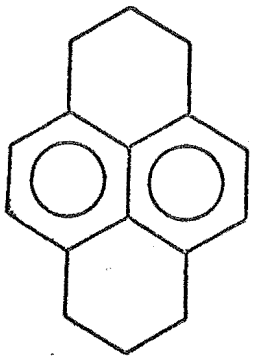

1,2,3,6,7,8-HEXAHYDROPYRENE

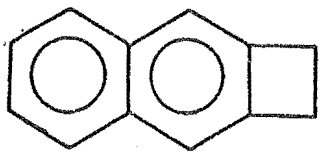

NAPHTHACYCLOBUTENE

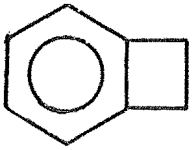

BENZOCYCLOBUTENE

also, but in the K/DME system the combined effects of the electrostatic and steric perturbations slow down this motion sufficiently to cause linebroadening. A change from tight to loose ion pairs with these two anions also involves significant changes in relative cation - anion geometry.

Cation jumping between double minima above six-membered rings has also been postulated[128,129] in peri-substituted alkyl naphthalenes, as well as in Goldberg and Bolton's later model[31] for naphthalene ion pairs. Iwaizumi[128] observed two linewidth alternation effects in acenaphthene [Fig. 5.20]: the first he explained in terms of cation exchange between positions above and below the molecular plane and the second he attributed to cation movement across the aromatic rings. As Reddoch[129] has recently shown, this should lead to broadening of the lines due to protons 4 and 5 as well. Although not reported by Iwaizumi, Reddoch detected this broadening on reinvestigating this system.* He also showed, using spin density calculations similar to those used in this work, that a similar type of second linewidth alternation noted by de Boer[29,32] in pyracene ion pairs [Fig. 5.20], is well accounted for by cation oscillation from one six-membered ring to the other. Earlier attempts to observe this movement experimentally with partially deuterated pyracene anions had been unsuccessful.[130] Cation movement from one aromatic ring to the other seems to account for the alternating linewidth effects observed in the 9,10-dihydroanthracene/K/DME: THF[131] and 1,2,3,6,7,8-hexahydropyrene/K/THF[132] systems [Fig. 5.20].

---

* In the K/DEE system used by Iwaizumi and Reddoch (-95°C), spectra of the closely-related 1,8DMN showed no selective broadening of the lines due to the methyl-protons or the protons on positions 4 and 5, at -107°C or -85°C.

Thus, there is a growing amount of evidence to support the type of cation movement proposed for the tight ion pairs with DMN anions.

Rieke investigated an interesting series of similar compounds in his studies of the effects of ring strain on spin densities, including the benzo- and naphtho-cyclobutene anions which have ethylene bridges at the 2 and 3 positions [Fig. 5.20]. The benzo-compound showed an alternating linewidth effect and inequivalent methylene protons[133,134] but Rieke found these protons were always equivalent in the naphtho- analogue.[135] He concluded that the cation was situated above the centre of the unsubstituted ring and was thus too far from the methylene protons to cause inequivalence. He also found that the a_5 and a_1 coupling constants were markedly dependent on the metal/solvent combination, with a_1 decreasing and a_5 increasing in poorly solvating systems, as found in this study for the 1,4- and 2,3-DMN systems. Unlike the DMNs in K/DME, the coupling constants were temperature independent from -50° to $+25^{\circ}C$. No broadening was reported for the lines from the protons at positions 4 and 5 in this or any other 2,3-alkyl substituted compound that Rieke studied.[72,73,135]

Although the introduction of a strained ring alters the spin distribution considerably,[72,135] the cation may be expected to occupy similar positions to those in the 1,4- and 2,3- DMN systems. Since the 2,3-naphthocyclobutene anion would have inequivalent cation sites along the y axis, the mean position of a cation oscillating between them would be more over the unsubstituted ring than the 9-10 bond and Rieke's reason for the equivalence of the methylene protons may still be valid.[135] The apparent lack of broadening in the K/DME system is surprising

but may reflect a greater steric interaction of the cation with the freely rotating methyl groups than with the rigid methylene protons. From the calculations in this chapter and those of Reddoch,[129] placing the cation over the centre of the unsubstituted ring should result in a substantial increase in the spin density of 5 and 8 positions, contrary to observation.[135] Hence the cation may be oscillating across the molecule in 2,3 naphthocyclobutene in a similar manner to that proposed for DMN ion pairs.

An unexpected feature of a comparison between the sodium and potassium DMN systems is the different order of the cation splitting in tight ion pair structures. For sodium pairs in THF and MTHF at 20°C, the sodium spin density increases in the order:

$$1,5 < 1,8 < N < 1,4 < 2,3 < 2,6 < 2,7.$$

At very low temperatures (< -80°C), the positions of '1,8' and 'N' reverse in MTHF, as do the positions of '2,3' and '2,6' below -30° in THF. On the other hand, the order of increasing potassium spin density in THF, MTHF and DEE is (at 20°C):

$$1,8 < 1,5 < N < 2,3 < 2,6 < 2,7 < 1,4.$$

In DEE and MTHF, '2,3' and 'N' tend to the same value at low temperatures (-70°C and -30°C respectively). For THF and MTHF, no potassium hfs was resolved for 1,8- and 1,5- DMN, and in THF for N as well.

Goldberg and Bolton[31] have suggested a model to account for the marked changes in cation spin density when alkyl groups are introduced into the naphthalene system, in terms of a 'steric' effect. They propose that in 1,5DMN, for instance, the cation, which is considered to be moving rapidly across the rings, is forced away from the positions of methyl substitution (1 and 5) toward the 4 and 8 positions; for 2,6 substitution they envisage

the cation oscillating between the two rings in a potential well that is "hardened" on the outsides by the proximity of the methyl groups. Using the cation spin density map calculated for naphthalene, they predicted these effects lead to a smaller cation spin density for 1,5DMN and a larger spin density for 2,6-substitution than is found in naphthalene.

This model successfully predicts the observed order of sodium and potassium spin densities to be:

$$1,8;\ 1,5 < N < 2,6;\ 2,7$$

Predictions when dimethyl substitution is in the same ring are not so obvious. The mean pcsition of the cation in these tight ion pairs is more over the unsubstituted ring than the centre of the molecule, but the precise details are not known. The sites the cation oscillates between are inequivalent, so the observed spin density depends on the relative occupation of each site [$a_{obs} = p_A a_A + p_B a_B$] which is also unknown.

The Bolton-Goldberg method[31] of calculating cation spin densities and the hyperconjugative - inductive model for the effects of substituting a methyl-group for a hydrogen [section 5.1] were combined to test whether calculated and experimental sodium hfs were in good agreement. Using an interionic distance of 3.0Å, this treatment produced the correct order of magnitude at the sites predicted to be minimum energy positions by the interaction energy calculations, for the 2,6-, 2,7-, 1,5- and possibly 2,3- DMN anions. However, the predicted values with the 1,8- and 1,4- compounds (especially 1,4DMN) were in very poor agreement, and it appears that approximations in this treatment are too severe to allow accurate spin densities to be confidently calculated. Hence information on cation position from these calculations is limited.

The observed difference in order of the metal coupling constants for Na and K indicates that tight ion pairs with the 1,4DMN anion and K^+ cation have a different structure to those with Na^+ as cation. It seems most likely that the K^+ ion, being larger*, will tend toward a mean position further away from the site of methyl substitution to minimize steric effects. This could arise from a greater time being spent at the most favoured site (greater p_A value) or from the actual sites being different for the two cations. Unfortunately, this cannot be tested by comparing the structure-dependent a_{Me} and a_5 coupling constants, because the two ions are of different size, and differing interionic distance also affects the proton splittings.

The observed order for the metal coupling constants in this series of dimethylnaphthalenes shows that the general predictions of the Goldberg-Bolton 'steric' model are followed - i.e. for α-methyl substitution lower cation spin densities should be found, with higher values expected for β-substitution. More subtle differences such as the order among the β- or α-substituted compounds, the effect of different metals and the effect of disubstitution in the same ring, require more detailed considerations taking account of the specific features of the entities involved.

5.11 The unsymmetric dimethylnaphthalenes

Spectra for the four unsymmetric dimethylnaphthalenes reduced in DME by potassium showed narrow lines at low temperatures but broadened considerably as the temperature was raised.

---

* Tight ion pairs with unsolvated cations are assumed.

Table 5.7: Additivity model for ring-proton splittings in the unsymmetric dimethylnaphthalenes.

Dimethyl derivative of naphthalene anion	Position	Expression for a_H	Calculated a_H
1,2-	3	$\beta + c + c'$	-2.44
	4	$\alpha + d + d'$	-4.52
	5	$\alpha + e + e'$	-5.37
	6	$\beta + f + f'$	-0.98
	7	$\beta + g + g'$	-2.58
	8	$\alpha + h + h'$	-4.78
1,3-	2	$\beta + b + c$	-1.82
	4	$\alpha + d + a'$	-4.06
	5	$\alpha + e + h'$	-5.06
	6	$\beta + f + g'$	-1.90
	7	$\beta + g + f'$	-1.66
	8	$\alpha + h + e'$	-5.09
1,6-	2	$\beta + b + f'$	-0.88
	3	$\beta + c + g'$	-2.42
	4	$\alpha + d + h'$	-4.25
	5	$\alpha + e + a'$	-4.87
	7	$\beta + g + c'$	-2.60
	8	$\alpha + h + d'$	-5.05
1,7-	2	$\beta + b + g'$	-1.80
	3	$\beta + c + f'$	-1.50
	4	$\alpha + d + e'$	-4.56
	5	$\alpha + e + d'$	-5.33
	6	$\beta + f + c'$	-1.92
	8	$\alpha + h + a'$	-4.59

The low temperature spectra were analysed by computer simulation and the experimental results are given in Table A.5, Appendix A.

In his extensive studies of methyl-substituted naphthalenes, Fraenkel[71] found that changes in the proton splittings caused by methyl substitution obeyed an additivity relationship, which may be stated as: methyl group substitution at positions i and j produces a change in the splitting at position k equal to the sum of the effects observed at k in radicals which are substituted only at i or only at j. The additivity relations are expected to be accurate when the substituent effects are small and the groups do not interact. Using Fraenkel's notation and values,* expressions for the ring-proton coupling constants for each position can be written and evaluated for the unsymmetric DMNs [Table 5.7]. These values are compared with those calculated by various MO theories in Table 5.8. The methyl-proton splittings may be confidently assigned on the basis of the MO calculations, but assignments for the ring-proton splittings must be more tentative. Those suggested [Table 5.8] were made by comparing the order of the splittings at different positions predicted by the various treatments; when the order varied, most weight was given to the additivity model followed by the simple HMO method, which gave the best results for the symmetric DMNs. The INDO calculations again produced the largest deviations from the experimental results and usually predicted the order within the large and small sets of splittings to be opposite that of the

---

* For a methyl group at position 1, the changes in the splittings at 2,3,4,5,6,7, and 8 positions are represented by b,c,d,e,f,g, and h, respectively; similarly, for a methyl group at position 2 the changes in the splittings are denoted a', c', d', e', f', g', and h', respectively. α and β are the proton splittings of the protons at positions 1 and 2 respectively in the naphthalene anion. All values were taken from Fraenkel's paper[71] and are based mainly on experimental results obtained from Na/DME systems.

Table 5.8: Calculated and experimental coupling constants[a] for the unsymmetric dimethylnaphthalenes.

Compound	Position	HMO	McL	INDO	Add.[b]	Exptal[c]
1,2DMN	3	2.1	1.8	0.4	2.44	2.31
	4	4.3	5.3	5.6	4.52	4.50
	5	4.9	6.2	4.7	5.37	5.42
	6	1.8	1.1	0.8	0.98	1.01
	7	1.9	1.2	0.9	2.58	2.65
	8	4.9	6.1	4.9	4.78	4.69
	CH_3-1	4.2	5.3	7.2	-	4.375
	CH_3-2	1.3	0.5	2.6	-	1.943
1,3DMN	2	1.7	1.2	0.9	1.82	1.88
	4	3.9	4.9	7.3	4.06	4.24
	5	4.8	5.9	5.3	5.06	5.07
	6	2.1	1.6	0.2	1.90	2.03
	7	1.6	0.7	2.1	1.66	1.76
	8	5.1	6.5	3.5	5.09	5.24
	CH_3-1	4.5	5.7	8.6	-	3.950
	CH_3-3	1.6	1.1	3.3	-	1.867
1,6DMN	2	1.3	0.4	1.3	0.88	1.11
	3	2.0	1.6	0.7	2.42	2.36
	4	4.2	5.1	5.2	4.25	4.10
	5	4.5	5.6	5.1	4.87	5.12
	7	2.1	1.5	0.8	2.60	2.76
	8	5.0	6.3	5.0	5.05	5.38
	CH_3-1	4.6	5.8	6.6	-	4.38
	CH_3-6	1.7	1.1	1.8	-	1.94
1,7DMN	2	1.6	0.9	1.2	1.80	1.87
	3	1.7	1.1	0.8	1.50	1.45
	4	4.4	5.5	5.1	4.56	4.54
	5	4.9	6.1	5.0	5.33	4.88
	6	2.3	1.8	0.6	1.92	1.95
	8	4.6	6.3	5.0	4.59	4.88
	CH_3-1	4.4	5.5	6.8		3.49
	CH_3-7	1.5	0.8	2.0		2.18

a) Footnotes a) - d) of Table 5.1 apply.

b) From Fraenkel's additivity relation.[71]

c) Suggested assignments.

other treatments. In general, the additivity model gives the most satisfactory fit with observed coupling constants.

The methyl-proton splittings can also be described by a similar type of additivity model. The results obtained for the unsymmetric DMNs allow the gaps in Fraenkel's model to be filled and further predictions made.

The methyl-proton splitting in 1-methylnaphthalene is denoted by P and changes produced in this splitting by methyl-group substitution at positions 2,3,4,5,6,7 and 8 are designated B,C,D,E,F,G, and H respectively; similarly, Q denotes the proton-methyl splitting in 2-methylnaphthalene and A', C', D', E', F', G', and H' represent changes in this splitting by methyl-group substitution at positions 1,3,4,5,6,7, and 8 respectively. If P and Q are taken to be 3.87 G and 1.71 G respectively, the experimental constants found by Fraenkel,[71] then all the remaining parameters may be determined from the experimental results obtained in this study. This approach has the advantage that all the experimental constants were determined under similar conditions. The splittings used were those found in K/DME systems at $\sim -70^{\circ}C$*, and the derived parameters are listed in Table 5.9.

Table 5.9: Additivity parameters for methyl-proton splittings in methyl-substituted naphthalenes.

Parameter	Value (G)	Parameter	Value
A	-	A'	+0.23
B	+0.51	B'	-
C	+0.08	C'	0.00
D	-0.63	D'	+0.16
E	+0.52	E'	-0.40
F	+0.11	F'	-0.49
G	-0.38	G'	+0.47
H	+0.69	H'	+0.47

* The value for P was found in the K/DME system at -76° and that for Q observed in a Na/DME system at -75°.

Table 5.10: Additivity model for the methyl-proton splittings in the symmetric tetramethylnaphthalene anions.

Tetramethyl derivative of naphthalene anion	Position	Expression	Calculated	Experimental
1458	1	P + D + E + H	4.45	4.35[a]
2367	2	Q + C' + F' + G'	1.69	1.62[b]
1234	1	P + B + C + D	3.83	3.74[c]
	2	Q + A' + C' + D'	2.10	1.98[c]
1256	1	P + B + E + F	3.83	
	2	Q + A' + E' + F'	1.05	
1278	1	P + B + G + H	4.69	
	2	Q + A' + G' + H'	2.88	
1357	1	P + C + E + G	4.09	
	2	Q + D' + F' + H'	1.85	
1368	1	P + C + F + H	4.75	
	2	Q + D' + E' + G'	1.94	
1467	1	P + D + F + G	2.97	
	2	Q + C' + E' + H'	1.78	

a) Ref 71; Na/DME at -91°C

b) Ref. 136; conditions unknown

c) Ref. 137; K/DME, Na/DME from -90° to +30°C.

Methyl-proton splittings in any methyl-substituted naphthalene compound can be predicted using these parameters. For instance, the predicted methyl-proton splittings in the symmetric tetramethylnaphthalenes are given in Table 5.10. Since the calculated values rely solely on experimental observations and have not been refined in any way, the agreement with the experimental results that are available is most satisfactory.

Although the spectra of all compounds broadened at higher temperatures, the spectra of the 1,3DMN in K/DME, where the substituents are on the same ring, showed the same type of selective broadening as that observed for the 1,4- and 2,3- DMNs in this system. The lines associated with the proton splittings of the 4, 5, and 8 protons and the 1 methyl group were less intense than expected at -87°C, and broadened considerably as the temperature was raised [Fig. 5.21]. The greater number of coupling constants and overlapping lines, and the reversible broadening of all lines at higher temperatures, prevent a more detailed analysis. The same model proposed for the 2,3- and 1,4- systems accounts for this linebroadening - i.e.: modulation of the spin densities of the 1, 4, 5, and 8 positions by movement of the cation between inequivalent sites, at a rate comparable to the inverse of the induced frequency changes. No selective broadening was observed for the 1,2- 1,6- or 1,7- DMN systems.

Since the linewidth effect was noted for the 2,3-, 1,4- and 1,3- DMN/K/DME systems, it is surprising it was not reported for the 1,2,3,4-tetramethylnaphthalene/K/DME system. Apparently spectra for this system were identical, from -90° to +30°C, to those found for the Na/DME system,[137] where broadening would not be predicted from the results of this project, and does not seem to be present from the published spectrum.[137] It is unlikely

FIGURE 5.21

ESR SPECTRA FOR THE 1,3DMN/K/DME SYSTEM

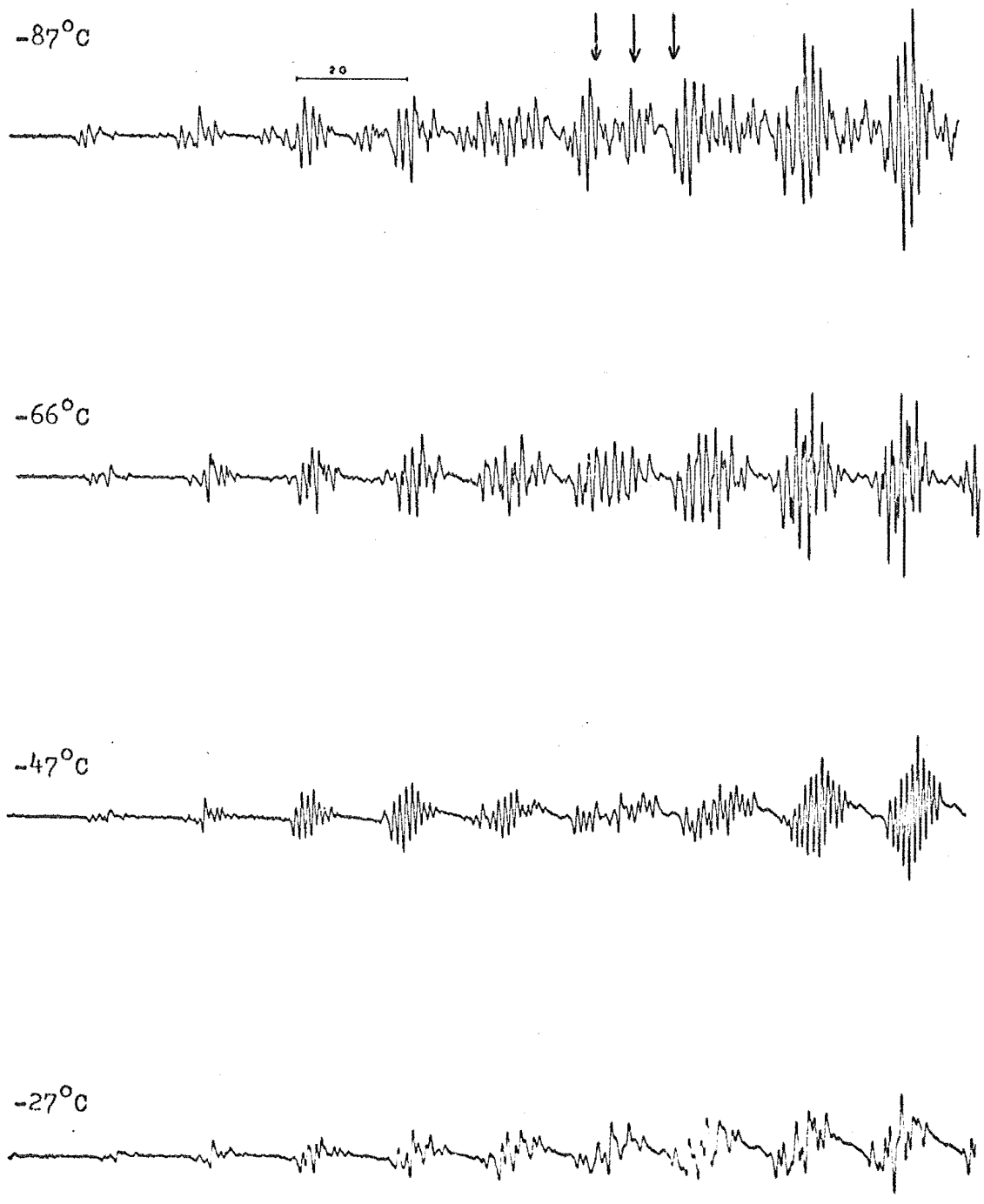

Regions of significant broadening arrowed

that the very slow exchange region has been reached where the cation is stationary above the unsubstituted ring, for then substantial differences in the proton coupling constants compared to those found for the 2,3- and 1,4- DMN systems [Table A.3] should result, contrary to observation.[137]

CHAPTER SIX

COMPARISON OF SYSTEMS

Since perylene, pyrene, and naphthalene radical ions were studied in this project, some of the effects on ion pair formation can be assessed. For instance, Table 6.1 compares the type of ion pairs found in the Na/MTHF system for the three anions. Some of the derived thermodynamic data can be directly compared to show the influence of the anion on a given process [Table 6.2]. Since large values of ΔH° and ΔS° indicate large changes in the state of solvation, the dissociation of perylene ion pairs involves significantly less solvent reorganisation than the dissociation of pyrene ion pairs.

Consideration of all the available results shows that for a given solvent, cation, and temperature, the extent of loose ion pair formation increases in the order $N << PY < PYL$. This is expected because the more extensive delocalization of the unpaired electron in the larger anions reduces the Coulombic energy required to separate the ions of a tight ion pair. The gain in solvation energy for these anion moieties is considered negligible.[36] It also follows that the 'tightness' of an ion pair structure will increase in the opposite order. A tighter structure does not necessarily result in a larger magnitude for the metal coupling constant under a given set of conditions. As discussed in section 3B.6, the magnitude depends not only on the interionic distance, but also on the relative positions of cation and anion, and the properties (particularly nodal properties) of the MOs of the particular anion. Thus, many pyrene ion pairs have a lower spin density on the cation than do

Table 6.1: Comparison of ion pair types for perylene, pyrene and naphthalene systems reduced with sodium in ether solvents.

Metal: Na

	PYL	PY	N
DME	LIP only	LIP only	LIP < -50°C; LIP⇌TIP (> -50°C)
THF	LIP only	LIP only	TIP only > +40°C; LIP⇌TIP; LIP only < -80°C.
MTHF	LIP low T; LIP⇌TIP (> -50°C)	LIP low T; LIP⇌TIP (> -50°C)	TIP only > -100°C; LIP⇌TIP (possibly < -100°C)
DEE	TIP only; or LIP low T; LIP⇌TIP > -110°C	TIP only	TIP only, $TIP_1 \rightleftharpoons TIP_2$

Table 6.2: Comparison of thermodynamic data for pyrene and perylene anion in common metal/solvent systems.

System	Process	ΔH° / kJ mol^{-1}	ΔS° / J K^{-1} mol^{-1}
PYL/K/MTHF	IP⇌FI	-9.6 ± 2	-155 ± 10
PY/K/MTHF	IP⇌FI	-19.3 ± 2	-210 ± 10
PYL/Cs/THF	IP⇌FI	-12.9 ± 2	-162 ± 10
PY/Cs/THF	IP⇌FI	-16.7 ± 2	-176 ± 10
PYL/Li/DEE[a)]	TIP⇌LIP	-34.3 ± 1.5	-171 ± 8
PY/Li/DEE	TIP⇌LIP	-34.3 ± 1	-172 ± 5

a) This process is postulated only on the basis of the a_{Li} vs T graph and may not exist.

the corresponding perylene systems, despite the looser ion pairs and greater interionic distances expected in the latter. The substantially greater cation spin densities in naphthalene systems do reflect the shorter interionic distances in these ion pairs.

All the anions have naphthalenic skeletons. In tight ion pairs with PY, N and the DMNs as anions, the cation* is envisaged as moving very rapidly between sites above the naphthalenic rings. In tight ion pair structures with the PYL anion, the most likely cation position seems to be between the two naphthalene systems. This may arise because less than half of the unpaired electron density is now located at each naphthalenic skeleton, so that Coulombic attraction above the rings is reduced. This may be no longer sufficient to drive the cation over the energy barriers for a rapid jumping process between the four equivalent sites.

The kinetic parameters derived in this project cannot be compared for anion effects because the metal and/or solvent varies also. Hirota has reported[46] that the N/Li/DEE system exhibits selective linebroadening of the hyperfine components of the lithium splitting, but does not appear to have published any kinetic parameters for this system. Since Li^+N^- ion pairs in tetrahydropyran and dioxane also show this effect,[88] the Li^+PY^- system in these solvents may also lead to linebroadening.

In all cases where the thermodynamic parameters of the conversion of tight to loose ion pairs were determined, negative ΔH° and ΔS° terms were found. Such changes are well-documented[19,40,45,47], and reflect the increased enthalpy of solvation and the greater freezing of solvent molecules about the

---

* For pyrene this applies only to the small cations like Li^+ and Na^+. Larger ions vibrate in a minimum above the centre of the molecule.

cation in loose ion pairs. Combining these thermodynamic conclusions with the observed effects on ion pair formation of varying cation, anion, solvent, and temperature, the conditions favouring the conversion of tight ion pairs to solvent-separated ion pairs may be summarised:

(1) Decreasing temperature: this reduces ΔG^{o}, since $\Delta G^{o} = \Delta H^{o} - T\Delta S^{o}$ and ΔS^{o} is negative;

(2) Increasing anion size: this increases electron delocalization which reduces the energy required to separate the ions and so leads to a more negative ΔH^{o} term;

(3) Decreasing cation size: while this increases the energy required to separate the ions ($\Delta H^{o}_{ion-ion}$), it also leads to a greater energy of solvation ($\Delta H^{o}_{ion-solvent}$) and a greater net negative ΔH^{o} term;

(4) Increasing solvating power of the solvent (DME > THF > MTHF > DEE): this depends on the coordinating ability and dielectric constant of each solvent in a complicated way,[37,99] and affects both the ΔH^{o} and ΔS^{o} terms.

The dimethylnaphthalenes behave similarly to naphthalene except where steric interactions become large. Since cation movement across the rings can be slowed down sufficiently to cause linebroadening in the 1,3-, 1,4-, and 2,3- DMN/K/DME systems, it might also be expected in a number of other DMN/metal/solvent systems. The larger cations, Rb and Cs, in the usual ether solvents or Li and Na in the larger glymes may be suitable combinations. A study of the tetramethylnaphthalenes (TMN) listed in Table 5.10 would be particularly interesting for two reasons: (1) to test the predictions of the additivity model [section 5.11], and (2) to investigate linebroadening effects. From the second point of view, the 1,2,3,4TMN/K/DME system might be reinvestigated,

for the broadening should be very apparent. The 1,4,6,7-compound, which could be synthesised by adapting Rieke's recent method,[138] would possess inequivalent cation sites but with steric interactions in both rings. The remaining symmetrical TMNs possess equivalent sites above each ring, but substantial steric effects. A study of these compounds could lead to much information on cation movement in substituted naphthalene systems.

APPENDIX A

Table A.1: Pyrene radical anion: coupling constants[a)]

System	Temperature[b)] (°C)	$\lvert a_\beta \rvert$[c)] (G)	$\lvert a_\alpha \rvert$[c)] (G)	$\lvert a_\gamma \rvert$[c)] (G)	$\lvert a_M \rvert$[c)] (G)
K/DME	+21	4.832	2.127	1.054	
	+7	4.832	2.127	1.048	
	-6	4.832	2.127	1.041	
	-23	4.832	2.127	1.035	
	-34	4.832	2.127	1.035	
	-48	4.832	2.127	1.035	
	-73	4.832	2.127	1.029	
	-83	4.832	2.127	1.022	
Li/DME	+25	4.902	2.156	1.068	
	+3	4.902	2.156	1.062	
	-17	4.902	2.156	1.055	
	-35	4.902	2.156	1.049	
	-55	4.902	2.156	1.042	
	-77	4.902	2.156	1.042	
Na/DME	+25	4.855	2.135	1.061	(0.025)
	+8	4.862	2.135	1.061	(0.019)
	-3	4.874	2.141	1.055	(0.013)
	-13	4.902	2.155	1.055	(0.006)
	-30	4.902	2.155	1.048	
	-45	4.902	2.155	1.048	
	-59	4.902	2.155	1.042	
	-79[67]	4.902	2.155	1.042	
	Segal[67]	4.856	2.139	1.024	
Cs/DME	+17[d]	4.797	2.117	1.055	(0.018)
	+2[d]	4.797	2.117	1.049	(0.013)
	-17[d]	4.797	2.117	1.035	(0.013)
	-35	4.797	2.117	1.029	(0.013)
	-55	4.797	2.117	1.029	(0.006)
	-73	4.797	2.117	1.023	(0.006)
	-84	4.797	2.117	1.016	(0.006)
K/THF	+20	4.807	2.102	1.041	(0.019)
	+2	4.807	2.108	1.035	(0.013)
	-17	4.807	2.115	1.035	(0.009)
	-28	4.807	2.121	1.029	(0.006)
	-51	4.807	2.121	1.022	
	-68[74]	4.807	2.121	1.016	
	Lyons[63]	4.80	2.11	1.03	
	Hoitjink[63] (-83)	4.75	2.08	1.09	

Table A.1 continued

System	Temperature (°C)	$\lvert a_\beta \rvert$ (G)	$\lvert a_\alpha \rvert$ (G)	$\lvert a_\gamma \rvert$ (G)	$\lvert a_M \rvert$ (G)
Na/THF	+32	4.797	2.116	1.055	(0.018)
	+22	4.797	2.122	1.048	(0.013)
	+11	4.797	2.122	1.041	(0.006)
	-5	4.797	2.122	1.035	
	-23	4.797	2.122	1.028	
	-40	4.797	2.122	1.022	
	-58	4.797	2.122	1.016	
Reddoch[69]	+25	4.815	2.125	1.040	
Hirota[75]	+25				0.0(nmr)
Li/THF	+35	4.830	2.130	1.055	(0.013)
	+18	4.830	2.130	1.049	(0.006)
	+2	4.830	2.130	1.042	
	-15	4.830	2.130	1.042	
	-32	4.830	2.130	1.035	
	-51	4.830	2.130	1.029	
	-62	4.830	2.130	1.022	
	-82	4.830	2.136	1.022	
Cs/THF					
Ion pair	+17	4.869	2.117	1.055	0.714
	+3	4.869	2.117	1.049	0.721
	-8	4.869	2.117	1.049	0.728
	-23	4.869	2.117	1.042	0.734
	-36	4.869	2.117	1.035	0.741
	-45	4.869	2.117	1.035	0.741
	-59	4.869	2.117	1.029	0.747
	-65	4.869	2.117	1.029	0.753
	-88	4.869	2.117	1.022	0.761
Free ion	+17	4.830	2.136	1.055	
	+3	4.830	2.136	1.049	
	-8	4.830	2.136	1.049	
	-23	4.830	2.136	1.042	
	-36	4.830	2.136	1.035	
	-45	4.830	2.136	1.035	
	-59	4.830	2.136	1.029	
	-65	4.830	2.136	1.029	
	-88	4.830	2.136	1.023	

Table A.1 continued

System	Temperature (°C)	$\lvert a_\beta \rvert$ (G)	$\lvert a_\alpha \rvert$ (G)	$\lvert a_\gamma \rvert$ (G)	$\lvert a_M \rvert$ (G)
Na/MTHF	+50	4.794	2.095	1.041	0.140
	+41	4.794	2.095	1.041	0.135
	+32	4.794	2.095	1.035	0.121
	+25	4.794	2.095	1.035	0.108
	+20	4.794	2.095	1.035	0.102
	+13	4.794	2.095	1.029	0.089
	+4	4.794	2.095	1.029	0.070
	-5	4.807	2.102	1.029	0.050
	-13	4.807	2.102	1.029	0.044
	-20	4.807	2.108	1.029	0.032
	-29	4.807	2.108	1.022	(0.019)
	-35	4.807	2.108	1.022	(0.006)
	-48	4.807	2.115	1.016	
	-58	4.807	2.115	1.016	
	-76	4.807	2.115	1.010	
Hirota[75]	+25	4.807	2.115	1.010	0.17(nmr)
Li/MTHF	+21	4.804	2.117	1.049	(0.012)
	+12	4.816	2.123	1.049	(0.006)
	+4	4.830	2.130	1.049	
	-15	4.850	2.136	1.042	
	-35	4.863	2.142	1.042	
	-52	4.863	2.142	1.035	
	-70	4.863	2.142	1.029	
	-89	4.863	2.142	1.029	
Second Species	+21	4.824	2.103	1.042	0.105
	+12	4.843	2.117	1.042	0.086
	+4	4.843	2.117	1.042	0.072
K/MTHF					
Ion pair	+23	4.862	2.108	1.054	0.057
	+15	4.862	2.108	1.048	0.057
	+7	4.862	2.108	1.048	0.057
	-5	4.862	2.108	1.041	0.057
	-13	4.862	2.108	1.041	0.057
	-22	4.862	2.108	1.035	0.057
	-29	4.862	2.108	1.028	0.057
	-41	4.849	2.108	1.028	0.057
	-58	4.849	2.108	1.022	0.057
	-67	4.849	2.108	1.016	0.051
	-71[e]				0.053
	-81[e]				0.050
	-88[e]				0.048
Free ion	-13	4.816	2.128	1.041	
	-22	4.816	2.128	1.035	
	-41	4.816	2.128	1.028	
	-58	4.816	2.128	1.022	
	-67	4.822	2.128	1.016	

Table A.1 continued

System	Temperature (°C)	$\lvert a_\beta \rvert$ (G)	$\lvert a_\alpha \rvert$ (G)	$\lvert a_\gamma \rvert$ (G)	$\lvert a_M \rvert$ (G)
Cs/MTHF	+13	4.836	2.091	1.049	0.773
	-2	4.836	2.091	1.042	0.780
	-17	4.849	2.092	1.042	0.786
	-29	4.849	2.092	1.035	0.800
	-42	4.849	2.092	1.029	0.806
	-53	4.849	2.103	1.023	0.812
	-63	4.849	2.110	1.023	0.819
	-83	4.875	2.123	1.016	0.832
K/DEE	+22	4.902	2.108	1.061	0.065
	+12	4.902	2.108	1.055	0.065
	0	4.902	2.108	1.055	0.065
	-11	4.908	2.108	1.055	0.072
	-20	4.908	2.108	1.048	0.072
	-28	4.922	2.116	1.048	0.072
	-37	4.922	2.116	1.048	0.072
	-48	4.922	2.116	1.041	0.078
	-59	4.914	2.116	1.035	0.078
	-64	4.922	2.122	1.035	0.078
	-78	4.914	2.122	1.028	0.078
	-90	4.914	2.122	1.028	0.085
Na/DEE	+16	4.807	2.089	1.035	0.051
	+3	4.807	2.095	1.029	0.044
	-12	4.807	2.102	1.022	0.038
	-21	4.807	2.102	1.022	0.032
	-28	4.807	2.102	1.022	(0.025)
	-54[f)]	4.807	2.114	1.016	
	-68[f)]	4.807	2.127	1.016	(0.006)
	-86[f)]	4.813	2.127	1.010	0.038
	-112[f)]	4.813	2.127	1.003	0.070

Table A.1 continued

System	Temperature (°C)	$\lvert a_\beta \rvert$ (G)	$\lvert a_\alpha \rvert$ (G)	$\lvert a_\gamma \rvert$ (G)	$\lvert a_M \rvert$ (G)
Li/DEE					
ion pair[g]	+20	4.771	2.136	1.029	0.180
	+10	4.771	2.136	1.029	0.190
	-5	4.771	2.136	1.029	0.203
	-18	4.771	2.136	1.029	0,216
	-27	4.785	2.148	1.022	0.223
	-37	4.797	2.156	1.022	0.223
	-45	4.797	2.156	1.022	0.218
	-53	4.804	2.156	1.022	0.210
	-66	4.817	2.156	1.016	0.164
	-77[h]	4.830	2.150	1.016	0.105
	-73[h]				0.130
	-83[h]				0.060
free ion	-54	4.889	2.156	1.022	
	-66	4.889	2.156	1.022	
	-77	4.889	2.156	1.022	
	-90	4.889	2.156	1.016	

Footnotes:

a) Values used to construct the computer simulated spectra which gave the best agreement with experimental spectra; smallest interval in computer simulations is 0.006 G.

b) $\pm$ 1.5°C

c) $\pm$ 0.015 G

d) Second species observed, but signal-to-noise ratio too poor to determine coupling constants: $\lvert a_{Cs} \rvert \sim 0.3$ G at +17°C.

e) From 1 G/40 cm spectra; below -70°C 10 G/40 cm spectra too difficult to simulate accurately because of changing a_K and Δg and overlapping of components.

f) In one sample a second species was observed; this had $\lvert a_M \rvert$ = 0.146 G at -112°C, 0.133 G at -86°C and -0.127 G at -68°C.

g) Coupling constants are for both ion pairs; a slight difference in a_β is discussed in the text.

h) From 1 G/40 cm spectra.

Table A.2: Perylene radical anion: coupling constants[a)]

System	Temperature (°C)	$\lvert a_\alpha \rvert$ (G)	$\lvert a_\beta \rvert$ (G)	$\lvert a_\gamma \rvert$ (G)	$\lvert a_M \rvert$ (G)
K/DME	-86	3.478	3.039	0.432	
	-73	3.478	3.039	0.432	
	-60	3.478	3.039	0.432	
	-39	3.472	3.026	0.432	
	-17	3.459	3.020	0.438	
	-6	3.453	3.020	0.438	
	+10	3.453	3.020	0.438	
Li/DME	-87	3.516	3.064	0.425	
	-81	3.516	3.064	0.425	
	-70	3.503	3.058	0.432	
	-49	3.503	3.058	0.432	
	-34	3.503	3.052	0.438	
	-19	3.503	3.052	0.438	
	-13	3.503	3.052	0.438	
	+1	3.503	3.045	0.444	
Na/DME	-83	3.484	3.052	0.438	
	-62	3.484	3.052	0.438	
	-46	3.484	3.045	0.438	
	-30	3.491	3.039	0.438	
	-14	3.491	3.039	0.444	
	+2	3.491	3.039	0.444	
	+18	3.491	3.039	0.444	
Cs/DME	-86	3.503	3.064	0.432	
	-74	3.503	3.064	0.432	
	-62	3.478	3.052	0.438	
	-51	3.472	3.045	0.438	
	-36	3.472	3.045	0.438	
	-20	3.472	3.045	0.444	
K/THF	-90	3.497	3.039	0.419	
	-73	3.497	3.039	0.419	
	-57	3.497	3.039	0.425	
	-39	3.497	3.039	0.425	
	-23	3.491	3.033	0.432	
	-4	3.491	3.033	0.438	
	+15	3.484	3.033	0.444	
Carrington[62]		4.11	3.09	0.46	

Table A.2 continued

System	Temperature (°C)	$\|a_\alpha\|$ (G)	$\|a_\beta\|$ (G)	$\|a_\gamma\|$ (G)	$\|a_M\|$ (G)
Na/THF	-81	3.478	3.020	0.419	
	-71	3.478	3.020	0.419	
	-66	3.478	3.020	0.419	
	-62	3.472	3.020	0.419	
	-54	3.472	3.014	0.419	
	-43	3.465	3.007	0.425	
	-35	3.465	3.007	0.432	
	-28	3.465	3.007	0.438	
Li/THF	-82	3.491	3.039	0.419	
	-66	3.484	3.033	0.419	
	-47	3.478	3.026	0.425	
	-29	3.472	3.026	0.432	
	-13	3.472	3.020	0.432	
	+3	3.472	3.020	0.438	
Hnoosh[82]		3.53	3.09	0.46	
Cs/THF					
Ion pair	-98	3.524	3.095	0.435	0.300
	-81	3.517	3.076	0.435	0.326
	-62	3.505	3.064	0.441	0.326
	-42	3.498	3.057	0.447	0.326
Free ion	-98	3.517	3.057	0.421	
	-81	3.492	3.038	0.421	
	-62	3.492	3.038	0.428	
	-42	3.492	3.038	0.435	
Na/MTHF					
Ion pair	-68	3.498	3.057	0.435	(0.006)
	-49	3.498	3.057	0.435	(0.012)
	-28	3.511	3.070	0.441	0.038
	-12	3.511	3.070	0.447	0.057
	+4	3.505	3.064	0.453	0.089
Free ion	-28	3.492	3.045	0.422	
	-12	3.492	3.045	0.428	
	+4	3.492	3.045	0.435	

Table A.2 continued

System	Temperature (°C)	$\|a_\alpha\|$ (G)	$\|a_\beta\|$ (G)	$\|a_\gamma\|$ (G)	$\|a_M\|$ (G)
Li/MTHF					
Ion pair	-105	3.524	3.095	0.435	
	-86	3.517	3.076	0.435	
	-67	3.498	3.057	0.435	
	-48	3.492	3.051	0.435	
	-28	3.479	3.038	0.441	
	-7	3.479	3.038	0.447	
	+15	3.473	3.025	0.447	
Free ion	-105	3.505	3.070	0.416	
	-86	3.505	3.051	0.422	
K/MTHF					
Ion pair	-105	3.505	3.070	0.435	
	-85	3.505	3.070	0.435	
	-65	3.505	3.064	0.435	
	-45	3.505	3.057	0.441	
	-25	3.505	3.057	0.447	(0.012)
	-5	3.505	3.057	0.450	(0.018)
	+15	3.505	3.057	0.450	(0.025)
Free ion	-105	3.505	3.045	0.416	
	-85	3.486	3.025	0.422	
	-45	3.473	3.012	0.428	
	-25	3.473	3.000	0.428	
Cs/MTHF					
Ion pair	-100	3.524	3.095	0.428	0.422
	-80	3.524	3.095	0.435	0.441
	-60	3.518	3.064	0.435	0.454
	-43	3.518	3.047	0.441	0.467
	-23	3.518	3.047	0.441	0.486
	-2	3.511	3.047	0.447	0.506
	+16	3.511	3.047	0.557	0.511
Free ion	-100	3.505	3.038	0.416	
	-80	3.505	3.038	0.416	
	-60	3.505	3.031	0.422	
K/DEE	-103	3.524	3.127	0.454	0.051
	-82	3.524	3.127	0.454	0.051
	-64	3.524	3.127	0.460	0.051
	-44	3.524	3.127	0.460	0.044
	-24	3.524	3.123	0.467	0.044
	-2	3.524	3.123	0.467	0.044

Table A.2 continued

System	Temperature (°C)	$\|a_\alpha\|$ (G)	$\|a_\beta\|$ (G)	$\|a_\gamma\|$ (G)	$\|a_M\|$ (G)
Na/DEE	-104	3.524	3.114	0.454	
	-97	3.524	3.114	0.454	
	-89	3.524	3.114	0.454	0.025
	-76	3.518	3.114	0.460	0.051
	-68	3.518	3.114	0.460	0.055
	-48	3.518	3.114	0.467	0.077
	-28	3.518	3.114	0.473	0.096
	-9	3.505	3.114	0.479	0.115
	+1				0.128
	+26				0.141
Li/DEE	-99	3.524	3.095	0.441	
	-79	3.524	3.095	0.441	
	-61	3.517	3.076	0.447	
	-43	3.524	3.076	0.447	(0.013)
	-23	3.486	3.057	0.454	0.032
	-3	3.473	3.057	0.460	0.051
	+17	3.447	3.031	0.460	0.057

a) Footnotes a) - c) of Table A.1

Table A.3: Proton Coupling constants for the symmetric dimethylnaphthalenes and naphthalene.[a)]

System	Temperature (°C)	$\|a_2\|$ (G)	$\|a_3\|$ (G)	$\|a_{CH_3}\|$ (G)	$\|a_4\|$ (G)
1,5DMN					
K/DME	-56	1.132	2.443	4.387	4.490
	+1	1.145	2.405	4.355	4.458
Na/DME	-88	1.126	2.462	4.393	4.490
	-71	1.126	2.436	4.374	4.483
	-55	1.126	2.398	4.336	4.452
	-33	1.126	2.347	4.259	4.374
Gerson[69]	-70	1.13	2.46	4.41	4.50
Peake[74]	-85	1.19	2.441	4.378	4.464
K/THF	-53	1.126	2.514	4.458	4.502
	-35	1.132	2.475	4.413	4.470
	+18	1.157	2.392	4.349	4.413
Na/THF	-86	1.100	2.449	4.413	4.477
	-10	1.126	2.507	4.381	4.425
K/MTHF	-101	1.100	2.564	4.477	4.477
	-46	1.132	2.495	4.419	4.458
	-8	1.132	2.436	4.343	4.381
Na/MTHF	-47	1.055	2.520	4.387	4.387
	-10	1.081	2.514	4.381	4.381
K/DEE	-102	1.126	2.507	4.400	4.400
	-28	1.164	2.449	4.374	4.419
1,8DMN					
K/DME	-56	1.657	1.714	4.560	4.662
	-20	1.625	1.720	4.541	4.611
	+16	1.611	1.733	4.541	4.566
Campion[71]	-70	1.680	1.680	4.538	4.677
Na/DME	-71	1.682	1.682	4.553	4.681
	-33	1.657	1.657	4.509	4.630
	-18	1.657	1.657	4.509	4.618
Gerson[69]	-70	1.70	1.70	4.61	4.73
Peake[74]	-85	1.678	1.678	4.535	4.665

Table A.3 continued

System	Temperature (°C)	$\|a_2\|$ (G)	$\|a_3\|$ (G)	$\|a_{CH_3}\|$ (G)	$\|a_4\|$ (G)
K/THF	-91	1.663	1.810	4.656	4.713
	-73	1.638	1.778	4.599	4.650
	0	1.599	1.733	4.534	4.566
Peake[74]	-90 to +40	1.678	1.678	4.535	4.665
Na/THF	-103	1.707	1.707	4.618	4.758
	-83	1.701	1.701	4.627	4.762
	-27	1.625	1.785	4.585	4.630
	+11	1.611	1.766	4.566	4.592
Peake[74]	-90	1.63	1.63	4.58	4.58
K/MTHF	-83	1.651	1.797	4.611	4.669
	-8	1.631	1.739	4.553	4.599
Peake[74]	-120 to -40	1.70	1.70	4.64	4.64
Na/MTHF	-84	1.644	1.835	4.630	4.694
	-65	1.644	1.835	4.637	4.688
	-28	1.599	1.804	4.579	4.599
	-10	1.586	1.804	4.560	4.560
K/DEE	-85	1.714	1.810	4.605	4.707
	-10	1.682	1.752	4.553	4.611
1,4DMN			$\|a_6\|$		$\|a_5\|$
K/DME	-69	1.663	1.829	3.300	5.416
	-28	1.669	1.829	3.175	5.513
	-9	1.657	1.823	3.108	5.519
	+11	1.651	1.816	3.076	5.506
Na/DME	-89	1.688	1.842	3.358	5.416
	-69	1.669	1.835	3.339	5.391
	-48	1.663	1.823	3.320	5.353
	-29	1.650	1.804	3.300	5.347
Gerson[69] Peake[74]	-70	1.63	1.79	3.26	5.17
	-85	1.679	1.858	3.361	5.439
Campion[71]	-70	1.671	1.832	3.343	5.393
K/THF	-74	1.694	1.848	3.102	5.672
	-35	1.682	1.848	3.083	5.647
	+2	1.663	1.842	3.057	5.603
de Waard[71]	-50	1.65	1.81	3.03	5.58

Table A.3 continued

System	Temperature (°C)	$\|a_2\|$ (G)	$\|a_6\|$ (G)	$\|a_{CH_3}\|$ (G)	$\|a_5\|$ (G)
Na/THF	-82	1.688	1.835	3.396	5.423
	-26	1.663	1.841	2.948	5.475
	+10	1.663	1.835	2.910	5.641
K/MTHF	-86	1.707	1.867	2.948	5.811
	-45	1.676	1.848	2.929	5.743
	-28	1.682	1.842	2.923	5.685
	+11	1.657	1.835	2.929	5.622
Na/MTHF	-86	1.695	1.861	2.789	5.865
	-28	1.669	1.855	2.795	5.813
	+9	1.650	1.823	2.795	5.769
K/DEE	-102	1.707	1.874	2.820	5.897
	-85	1.701	1.874	2.833	5.890
	-46	1.688	1.855	2.820	5.794
	+10	1.663	1.842	2.826	5.718
2,7DMN		$\|a_3\|$	$\|a_{CH_3}\|$	$\|a_1\|$	$\|a_4\|$
K/DME	-89	1.797	2.200	4.413	5.231
	-49	1.810	2.168	4.400	5.231
	-31	1.810	2.149	4.368	5.200
	-12	1.816	2.149	4.343	5.200
Na/DME	-88	1.791	2.200	4.406	5.218
[69]	-36	1.791	2.194	4.368	5.206
Gerson [74]	-70	1.76	2.16	4.32	5.12
Peake	-85	1.784	2.195	4.386	5.215
K/THF	-74	1.861	2.168	4.419	5.212
	-1	1.835	2.136	4.381	5.200
Na/THF	-86	1.785	2.200	4.419	5.238
	-45	1.835	2.130	4.355	5.193
	-10	1.842	2.111	4.349	5.174
K/MTHF	-86	1.861	2.200	4.419	5.231
	-68	1.867	2.194	4.425	5.237
	-10	1.835	2.136	4.336	5.181

Table A.3 continued

System	Temperature (°C)	$\|a_3\|$ (G)	$\|a_{CH_3}\|$ (G)	$\|a_1\|$ (G)	$\|a_4\|$ (G)
Na/MTHF	-65	1.874	2.142	4.400	5.206
	-27	1.835	2.085	4.324	5.097
	+10	1.848	2.085	4.317	5.110
K/DEE	-85	1.861	2.174	4.400	5.244
	-65	1.842	2.155	4.375	5.219
	-9	1.816	2.117	4.324	5.161
2,3DMN		$\|a_{CH_3}\|$	$\|a_6\|$	$\|a_1\|$	$\|a_5\|$
K/DME	-85	1.714	1.797	4.733	5.033
	-45	1.707	1.785	4.515	5.078
	-17	1.739	1.739	4.432	5.135
Rieke[72]	-65	1.7	1.8	4.7	5.0
	+25	1.75	1.75	4.32	5.25
Na/DME	-74	1.688	1.779	4.681	4.937
	-57	1.682	1.758	4.662	4.893
	-39	1.688	1.752	4.669	4.886
Gerson[69]	-70	1.69	1.76	4.67	4.93
Peake[74]	-85	1.701	1.767	4.729	5.002
K/THF	-73	1.739	1.810	4.355	5.309
	-36	1.739	1.797	4.336	5.238
	+1	1.733	1.758	4.336	5.238
Peake[74]	-90 to +40	1.78	1.78	4.40	5.38
Na/THF	-84	1.688	1.758	4.681	4.963
	-44	1.739	1.810	4.331	5.155
	-10	1.739	1.791	4.266	5.225
Peake[74]	-95	1.701	1.767	4.729	5.002
K/MTHF	-89	1.766	1.861	4.297	5.525
	-48	1.752	1.816	4.259	5.378
	+10	1.739	1.791	4.259	5.231
Na/MTHF	-84	1.766	1.861	4.137	5.590
	-65	1.739	1.835	4.106	5.410
	+10	1.739	1.797	4.080	5.366
K/DEE	-47	1.739	1.804	4.183	5.340
	-29	1.746	1.816	4.190	5.398
	-11	1.739	1.810	4.163	5.404

Table A.3 continued

System	Temperature (°C)	$\lvert a_{CH_3} \rvert$ (G)	$\lvert a_3 \rvert$ (G)	$\lvert a_1 \rvert$ (G)	$\lvert a_4 \rvert$ (G)
2,6DMN					
K/DME	-72	1.222	2.724	4.681	4.835
	-39	1.183	2.757	4.643	4.822
	+17	1.126	2.757	4.553	4.758
Na/DME	-77	1.260	2.743	4.758	4.912
	-55	1.222	2.705	4.681	4.835
	-36	1.209	2.686	4.643	4.797
	-18	1.189	2.648	2.585	4.719
Gerson[69]	-70	1.22	2.68	4.65	4.79
Peake[74]	-85	1.223	2.702	4.675	4.914
K/THF	-74	1.216	2.795	4.681	4.866
	-18	1.164	2.776	4.605	4.803
	+1	1.138	2.757	4.566	4.765
Na/THF	-82	1.266	2.623	4.662	4.790
	-45	1.195	2.770	4.649	4.822
	-9	1.157	2.795	4.605	4.797
	+11	1.151	2.795	4.585	4.778
K/MTHF	-103	1.228	2.770	4.643	4.835
	-47	1.189	2.789	4.624	4.816
	-8	1.157	2.782	4.605	4.790
Na/MTHF	-83	1.241	2.801	4.670	4.866
	-65	1.216	2.801	4.675	4.866
	-28	1.183	2.782	4.599	4.803
	+10	1.157	2.763	4.553	4.752
K/DEE	-84	1.209	2.814	4.669	4.860
	-46	1.164	2.798	4.605	4.813
	-29	1.145	2.789	4.585	4.784
	-10	1.138	2.782	4.578	4.777
	+11	1.132	2.776	4.532	4.745

Table A.3 continued

System	Temperature (°C)	$\|a_1\|$ (G)	$\|a_2\|$ (G)
N			
K/DME	-75	4.965	1.842
	-18	4.925	1.835
	Reddoch[49] +26	4.91	1.835
Na/DME	-89	4.975	1.842
	-19	4.918	1.816
	Reddoch[49] +26	4.92	1.825
K/THF	-93	4.985	1.865
	-56	4.930	1.848
	+20	4.908	1.838
	Reddoch[49] +26	4.91	1.84
Na/THF	-98	4.975	1.838
	-45	4.910	1.843
	Reddoch[49] +26	4.91	1.85
K/MTHF	-104	4.985	1.878
	-66	4.960	1.872
	-46	4.944	1.861
	-26	4.886	1.842
	+12	4.852	1.828
Na/MTHF	-66	4.956	1.874
	-39	4.925	1.858
	-11	4.905	1.850
	+18	4.859	1.838
Na/DEE	-100	4.925	1.867
	-76	4.888	1.861
	-10	4.857	1.852
K/DEE	-67	4.973	1.888
	+10	4.890	1.843

a) Footnotes a) - c) of Table A.1

Table A.4: Alkali metal hyperfine splittings for the dimethylnaphthalenes and naphthalene.[a)]

System	Temperature (°C)	$\lvert a_M \rvert$ (G)
1,5DMN/Na/THF	-47	0.429
	-37	0.550
	-27	0.656
	-19	0.716
	-10	0.748
	-1	0.718
	+10	0.812
1,5DMN/Na/MTHF	-101	0.531
	-96	0.537
	-86	0.576
	-76	0.607
	-64	0.626
	-57	0.653
	-47	0.684
	-37	0.710
	-28	0.741
	-17	0.781
	-10	0.806
	+1	0.851
	+9	0.889
	+19	0.908
1,5DMN/K/DEE	-82	(0.026)
	-64	0.032
	-46	0.038
	-28	0.044
	-9	0.047
	+10	0.054
1,4DMN/K/DME	+19	(0.032)
	+31	(0.051)
	+42	(0.063)
1,4DMN/K/THF	-74	(0.025)
	-54	0.032
	-35	0.044
	-17	0.051
	+2	0.057
	+21	0.070

Table A.4 continued

System	Temperature (°C)	$\|a_M\|$ (G)
1,4DMN/Na/THF	-54	0.422
	-46	0.633
	-37	0.767
	-28	0.832
	-26	0.832
	-19	0.901
	-9	0.931
	-1	0.978
	+10	1.004
	+18	1.029
1,4DMN/K/MTHF	-101	0.044
	-86	0.051
	-66	0.057
	-45	0.066
	-28	0.077
	-8	0.084
	+11	0.090
	+31	0.106
1,4DMN/Na/MTHF	-113	0.754
	-103	0.773
	-86	0.806
	-75	0.854
	-67	0.863
	-58	0.901
	-48	0.928
	-36	0.966
	-28	0.985
	-17	1.010
	-10	1.048
	0	1.100
	+9	1.138
	+18	1.177
1,4DMN/K/DEE	-102	0.096
	-85	0.103
	-75	0.103
	-67	0.109
	-56	0.113
	-46	0.115
	-38	0.120
	-27	0.122
	-19	0.125
	-10	0.128
	0	0.134
	+10	0.141
	+18	0.147

Table A.4 continued

System	Temperature (°C)	$\|a_M\|$ (G)
1,8DMN/Na/THF	-46	0.512
	-36	0.678
	-27	0.754
	-18	0.806
	-9	0.838
	+1	0.876
	+11	0.902
	+18	0.928
1,8DMN/Na/MTHF	-103	0.742
	-94	0.748
	-84	0.774
	-74	0.793
	-65	0.819
	-55	0.827
	-45	0.845
	-38	0.882
	-28	0.901
	-19	0.928
	-10	0.947
	+1	1.004
	+10	1.017
	+19	1.055
1,8DMN/K/DEE	-29	(0.032)
	-10	(0.036)
	+9	(0.038)
2,3DMN/K/DME	-17	(0.025)
	-2	(0.032)
	+17	(0.044)
2,3DMN/Na/DME	-3	0.185
	+14	0.403
	+37	0.754
2,3DMN/K/THF	-18	(0.025)
	-1	0.032
	+18	0.038
2,3DMN/Na/THF	-73	0.428
	-64	0.473
	-53	0.729
	-49	0.787
	-44	0.863
	-37	0.895
	-27	0.991

Table A.4 continued

System	Temperature (°C)	$\|a_M\|$ (G)
	-19	1.042
	-10	1.081
	+1	1.132
	+10	1.157
	+18	1.182
2,3DMN/K/MTHF	-29	(0.025)
	-11	0.033
	-5	0.038
	+1	0.040
	+6	0.042
	+10	0.044
	+15	0.051
	+29	0.057
2,3DMN/Na/MTHF	-111	0.806
	-101	0.863
	-95	0.869
	-84	0.921
	-75	0.928
	-65	0.966
	-56	1.004
	-46	1.036
	-37	1.081
	-28	1.107
	-19	1.151
	-10	1.183
	0	1.216
	+10	1.247
	+19	1.291
2,3DMN/K/DEE	-102	0.054
	-85	0.054
	-66	0.057
	-47	0.064
	-29	0.070
	-11	0.070
	-9	0.077
	+1	0.081
	+9	0.084
	+19	0.090
2,6DMN/K/DME	+17	(0.032)
	+29	0.044
	+36	0.051

Table A.4 continued

System	Temperature (°C)	$\|a_M\|$ (G)
2,6DMN/Na/DME	+1	0.185
2,6DMN/K/THF	-36	(0.025)
	-18	0.032
	+1	0.038
	+19	0.044
	+36	0.064
2,6DMN/Na/THF	-62	0.447
	-55	0.595
	-50	0.685
	-45	0.787
	-36	0.908
	-26	1.004
	-18	1.055
	-9	1.119
	+2	1.144
	+11	1.189
	+18	1.222
2,6DMN/K/MTHF	-66	(0.025)
	-47	0.032
	-28	0.038
	-8	0.051
	+11	0.057
	+31	0.070
2,6DMN/Na/MTHF	-111	0.985
	-102	1.029
	-92	1.029
	-83	1.094
	-73	1.107
	-65	1.151
	-56	1.178
	-48	1.203
	-38	1.209
	-28	1.254
	-20	1.284
	-10	1.317
	+1	1.363
	+10	1.401
	+19	1.432

Table A.4 continued

System	Temperature (°C)	$\|a_M\|$ (G)
2,6DMN/K/DEE	-84	0.081
	-65	0.081
	-46	0.084
	-29	0.087
	-10	0.094
	+11	0.101
	+20	0.103
2,7DMN/K/DME	-12	(0.038)
	+11	(0.051)
	+25	(0.057)
2,7DMN/Na/DME	-36	(0.038)
	-18	(0.051)
2,7DMN/K/THF	-74	(0.02)
	-56	0.028
	-36	0.038
	-19	0.044
	-1	0.051
	+17	0.057
2,7DMN/Na/THF	-61	0.633
	-55	0.735
	-48	0.838
	-45	0.914
	-37	1.029
	-27	1.094
	-10	1.209
	-1	1.235
	+9	1.279
	+18	1.311
2,7DMN/K/MTHF	-86	0.032
	-75	0.035
	-68	0.041
	-47	0.051
	-28	0.059
	-10	0.070
	+9	0.077
	+28	0.084

Table A.4 continued

System	Temperature (°C)	$\|a_M\|$ (G)
2,7DMN/Na/MTHF	-115	1.094
	-105	1.100
	-98	1.126
	-85	1.189
	-76	1.209
	-65	1.247
	-56	1.260
	-46	1.298
	-37	1.324
	-27	1.336
	-19	1.394
	-10	1.458
	+1	1.477
	+10	1.510
	+19	1.560
2,7DMN/K/DEE	-103	0.096
	-85	0.096
	-65	0.096
	-46	0.103
	-28	0.103
	-9	0.109
	+11	0.122
N/Na/DME	+8	0.153
	+13	0.251
	+22	0.347
N/Na/THF	-64	0.176
	-54	0.368
	-45	0.579
	-35	0.691
	-23	0.832
	-11	0.891
	+4	0.945
	+18	1.007
N/Na/MTHF	-136	0.592
	-126	0.655
	-106	0.679
	-101	0.711
	-92	0.710

Table A.4 continued

System	Temperature (°C)	$\|a_M\|$ (G)
N/Na/MTHF (ctd)	-82	0.760
	-73	0.781
	-66	0.814
	-57	0.834
	-48	0.875
	-39	0.899
	-30	0.931
	-21	0.957
	-11	0.995
	-2	1.022
	+9	1.071
	+18	1.095
N/K/MTHF	-27	(0.025)
	-9	0.032
	+11	0.038
	+29	0.044
N/Na/DEE	-124	0.957
	-113	1.010
	-110	1.091
	-95	1.232
	-86	1.304
	-76	1.380
	-65	1.506
	-57	1.536
	-47	1.662
	-38	1.720
	-27	1.818
	-19	1.878
	-10	1.944
	-1	1.991
	+9	2.014
N/K/DEE	-103	0.057
	-86	0.057
	-67	0.057
	-48	0.057
	-28	0.060
	-10	0.060
	+10	0.063

a) Footnotes a) - c) of Table A.1

Table A.5: Proton Coupling Constants for the unsymmetric Dimethylnaphthalenes.[a)]

System	1,2DMN/K/DME	1,3DMN/K/DME
Temperature	-85°C	-87°C
	$\lvert a_H \rvert$ (G)	$\lvert a_H \rvert$ (G)
	1.010	1.759
	2.305	1.880
	2.648	2.032
	4.502	4.242
	4.693	5.074
	5.423	5.239
	$\lvert a_{CH_3} \rvert$ (G)	$\lvert a_{CH_3} \rvert$ (G)
	1.943	1.867
	4.375	3.950

System	1,6DMN/K/DME	1,7DMN/K/DME	
Temperature	-83°C	-84°C	-61°C
	$\lvert a_H \rvert$ (G)	$\lvert a_H \rvert$ (G)	$\lvert a_H \rvert$ (G)
	1.105	1.448	1.441
	2.362	1.949	1.949
	2.762	1.867	1.892
	4.102	1.883	4.909
	5.124	4.883	4.870
	5.378	4.540	4.540
	$\lvert a_{CH_3} \rvert$ (G)	$\lvert a_{CH_3} \rvert$ (G)	$\lvert a_{CH_3} \rvert$ (G)
	1.308	2.184	2.140
	3.975	3.492	3.480

a) Footnotes a) - c) of Table A.1

References

1. A. Carrington and A. D. McLachlan, "Introduction to Magnetic Resonance", Harper and Row, New York, 1967; P. B. Ayscough, "Electron Spin Resonance in Chemistry", Meuthuen, London, 1967; J. E. Wertz and J. R. Bolton, "Electron Spin Resonance: Elementary Theory and Practical Applications," McGraw-Hill, New York, 1972.

2. M. Berthelot, Ann. Chem., 12, 155 (1867).

3. W. Schlenk and T. Weikel, Chem. Ber., 44, 1182 (1911); W. Schlenk and E. Bergmann, Ann. Chem., 463, 91 (1928).

4. S. Sugden, Trans. Faraday Soc., 30, 18 (1934).

5. R. Willstatter, F. Seitz and E. Bumm, Chem. Ber., 61, 871 (1928).

6. N. D. Scott, J. F. Walker and V. L. Hansley, J. Am. Chem. Soc., 58, 2442 (1936).

7. W. Huckel and H. Bretschneider, Ann. Chem., 540, 157 (1939).

8. D. Lipkin, D. E. Paul, J. Townsend and S. I. Weissman, Science, 117, 534 (1953); S. I. Weissman, J. Townsend, D. E. Paul and G. E. Pake, J. Chem. Phys., 21, 2227 (1953).

9. D. E. Paul, D. Lipkin and S. I. Weissman, J. Am. Chem. Soc., 78, 116 (1956).

10. G. J. Hoijtink, J. van Schooten, E. de Boer and W. Y. Aalbersberg, Rec. Trav. Chim., 73, 355 (1954); G. J. Hoijtink, Rec. Trav. Chim., 73, 895 (1954).

11. G. J. Hoijtink, E. de Boer, P. H. van der Meij and W. P. Weijland, Rec. Trav. Chim., 75, 487 (1956).

12. P. Balk, G. J. Hoijtink and J.W.H. Schreurs, Rec. Trav. Chim., 76, 813 (1957); P. Balk, S. de Bruijn and G. J. Hoijtink, Rec. Trav. Chim., 76, 907 (1957); J.H.K. Buschow, J.Dieleman and G. J. Hoijtink, Mol. Phys., 7, 1 (1963).

13. S. I. Weissman and E. de Boer, J. Am. Chem. Soc., 80, 4549 (1958).

14. T. R. Tuttle, S. I. Weissman and E. de Boer, J. Phys. Chem., 61, 28 (1957); P. Balk, S. de Bruijn and G. J. Hoijtink, Rec. Trav. Chim., 76, 860 (1957).

15. H. McConnell, J. Chem. Phys., 24, 764 (1956); H. M. McConnell and D. B. Chesnut, J. Chem. Phys., 28, 107 (1958).

16. A. D. McLachlan, Mol. Phys., 3, 233 (1960).

17. F. C. Adam and S. I. Weissman, J. Am. Chem. Soc., 80, 1518 (1958).

18. N. M. Atherton and S. I. Weissman, J. Am. Chem. Soc., 83, 1330 (1961).

19. M. Szwarc, Ed., "Ions and Ion Pairs in Organic Reactions," Vol. 1, Wiley - Interscience. New York, N.Y., 1972.

20. N. Bjerrum, Kgt. dauske Vidensk. Selsk., 7, 9 (1926).

21. R. M. Fuoss and C. A. Kraus, J. Am. Chem. Soc., 55, 2387 (1933); R. M. Fuoss, Trans. Faraday Soc., 30, 967 (1934).

22. C. A. Kraus, J. Phys. Chem., 60, 129 (1956).

23. R. M. Fuoss, J. Am. Chem. Soc., 80, 5059 (1958).

24. J. T. Denison and J. B. Ramsey, J. Am. Chem. Soc., 77, 2615 (1955).

25. M. Born, Z. Physik, 1, 45 (1920).

26. Y. H. Inami, H. K. Bodeusch and J. B. Ramsey, J. Am. Chem. Soc., 83, 4745 (1961).

27. W. R. Gilkerson, J. Chem. Phys., 25, 1199 (1956).

28. J. F. Coetzee and C. D. Ritchie, Ed., "Solute-Solvent Interactions", Marcel Dekker, New York, 1969.

29. S. Aono and K. Oohashi, Prog. Theoret. Phys., 30, 162 (1963); 32, 1 (1964); E. de Boer, Rec. Trav. Chim., 84, 609 (1965).

30. G. W. Canters, C. Corvaja and E. de Boer, J. Chem. Phys., 54, 3026 (1971).

31. I. B. Goldberg and J. R. Bolton, J. Phys. Chem., 74, 1965 (1970).

32. E. de Boer and E. L. Mackor, Proc. Chem. Soc., 23, (1963); J. Am. Chem. Soc., 86, 1513 (1964).

33. M.C.R. Symons, J. Phys. Chem., 71, 172 (1967).

34. R. L. Ward and S. I. Weissman, J. Am. Chem. Soc., 79, 2086 (1957); P. J. Zandstra and S. I. Weissman, J. Chem. Phys., 35, 757 (1961); J. Am. Chem. Soc., 84, 4408 (1962).

35. J. Jagur-Grodzinski, M. Feld, S. L. Yang and M. Szwarc, J. Phys. Chem., 69, 628 (1965).

36. R. V. Slates and M. Szwarc, J. Phys. Chem., 69, 4124 (1965); P. Chang, R. V. Slates and M. Szwarc, J. Phys. Chem., 70, 3180 (1966).

37. A. I. Shatenshtein, E. S. Petrov and E. A. Yakovleva, J. Polymer Sci. C, 16, 1729 (1967).

38. H.V. Carter, B.J. McClelland and E. Warhurst, Trans. Faraday Soc., 56, 455 (1960), N. Hirota and S.I. Weissman, J. Am. Chem. Soc., 86, 2538 (1964); J.F. Garst, C. Hewitt, D. Walmsley and W. Richards, J. Am. Chem. Soc., 83, 5034 (1961).

39. B. J. McClelland, Trans. Faraday Soc., 57, 1458 (1961).

40. T. E. Hogen-Esch and J. Smid, J. Am. Chem. Soc., 88, 307, 318 (1966).

41. S. Winstein, E. Clippinger, A. H. Fainberg and G. C. Robinson, J. Am. Chem. Soc., 76, 2597 (1954).

42. H. Sadek and R. M. Fuoss, J. Am. Chem. Soc., 76, 5905 (1954).

43. E. Grunwald, Anal. Chem., 26, 1696 (1954).

44. N. Hirota and R. Kreilick, J. Am. Chem. Soc., 88, 614 (1966); A. Crowley, N. Hirota and R. Kreilick, J. Chem. Phys., 46, 4815 (1967).

45. N. Hirota, J. Phys. Chem., 71, 127 (1967).

46. N. Hirota, J. Am. Chem. Soc., 90, 3603 (1968).

47. N. Hirota, R. Carraway and W. Schook, J. Am. Chem. Soc., 90, 3611 (1968).

48. K. Hofelmann, J. Jagur-Grodzinski and M. Szwarc, J. Am. Chem. Soc., 91, 4645 (1969).

49. C. L. Dodson and A. H. Reddoch, J. Chem. Phys., 48, 3226 (1968).

50. W. G. Williams, R. J. Pritchett and G. K. Fraenkel, J. Chem. Phys., 52, 5584 (1970).

51. G. J. Hoijtink, J. Townsend and S. I. Weissman, J. Chem. Phys. 34, 507 (1961).

52. H. Nishiguchi, Y. Nakai, K. Nakamura, K. Ishizu, Y. Deguchi and H. Takaki, Mol. Phys., 9, 153 (1965).

53. T. Takeshita and N. Hirota, J. Chem. Phys., 58, 3745 (1973).

54. K. Mobius, Zeit. Naturforschg., 20A, 1102 (1965).

55. A. H. Reddoch, C. L. Dodson and D. H. Paskovich, J. Chem. Phys., 52, 2318 (1970).

56. B. G. Segal as cited by O. W. Howarth and G. K. Fraenkel, J. Chem. Phys., 52, 6258 (1970).

57. N. Hirota, in "Radical Ions", E. T. Kaiser and L. Kevan, Eds., Interscience, New York, 1968, Chapter 2.

58. K. Suga and S. Aoyagui, Bull. Chem. Soc. Japan, 45, 1375 (1972).

59. M. S. Blois, "Free Radicals in Biological Systems", Academic Press, New York, 1961.

60. B. G. Segal, M. Kaplan and G. K. Fraenkel, J. Chem. Phys., 43, 4191 (1965).

61. L. E. Lyons, J. E. Moore and G. C. Morris, Aust. J. Chem., 21, 1337 (1968).

62. A. Carrington, F. Dravnieks and M.C.R. Symons, J. Chem. Soc. (London), 947 (1959).

63. J. P. Colpa and J. R. Bolton, Mol. Phys., 6, 273 (1963).

64. J. R. Bolton, J. Phys. Chem., 71, 3702 (1967).

65. M. H. Hnoosh and R. A. Zingaro, J. Am. Chem. Soc., 92, 4388 (1970).

66. D.J.M. Fassaert and E. de Boer, Mol. Phys., 21, 485 (1971).

67. A. Reymond and G. K. Fraenkel, J. Phys. Chem., 71, 4570 (1967).

68. C. de Waard and J.C.M. Henning, Phys. Lett., 4, 31 (1963).

69. F. Gerson, B. Weidmann and E. Heilbronner, Helv. Chim. Acta., 47, 1951 (1964).

70. V. A. Maximadsky and F. Dorr, Naturforschg., 196, 359 (1964).

71. R. E. Moss, N. A. Ashford, R. G. Lawler and G. K. Fraenkel, J. Chem. Phys., 51, 1765 (1969).

72. R. D. Rieke, C. F. Meares and L. I. Rieke, Tett. Lett., 5275 (1968).

73. R. D. Rieke, S. E. Bales, C. F. Meares, L. I. Rieke and C. M. Milliren, J. Org. Chem., 39, 2276 (1974).

74. B. M. Peake, Ph.D. Thesis, University of Canterbury, Christchurch, 1971.

75. J. R. Bolton and G. K. Fraenkel, J. Chem. Phys., 40, 3307 (1964).

76. D. Casson and B. J. Tabner, J. Chem. Soc. (London) B., 572 (1969).

77. E. De Barry Barnett and F. G. Sanders, Chem. Soc. (London), 434 (1933).

78. W. J. Mitchell, R. D. Topsom and J. Vaughan, J. Chem. Soc., (London), 2526 (1962).

79. R. A. Friedal and M. Orchin, "Ultraviolet Spectra of Aromatic Compounds," J. Wiley and Sons, New York, 1951, No. 563; A. D. Campbell, R. A. Elder and G. W. Emerson, J. Chem. Soc. (London), 3526 (1959).

80. P. A. Dobosh, "CNINDO: CNDO and INDO Molecular Orbital Program (FORTRAN IV)," Quantum Chemistry Program Exchange, Program No. 141.

81. P. Graceffa and T. R. Tuttle, J. Chem. Phys., 50, 1908 (1969).

82. R. W. Fessenden, J. Chem. Phys., 37, 747 (1962).

83. C. Gooijer and C. Maclean, Mol. Phys., 27, 105 (1974).

84. A. C. Aten, J. Dieleman and G. J. Hoijtink, Disc. Faraday Soc., 29, 182 (1960).

85. M. T. Jones, M. Komarynsky and R. D. Rataiczak, J. Phys. Chem., 75, 2769 (1971).

86. G. W. Canters, E. de Boer, B.M.P. Hendricks and A.A.K. Klaassen, Proc. Coll. Ampere, XV, 242 (1969).

87. N. M. Atherton, Chem. Comm., 254 (1966).

88. P. B. Ayscough and F. B. Sargent, J. Chem. Soc. (London), B, 900 (1966).

89. R. D. Allendoerfer and R. J. Papez, J. Phys. Chem., 76, 1012 (1972).

90. D. Nicholls, C. Sutphen and M. Szwarc, J. Phys. Chem., 72, 1021 (1968).

91. C. Carvajal, K. J. Tolle, J. Smid and M. Szwarc, J. Am. Chem. Soc., 87, 5548 (1965).

92. A. G. Evans, J. C. Evans, P. J. Emes, C. L. James and P. J. Pomery, J. Chem. Soc. (London) B, 1484 (1971).

93. G. K. Fraenkel, J. Phys. Chem., 71, 139 (1967).

94. Esr Spectra Simulation Program Version 8, from University of York, England.

95. H. S. Gutowsky and C. H. Holm, J. Chem. Phys., 25, 1228 (1956).

96. S. A. Al-Baldawi and T. E. Gough, Can. J. Chem., 48, 2798 (1970). J.H. Sharp and M.C.R. Symons, Chapter 5 of Ref. 1.

97. G. W. Canters, E. de Boer, B.M.P. Hendricks and H. van Willigen, Chem. Phys. Lett., 1, 627 (1968).

98. B.M.P. Hendriks, G. W. Canters, C. Corvaja, J.W.M. de Boer and E. de Boer, Mol. Phys., 20, 193 (1971).

99. L. L. Chan and J. Smid, J. Am. Chem. Soc., 90, 4654 (1968).

100. M. Iwaizumi, M. Suzuki, T. Isobe and H. Azumi, Bull Chem. Soc. Japan, 40, 1325, (1967).

101. A. H. Reddoch, J. Chem. Phys., 43, 225 (1965).

102. A. Streitwieser, "Molecular Orbital Theory for Organic Chemists," Wiley, New York, 1961.

103. L. C. Snyder and T. Amos, J. Chem. Phys., 42, 3670 (1965).

104. J. A. Pople and D. L. Beveridge, "Approximate Molecular Orbital Theory," McGraw-Hill, New York, 1970.

105. M. Karplus and G. K. Fraenkel, J. Chem. Phys., 35, 1312 (1961).

106. J. Freed and G. K. Fraenkel, J. Chem. Phys., 39, 326 (1963).

107. E. de Boer and E. L. Mackor, J. Chem. Phys., 38, 1450 (1963).

108. J. R. Bolton and G. K. Fraenkel, J. Chem. Phys., 40, 3307 (1964); 41, 944 (1964).

109. R. D. Allendoerfer, J. Chem. Phys., 55, 3615 (1971).

110. A. Rainis and M. Szwarc, J. Am. Chem. Soc., 96, 3008 (1974).

111. D. M. Donaldson, J. M. Robertson and J. G. White, Proc. Roy. Soc. (London), 220A, 311 (1953); C. A. Coulson and P. N. Skancke, J. Chem. Soc. (London), 2775 (1962).

112. M. Brustolon, C. Corvaja and L. Pasimeni, J. Chem. Soc. (Faraday II), 68, 2150 (1972).

113. A. J. Stone, Mol. Phys., 6, 509 (1963).

114. J. R. Bolton, A. Carrington and A. D. McLachlan, Mol. Phys., 5, 31 (1962); J. P. Colpa and E. de Boer, Mol. Phys., 7, 333 (1964).

115. J. A. Valenzuela and A. J. Bard, J. Phys. Chem., 73, 779 (1969).

116. D. Lazdins and M. Karplus, J. Am. Chem. Soc., 87, 920 (1965).

117. A. D. McLachlan, Mol. Phys., 1, 233 (1958); H. L. Strauss and G. K. Fraenkel, J. Chem. Phys., 35, 1738 (1961).

118. D. Bright, I. E. Maxwell and J. de Boer, J. Chem. Soc. (Perkin II), 2101 (1973).

119. D. Doddrell and P. R. Wells, J. Chem. Soc. (Perkin II), 1333 (1973); N. K. Wilson and J. B. Stothers, J. Mag. Res., 15, 31 (1974).

120. F. F. Yew, R. J. Kurland and B. J. Mair, Anal. Chem., 36, 843 (1964); A. Saika, A. Kawamori, and R. Takagi, J. Mag. Res., 7, 324 (1972).

121. C. Maclean and E. L. Mackor, Mol. Phys. 3, 223 (1960).

122. Y. Karasawa, G. Levin and M. Szwarc, J. Am. Chem. Soc., 93, 4614 (1971).

123. T. R. Tuttle, J. C. Danner and P. Graceffa, J. Phys. Chem., 76, 2866 (1972).

124. R. Chang and C. S. Johnson, J. Am. Chem. Soc., 88, 2338 (1966).

125. P. Graceffa and T. R. Tuttle, J. Phys. Chem., 77, 1566 (1973).

126. J. A. Pople, W. G. Schneider and H. J. Berstein, "High Resolution Nuclear Magnetic Resonance," McGraw-Hill Book Co., New York, 1959, pp 221-222.

127. L. Lee, R. Adams, J. Jagur-Grodzinski and M. Szwarc, J. Am. Chem. Soc., 93, 4149 (1971).

128. M. Iwaizumu, M. Suzuki, T. Isobe and H. Azumi, Bull. Chem. Soc. Japan, 40, 2754 (1967).

129. A. H. Reddoch, J. Mag. Res., 15, 75 (1974).

130. A. H. Reddoch, Chem. Phys. Lett., 10, 108 (1971).

131. M. Iwaizumi and J. R. Bolton, J. Mag. Res., 2, 278 (1970).

132. M. Iwaizumi and T. Isobe, Bull. Chem. Soc. Japan, 38, 1547 (1965).

133. R. D. Rieke, S. E. Bales, P. M. Hudnall, and C. F. Meares J. Am. Chem. Soc., 92, 1418 (1970); 93, 697 (1971).

134. R. D. Rieke and S. E. Bales, Chem. Phys. Lett., 12, 631 (1972).

135. R. D. Rieke and S. E. Bales, Tett. Lett., 2439 (1972).

136. J. R. Bolton, Ph.D. Thesis, Cambridge University, Cambridge, 1963, as quoted in Ref. 71.

137. F. Gerson, B. M. Peake and G. M. Whitesides, Org. Mag. Res., 4, 361 (1972).

138. R. D. Rieke, K. White and E. McBride, J. Org. Chem., 38, 1430 (1973).

^{13}C COUPLING IN THE E.S.R. SPECTRUM OF THE PYRENE ANION IN TETRAHYDROFURAN

By R. F. C. CLARIDGE,* C. M. KIRK,* and B. M. PEAKE†

[Manuscript received 4 April 1973]

Abstract

Examination of the e.s.r. spectrum of pyrene anion in tetrahydrofuran under conditions of high resolution has yielded the ^{13}C hyperfine coupling parameters for five of the six carbon positions. The parameters agree well with those calculated by molecular orbital methods. No evidence of ion pair formation was found under the conditions used in these experiments.

In the numerous reports of e.s.r. studies on ion pair formation between aromatic radical anions and alkali metals controversy has existed over the relative locations of the anion and cation.[1] Lyons, Moore, and Morris[2] in a report on the potassium–pyrene system in tetrahydrofuran note the existence of small peaks not due to the major species. By the use of stick spectra they have assigned these to the outer pair of lines of a quartet arising from a K^+ pyrene$^-$ ion pair with a metal hyperfine spacing of 0·14 G. The possibility that these extra lines arise from the 1·1% ^{13}C present in natural abundance was discounted because the intensities of the lines relative to the major peaks were too great and showed an apparent temperature dependence. On lowering the temperature, certain of these lines were found to broaden which was interpreted in terms of a linewidth alternation arising from the migration of the K^+ cation between the equivalent sites 2 and 7 (see structure (1)).

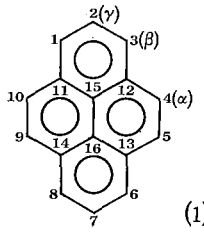

(1)

We have re-examined the potassium–pyrene system in tetrahydrofuran and wish to report that by allowing for ^{13}C coupling constants we have been able to explain the observed spectrum.

Under high resolution the spectrum appears to be more complex than indicated by Lyons and cannot be explained by a simple linewidth alternation effect. The ^{13}C

* Chemistry Department, University of Canterbury, Christchurch, New Zealand.
† Chemistry Department, University of Otago, Dunedin, New Zealand.

[1] De Boer, E., and Mackor, E. L., *J. Am. chem. Soc.*, 1964, **86**, 1513; Iwaizumi, M., and Bolton, J. R., *J. magn. Resonance*, 1970, **2**, 279; Reddoch, A. H., *Chem. Phys. Lett.*, 1971, **10**, 108.
[2] Lyons, L. E., Moore, J. E., and Morris, G. C., *Aust. J. Chem.*, 1968, **21**, 1337.

coupling constants were determined by analysing the extreme ends of the spectrum (Fig. 1) to avoid complication caused by overlapping lines. As pointed out by Bolton and Fraenkel[3] the need for high resolution and a high signal-to-noise ratio places stringent requirements on the spectrometer. To achieve the desired sensitivity a long time constant (10 s) and a slow scan rate (10 G/2 hr) had to be used. Because of the remaining noise level and the drift in the magnetic field (1 part in 10^5) over the long scan time, the ^{13}C coupling constants cannot be quoted as accurately as the proton parameters. Spectra were recorded using 10-kHz modulation to reduce instrumental line broadening.

Using the coupling constants, linewidths, and ratios relative to the parent proton peaks* of Table 1 we have obtained excellent simulation of the low-field spectral region. In the remainder of the spectrum where there are overlapping lines and the added complication that the low- and high-field components of the ^{13}C lines can have different linewidths, the agreement is remarkable. All features of the spectrum are accounted for.

TABLE 1

HYPERFINE COUPLING CONSTANTS, IN GAUSS, AT −30°C

Position	Constant[a]	Linewidth	Percentage
A_1^H	(−)4·813	0·03	
A_2^H	(+)1·029	0·03	
A_4^H	(−)2·121	0·03	
A_1^C	+7·10	0·06	2·2
A_2^C	−6·00	0·04	1·1
A_4^C	(+)1·84	0·04	2·2
A_{11}^C	(−)2·58	0·03	2·2
A_{15}^C	<0·20	—	—

[a] Proton constants ±0·005 G, ^{13}C constants ±0·01 G. Signs in brackets are predicted by theory, the others are determined from experiment.

The proton coupling constants have previously been assigned.[2,4] The ^{13}C assignments are based on a comparison of the experimental parameters with calculated spin densities.[5–9] All the calculations shown in Table 2 predict positive coupling constants for positions 1 and 4, and negative constants for positions 2, 11, and 15. The two largest observed coupling constants have been assigned to positions 1 and 2 respectively on the basis of their magnitudes, intensity ratio, and signs. The signs were

* The intensity of each ^{13}C satellite relative to the parent line is given by $(n/2)\times 0{\cdot}011$ where n is the number of equivalent positions capable of accommodating the ^{13}C nucleus.

[3] Bolton, J. R., and Fraenkel, G. K., *J. chem. Phys.*, 1964, **41**, 944; Bolton, J. R., and Fraenkel, G. K., *J. chem. Phys.*, 1964, **40**, 3307.

[4] De Boer, E., and Mackor, E. L., *J. chem. Phys.*, 1963, **38**, 1450.

[5] Streitwieser, A., "Molecular Orbital Theory for Organic Chemists," (John Wiley: New York 1961).

[6] McLachlan, A. D., *Molec. Phys.*, 1960, **3**, 232.

[7] Snyder, L. C., and Amos, A. T., *J. chem. Phys.*, 1965, **42**, 3670.

[8] Karplus, M., and Fraenkel, G. K., *J. chem. Phys.*, 1961, **35**, 1312.

[9] Pople, J. A., and Beveridge, D. L., "Approximate Molecular Orbital Theory," (McGraw–Hill: New York 1970).

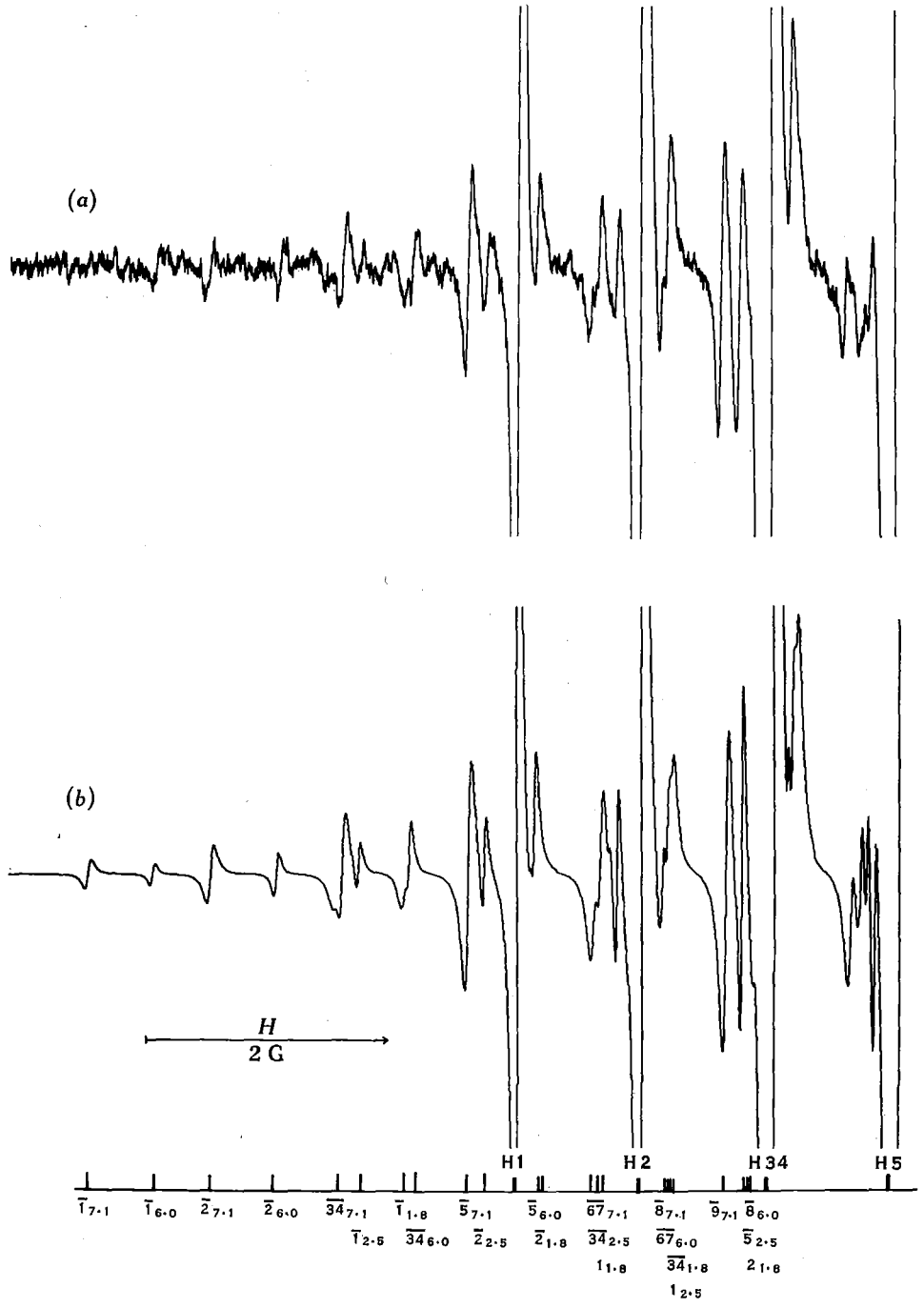

Fig. 1.—Low-field region of the spectrum of K^+ pyrene$^-$ in tetrahydrofuran. (*a*) Observed; (*b*) computer simulation. The large lines labelled H1, H2 etc. are the outermost lines due to the protons. The remaining lines are due to ^{13}C and are labelled as low-field, $\bar{1}$, or high-field, 1, satellites of the proton lines. The subscripts are the respective coupling constants.

To accompany thesis by Kirk, C.M. " ESR studies of radical ions

determined by observing the relative linewidths of the high- and low-field components of the lines.[5] The two remaining constants observed were present in equal ratios (2·2%) and since they were of similar magnitude, 1·84 and 2·59 G, could not be distinguished by comparison with the calculated values for positions 4 and 11. Examination of the high- and low-field components did not reveal the sign of either constant because of accidental overlap of lines. However, on the basis that linewidth broadening due to the anisotropic dipolar interactions is approximately proportional to the square of local spin density,[3] the splitting (2·59 G) with the narrowest linewidth has been assigned to position 11. The 1·85 G constant has therefore been assigned to position 4, since the remaining position, 15, was predicted to give a 1·1% ^{13}C constant with a much smaller coupling constant. This final coupling constant could not be observed and it was concluded that it was less than 0·20 G and masked by the more intense proton lines.

TABLE 2

CALCULATED AND EXPERIMENTAL ^{13}C CONSTANTS AND SPIN DENSITIES

Position	Spin densities $\rho^{\pi}(C_i)$			Coupling constants A^C				
	HMO[a]	MCL[b]	UHF[c]	HMO[d]	MCL[d]	UHF[d]	INDO[e]	Exptl
1	0·136	0·187	0·174	+4·467	+7·352	+6·625	+9·9	+7·10
2	0	−0·052	−0·042	−3·781	−7·050	−6·332	−7·1	−6·00
4	0·087	0·092	0·085	+1·512	+1·968	+1·692	−2·9	(+)1·84
11	0·027	0·002	0·011	−2·276	−3·650	−3·278	—	(−)2·58
15	0	−0·012	−0·001	−0·751	−0·255	−0·389	—	0·20

[a] Simple Hückel method, ref. 5.
[b] McLachlan method, ref. 6.
[c] Unrestricted Hartree–Fock method, ref. 7.
[d] Calculated (ref. 8) using

$$A^C = 35{\cdot}6\rho^{\pi}(C) - 13{\cdot}9\sum_i \rho^{\pi}(C_i) \quad \text{for C–C}_2\text{H fragments}$$

$$A^C = 30{\cdot}5\rho^{\pi}(C) - 13{\cdot}9\sum_i \rho^{\pi}(C_i) \quad \text{for C–C}_3 \text{ fragments}$$

[e] Ref. 9.

Finally, the apparent selective broadening observed by Lyons *et al.* has a simple explanation. Measurements show that the majority of the lines which overlap at position A (of ref.[2]) are ^{13}C satellites of the γ proton lines, whereas the main ^{13}C components at position B of ref.[2] are not. It is a change in the γ proton coupling constant with temperature rather than any linewidth broadening effect due to cation migration between positions 2 and 7 on the pyrene molecule which is responsible for the observed broadening. With the resolution obtained in these experiments (mean linewidth 0·030 G) components of a potassium coupling constant of 0·14 G should have been visible.

The question of the relative positions of the cation and the anion in the pyrene system remains unsolved. Further work will be necessary to establish whether migration of the cation can be observed.

Acknowledgment

This work was supported by funds from the New Zealand University Grants Committee.